



UNIVERSITY GRANTS COMMISSION

BAHADURSHAH ZAFAR MARG

NEW DELHI-110002

A Final Report

On

Major Research Project

Entitled

**“Design, Synthesis and Screening of Some Novel Tyrosine Kinase Inhibitors as
Anticancer Agent”**

(F. No. 41-752/2012 (SR), dated 23/07/2012)

Principal Investigator

Dr. Santosh. R. Butle

Assistant Professor,

School of Pharmacy,

Swami Ramanand Teerth Marathwada University

Vishnupuri, Nanded – 431605 (MS)

butlesr@gmail.com; butlesr@srtmun.ac.in

INDEX

Sr. No.	Title	Page No.
1.	Introduction	1
2.	Objectives of Study	2
3.	Plan of Work	3
4.	Designing of Anticancer Drug Molecules	4
4.1	Designing of Phthalazine Derivatives	08
4.1.1	Designing of 1,6-Disubstituted Phthalazine Derivatives	08
4.1.2	Designing of Aminophthalazine Derivatives	23
4.2	Designing of Quinazoline Derivatives	41
4.2.1	Designing of N-[4-Amino-2-(4-Methylphenyl)quinazoline-6-yl]acetamide derivatives	42
4.2.2	Designing of N-[2-(4-methylphenyl)-4-(substituted aniline)-3, 4-dihydro quinazolin-6-yl] acetamide derivatives	57
4.3	Designing of 4-Anilinoquinazoline Derivatives	73
4.4	Designing of Pyrido[2,3-D]Pyrimidine Derivatives	90
5.	Synthesis of Anticancer Drug Molecules	113
5.1	Synthesis of Phthalazine Derivatives	115
5.1.1	Synthesis of 1,6-Disubstituted Phthalazine Derivatives	115
5.1.2	Synthesis of Aminophthalazine Derivatives	124
5.2	Synthesis of Quinazoline Derivatives	130
5.2.1	Synthesis of N-[4-Amino-2-(4-Methylphenyl)quinazoline-6-yl]acetamide derivatives	130
5.2.2	Synthesis of N-[2-(4-methylphenyl)-4-(substituted aniline)-3, 4-dihydro quinazolin-6-yl] acetamide derivatives	134
5.3	Synthesis of 4-Anilinoquinazoline Derivatives	139
5.4	Synthesis of Pyrido[2,3-D]Pyrimidine Derivatives	142
6.	Anticancer Activity	163
7.	Conclusion	166
8.	Future Scope	169
9.	Acknowledgement	169
10.	References	170
11.	Research Outcomes: PG Students Degree Awarded	175
12.	Research Outcomes: PhD Students Registered and Awarded	176
13.	Research Outcomes: Research Paper Published/Accepted/Communicated	177
14.	Research Outcome: Poster Presented	178

1. INTRODUCTION:

In India around 8 lakh cases of cancer are reported every year. Half of them succumb to the disease. Cancer incidences are expected to double by 2020, because of changing life style, industrialization, indiscriminate use of pesticides, adulterants, and consumption of drugs and tobacco. The chemotherapy of cancer has become increasingly important in the recent years. But the cancer chemotherapy has received no spectacular breakthrough of the kind that the discovery of penicillin provided for antibacterial chemotherapy. Most of the anticancer agents used currently in clinical practice are highly toxic and causes bone marrow depression, which results in leukopenia and thrombocytopenia. The other side effects of the presently used anticancer agents are gastrointestinal hemorrhage, stomatitis, and esophagopharyngitis, hemorrhagic cystitis which may be fatal, alopecia, nausea, kidney damage, and myelosuppression. Therefore, the development of new anticancer agents which will selectively kill neoplastic cells only, has become the important objective in the research in this field.

Tyrosine Kinase is an enzyme which transports phosphates from ATP to a protein's tyrosine residue. Therefore, a Tyrosine Kinase inhibitor prevents the phosphate groups from being transferred. Research indicates that mutations which make Tyrosine Kinases constantly active can be a contributing factor in the development of cancerous cells. So, when an inhibitor is used, the cell communication and reproduction is reduced, and cancerous cell growth will be reduced to the point of stopping tumor growth. A comparative molecular field analysis (CoMFA), ligand- based drug design tool, one of the most commonly used three dimensional quantitative structure-activity relationship (3D-QSAR) programs, are applied to the number of different classes of Tyrosine Kinase inhibitors. We aim to design and develop, potent, selective, non toxic, and cost effective Tyrosine Kinase inhibitor analogs by Computer Aided Drug Design (CADD) and molecular modeling studies, in order to prepare more effective analogs.

Significance of the study:

Tyrosine Kinases are important mediators of the signaling cascade, determining key roles in diverse biological processes like growth, differentiation, metabolism and apoptosis in response to external and internal stimuli. Recent advances have implicated the role of

tyrosine kinase in the pathophysiology of cancer. Though their activity is tightly regulated in normal cells, they may acquire transforming functions due to mutations), overexpression and autocrine paracrine stimulation, leading to malignancy. Constitutive oncogenic activation in cancer cells can be blocked by selective tyrosine kinase inhibitors and thus considered as a promising approach for innovative genome based therapeutics. The modes of oncogenic activation and the different approaches for tyrosine kinase inhibition, like small molecule inhibitors, monoclonal antibodies, heat shock proteins, immunoconjugates, antisense and peptide drugs are reported in case of the important molecules. As angiogenesis is a major event in cancer growth and proliferation, tyrosine kinase inhibitors as a target for anti-angiogenesis can be aptly applied as a new mode of cancer therapy.

2. OBJECTIVES OF STUDY:

Chemotherapy is widely used for the treatment of many dreadful cancers, but still scientist are unsuccessful in developing the promising agent that selectively kill only cancer cells, without harming normal cells. Therefore, the development of novel anticancer agents with an increase efficacy and low toxicity is the prime objective of the present study.

For these reasons, the objectives of the present study are to design and synthesize tyrosine kinase inhibitor analogs. The base molecules structure will be modified to increase the cell permeability, confer more stability, and structure rigidity. Using the pharmacophore structure of base molecules, new chemical entities will be designed, and synthesized with the aim of optimizing the pharmacology of the pharmacophore molecule, as a potential anticancer agent. The synthesized compounds will be evaluated for their anticancer activity.

Objectives of the Project

- i. The prime objective of the present study is to develop novel tyrosine kinase inhibitors as anticancer agents with increased efficacy and low toxicity.
- ii. The base molecules structure will be modified in order to increase the cell permeability, confer more stability, and structure rigidity. Using the pharmacophore structure of base molecules, new chemical entities will be designed, and synthesized

with the aim of optimizing the pharmacology of the molecule, as a potential anticancer agent.

- iii. The designing of novel compounds shall be carried out using molecular modeling studies by Schrodinger software.
- iv. The proposed compounds shall be synthesized by known standard method.
- v. The synthesized compounds shall be confirmed by using IR, Mass & NMR Spectroscopy.
- vi. The synthesized compounds then shall be evaluated for their anticancer activity.

3. PLAN OF WORK:

In order to achieve the objectives of the project, the present work was planned as -

- 1. To carry out the comprehensive literature survey of tyrosine kinase inhibitors.
- 2. Designing of novel tyrosine kinase inhibitors by using molecular modeling and docking study.
- 3. To select and optimize the scheme for the synthesis of proposed compounds.
- 4. To synthesize proposed compounds.
- 5. To confirm the structures of the synthesized compounds by spectral and elemental analysis such as:
 - a. Physical properties like nature, colour, solubility, M.P., and R_f value
 - b. Structural elucidation using IR, Mass and 1H NMR.
- 6. To evaluate the synthesized compounds for anticancer activity by the known standard methods.

4. DESIGNING OF ANTICANCER DRUG MOLECULES:

Molecular modeling has become a valuable and essential tool to medicinal chemists in the drug design process. Molecular modeling describes the generation, manipulation or representation of three-dimensional structures of molecules and associated physicochemical properties. It involves a range of computerized techniques based on theoretical chemistry methods and experimental data to predict molecular and biological properties. Molecular modeling can be defined as an application of computers to generate, manipulate, calculate and predict realistic molecular structures and associated properties. The computational approaches in particular molecular mechanics is to obtain energetic and structural information for biomolecules.

Molecular modeling can be considered as a range of computerized techniques based on theoretical chemistry methods and experimental data that can be used either to analyze molecules and molecular systems or to predict molecular, chemical, and biochemical properties. It serves as a bridge between theory and experiment to:

1. Extract results for a particular model.
2. Compare experimental results of the system.
3. Compare theoretical predictions for the model.
4. Help understanding and interpreting experimental observations
5. Correlate between microscopic details at atomic and molecular level and macroscopic properties.
6. Provide information not available from real experiments.

Thus, molecular modeling can be defined as the generation, manipulation, calculation, and prediction of realistic molecular structures and associated physicochemical as well as biochemical properties by the use of a computer. It is primarily a mean of communication between scientist and computer, the imperative interface between human-comprehensive symbolism, and the mathematical description of the molecule.

Functions of the Molecular Modeling:

1. Structure retrieval or generation:

Crystal structures of organic compounds can be found in the Cambridge Crystallographic Data files (<http://www.ccdc.cam.ac.uk/>). Those that do not exist may be generated by 3D rendering software. The 3D structural coordinates of biomacromolecules can be retrieved from

Protein Data Bank (<http://www.rcsb.org/pdb/>).

2. Structural visualization:

Computer graphics is the most effective means for visualization and interactive manipulation of molecules and molecular systems. Numerous software programs (e.g., Cn3D, RasMol and KineMage,) are available for visualization, management, and manipulation of molecular structures.

3. Energy calculation and minimization:

One of the fundamental properties of molecules is their energy content and energy level. Three major theoretical computational methods of their calculation include empirical (molecular mechanics), semi-empirical, and ab initio (quantum mechanics) approaches. Energy minimization results in geometry optimization of the molecular structure.

4. Dynamics simulation and conformation search:

Solving motion of nuclei in the average field of the electrons is called quantum dynamics. Solution to the Newton's equation of motion for the nuclei is known as molecular dynamics. Integration of Newton's equation of motion for all atoms in the system generates molecular trajectories. Conformation search is carried out by repeating the process by rotating reference bonds (dihedral angles) of the molecule under investigation for finding lowest energy conformations of molecular systems.

5. Calculation of molecular properties:

Molecular modeling methods will be helpful in estimating or computing properties (i.e., interpolating properties, extrapolating properties, and computing properties). Some computing properties are boiling point, molar volume, solubility, heat capacity, density,

thermodynamic quantities, molar refractivity, magnetic susceptibility, dipole moment, partial atomic charge, ionization potential, electrostatic potential, Van Der Waals surface area, and solvent accessible surface area.

6. Structure superposition and alignment:

Computing activities and properties of molecules often involves comparisons across a homologous series. Such techniques require superposition or alignment of structures.

7. Molecular interactions, docking:

The intermolecular interaction in a ligand-receptor complex is important and requires difficult modeling exercises. Usually the receptor (e.g., protein) is kept rigid or partially rigid while the conformation of ligand molecule is allowed to change.

METHODOLOGY:

Steps of the molecular modeling:

1. Preparing a Library of Compounds.
2. Preparing the Protein
3. Preparing the Ligands
4. Generating the Receptor Grid
5. Docking the Ligands
6. Examining Poses

Software and Hardware Used:

Schrodinger-2012 was run on a Windows XP based Core i5 2.66 GHz PC (with 4 GB of memory). The molecular docking tool, Glide Docking version 2012 software was used for ligand docking studies into the protein DNA Gyrase with PDB code (1YWN, 2P2H, 3XIR, 3EWH, 3VHE, 3VNT, 4AG8, 4ASE) having a co-crystallized ligand Clorobiocin. Glide Docking is one of the most accurate docking programmes available for ligand-protein, protein-protein binding studies. Glide is validated software designed for calculating the accurate binding interaction energies of the 3-D structures of a known protein receptor with ligand or another protein molecule.

Docking Simulations:

Docking simulations have been performed using Glide Docking software, which combines differential evolution with a cavity prediction algorithm. The guided differential evolution algorithm combines the differential evolution optimization technique with a cavity prediction algorithm. Differential evolution (DE) has been successfully applied to molecular docking. Fast and accurate identification of potential binding modes during the search process is made by the use of predicted cavities. The docking scoring function of Glide make use of piece-wise linear potential (PLP) and is further extended in Glide Dock. The docking scoring function takes hydrogen bond directionality into account. The highest ranked poses are again re-ranked to increase the docking accuracy further. Only the ligand properties were represented in the individuals, as the protein has limited side chain flexibility during the docking process. The fitness of a candidate solution is the sum of the intermolecular interaction energy between the ligand and the protein, and the intra-molecular interaction energy of the ligand. The docking scoring function, G-score, is defined by the following energy terms.

$$G_{\text{score}} = E_{\text{intra}} + E_{\text{inter}}$$

Where, E_{inter} is the ligand–protein interaction energy:

$$E_{\text{inter}} = \sum_{i \in \text{ligand}} \sum_{j \in \text{protein}} \left[E_{\text{PLP}}(r_{ij}) + 332.0 \frac{q_i q_j}{4\pi\epsilon_0 r_{ij}^2} \right] \quad (2)$$

The summation runs over all heavy atoms in the ligand and all heavy atoms in the protein, including cofactor atoms and water molecule atoms that might be present. The second term of the (2) describes the electrostatic interactions between charged atoms.

E_{intra} is the internal energy of the ligand:

$$E_{\text{intra}} = \sum_{i \in \text{ligand}} \sum_{j \in \text{ligand}} E_{\text{PLP}}(r_{ij}) + \sum_{\text{flexible bonds}} A[1 - \cos(m^* \theta - \theta_0)] + E_{\text{clash}} \quad (3)$$

The double summation is between all atom pairs in the ligand, excluding atom pairs that are connected by two bonds or less. The second term is a torsional energy term, parameterized according to the hybridization types of the bonded atoms; θ is the torsional angle of the bond. The last term, Eclash, assigns a penalty of 1000 if the distance between two atoms (more than two bonds apart) is less than 2.0 Å. Thus, the Eclash term punishes infeasible ligand conformations.

Our present study makes use of docking templates so as to focus the search. Templates are implemented as scoring functions, rewarding poses similar to the specific pattern. A template is a collection of groups, where each group represents a chemical feature for an atom such as hydrogen acceptor atoms or donor atoms. Each template group contains a number of centers: optimal 3D positions for the group feature.

Following Gaussian formula is used for rewarding each group centre:

$$e = \omega * \exp\left(\frac{-d^2}{r_0^2}\right), \quad (4)$$

Where d is the distance from the position of the atom to the centre in the group. ω is a weight factor for the template group and r_0 is a distance parameter.

THE FOLLOWING DRUG MOLECULES WERE DESIGNED

1. DESIGNING OF PHTHALAZINE DERIVATIVES
2. DESIGNING OF QUINAZOLINE DERIVATIVES
3. DESIGNING OF 4-ANILINOQUINAZOLINE DERIVATIVES
4. DESIGNING OF PYRIDO[2,3-D]PYRIMIDINE DERIVATIVES

4.1. DESIGNING OF PHTHALAZINE DERIVATIVE

4.1.1. Designing Of 1,6-Disubstituted Phthalazine Derivatives:

Selection and Preparation of Protein Structures:

The co-crystal structure of DNA Gyrase PDB-ID (1YWN, 2P2H, 3XIR, 3EWH, 3VHE, 3VNT, 4AG8, 4ASE) was obtained from protein data bank. The typical structure file from the PDB is not suitable for immediate use in molecular modeling calculations as the

PDB structure file consists only of heavy atoms and may include a co-crystallized ligand, water molecules, metal ions, and cofactors. Some structures are metameric and may need to be reduced to a single unit. PDB structures may be missing the information on connectivity, which must be assigned along with bond orders and formal charges. Glide Dockers has therefore assembled a set of tools to prepare proteins in a form that is suitable for modeling calculations. All structures were prepared for docking using the ‘protein preparation tools’ in Glide Dockers. Water molecules in the crystal structures were deleted. In preparation component, after ensuring chemical correctness, the hydrogen’s were added where hydrogen atoms were missing.

Protein Preparation Steps

In protein preparation step, select the PDB-ID, download into the workspace, and import a pre process

1. Import and Process

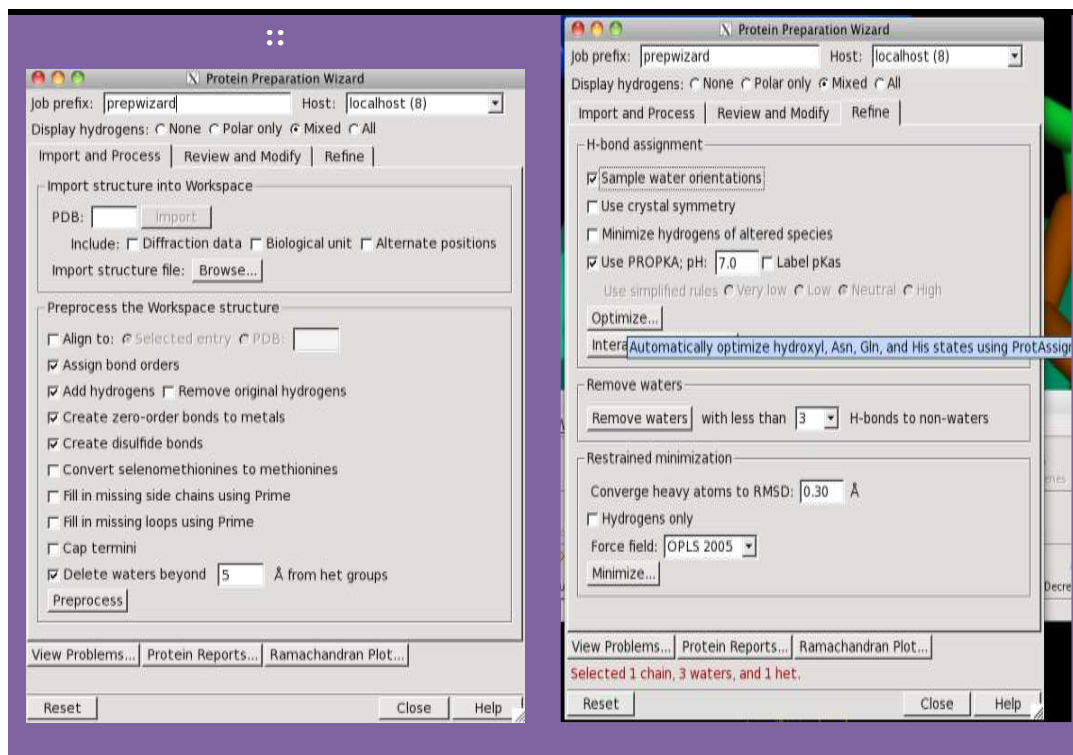


Fig: Protein preparation steps

Select all the tools, such as convert selenomethionine to methionine, fill missing side chain by using prime, cap termini, preprocess, review and modify, refine the protein structure.

Ligand Preparation:

The series of ethyl 1-(amino) phthalazine-6-carboxylate, -{1-[amino]phthalazin-6-yl}ethanol and its derivatives structures were drawn in ChemDraw ® 8.0 (Cambridge Soft, Cambridge, MA, USA) and exported to Glide Dock. Where they were further prepared, Choose Tasks > Ligand Preparation or Applications > LigPrep. Along with the proteins (charges and protonation states were assigned) by the docking engine.

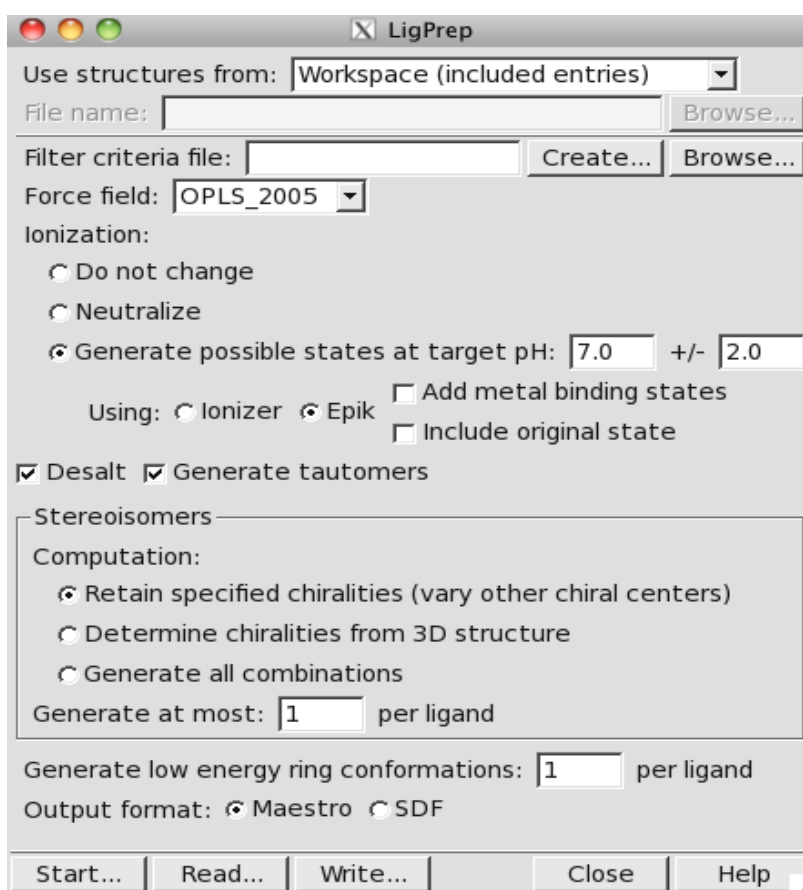


Fig: Ligand preparation

Generating the Receptor Grid:

Choose Tasks > Docking > Grid Generation or Applications > Glide > Receptor Grid Generation. Display the prepared receptor in the workspace. Pick the ligand to define the grid centre. Adjust the size of the active site in the Site tab to accommodate larger ligands, if

necessary. Add any hydrogen-bond, metal, positional or hydrophobic constraints in the constraints tab. Pick any rotatable hydroxyl groups in the active site if such groups could rotate during docking. Start the grid generation job.

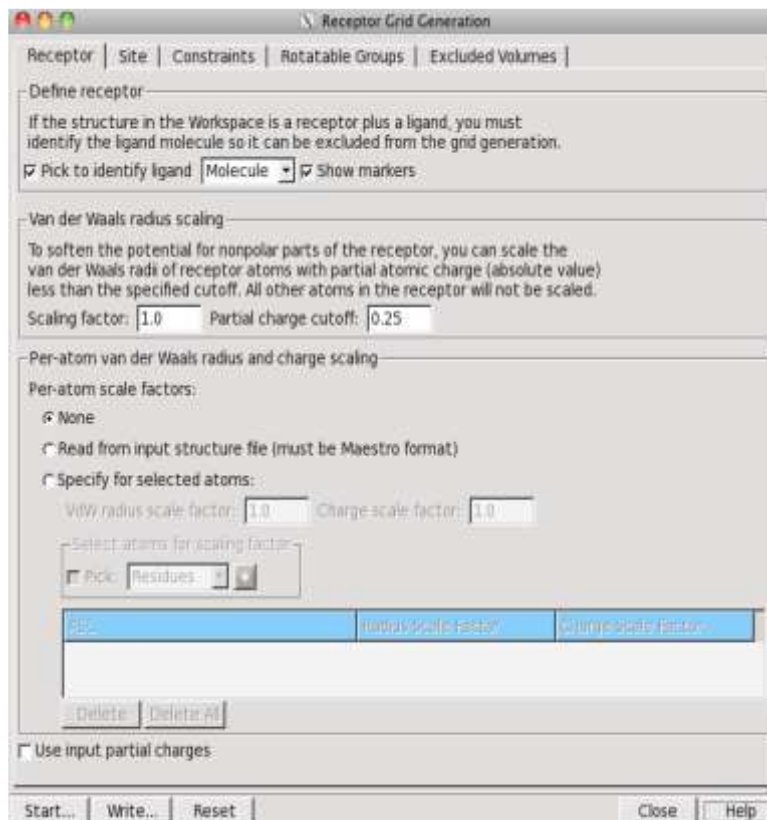


Fig: Receptor grid generation

Docking the Ligands:

Choose Tasks > Docking > Glide Docking or Applications > Glide > Ligand Docking. Specify the receptor grid to use. Select the docking precision:

1. HTVS for initial screen of millions of compounds (limited conformational search but fast)
2. SP for thousands of compounds (better coverage of conformational space)
3. XP for tens or hundreds of compounds (high accuracy on docked poses)

If we chose XP, select, write XP descriptor information if you want to visualize interaction terms. Select Add Epik state penalties to docking score, if Epik was used in ligand preparation (especially for metalloproteinase). Specify the ligand file to use, in the Ligands

tab. If you want to set up constraints to a reference ligand core or calculate RMSD to this core, you can do this in the Core tab. Select the receptor constraints you want to use in the Constraints tab, and supply any required information. If the ligands are very flexible, you can apply constraints on ligand torsions in the Torsional Constraints tab, to reduce the torsional degrees of freedom. Set the number of poses per ligand and total number of poses in the Output tab. Use post-docking minimization if you want to improve pose geometries. Select Write per-residue interaction scores for residues within N Å of grid centre if you want to examine interactions of ligand poses with the receptor, and set the cut-off distance. Click Start to run the job. If the ligand file is large, distribute the job over multiple processors if possible.

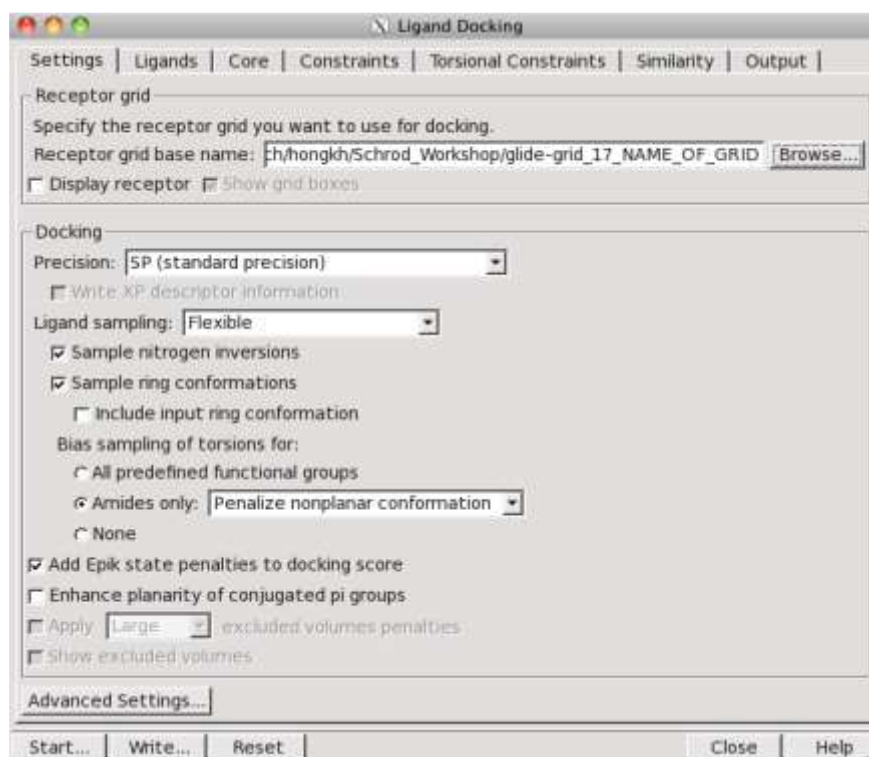


Fig: Docking of ligand

Interpretation of Results:

All the designed compounds were docked into the active sites of EGFR receptor PDB ID (1YWN, 2P2H, 3XIR, 3EWH, 3VHE, 3VNT, 4AG8, 4ASE) for studying the binding mode of designed compounds and further screening to sort out the best compound having good binding affinity which was compared with binding mode of EGFR receptor Inhibitors

like Vatalanib results of which are depicted in following table. The reliability of the docking results was first checked by comparing the best docking poses obtained for the co-crystallized inhibitor with its bound conformation. This was done by removing co-crystallized ligand from their active site and subjecting again to docking into the binding pocket in the conformation found in the crystal structure. The accurate prediction of protein-ligand interaction geometries is essential for the success of virtual screening.

Glide Dock Score:

The results of the docking studies are presented in the form of Glide Dock Score. The 1YWN, 2P2H, 3XIR, 3EWH, 3VHE, 3VNT, 4AG8, 4ASE glide dock score are presented as negative values, indicating that more the negative values more are the binding interactions.

The docking studies were performed for the synthesized compounds (24ligands) with protein and the results were compared with the ligand Vatalanib which was used as standard for an EGFR receptor screening. The docked complexes of the designed compounds along with the ligand receptor poses have been shown in the figures.

The docking scoring function (*G- Score*) is defined by the following energy terms:

$$G_{\text{score}} = E_{\text{intra}} + E_{\text{inter}}$$

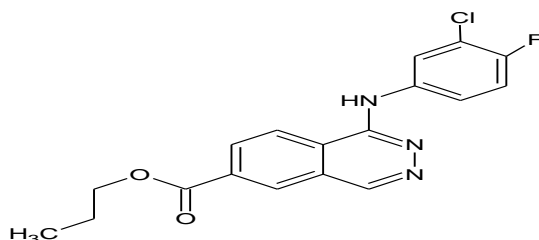
Where,

E-inter is the ligand-protein interaction energy

E-intra is the internal energy of the ligand

Induced-Fit Docking Studies of the Active and Inactive States of Protein Tyrosine Kinases:

Docking of Vmol 21



Propyl 1-[(3-chloro-4-fluorophenyl) amino] phthalazine-6-carboxylate

Method:**Generation of enzyme structures:**

Virtual screening by docking requires an accurate 3D structure of the considered target. The crystal structure of VEGFR-2 kinase domain with its bound to the inhibitor Propyl 1-[(3-chloro-4-fluorophenyl) amino] phthalazine-6-carboxylate.

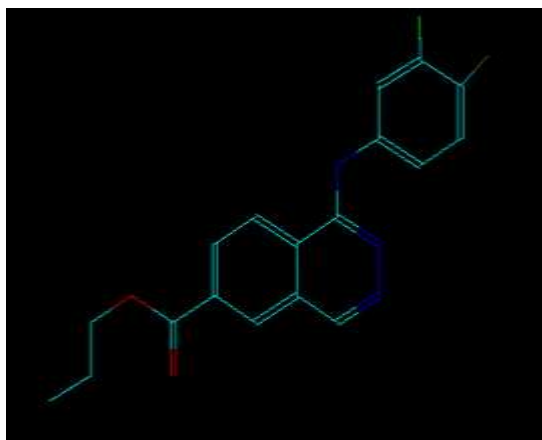


Fig: Structure of Propyl 1-[(3-chloro-4-fluorophenyl) amino] phthalazine-6-carboxylate

Computational protein structure preparation:

The coordinates for all protein–ligand complexes were obtained from the RCSB Protein Data Bank (PDB). Protein structures of 3VHE was prepared using the Schrodinger's Protein Preparation Wizard module

PDB-3VHE

A docking study with two pharmacophore models was routinely used in lead identification and optimization in library focusing, evaluation, and prioritization of virtual high-throughput screening results. The superposition of the crystal structures of the ABL/Vatalanib complex (PDB id: 3VHE) Hydrogen atoms were added and the side chain structures of Gln and were flipped if necessary in order to provide maximum degree of hydrogen bond interactions.



Fig: X-ray crystal structures of the active ABL conformation (green cartoon), the inactive ABL conformation (yellow), and the EGFR (red).

Induced-fit docking

The protein structures of 3VNT were applied with the induced-fit docking (IFD) method in the Schrodinger software suite. The structurally diverse 24 tyrosine kinase inhibitors were selected mol file. All ligands were prepared using LigPrep and were optimized with the OPLS force field in the Macro Model module in Schrodinger. Ligands were docked to the rigid protein using the soften-potential docking in the Glide program with the Van der Waals radii scaling of 0.7 for the proteins. The resulting top 20 poses of ligands were used to sample the protein plasticity using the Prime program in the Schrodinger suite. Residues having at least one atom within 5Å° of any of the 20 ligand poses were subject to a conformational search and minimization while residues outside the zone were held fixed. The resulting 20 new receptor conformations were taken forward for redocking. In this redocking stage, Glide docking parameters were set to the default hard potential function, i.e., the van der Waals radii scaling is 1.0. The Glide XP (extra precision) was used for all docking calculations.

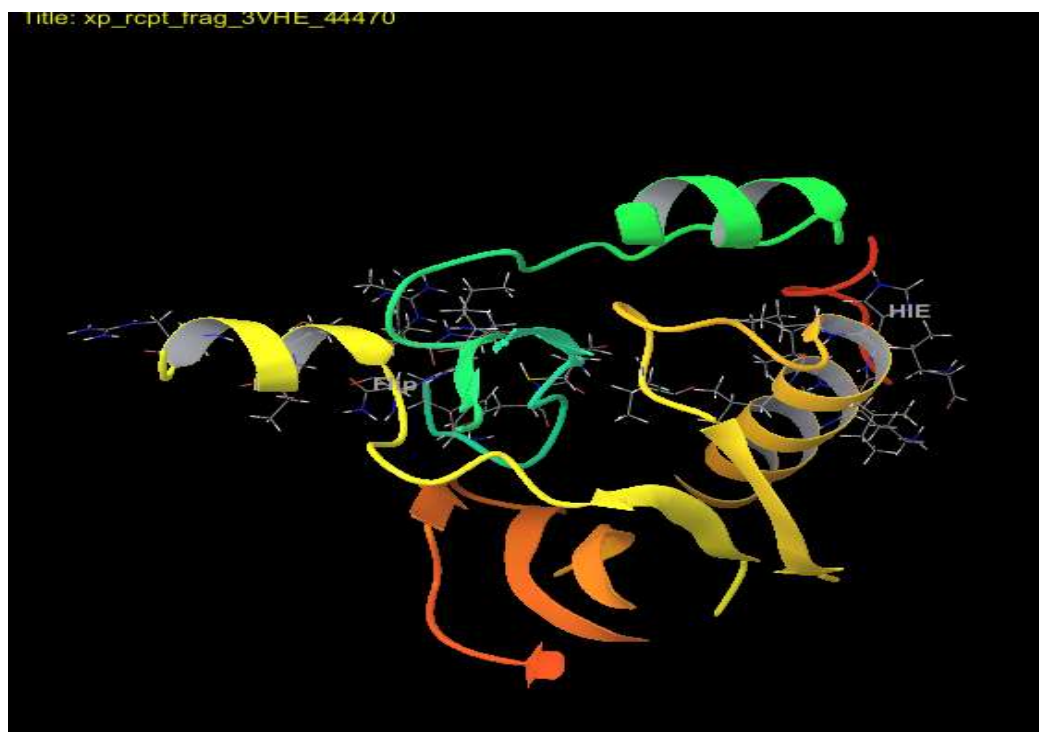
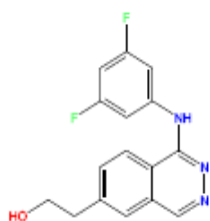


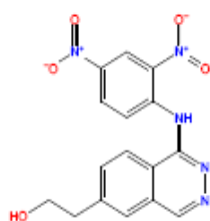
Fig: Induced fit docking

Structures of docked ligand

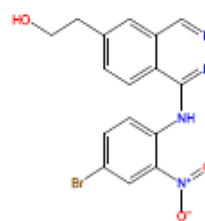
Structures of ligand having -{1-[amino]phthalazin-6-yl}ethanol and its derivatives



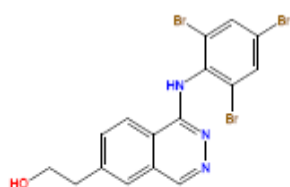
title: mol 1



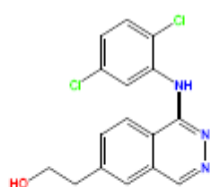
title: mol 2



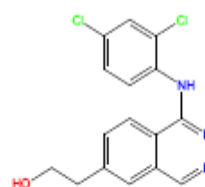
title: mol 3



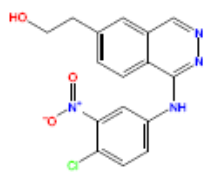
title: mol 4



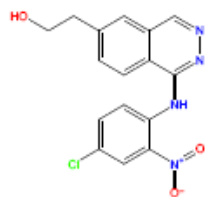
title: mol 5



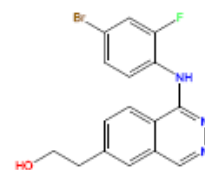
title: mol 6



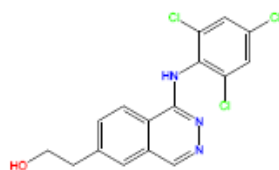
title: mol 7



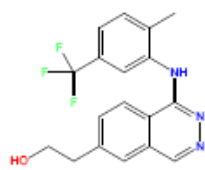
title: mol 8



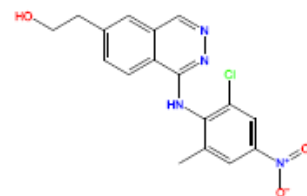
title: mol 9 active



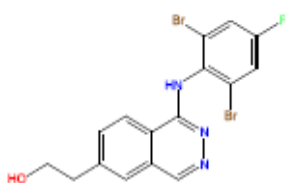
title: mol 10



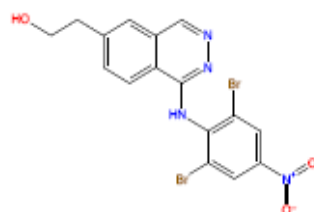
title: mol 11



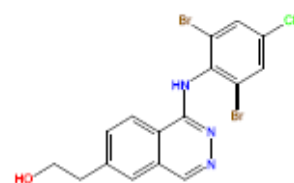
title: mol 12



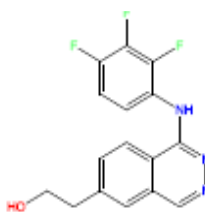
title: mol 13



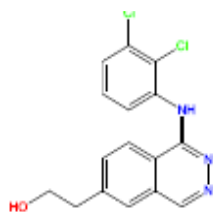
title: mol 14



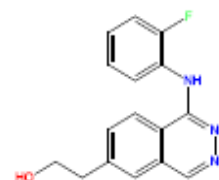
title: mol 15



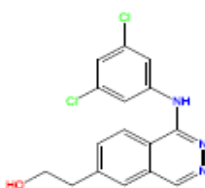
title: mol 16 active



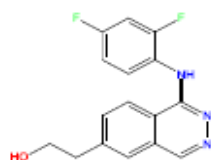
title: mol 17



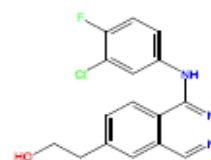
title: mol 18 active



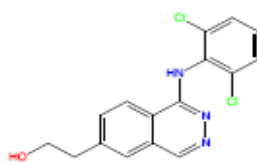
title: mol 19 average



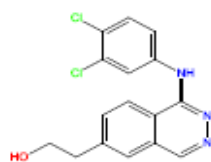
title: mol 20 active



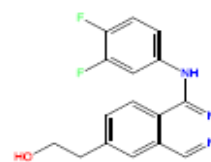
title: mol 21



title: mol 22

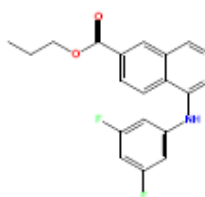


title: mol 23

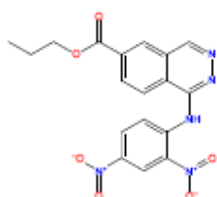


title: mol 24 active

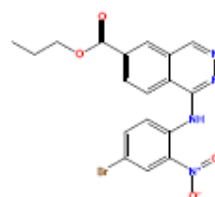
Structures of ligand having propyl 1-(amino) phthalazine-6-carboxylate



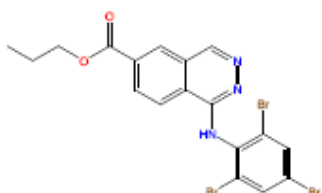
title: v mol 1



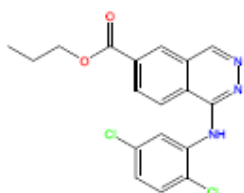
title: v mol 2



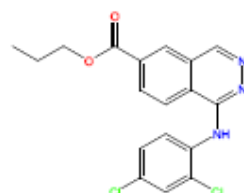
title: v mol 3



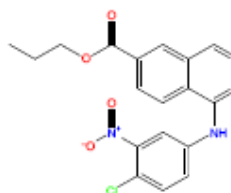
title: v mol 4



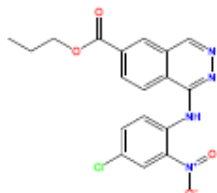
title: v mol 5



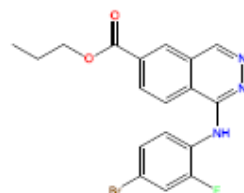
title: v mol 6



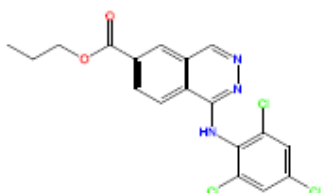
title: v mol 7



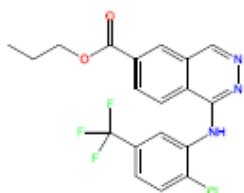
title: v mol 8



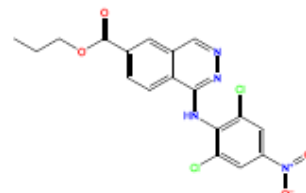
title: v mol 9 average



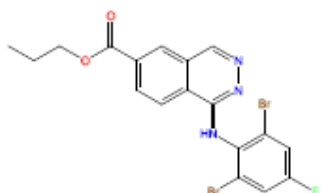
title: v mol 10



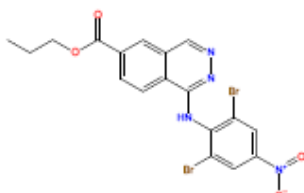
title: v mol 11



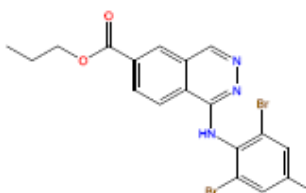
title: v mol 12



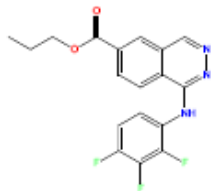
title: v mol 13



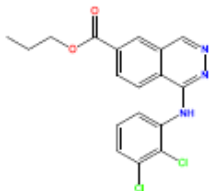
title: v mol 14



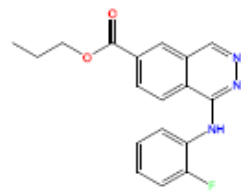
title: v mol 15



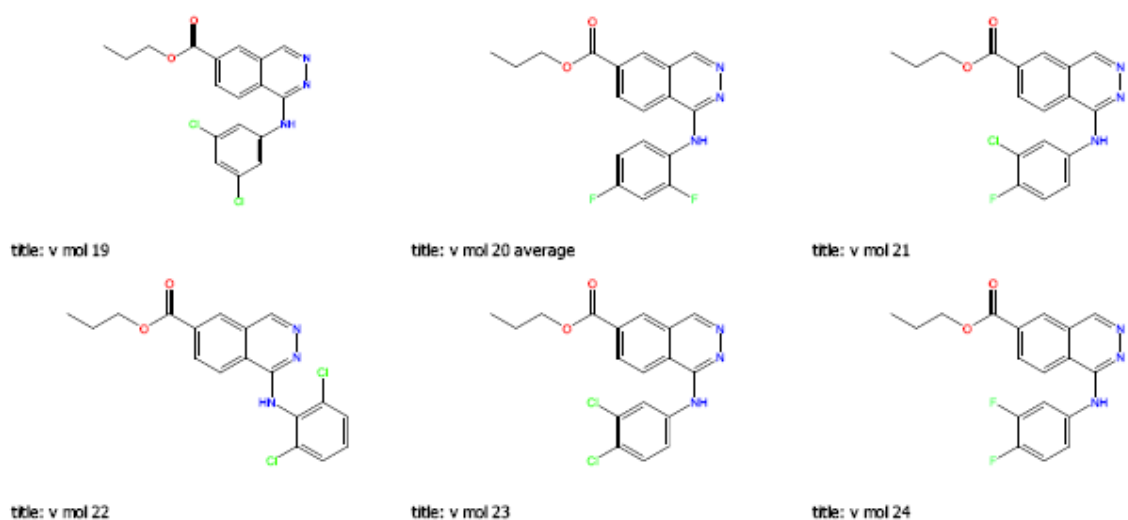
title: v mol 16



title: v mol 17



title: v mol 18 average



Glide docking

The rigid receptor docking using the Glide program was carried out against the three receptors using the same set of ligands. The scaling factor for protein van der Waals radii was 1.0 in the receptor grid generation. The ligands in the active sites were used as the centroid to generate the grid files for the docking. The default grid size was adopted from the Glide program. No constraints were applied for all the docking studies.

Name	QScore	DockScore	LipophilicEa	ProtEn	ProtEnHB	ProtEnPam	HBond	Electro	Stemap	mCal	CBR	LowMW	Penalties	HBPenal	ExposPenal	RotPenal	EpkStatePe	Similarity	Activity
v mol 21	-8.9	-	-6.3	-1.3	0.0	0.0	-0.7	-0.0	-0.6	0.0	0.0	-0.3	0.0	0.0	0.0	0.3	-	1.0	-
mol 17	-8.2	-	-6.4	-1.8	0.0	0.0	-0.7	-0.3	0.0	0.0	0.0	-0.4	1.0	0.0	0.0	0.3	-	0.4	-
mol 26 active	-8.2	-	-6.0	-1.6	0.0	0.0	-0.7	-0.2	-0.6	0.0	0.0	-0.4	1.0	0.0	0.0	0.3	-	0.4	-
mol 20 active	-7.9	-	-6.0	-1.5	0.0	0.0	-0.7	-0.2	-0.4	0.0	0.0	-0.5	1.0	0.0	0.0	0.3	-	0.4	-
mol 21	-7.9	-	-6.1	-1.4	0.0	0.0	-1.2	-0.4	-0.1	0.0	0.0	-0.4	1.5	0.0	0.0	0.3	-	0.2	-
mol 23	-7.6	-	-6.1	-1.3	0.0	0.0	-1.2	-0.5	0.0	0.0	0.0	-0.4	1.5	0.0	0.0	0.3	-	0.2	-
mol 6	-7.6	-	-6.6	-1.4	0.0	0.0	-0.7	-0.2	0.0	0.0	0.0	-0.4	1.5	0.0	0.0	0.3	-	0.3	-
mol 9 active	-7.5	-	-5.8	-1.4	0	0.0	-1.2	-0.5	-0.1	0.0	0.0	-0.3	1.5	0.0	0.0	0.2	-	0.2	-
mol 21-2	-7.8	-	-6.0	-1.4	0.0	0.0	-0.7	-0.3	-0.3	0.0	0.0	-0.4	1.0	0.0	0.0	0.3	-	0.4	-
mol 22	-7.2	-	-6.1	-1.5	0.0	0.0	-0.7	-0.3	0.0	0.0	0.0	-0.4	1.5	0.0	0.0	0.3	-	0.3	-
mol 10	-7.0	-	-6.2	-1.4	0.0	0.0	-0.7	-0.1	0.0	0.0	0.0	-0.3	1.5	0.0	0.0	0.2	-	0.3	-
mol 26 active-2	-7.5	-	-5.8	-1.3	0.0	0.0	-0.7	-0.2	-0.3	0.0	0.0	-0.4	1.0	0.0	0.0	0.3	-	0.4	-
mol 6-2	-7.5	-	-6.5	-1.4	0.0	0.0	-0.7	-0.3	0.0	0.0	0.0	-0.4	1.5	0.0	0.0	0.3	-	0.3	-
mol 17-2	-7.5	-	-6.5	-1.5	0.0	0.0	-0.7	-0.3	0.0	0.0	0.0	-0.4	1.5	0.0	0.0	0.3	-	0.3	-
mol 1	-7.5	-	-5.7	-1.4	0.0	0.0	-0.7	-0.3	-0.1	0.0	0.0	-0.5	1.0	0.0	0.0	0.3	-	0.4	-
mol 7	-7.5	-	-6.3	-1.0	0.0	0.0	-0.7	-0.4	0.0	0.0	0.0	-0.3	1.0	0.0	0.0	0.3	-	0.4	-
v mol 27	-6.7	-	-5.6	-1.1	0.0	0.0	-0.3	-0.4	-0.4	0.0	0.0	-0.1	1.0	0.0	0.0	0.2	-	0.3	-
v mol 22	-6.7	-	-6.5	-1.0	0.0	0.0	0.0	0.1	-0.2	0.0	0.0	-0.2	1.0	0.0	0.0	0.3	-	0.4	-
mol 28 active	-7.2	-	-5.6	-1.3	0.0	0.0	-0.7	-0.4	-0.2	0.0	0.0	-0.5	1.0	0.0	0.0	0.4	-	0.4	-

Fig: Glide Dock Scores

Results and Discussion

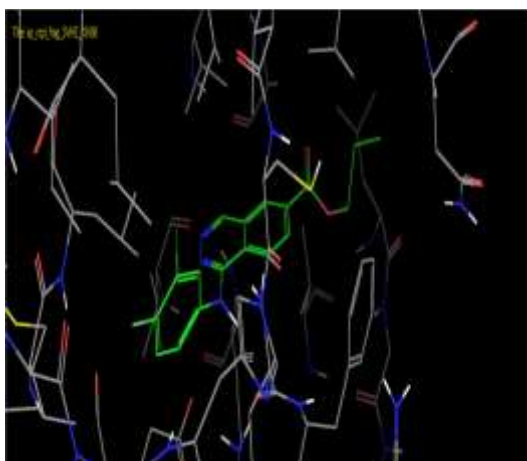
1. Virtual docking

We have applied the GLIDE docking method to twenty four analogues of 1,6-disubstituted phthalazine which are inhibitors of tyrosine protein kinases to build a binding affinity model for the epidermal growth factor receptor that was then used to compute the free energy of binding for this kinase. The ligand preparation procedure generated different training sets of the inhibitors whose scoring function is given in below Table. These different structures were found by using different orientations of the inhibitors and different positions of the hydrogen's. The results of docking and scoring are given in below Table. According to the table we see that among all the energy parameters the largest contribution for binding energy comes from Vander Waals interactions.

Table: Average Vander Waals (vdw), electrostatic (coul) and Site energy (site) after GLIDE docking.

Analogues	E vdw	E coul	E site	Docking score	Energy
Vmol 21	-6.3	-0.0	-0.6	-8.9	-6.3
Vmol 17	-6.4	-0.3	-0.0	-8.2	-6.7
Mol 16	-6.0	-0.2	-0.6	-8.2	-6.2
Mol 15	-6.0	-0.2	-0.4	-7.9	-6.2
Mol 21	-6.1	-0.4	-0.1	-7.9	-6.5
Mol 23	-6.1	-0.5	-0.0	-7.6	-6.6
Mol 6	-6.6	-0.2	-0.0	-7.6	-6.8
Mol 9	-5.8	-0.5	-0.1	-7.5	-6.3

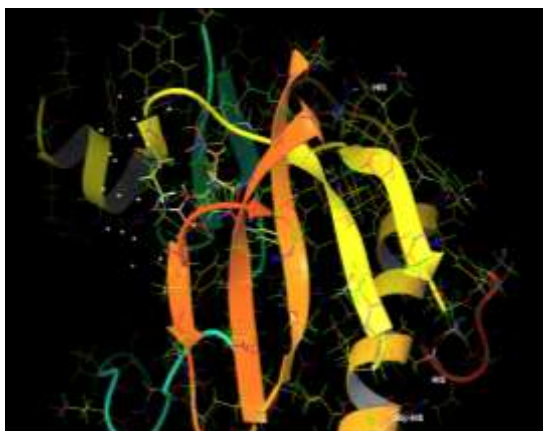
The energy data are written according to the structure generated by the docking program. The best docked poses are written in table. All energies are given in Kcal/mol.



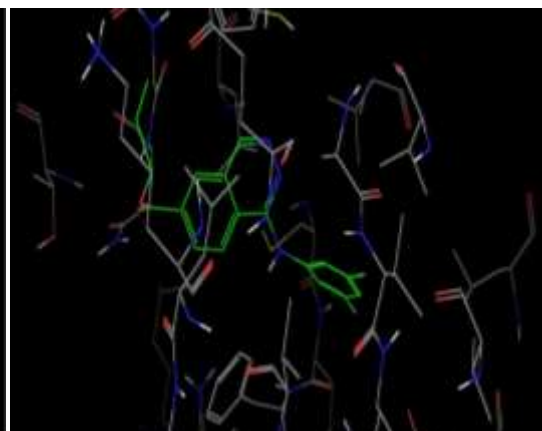
(a)



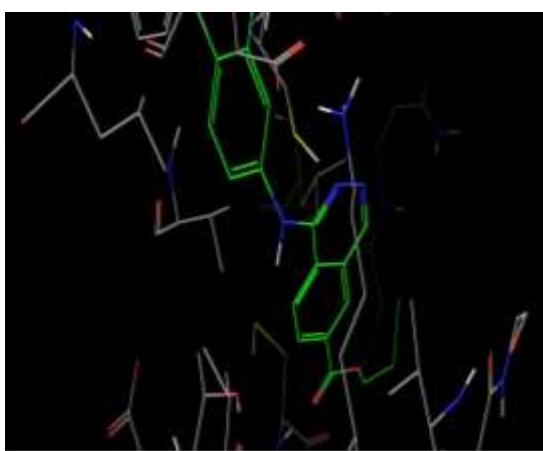
(b)



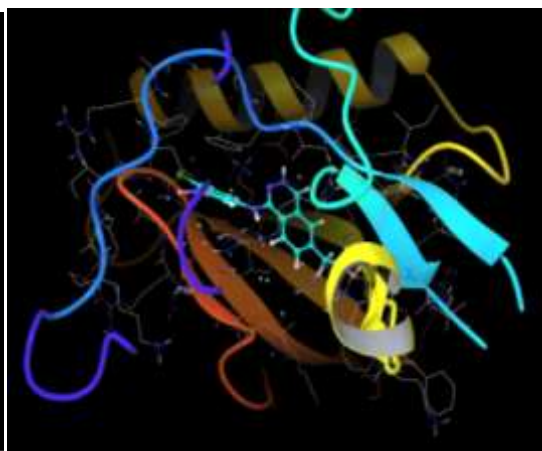
(c)



(d)



(e)



(f)

Figure: Structures of the different kinase inhibitors bound to the protein 3VNT. Only residues that undergo significant movement or are hydrogen bonded to the ligand are shown

2. Induced fit results

In virtual docking the ligands are docked into binding site of the receptor where the receptor is held rigid and the ligand is free to move. We have also taken into account receptor flexibility by induced fit docking. In induced fit docking, we obtained different poses of all the best docked analogues. The results of the induced fit docking are given in below Table, which displays the best docked poses. From the results of the induced fit docking, it is clear that there are some considerable changes in the docking scores and energies of the docked complexes.

Table: Results of the induced fit docking

Analogues	Docking Energy	Docking score
Vmol 21	-6.3	-8.9
Vmol 17	-6.7	-8.2
Mol 16	-6.2	-8.2
Mol 15	-6.2	-7.9
Mol 21	-6.5	-7.9
Mol 23	-6.6	-7.6
Mol 6	-6.8	-7.6
Mol 9	-6.3	-7.5

Docking energy is written only for the best docked poses. All energy values are given in Kcal/mol

Conclusion

The glide score can be used as a semi-quantitative descriptor for the ability of ligands to bind to a specific conformation of the protein receptor. Generally speaking for low glide score good ligand affinity to the receptor may be expected. According to the glide score the results of the inhibition for the VEGF receptor may be arranged in the following manner: Vmol 21> Vmol 17>mol 16> mol 15> mo21> mol 23>mol 6> mol 9>mol17.

Docking studies performed by GLIDE has confirmed that above inhibitors fit into the binding pocket of the VEGF receptor. From the results we may observe that for successful docking, intermolecular hydrogen bonding and lipophilic interactions between the ligand and

the receptor are very important.

A comparison of the induced fit and virtual docking gives the role of protein flexibility. It is obvious from the results that a combined method of soft docking and side chain optimization gives better results. It is also clear that an average distribution of docking free energy ranging from 2 kcal/mol or more, is sufficient to mis-rank a potential drug candidate as a weak binder. However, by combining the MM-GB/SA and relaxed complex methods we are able to show the best ranked binding modes.

4.1.2. Designing of Aminophthalazine Derivatives

Protein preparation

A typical PDB structure file consists only of heavy atoms, can contain waters, cofactors, metal ions and can be multimeric. Terminal amide groups can also be misaligned, because the X-ray structure analysis cannot usually distinguish between O and NH₂. Ionization and tautomeric states are also generally unassigned. Glide calculations use an all-atom force field for accurate energy evaluation. Thus, Glide requires bond orders and ionization states to be properly assigned and performs better when side chains are reoriented when necessary and steric clashes are relieved.

The crystal structure of vascular epidermal growth factor receptor tyrosine kinase domain was obtained from PDB database (Mc Tighe M., 2000) with PDB ID 4AG8 (Murray B. W., 2012).

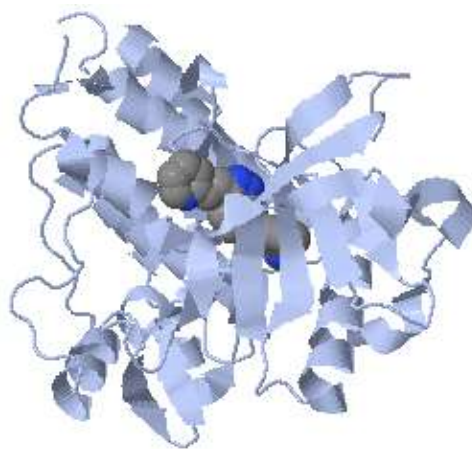


Figure: The crystal structure of VEGFR

Steps involved in protein preparation wizard

1. Import a ligand/protein co-crystallized structure from PDB.



Figure: PDB file step

2. Simplify multimeric complexes.

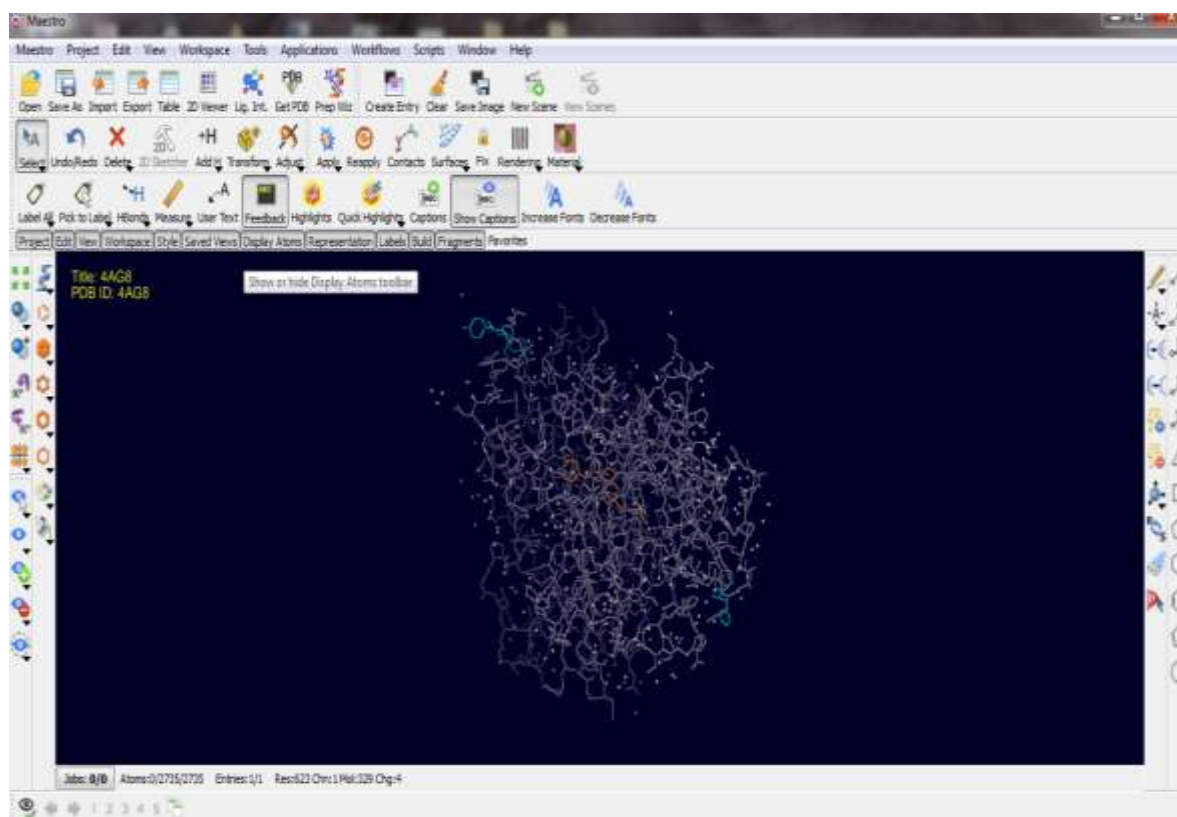


Figure: Multimeric structure of 4AG8

From Workflows tab, choose protein preparation Wizard.

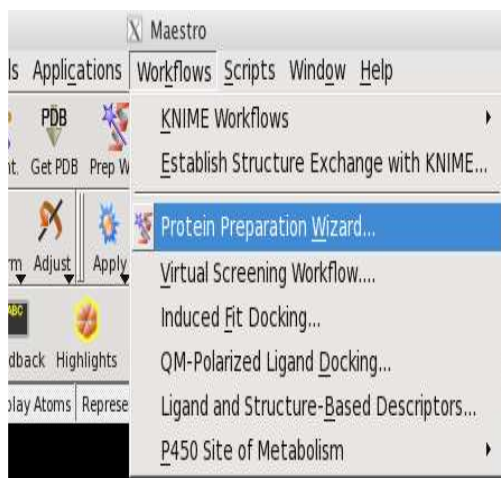


Figure: Protein preparation wizard step

After selecting protein preparation wizard, select import and process tab and import the protein structure from protein data bank and select the options as shown in this window.

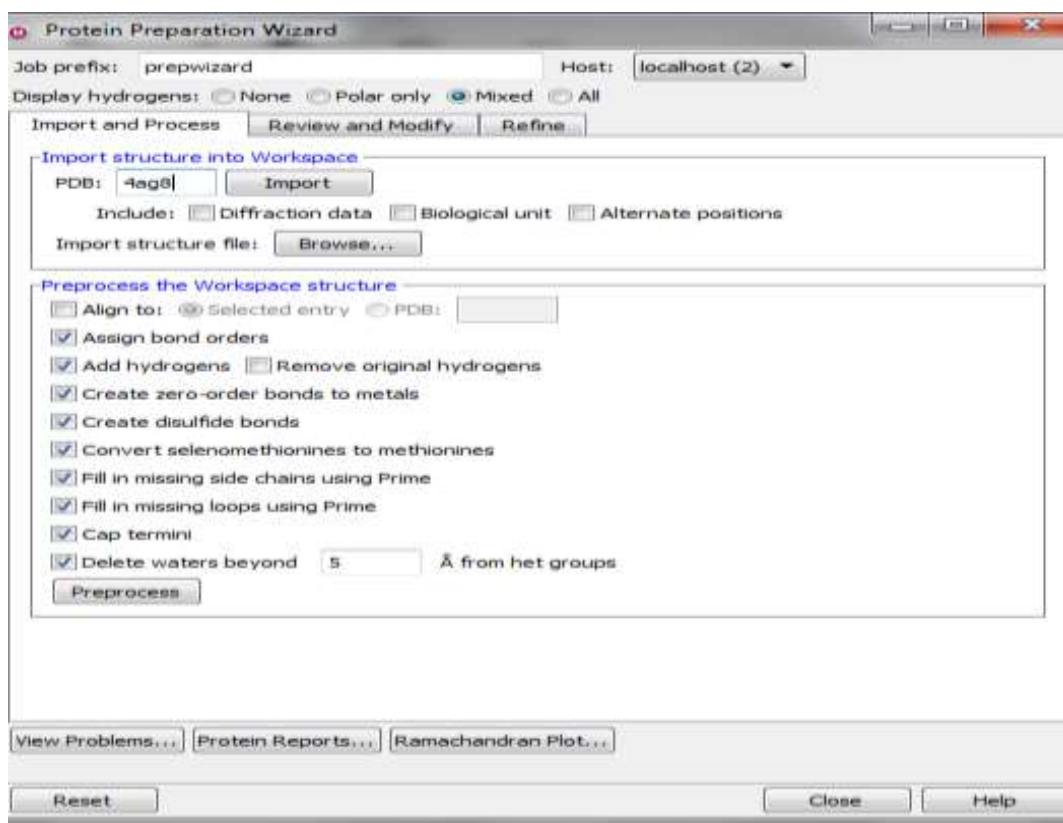


Figure: Protein preparation wizard (import and process step).

The typical structure file from the PDB is not suitable for immediate use in molecular modeling calculations as the PDB structure file consists only of heavy atoms and may include a co-crystallized ligand, water molecules, metal ions, and cofactors. Some structures are metameric and may need to be reduced to a single unit for that purpose go to next review and modify tab and remove unnecessary water molecule by selecting this chain name i.e. B and delete it.

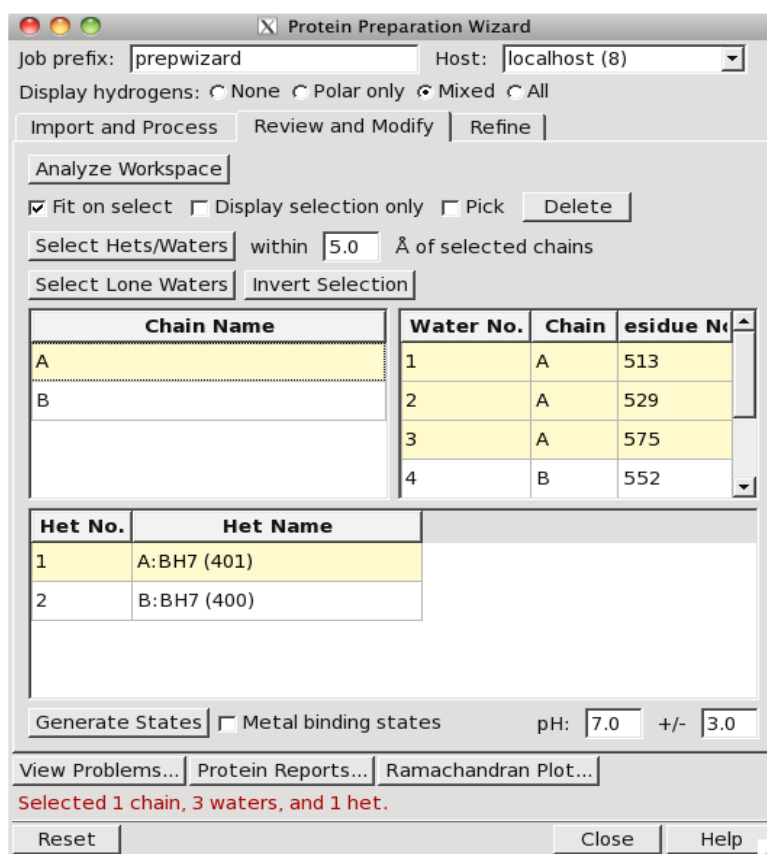


Figure: Protein preparation wizard (review and modify of chain 4AG8 step)

After this process only one chain name is observed in the tab. After that go to the view problem tab if there are any problems then minimize that and move toward refine process. In refinement process select sample water orientations and set use PROPKA pH 7.0 then optimize it.

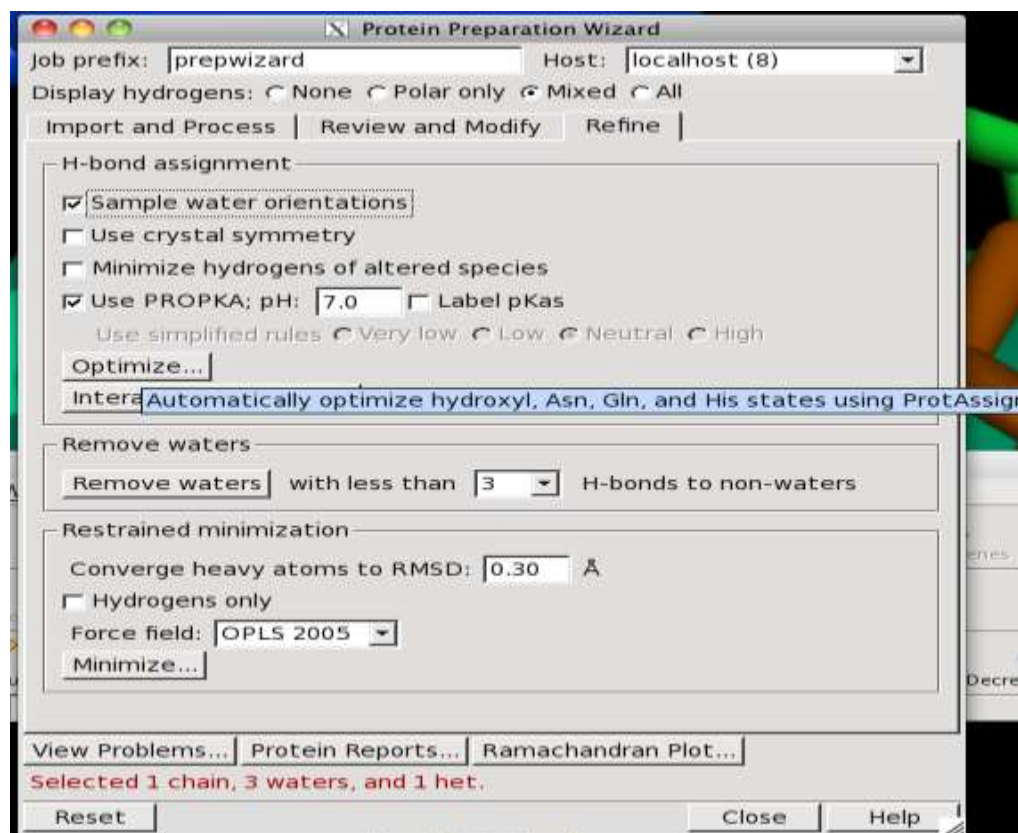


Figure: Protein preparation wizard (Refine step)

After completion of optimization process select 3 H-bond to non-water and in restrained minimization select 0.30 Å converge heavy atoms to RMSD and select force field OPLS 2005 and click on minimize to run this job. After the process is done, a message pops up as shown below. Click Incorporate Now.

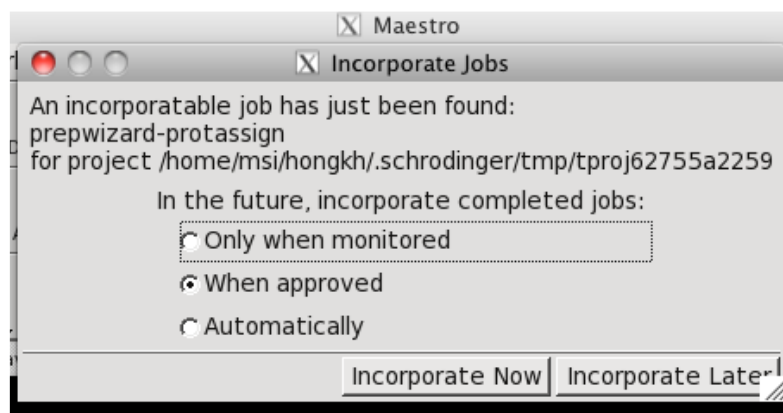


Figure: Incorporation job of prep wizard step

Ligand preparation

Structures supplied to glide must meet the following conditions

1. They must be three-dimensional (3D).
2. They must have realistic bond lengths and bond angles.
3. They must each consist of a single molecule that has no covalent bonds to the receptor, with no accompanying fragments, such as counter ions and solvent molecules.
4. They must have all their hydrogen's
5. They must have an appropriate protonation state for physiological pH values.

The series of Aminophthalazine derivatives structures were drawn using the LigPrep module of the Maestro software. Where they were further prepared Choose Tasks from Applications, choose LigPrep. Then, LigPrep window will be displayed. After that browse prepared 2D structure in the format of MDL Molefile [V2000] (*.mol) in LigPrep tab. Set pH 7.0 +/- 2.0, select Desalt, generate tautomers, Retain specified chiralities, select 1 for generate at most per ligand, select 1 for generate low energy ring confirmation and click start to run the job.

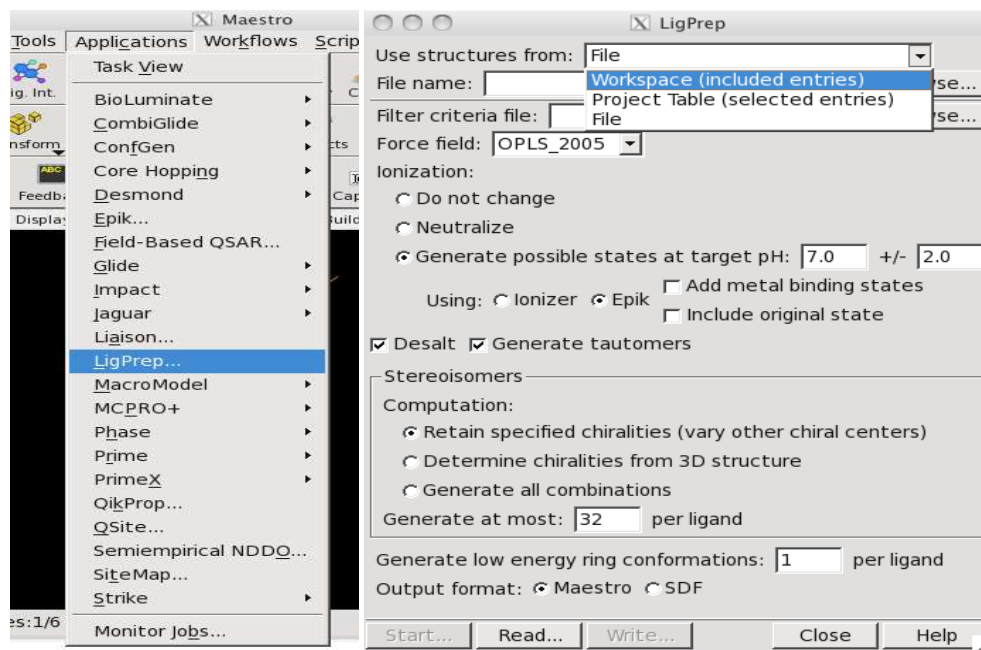
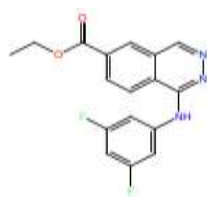
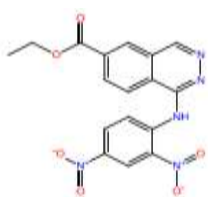


Figure: A) Selection of LigPrep. Step B) LigPrep step window display

Prepared ligand for docking



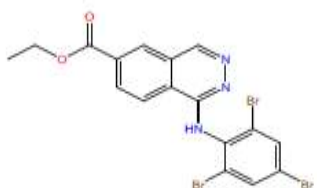
title: 1



title: 2



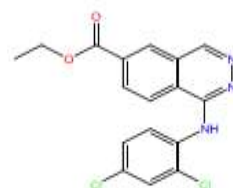
title: 3



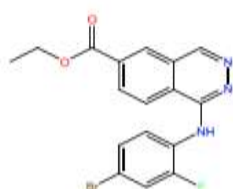
title: 4



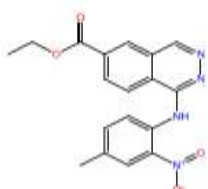
title: 5



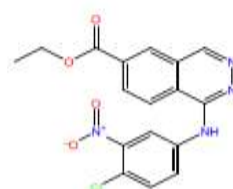
title: 6



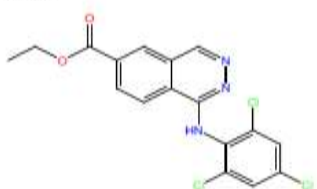
title: 7 active



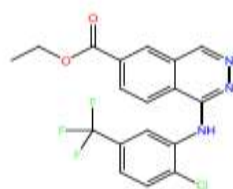
title: 8



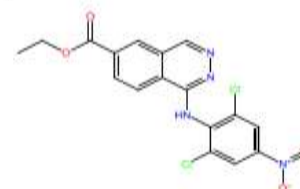
title: 9



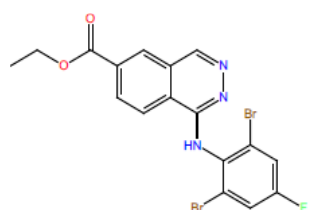
title: 10



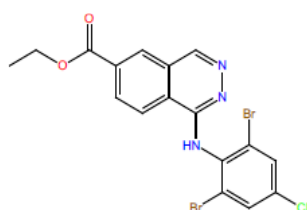
title: 11



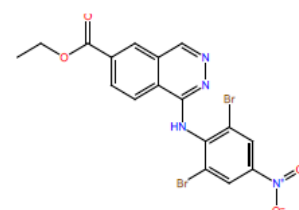
title: 12



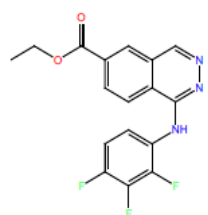
title: 13



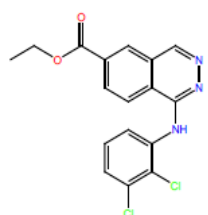
title: 14



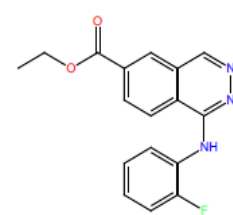
title: 15



title: 16 active



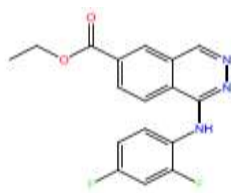
title: 17



title: 18 active



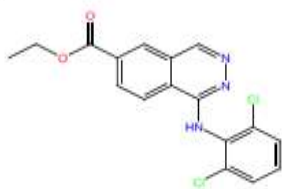
title: 19



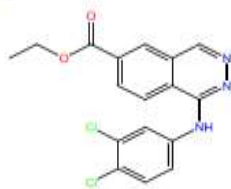
title: 20 active



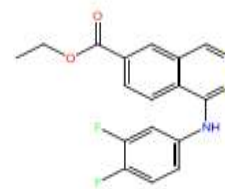
title: 21



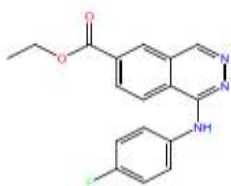
title: 22



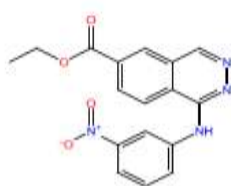
title: 23



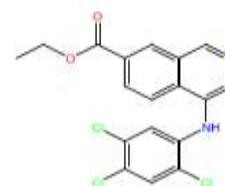
title: 24



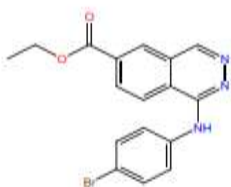
title: 25



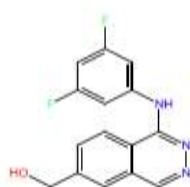
title: 26



title: 27



title: 28 active



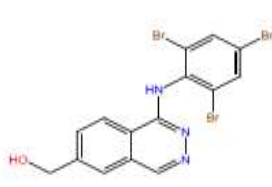
title: a1



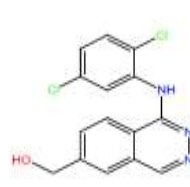
title: a2



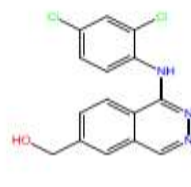
title: a3



title: a4



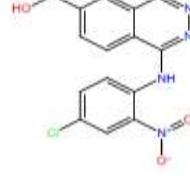
title: a5



title: a6



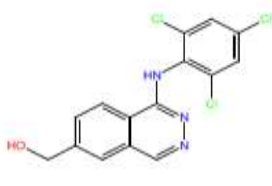
title: a7



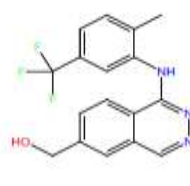
title: a8



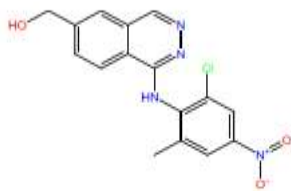
title: a9 active



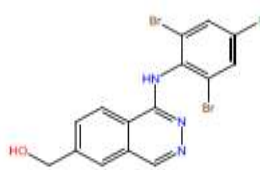
title: a10



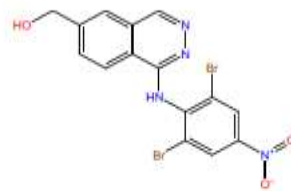
title: a11 active



title: a12 active



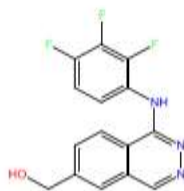
title: a13



title: a14



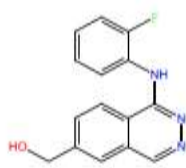
title: a15



title: a16 active



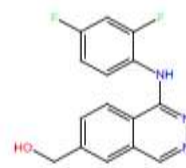
title: a17



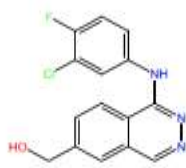
title: a18 active



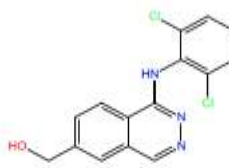
title: a19



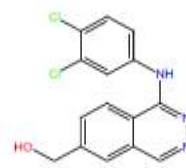
title: a20 active



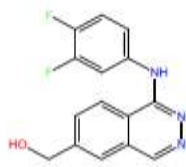
title: a21



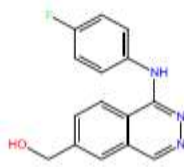
title: a22



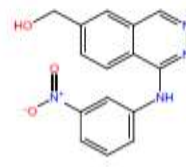
title: a23 active



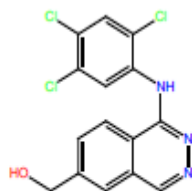
title: a24 active



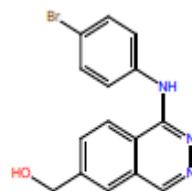
title: a25 active



title: a26



title: a27 active



title: a28 active

Receptor grid generation

To open the Receptor grid generation panel, choose Receptor Grid Generation from the Applications bar choose the Glide submenu in that receptor grid generation.



Figure: Selection of receptor grid through application.

After selecting receptor grid generation, select receptor tab and pick the ligand to identify i.e. molecule form ligand moiety, the Van der Waals radius scaling factor in the range of 1 and partial charge cut off at 0.25, use the input partial charges as shown in this window.

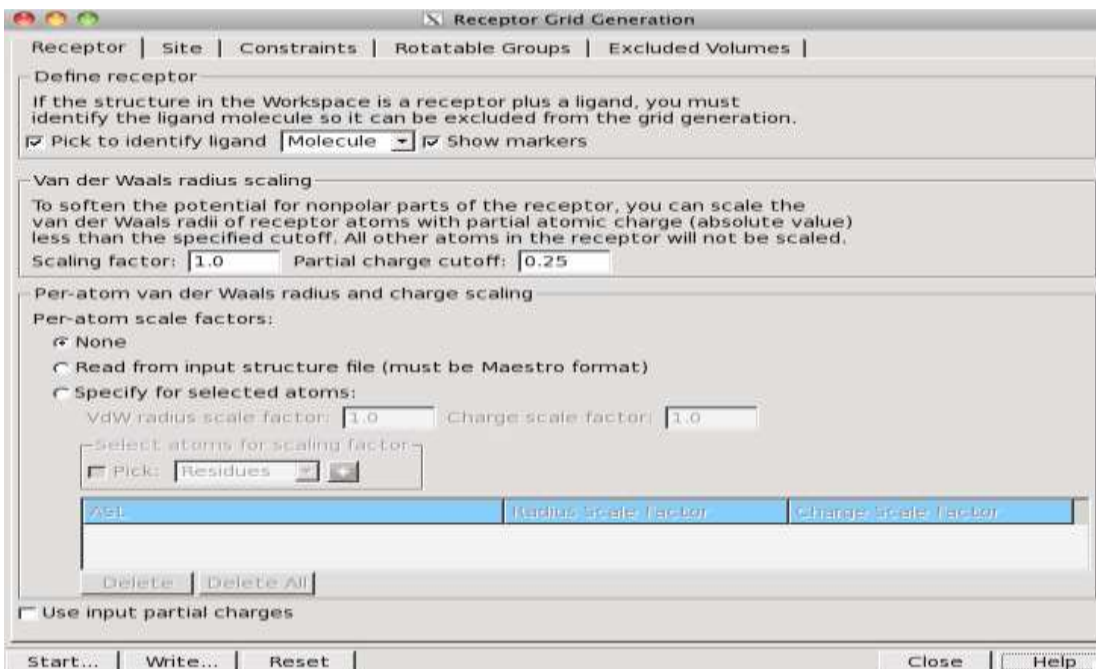


Figure: Receptor grid generation (Receptors ligand selection and other factor)

Then all factor like site, rotatable group, excluded volumes, constraints kept constant. Then run the receptor grid generation following window will come and run it as shown in this window.

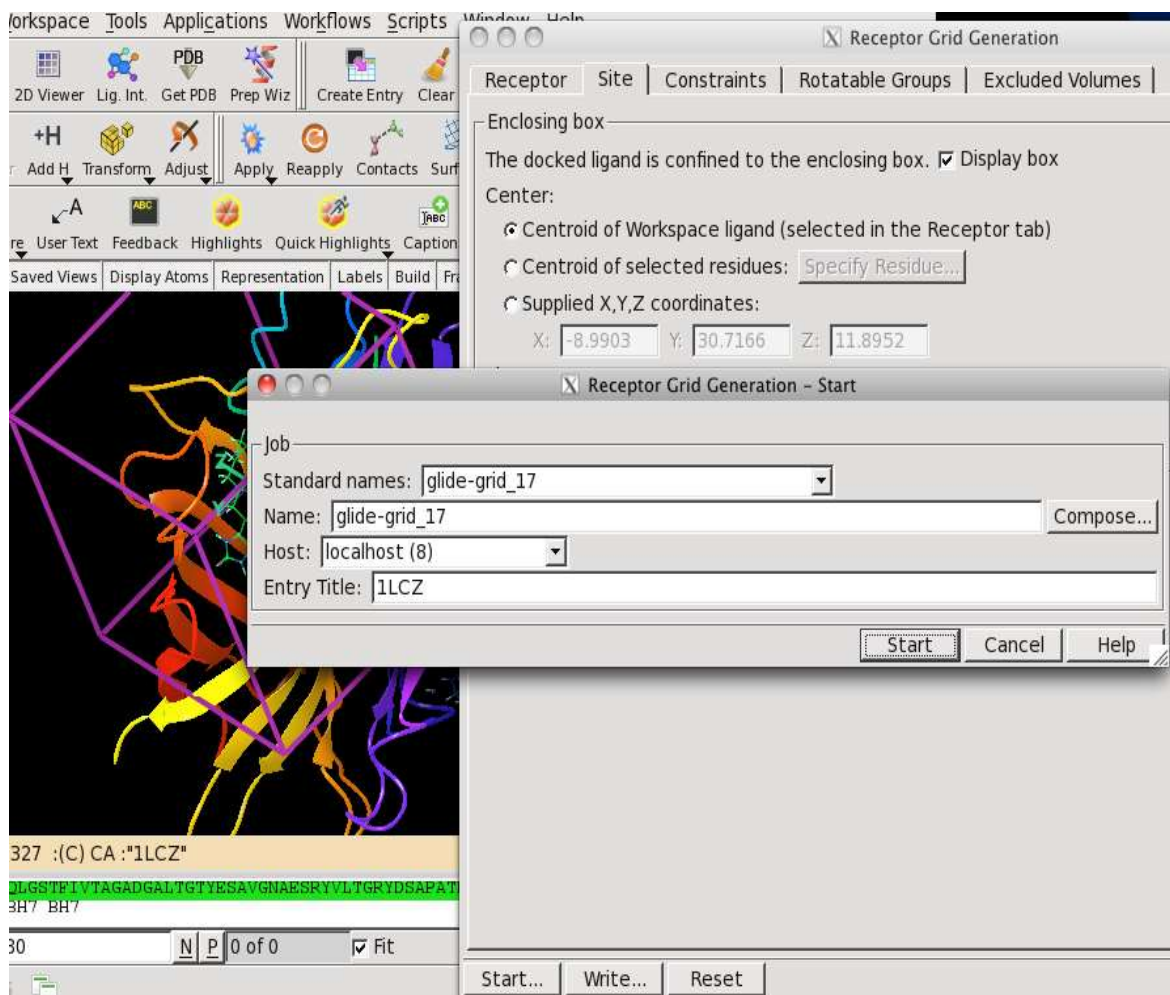


Figure: Receptor grid generation (selection of site and other factor) running job window display.

Glide docking (ligand docking)

Prepared ligand and receptor were used as the initial coordinates for docking purposes. We have used epidermal growth factor receptor tyrosine kinase as the target receptor. The stage for ligand docking was the receptor grid generation; for that purpose we have used the kinase protein structure complexes with Erlotinib. For ligand docking go to Applications>> Glide >> Ligand Docking.

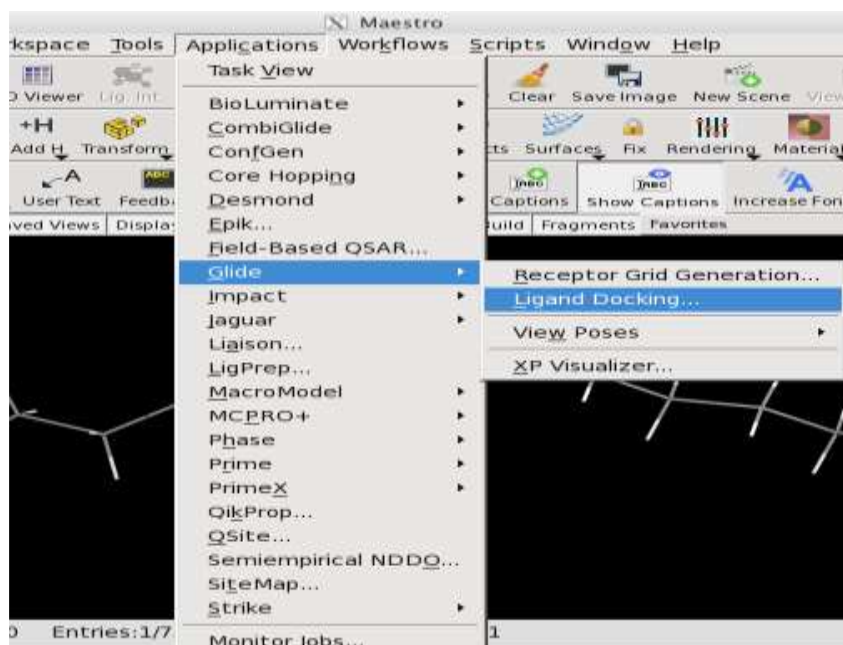


Figure: Selection of Ligand Docking step

Ligand docking window is shown below. In this tab select settings, select SP (standard precision), select Flexible for ligand sampling, select sample nitrogen inversions, select sample ring confirmation, select penalize non planar conformation for amides only.

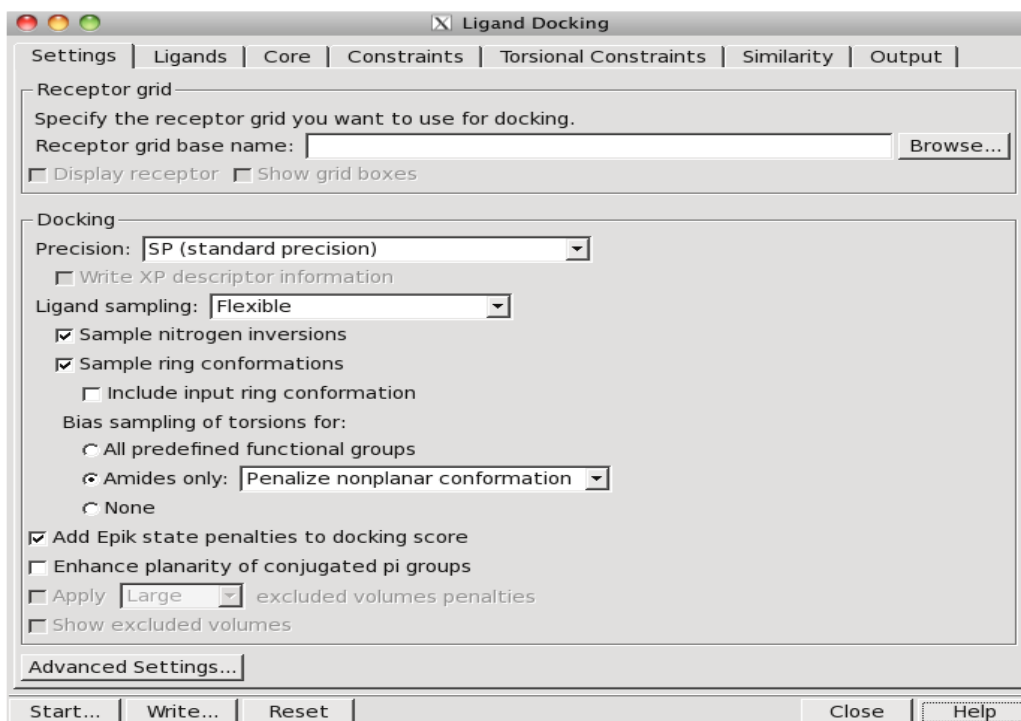


Figure: Ligand docking (selection of settings step)

From Ligands tab, indicate where you will get the ligand from workspace and select value as shown in figure. Click output tab.

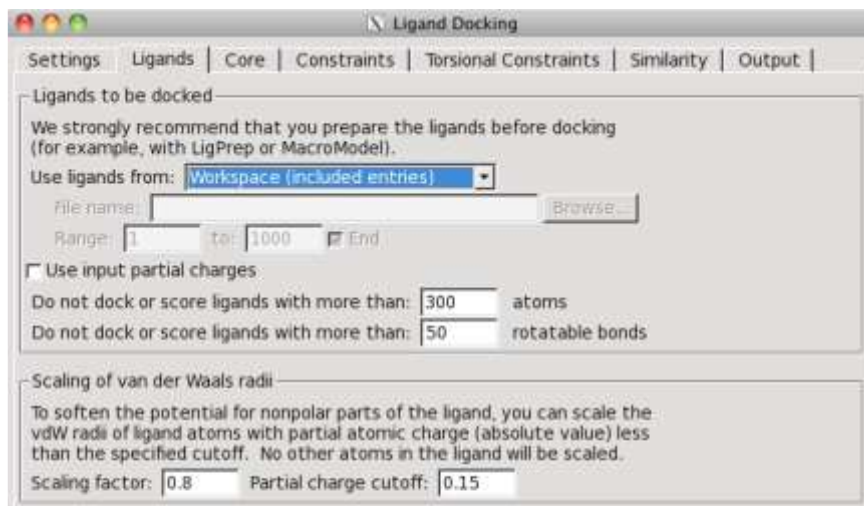


Figure: Ligand docking (Ligand selection step)

From Output tab, choose the options for a docking simulation. Then, click Start.

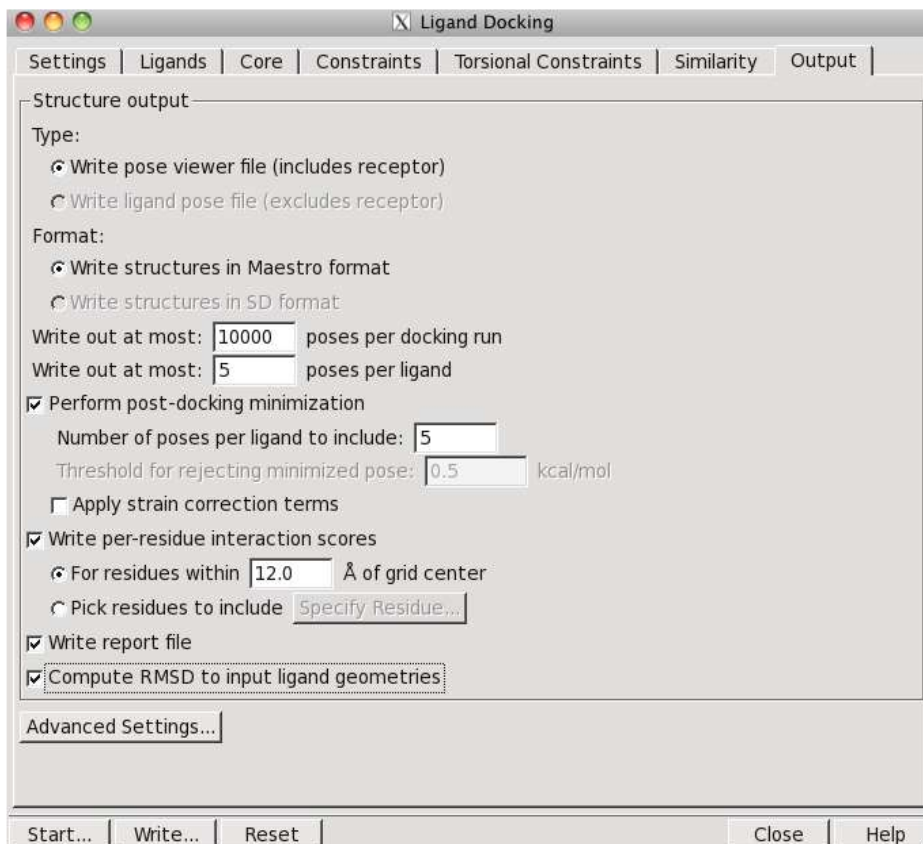


Figure: Ligand docking (output step)

After that, you will see the window below ask an output file name of the docking simulation. Add the file name and click Start to run the job.

Host Name	Processors	Use
localhost	8	8

Figure: Ligand docking (final preparation step)

After docking, we have performed post-docking minimization to improve the geometry of the poses. The post-docking minimization specifies a full force-field minimization of those poses which are considered for the final scoring. After docking, the results were used for binding energy calculations and docking scores.

Analysis Docking Poses

The View Poses facility in the Project Table panel enables to display the ligand poses with the receptor in the Workspace, along with hydrogen bonds, bad and ugly contacts, and per-residue interaction information. For Glide SP and XP docking runs, visualize the contributions to the XP docking score, provided that descriptor information was requested in the docking run. The Project Table panel offers a special facility for viewing poses from a pose viewer file. To use this facility you must select a single entry group. The group must contain the receptor as the first entry in the group, followed by the ligands. This is the normal situation when import a pose viewer file into the project. To start viewing poses, choose Setup from the View Poses submenu. The receptor is locked in the Workspace, and the first ligand entry is included.

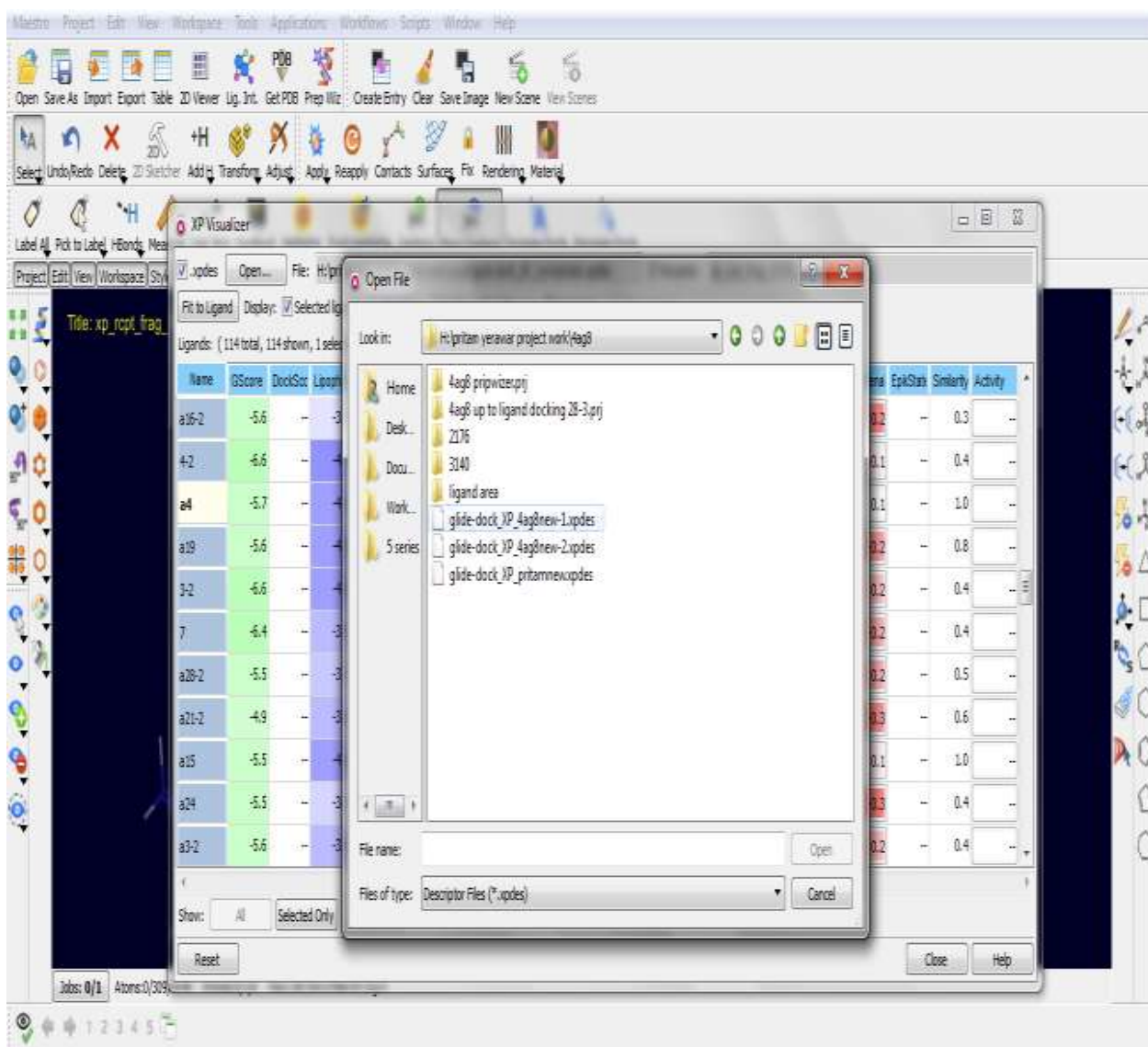


Fig: Analyzing of docking poses through generated (.xpdes) file

Molecular docking results of selected Aminophthalazine derivatives

In present work the GLIDE docking was applied for proposed 56 ligands to build a binding affinity model for the vascular epidermal growth factor receptor that was then used to compute the free energy of binding for this kinase. The docking score of respected ligands are shown in below Table.

Table: Glide docking score of selected Aminophthalazine derivatives

.xodes		Open...	File: D:\Eduve\pritam yerawar project work\Ags\glide-dock\XP_gltamnew.xodes										Receptor: xp_rcpt_frag_4408_13788														
Fit to Ligand		Display:	<input checked="" type="checkbox"/> Selected ligands		<input type="checkbox"/> XP Waters		<input type="checkbox"/> Hydrophobic/philic map		<input checked="" type="checkbox"/> Similarities		<input type="checkbox"/> Relative Scores																
Ligands: (114 total, 114 shown, 1 selected)		<input checked="" type="checkbox"/> Narrow columns		Set Column Order...		<input checked="" type="checkbox"/> Conditional coloring		Edit...																			
Name	QScore	DockScore	Lipophilicity	Proton	ProtonHB	ProtonPair	HBond	Electro	Stemap	mCat	CBR	LowMW	Penalties	HBondPen	ExposPen	RdPenal	EpikStatePe	Similarity	Activity								
22	-11.1	-	-6.3	-2.2	-1.0	0.0	-0.7	-0.3	-0.4	0.0	0.0	-0.3	0.0	0.0	0.0	0.2	-	1.0									
a22	-9.2	-	-6.3	-1.9	0.0	0.0	-0.7	-0.1	0.0	0.0	0.0	-0.4	0.0	0.0	0.0	0.2	-	0.4									
23	-9.1	-	-6.6	-1.2	-0.9	0.0	-0.6	-0.3	-0.4	0.0	0.0	-0.3	1.0	0.0	0.0	0.2	-	0.3									
26	-9.0	-	-6.3	-1.1	-1.0	0.0	-0.6	-0.3	-0.4	0.0	0.0	-0.4	1.0	0.0	0.0	0.3	-	0.3									
21	-8.6	-	-6.0	-1.2	-1.0	0.0	-0.7	-0.2	-0.4	0.0	0.0	-0.3	1.0	0.0	0.0	0.3	-	0.3									
a11	-8.2	-	-4.6	-1.2	0.0	0.0	-0.7	-0.6	-0.9	0.0	0.0	-0.4	0.0	0.0	0.0	0.2	-	0.1									
1	-7.9	-	-6.3	-1.3	0.0	0.0	-0.2	-0.2	-0.6	0.0	0.0	-0.4	1.0	0.0	0.0	0.3	-	0.2									
25	-7.8	-	-6.3	-1.3	0.0	0.0	-0.2	-0.2	-0.4	0.0	0.0	-0.5	1.0	0.0	0.0	0.3	-	0.2									
a7	-7.8	-	-6.4	-1.3	0.0	0.0	-0.8	-0.2	0.0	0.0	0.0	-0.4	1.0	0.0	0.0	0.2	-	0.2									
28	-7.7	-	-6.3	-1.3	0.0	0.0	-0.2	-0.3	-0.4	0.0	0.0	-0.3	1.0	0.0	0.0	0.2	-	0.2									
24	-7.7	-	-6.4	-1.3	0.0	0.0	-0.2	-0.3	-0.4	0.0	0.0	-0.4	1.0	0.0	0.0	0.3	-	0.2									
a13	-7.8	-	-5.0	-2.0	0.0	0.0	-0.7	-0.2	0.0	0.0	0.0	-0.1	0.0	0.0	0.0	0.1	-	0.2									
a1	-7.8	-	-5.6	-1.4	0.0	0.0	-0.9	-0.4	-0.3	0.0	0.0	-0.5	1.0	0.0	0.0	0.3	-	0.2									
a26	-7.7	-	-5.6	-1.4	0.0	0.0	-0.9	-0.6	0.0	0.0	0.0	-0.5	1.0	0.0	0.0	0.3	-	0.2									
20	-7.6	-	-6.3	-1.4	0.0	0.0	0.0	-0.3	-0.6	0.0	0.0	-0.4	1.0	0.0	0.0	0.3	-	0.2									
36	-7.6	-	-6.3	-1.3	0.0	0.0	-0.2	-0.3	-0.4	0.0	0.0	-0.3	1.0	0.0	0.0	0.3	-	0.2									
a23	-7.7	-	-6.0	-1.4	0.0	0.0	-0.8	-0.4	0.0	0.0	0.0	-0.4	1.0	0.0	0.0	0.2	-	0.2									
7	-7.5	-	-6.4	-1.3	0.0	0.0	-0.0	-0.3	-0.5	0.0	0.0	-0.2	1.0	0.0	0.0	0.2	-	0.2									
a28	-7.6	-	-5.9	-1.3	0.0	0.0	-0.9	-0.3	0.0	0.0	0.0	-0.4	1.0	0.0	0.0	0.2	-	0.2									
38	-7.5	-	-6.2	-1.4	0.0	0.0	0.0	-0.3	-0.5	0.0	0.0	-0.5	1.0	0.0	0.0	0.3	-	0.2									
a16	-7.6	-	-5.8	-1.3	0.0	0.0	-0.9	-0.4	-0.1	0.0	0.0	-0.5	1.0	0.0	0.0	0.2	-	0.2									
a21	-7.6	-	-6.2	-1.3	0.0	0.0	-0.5	-0.2	-0.1	0.0	0.0	-0.5	1.0	0.0	0.0	0.3	-	0.2									
6	-7.4	-	-6.4	-1.3	0.0	0.0	0.0	-0.3	-0.4	0.0	0.0	-0.3	1.0	0.0	0.0	0.2	-	0.2									
17	-7.4	-	-6.4	-1.3	0.0	0.0	0.0	-0.3	-0.4	0.0	0.0	-0.3	1.0	0.0	0.0	0.2	-	0.2									
a19	-7.5	-	-5.8	-1.3	0.0	0.0	-0.8	-0.4	0.0	0.0	0.0	-0.4	1.0	0.0	0.0	0.2	-	0.2									
9	-7.4	-	-6.3	-1.4	0.0	0.0	0.0	-0.3	-0.4	0.0	0.0	-0.3	1.0	0.0	0.0	0.2	-	0.2									
29	-7.4	-	-6.3	-1.3	0.0	0.0	0.0	-0.2	-0.4	0.0	0.0	-0.3	1.0	0.0	0.0	0.2	-	0.2									
a18	-7.5	-	-5.7	-1.3	0.0	0.0	-0.8	-0.4	-0.1	0.0	0.0	-0.5	1.0	0.0	0.0	0.3	-	0.2									

The ligand structure 1, 22, a11 and a22 shows high docking score on EGFR protein structure.

Detail interactions of ligands with EGFR protein structure (PDB ID 1M17) are shown in below Figure.

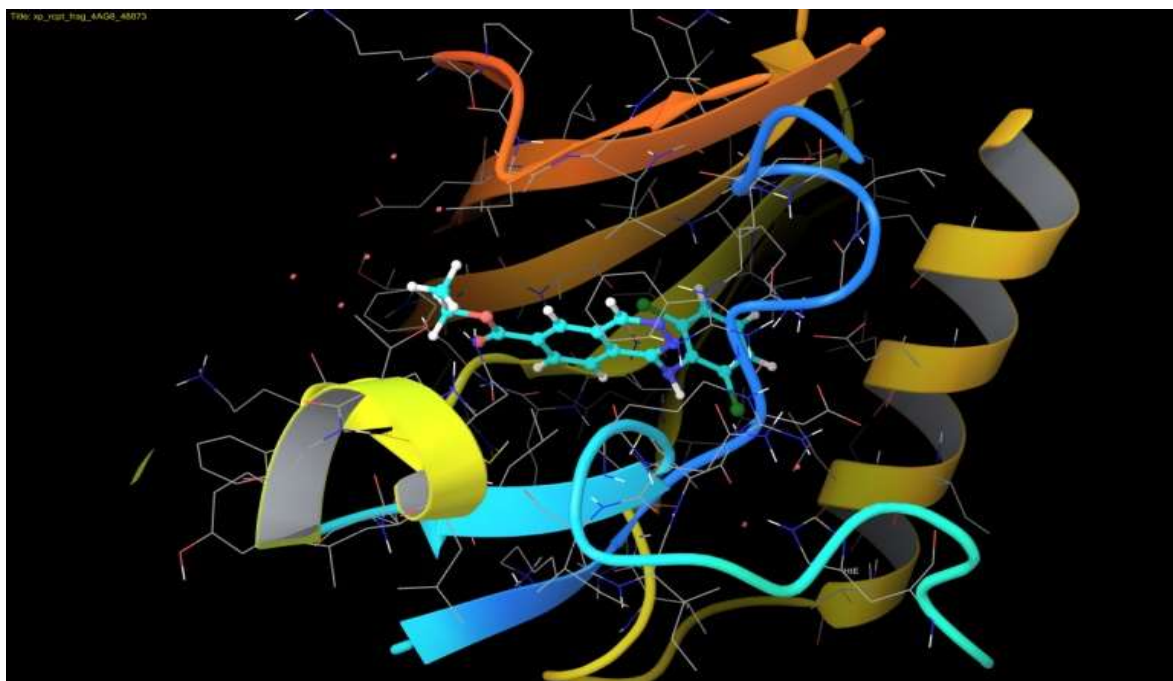
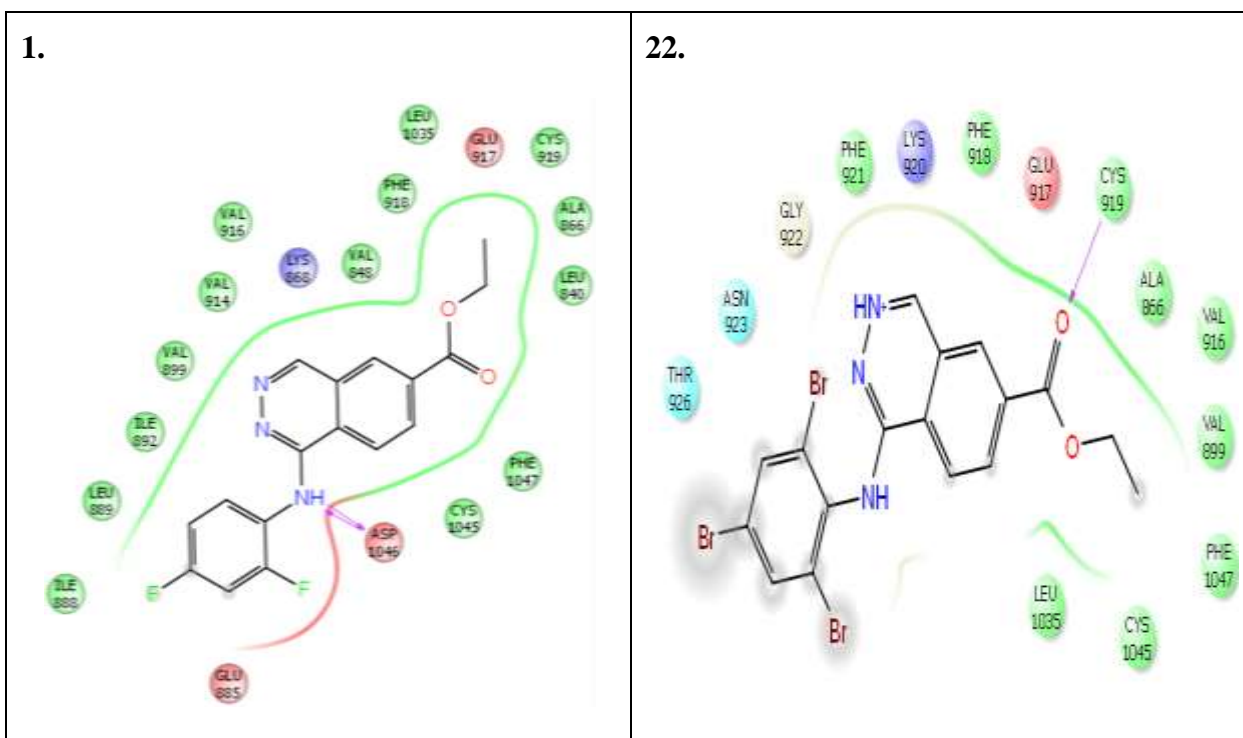


Figure 5.4.1.: Ligand interaction diagram with Vascular Epidermal Growth Factor receptor.



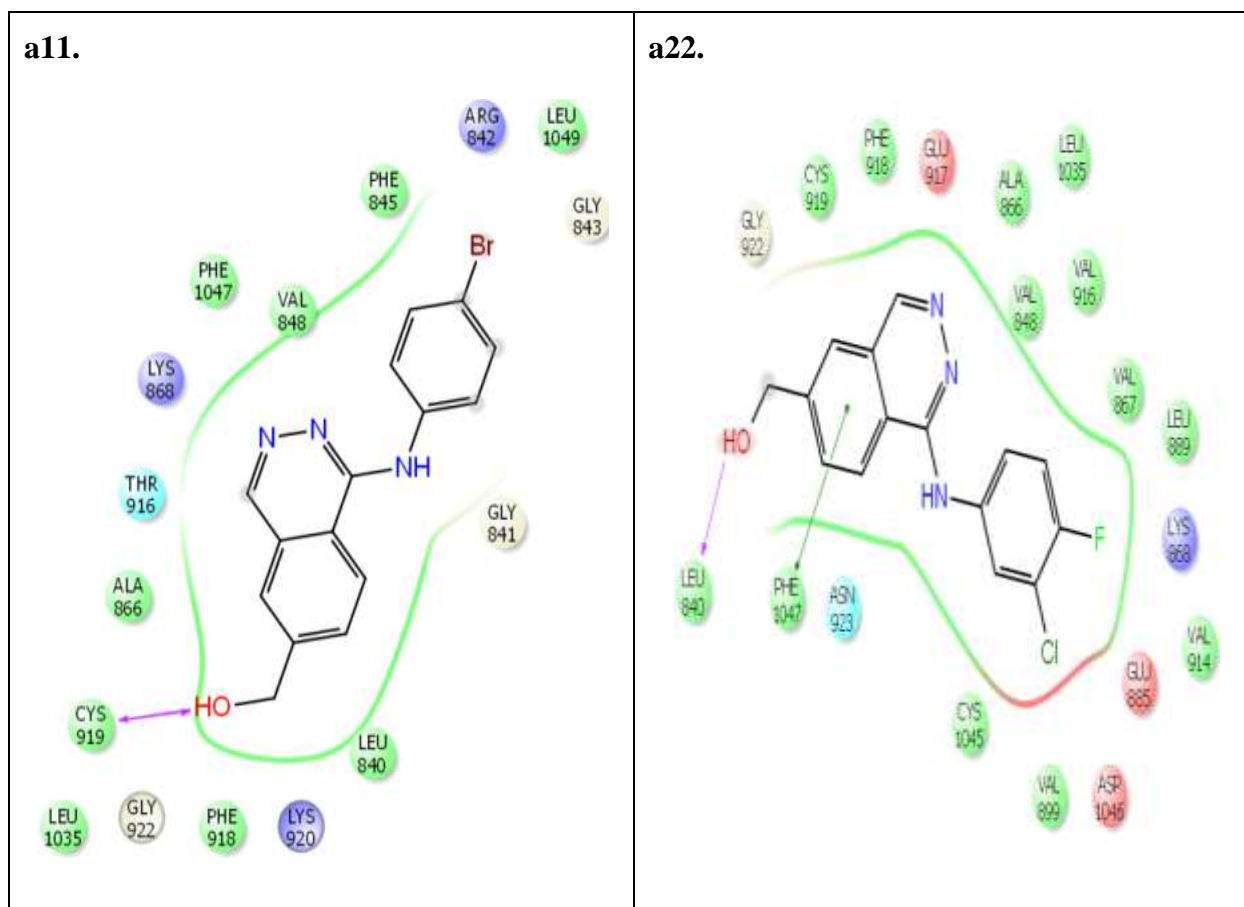


Figure: Ligand interaction diagram with Vascular Epidermal Growth Factor receptor

Results

The glide docking score can be used as a semi-quantitative descriptor for the ability of ligands to bind to a specific conformation of the protein receptor. Generally speaking for low glide score good ligand affinity to the receptor may be expected. According to the glide score, the results of the inhibition for the VEGFR human tyrosine kinase receptor may be arranged in the following manner: 22>a22>a11> 1. Docking studies performed by GLIDE has confirmed that above inhibitors fit into the binding pocket of the VEGFR kinase receptor.

4.2 DESIGNING OF QUINAZOLINE DERIVATIVES

4.2.1 Designing Of N-[4-Amino-2-(4-Methylphenyl)quinazoline-6-yl]acetamide derivatives

Protein preparation

A characteristic PDB structure file consists only of heavy atoms, waters, cofactors, and metal ions, and can be multimeric. Terminal amide groups should be misaligned, because the X-ray structure analysis cannot usually distinguish between O and NH₂. Ionization and tautomeric states are also generally unassigned. Glide calculations use an all-atom force field for accurate energy evaluation. Thus, Glide requires bond orders and ionization states to be properly assigned and performs better when side chains are reoriented when necessary and steric clashes are relieved.

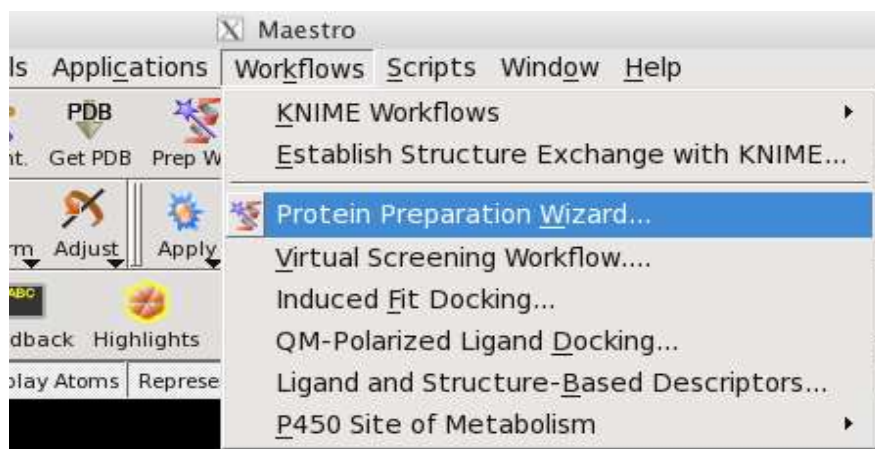


Fig: Protein preparation wizard

Steps involved in protein preparation wizard

1. Import a ligand/protein co-crystallized structure from PDB
2. Simplify multimeric complexes.

Determine whether the protein-ligand complex is a dimer or other multimer containing duplicate binding sites and duplicate chains that are redundant. If the structure is a multimer with duplicate binding sites, remove redundant binding sites and the associated chains by picking and deleting molecules or chains. Locate any waters you want to keep and then delete all others. These waters are identified by the oxygen atom, and usually do not

have hydrogens attached. Generally, all waters are deleted and retained only coordinated to metals. If waters are kept, hydrogens will be added to them by the preparation component of the protein preparation job. And, check that these water molecules are correctly oriented.

4. Adjust the protein, metal ions, and cofactors.
5. Adjust the ligand bond orders and formal charges.
6. Run a restrained minimization of the protein structure.
7. Review the prepared structures.

Checking the Protein Structures

1. Check the Orientation of Water Molecules
2. Check for Steric Clashes
3. Resolving H-Bonding Conflicts
4. Docking the Native Ligand

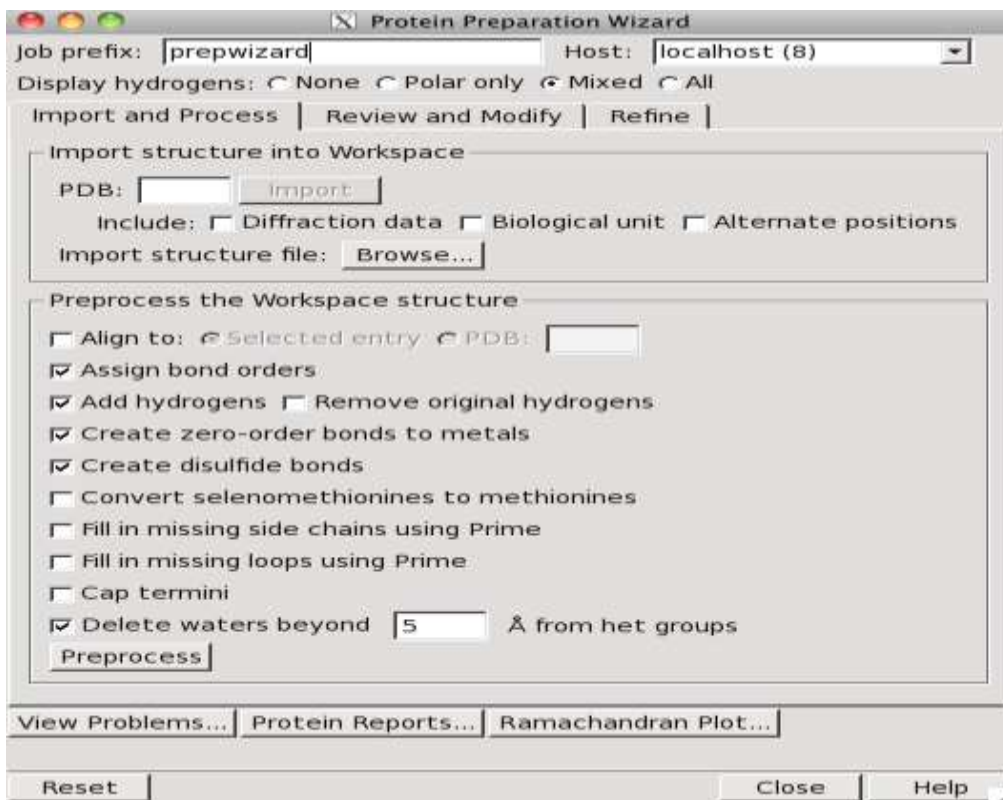


Fig: Protein preparation (import and process)

Protein Preparation Wizard

Job prefix: Host:

Display hydrogens: ☐ None ☐ Polar only ☒ Mixed ☐ All

Import and Process | Review and Modify | Refine |

Analyze Workspace

☒ Fit on select ☐ Display selection only ☐ Pick

Select Hets/Waters within Å of selected chains

Select Lone Waters

Chain Name	Water No.	Chain	esidue No
A	1	A	513
B	2	A	529
	3	A	575
	4	B	552

Het No.	Het Name
1	A:BH7 (401)
2	B:BH7 (400)

Generate States ☐ Metal binding states pH: +/-

Selected 1 chain, 3 waters, and 1 het.

Fig: Protein preparation wizard (Review and modify)

Protein Preparation Wizard

Job prefix: Host:

Display hydrogens: ☐ None ☐ Polar only ☒ Mixed ☐ All

Import and Process | Review and Modify | Refine |

H-bond assignment

☒ Sample water orientations

☐ Use crystal symmetry

☐ Minimize hydrogens of altered species

☒ Use PROPKA; pH: ☐ Label pKas

Use simplified rules ☐ Very low ☐ Low ☒ Neutral ☐ High

Intermolecular states: Automatically optimize hydroxyl, Asn, Gln, and His states using PROPKA

Remove waters

with less than H-bonds to non-waters

Restrained minimization

Converge heavy atoms to RMSD: Å

☐ Hydrogens only

Force field:

Fig: Protein preparation wizard (Refine)

Ligand Preparation

Convert structure format > Select structures > Add hydrogen atoms > Remove unwanted molecules > Neutralize charged groups > Generate ionization states > Generate tautomers > Filter structures > Generate alternative chiralities > Generate low-energy ring conformations > Remove problematic structures > Optimize the geometries > Convert output file.

To start the LigPrep choose the Applications menu. With the help of LigPrep single low energy 3D structure can produce with correct chiralities for each input structure. Also produce structures with various ionization states, tautomers, stereo chemistries, ring conformations and remove the molecules using various criteria. Remove the unwanted hydrogens, add hydrogens and minimize the ligand structure with the help of default options in the LigPrep panel.

To generate several different output structures for each input structure the default pH range must be 5.0 to 9.0. To generate the ionization states use either the ionizer or Epik. Epik generate states which are more suitable for metal binding. Select desalt and generate the tautomers by default. If more than 8 tautomers are possible then select the most likely tautomers. The stereoizer generates two stereoisomers per chiral centre in the ligand up to maximum limit. Determine chiralities from 3D structure ignore input file chiralities and takes chirality information from the 3D geometry. Generate all combinations varies the stereochemistry up to a maximum number of structures specified by generate at most max per ligand. The default maximum is 32.

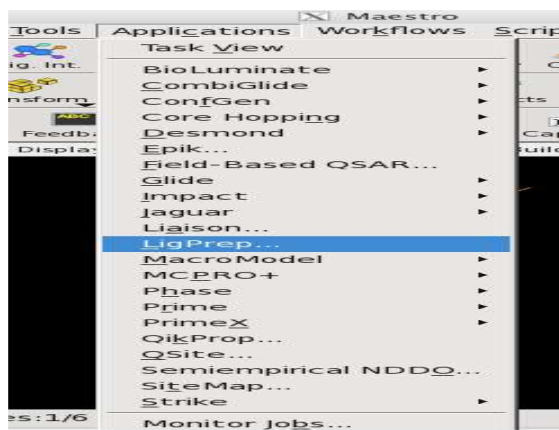


Fig: Selection of LigPrep from Application

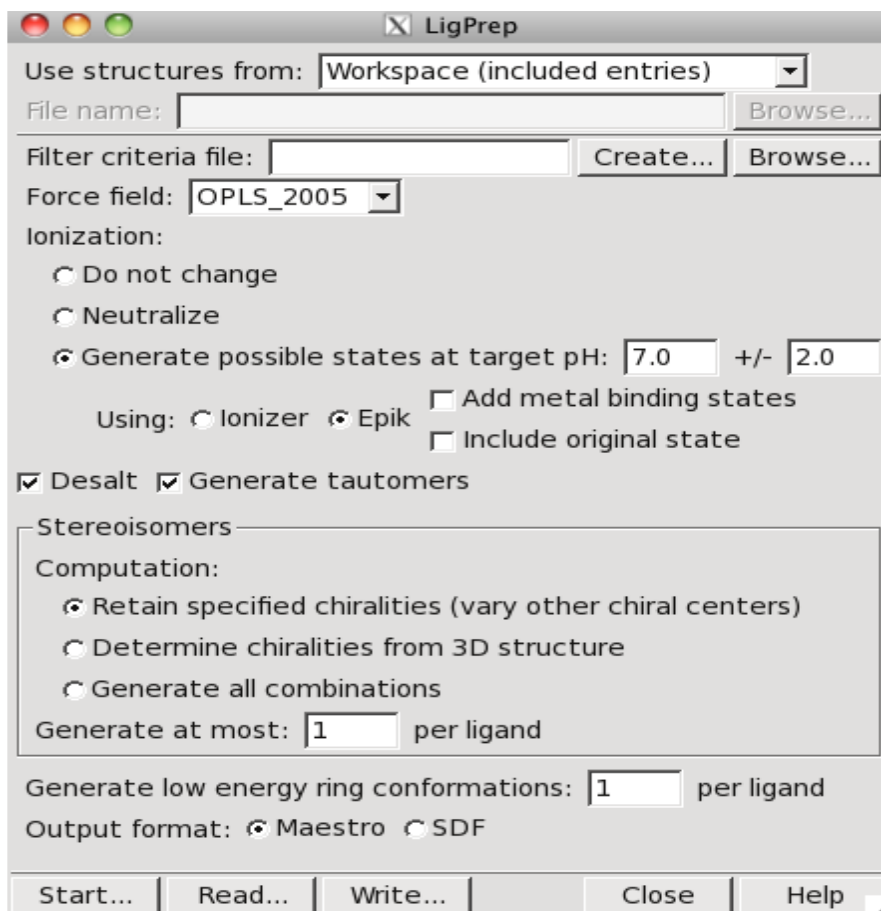


Fig: Ligand preparation window display

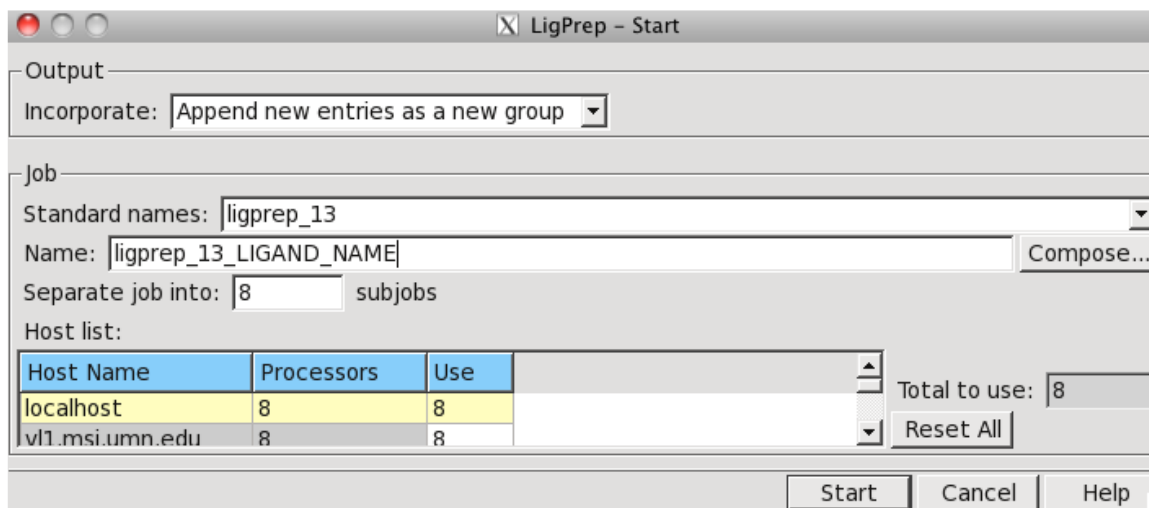
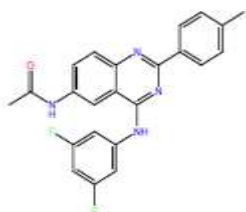
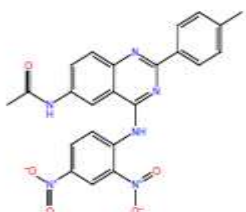


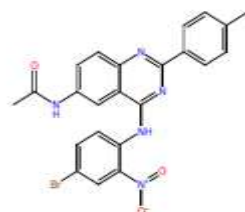
Fig: Ligand preparation-start



title: mol1



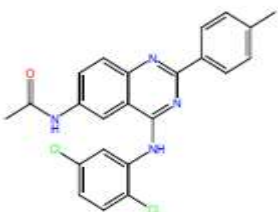
title: mol2



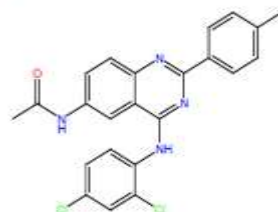
title: mol3



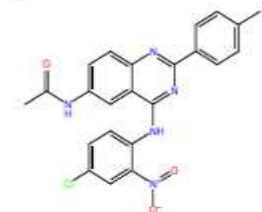
title: mol4



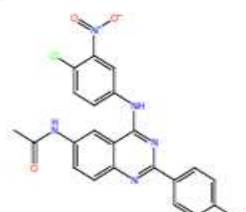
title: mol5



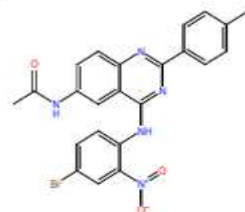
title: mol6



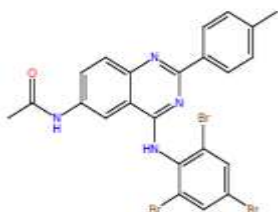
title: mol7



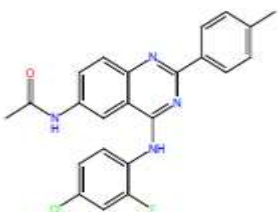
title: mol8



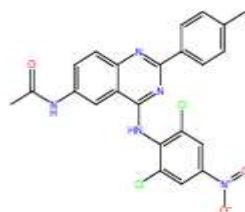
title: mol9



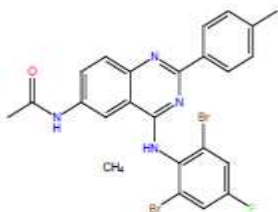
title: mol10



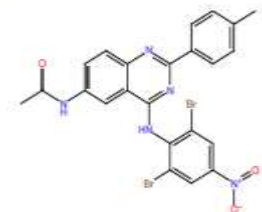
title: mol11



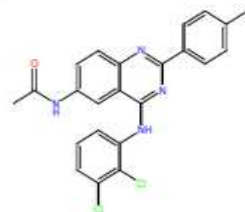
title: mol12



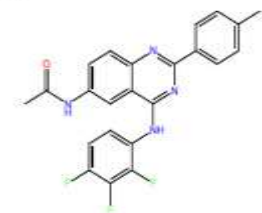
title: mol13



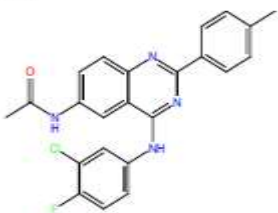
title: mol14



title: mol15



title: mol16



title: mol17



title: mol18

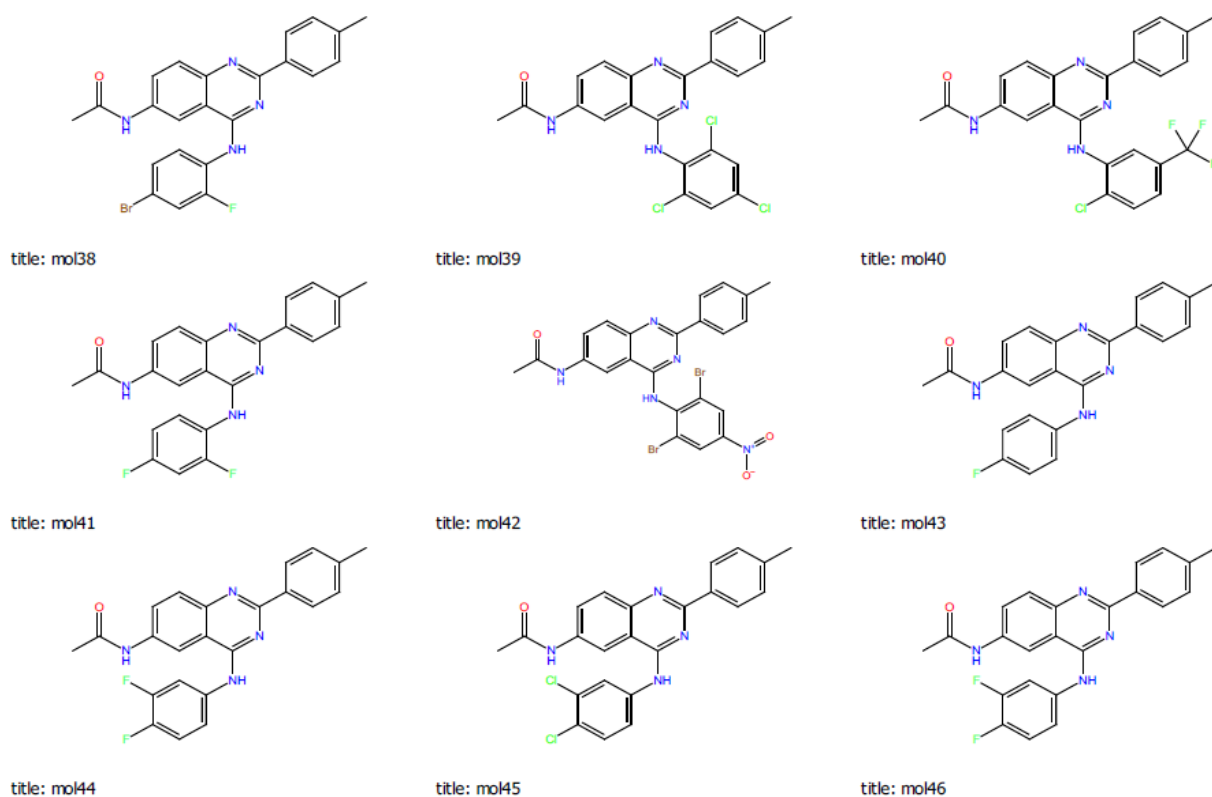


Fig: Chemical structures of different quinazoline derivatives in their minimized positions.
Non-carbon hydrogens are colored in blue.

Receptor Grid Generation

These are some steps to be followed for generation of receptor grid

1. Choose Tasks > Docking > Grid Generation or Applications > Glide > Receptor Grid Generation.
2. Display the prepared receptor in the Workspace.
3. Pick the ligand to define the grid centre.
4. Adjust the size of the active site in the Site tab to accommodate larger ligands, if necessary.
5. Add any hydrogen-bond, metal, positional, or hydrophobic constraints in the Constraints tab.

6. Pick any rotatable hydroxyl groups in the active site if such groups could rotate during docking.
7. Start the grid generation job

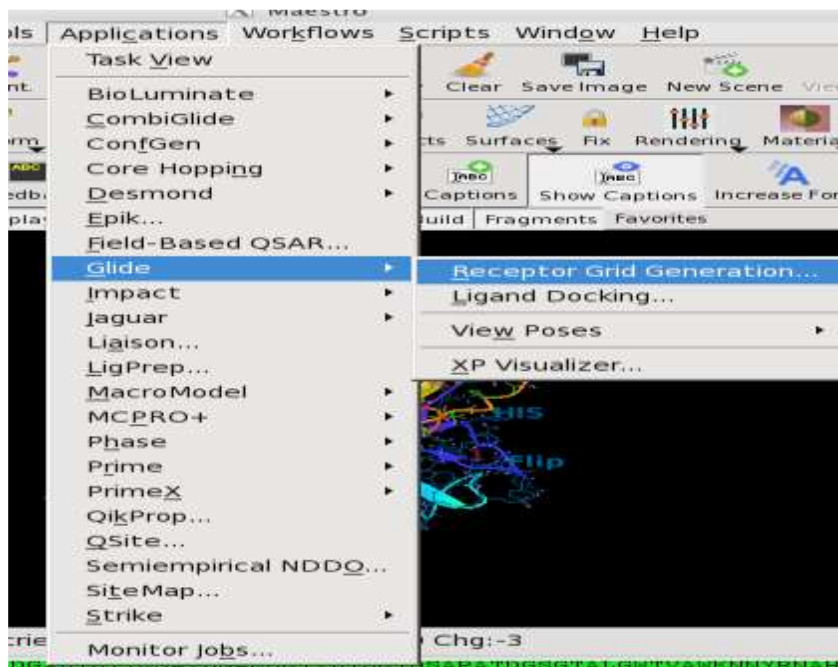


Fig: Selection of Glide -Receptor grid generation from Application panel

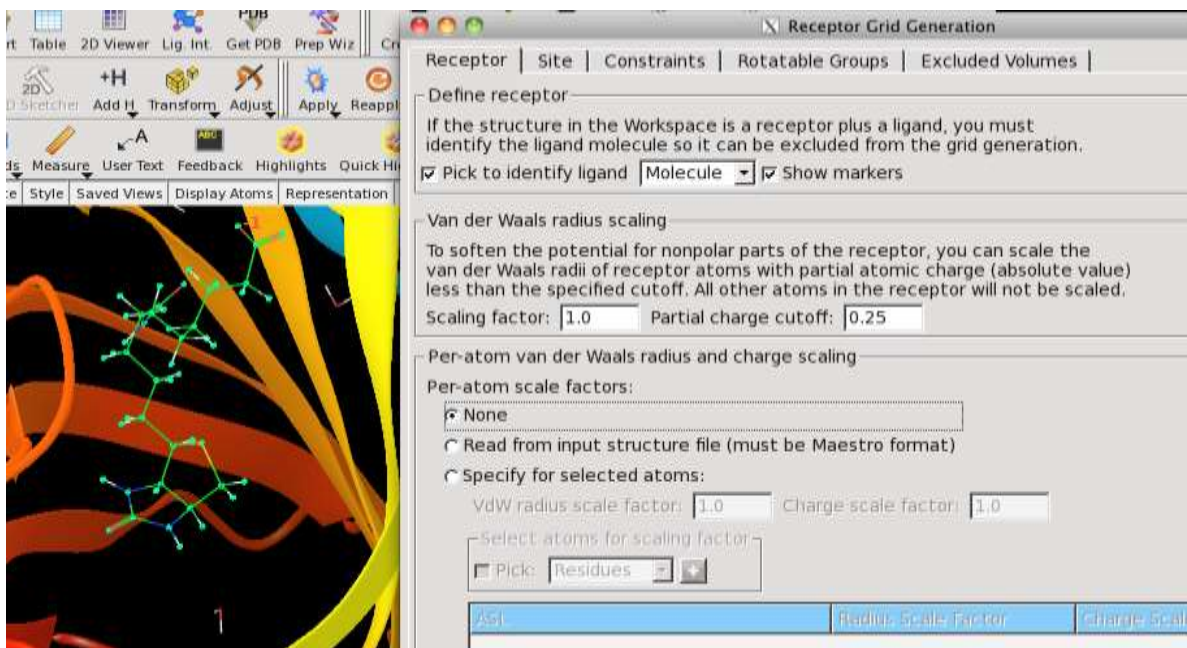


Fig: Receptor grid generation

Ligand Docking

Glide ligand docking job requires a set of previously calculated receptor grids and one or more ligand structures. Open the Ligand Docking panel; choose Ligand Docking from the Glide submenu of the Applications menu.

The Ligand Docking panel has six tabs such as settings, ligands, core, constraints, similarity and output.

Specifying the Receptor Grid

Click Browse in the Receptor grid section of the Settings tab to open a file selector and choose a grid file or a compressed grid archive (.zip). The file name, without the extension, is displayed in the Receptor grid base name text box.

Selecting the Docking Precision

There are three choices of docking precision, given under Precision in the Docking section.

HTVS (high-throughput virtual screening)-High-throughput virtual screening (HTVS) docking is intended for the rapid screening of very large numbers of ligands.

SP (standard precision)-Standard-precision (SP) docking is appropriate for screening ligands of unknown quality in large numbers. Standard precision is the default.

XP(extra precision)- Extra-precision (XP) docking and scoring is a more powerful and discriminating procedure, which takes longer to run than SP. XP is designed to be used on ligand poses that have a high score using SP docking. If want to dock a set of ligands using a progression of precision, then use the Virtual Screening Workflow to set up and run the docking jobs.

Selection of Initial Poses

The selection of initial poses section of the box control the way poses pass through the filters for the initial geometric and complementarity “fit” between the ligand and receptor molecules. The grids for this stage contain values of a scoring functions, it would be to place ligand atoms of given general types in given elementary cubes of the grid. These cubes have a constant spacing of 1 Å.

The “rough score” for a given pose of the ligand relative to the receptor is simply the sum of the appropriate grid scores for each of its atoms. Poses that pass these initial screens enter the final stage of the algorithm, which involves evaluation and minimization of a grid approximation to the OPLS-AA non-bonded ligand-receptor interaction energy. Keep initial poses per ligand for the initial phase of docking. This text box sets the maximum number of poses per ligand to pass to the grid refinement calculation. The value must be a positive integer. The default setting depends on the type of scoring window for keeping initial poses.

Visualizing Docking Results

The View Poses facility in the Project Table panel enables to display the ligand poses with the receptor in the Workspace, along with hydrogen bonds, bad and ugly contacts, and per residue interaction information. For Glide SP and XP docking runs, visualize the contributions to the XP docking score, provided that descriptor information was requested in the docking run. The Project Table panel offers a special facility for viewing poses from a pose viewer file. To use this facility select a single entry group. The group must contain the receptor as the first entry in the group, followed by the ligands. This is the normal situation when import a pose viewer file into the project. To start viewing poses, choose Setup from the View Poses submenu. The receptor is locked in the Workspace, and the first ligand entry is included.

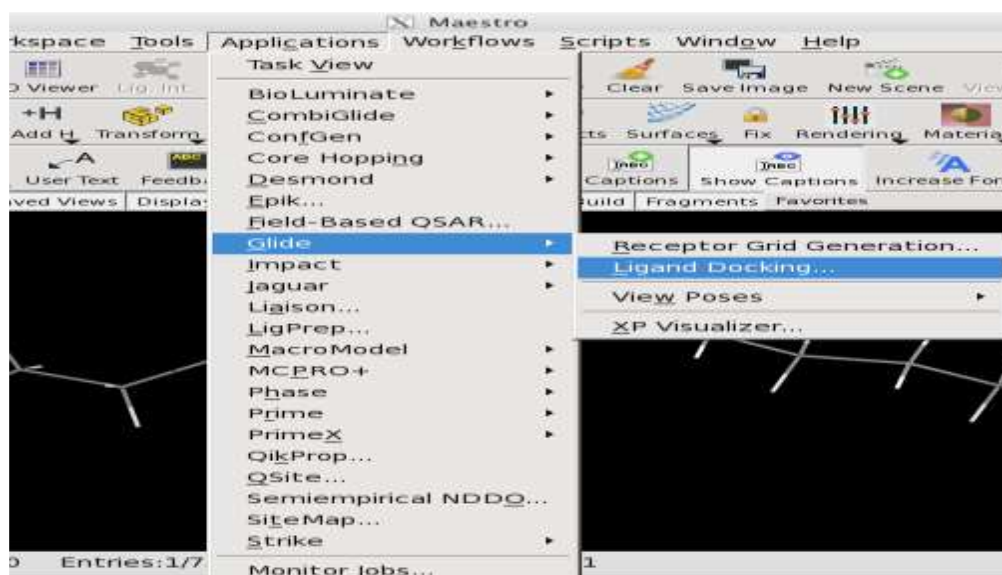


Fig: Selection of ligand docking from Application panel

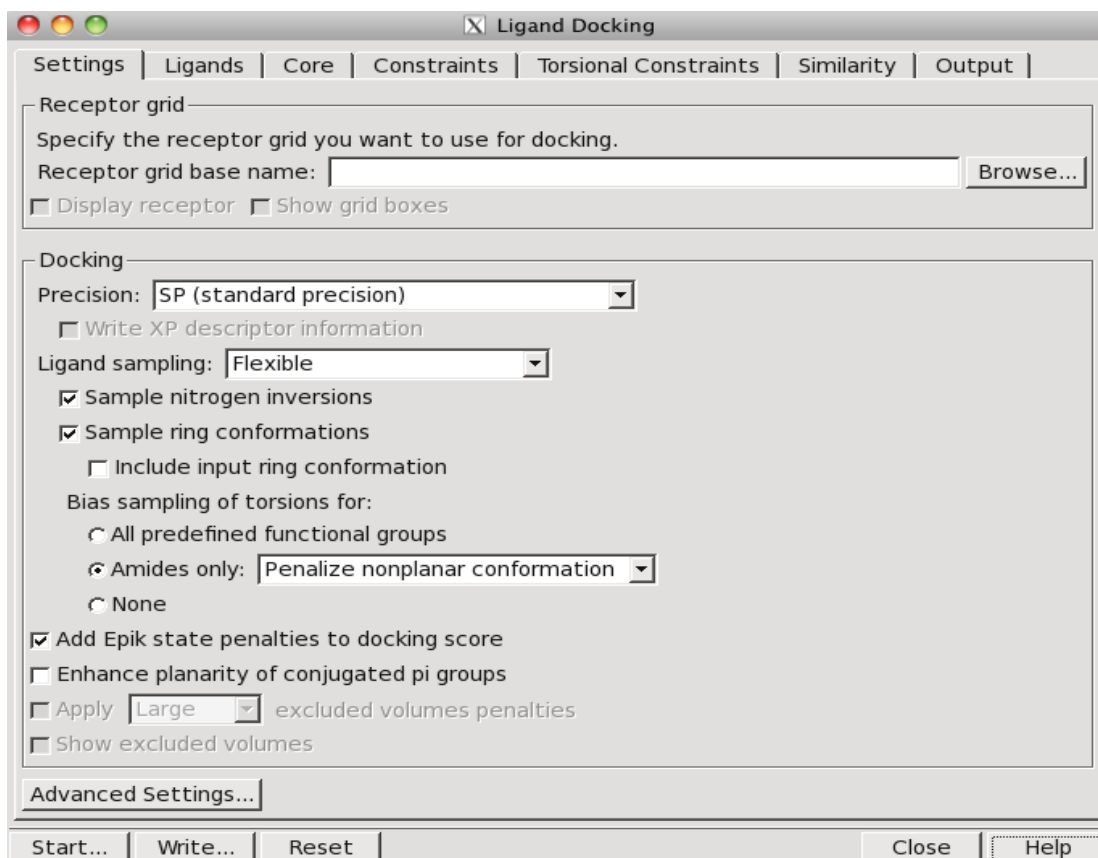


Fig: Ligand docking -settings

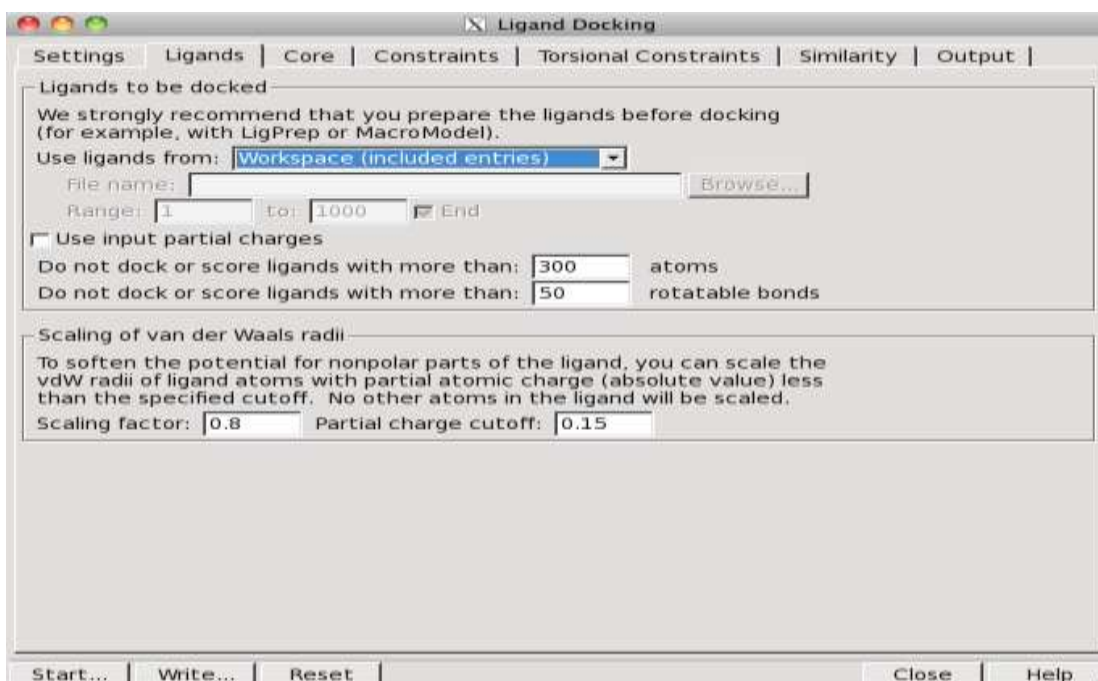


Fig: Ligand docking-Ligands

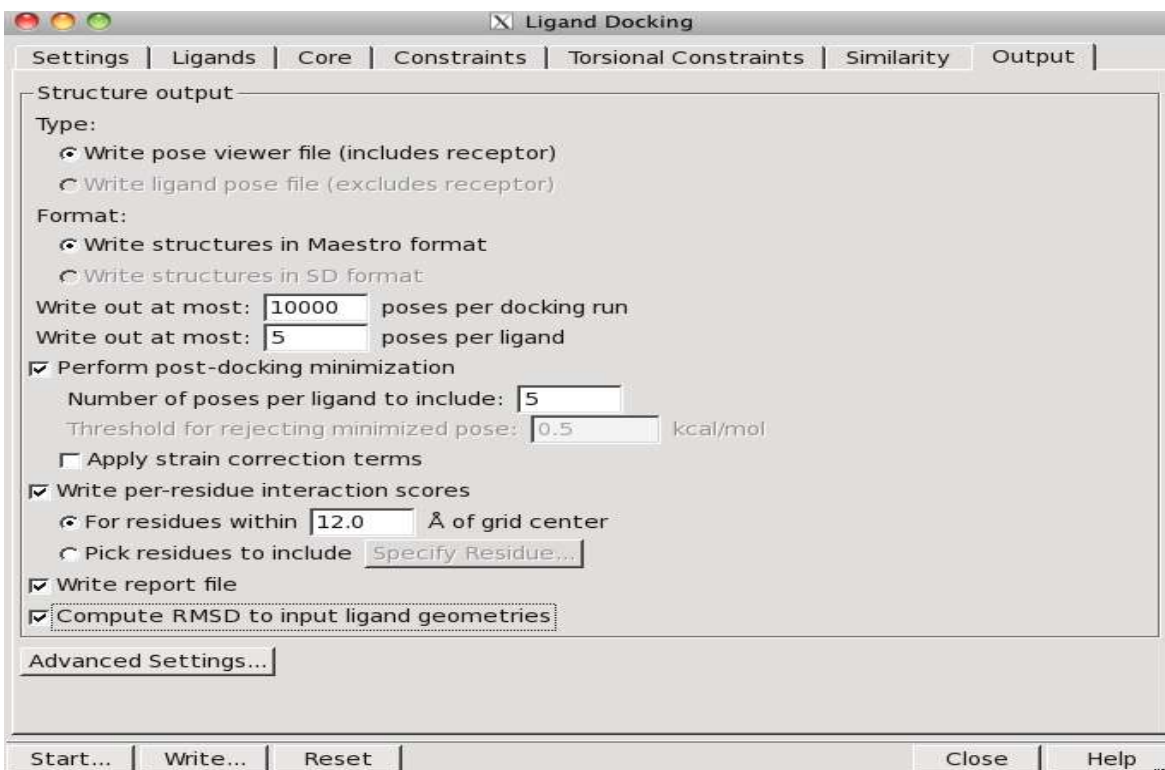


Fig: Ligand docking –output

Project Table --- Scratch Project

Table | Select | Entry | Property | Group | ePlayer

Import | Export | 2D Viewer | Plot | Sort | Find/Replace | Feedback | Color | Calculator

Columns | Tree | Show | 2D Structure | Show Family | Hide Family

Row	Stars	In	Title	Entry ID	PDB Title	PDB ID	PDB
73	☆☆☆☆		1LCZ_LIGAND	73	STREP...	1LCZ	
[6]			[3] - glide-dock_SP_96_NAME...				
74	☆☆☆☆		1LCZ	74			
75	☆☆☆☆		1LCZ_LIGAND	75	STREP...	1LCZ	
76	☆☆☆☆		1LCZ_LIGAND	76	STREP...	1LCZ	
77	☆☆☆☆		1LCZ_LIGAND	77	STREP...	1LCZ	
78	☆☆☆☆		1LCZ_LIGAND	78	STREP...	1LCZ	
79	☆☆☆☆		1LCZ_LIGAND	79	STREP...	1LCZ	

Find: Options Next Previous Replace with: Replace Replace All

Entries: 79 total, 79 shown, 6 selected, 2 included Groups: 3 total, 1 selected

Fig: Project Table

Results and discussion:

Virtual docking

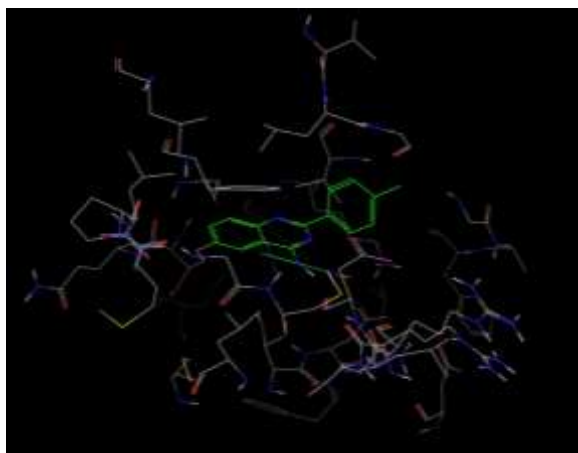
Glide docking method have applied to inhibitors of tyrosine protein kinases to build a binding affinity model for EGFR that was then used to compute the free energy of binding energy of binding for this kinase.

The ligand preparation procedure generated different training sets of the inhibitors whose scoring function is given in below Table. These different structures were found by using different orientations of the inhibitors and different positions of the hydrogens. The results of docking and scoring are given in below Table. According to the table we see that among all the energy parameters the largest contribution for binding energy comes from Vander Waals interactions.

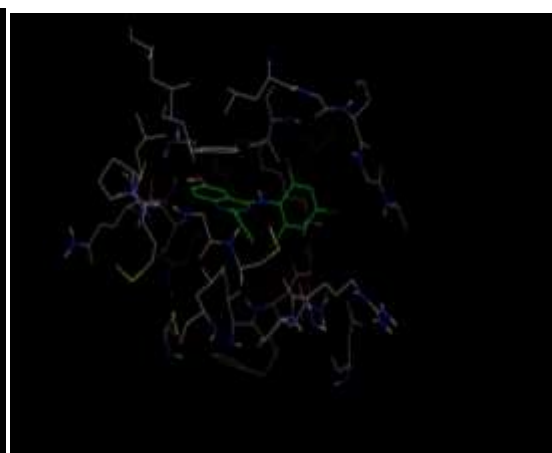
Table: Energy data of the structures generated by the docking program.

Compounds	E_{vdw}	E_{coul}	E_{site}	Docking score	Energy
Mol 1	-5.5	-0.4	-0.7	-7.6	-5.9
Mol 5 (comp 1)	-6.1	-0.2	-0.6	-6.3	-6.3
Mol 12 (comp 4)	-3.6	-0.4	-0.0	-6.5	-4.0
Mol 21	-5.5	-0.2	-0.2	-7.8	-5.7
Mol 24	-6.3	-0.3	-0.3	-7.7	-6.6
Mol 30	-6.1	-0.2	-0.3	-7.7	-6.3
Mol 39(comp 2)	-4.0	-0.4	-0.1	-6.5	-4.4
Mol 50(comp 3)	-6.4	-0.2	-0.3	-7.8	-6.6

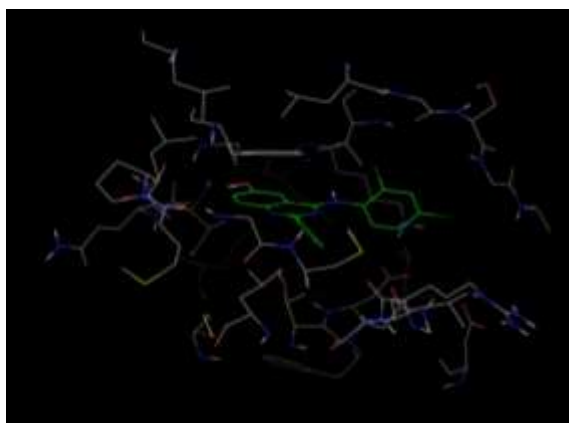
The energy data are written according to the structure generated by the docking program. The best docked poses are written in table. All energies are given in Kcal/mol.



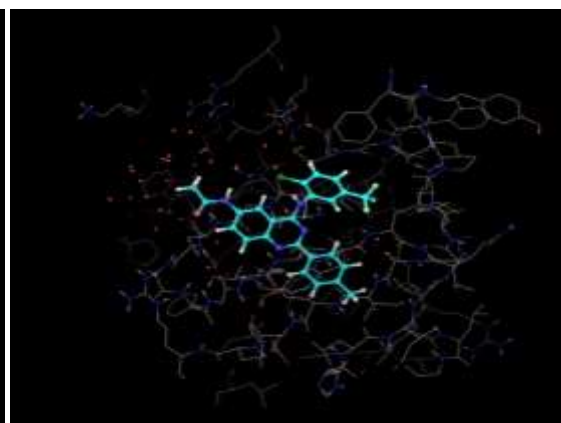
(a)



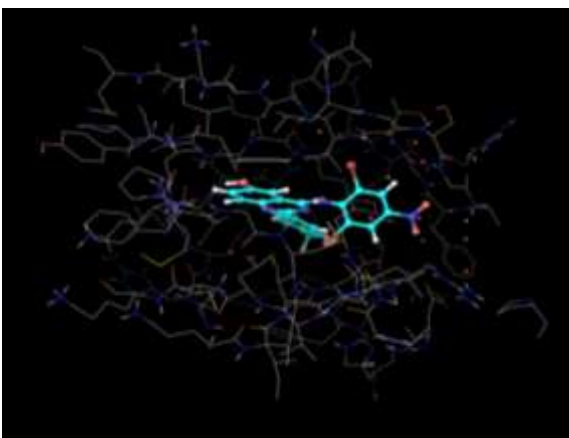
(b)



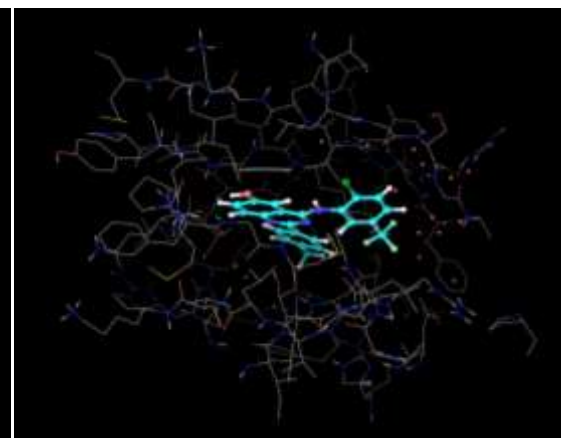
(c)



(d)



(e)



(f)

Figure: Structures of the different kinase inhibitors bound to the protein 3w32. Only residues that undergo significant movement or are hydrogen bonded to the ligand are shown.

Induced fit results

In virtual docking the ligands are docked into binding site of the receptor where the receptor is held rigid and the ligand is free to move. We have also taken into account receptor flexibility by induced fit docking. In induced fit docking, we obtained different poses of all the best docked analogues. The results of the induced fit docking are given in below Table, which displays the best docked poses. From the results of the induced fit docking, it is clear that there are some considerable changes in the docking scores and energies of the docked complexes.

Table: Results of the induced fit docking

Compounds	Docking score	Energy
Mol 1	-7.6	-5.9
Mol 5 (comp 1)	-6.3	-6.3
Mol 12 (comp 4)	-6.5	-4.0
Mol 21	-7.8	-5.7
Mol 24	-7.7	-6.6
Mol 30	-7.7	-6.3
Mol 39(comp 2)	-6.5	-4.4
Mol 50(comp 3)	-7.8	-6.6

Docking energy is written only for the best docked poses. All energy values are given in Kcal/mol.

Conclusion:

The glide score can be used as a semi-quantitative descriptor for the ability of ligands to bind to a specific conformation of the protein receptor. Generally speaking for low glide score good ligand affinity to the receptor may be expected. According to the glide score the results of the inhibition for the EGFR may be arranged in the following manner: mol21> mol150> mol24>mol30> mol1> mol2>mol39> mol5.

Docking studies performed by GLIDE has confirmed that above inhibitors fit into the binding pocket of the EGF receptor. From the results we may observe that for successful docking, intermolecular hydrogen bonding and lipophilic interactions between the ligand and the receptor are very important.

A comparison of the induced fit and virtual docking gives the role of protein flexibility. It is obvious from the results that a combined method of soft docking and side chain optimization gives better results. It is also clear that an average distribution of docking free energy ranging from 2 kcal/mol or more, is sufficient to mis-rank a potential drug candidate as a weak binder. However, by combining the MM-GB/SA and relaxed complex methods we are able to show the best ranked binding modes.

4.2.2 Designing of N-[2-(4-methylphenyl)-4-(substituted aniline)-3, 4-dihydroquinazolin-6-yl] acetamide

Protein preparation

A characteristic PDB structure file consists only of heavy atoms, waters, cofactors, and metal ions, and can be multimeric. Terminal amide groups should be misaligned, because the X-ray structure analysis cannot usually distinguish between O and NH₂. Ionization and tautomeric states are also generally unassigned. Glide calculations use an all-atom force field for accurate energy evaluation. Thus, Glide requires bond orders and ionization states to be properly assigned and performs better when side chains are reoriented when necessary and steric clashes are relieved.

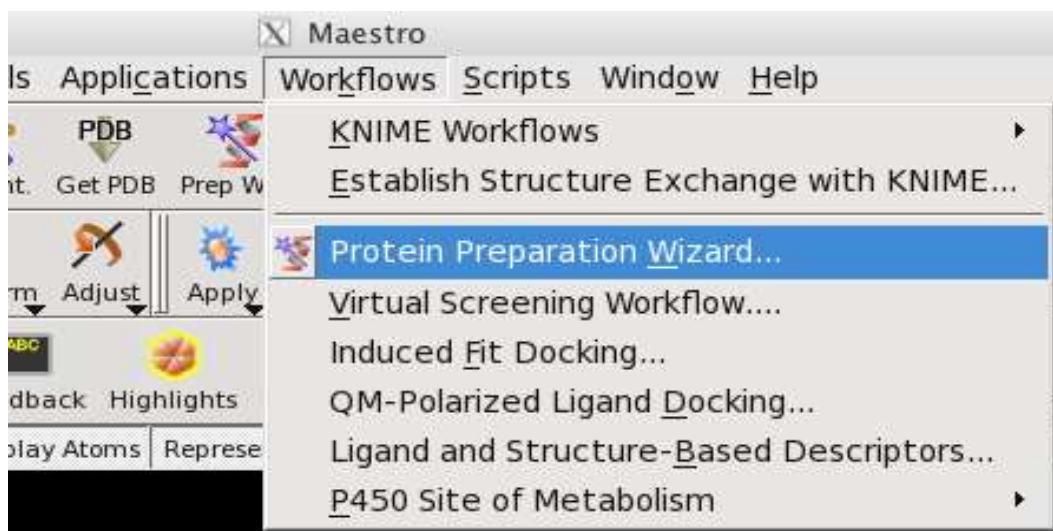


Fig: Protein preparation wizard

Steps involved in protein preparation wizard

1. Import a ligand/protein co-crystallized structure from PDB.
2. Simplify multimeric complexes.
3. Determine whether the protein-ligand complex is a dimer or other multimer containing duplicate binding sites and duplicate chains that are redundant. If the structure is a multimer with duplicate binding sites, remove redundant binding sites and the associated chains by picking and deleting molecules or chains. Locate any waters you want to keep and then delete all others. These waters are identified by the oxygen atom, and usually do not have hydrogens attached. Generally, all waters are deleted and retained only coordinated to metals. If waters are kept, hydrogens will be added to them by the preparation component of the protein preparation job. And, check that these water molecules are correctly oriented.
4. Adjust the protein, metal ions, and cofactors.
5. Adjust the ligand bond orders and formal charges.
6. Run a restrained minimization of the protein structure.
7. Review the prepared structures.

Checking the Protein Structures

1. Check the Orientation of Water Molecules
2. Check for Steric Clashes
3. Resolving H-Bonding Conflicts
4. Docking the Native Ligand

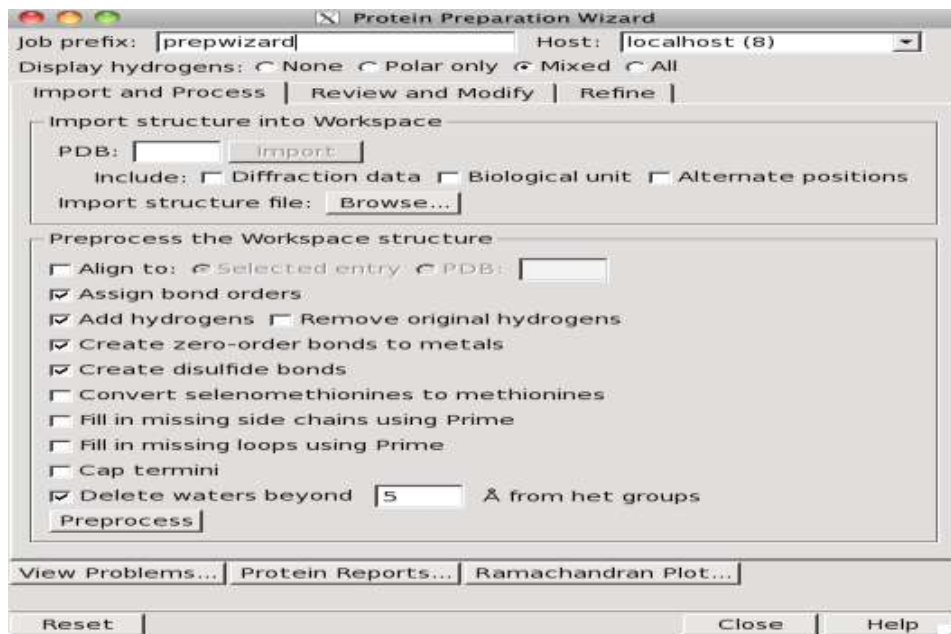


Fig: Protein preparation (import and process)

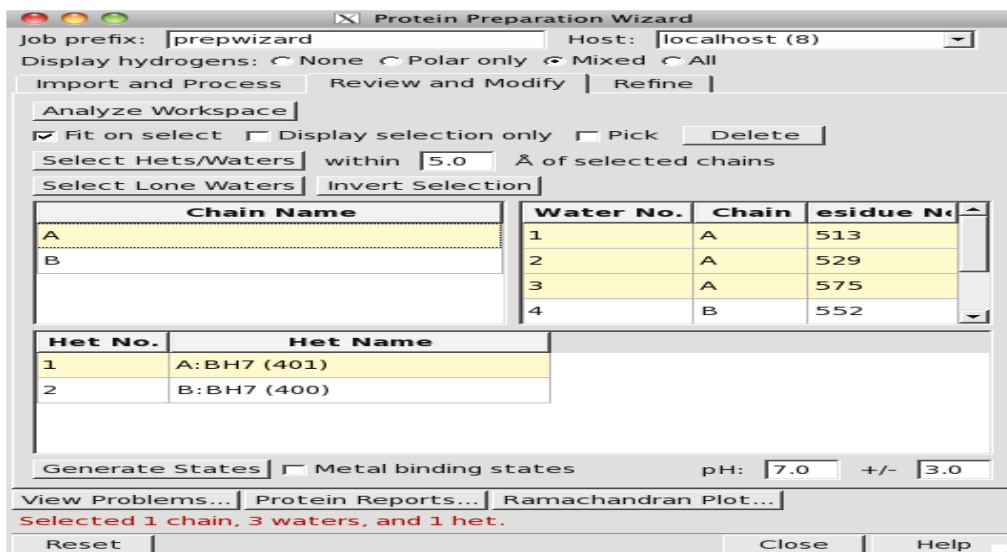


Fig: Protein preparation wizard (Review and modify)

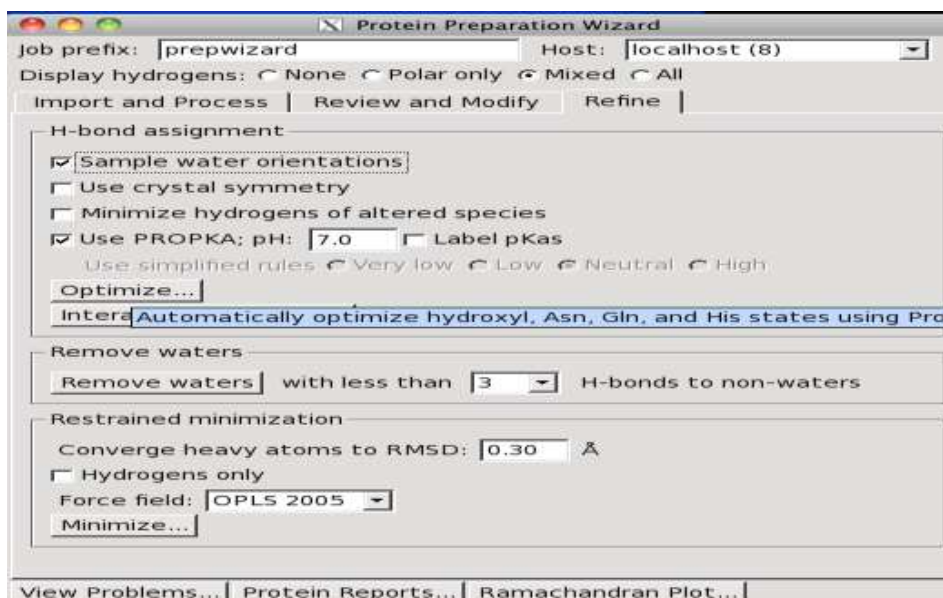


Fig: Protein preparation wizard (Refine)

Ligand Preparation

Structures supplied to Glide must meet the following conditions:

1. They must be three-dimensional (3D).
2. They must have realistic bond lengths and bond angles.
3. They must consist of a single molecule that has no covalent bonds to the receptor, with no accompanying fragments, such as counter ions and solvent molecules.
4. They must have all their hydrogens.
5. They must have an appropriate protonation state for physiological pH values.

The steps are listed below

Convert structure format > Select structures > Add hydrogen atoms > Remove unwanted molecules > Neutralize charged groups > Generate ionization states > Generate tautomers > Filter structures > Generate alternative chiralities > Generate low-energy ring conformations > Remove problematic structures > Optimize the geometries > Convert output file.

To start the LigPrep choose the Applications menu. With the help of LigPrep single low energy 3D structure can produce with correct chiralities for each input structure. Also produce structures with various ionization states, tautomers, stereochemistries, ring

conformations and remove the molecules using various criteria. Remove the unwanted hydrogens, add hydrogens and minimize the ligand structure with the help of default options in the LigPrep panel.

To generate several different output structures for each input structure the default pH range must be 5.0 to 9.0. To generate the ionization states use either the ionizer or Epik. Epik generate states which are more suitable for metal binding.

Select desalt and generate the tautomers by default. If more than 8 tautomers are possible then select the most likely tautomers. The stereoizer generates two stereoisomers per chiral centre in the ligand up to maximum limit. Determine chiralities from 3D structure ignore input file chiralities and takes chirality information from the 3D geometry.

Generate all combinations varies the stereochemistry up to a maximum number of structures specified by generate at most max per ligand. The default maximum is 7.

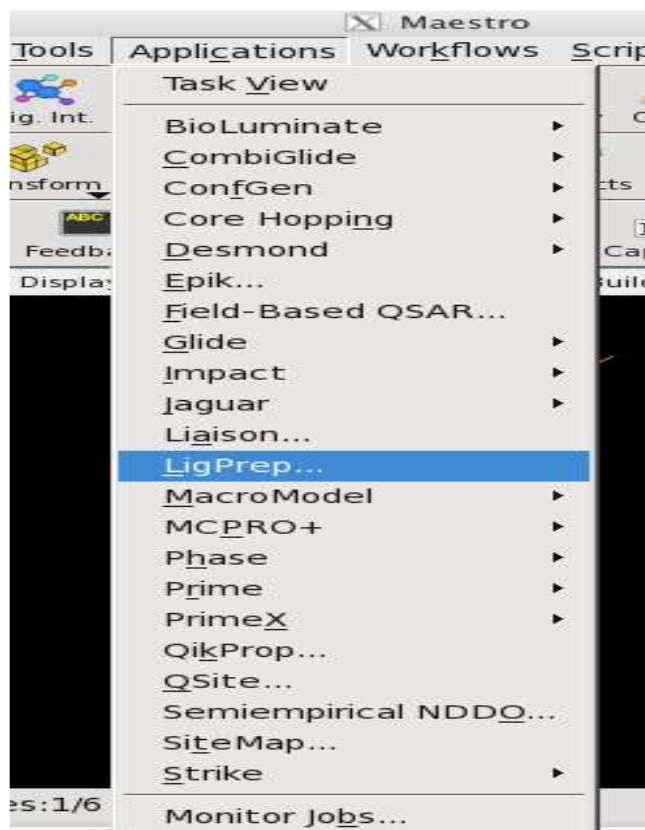


Fig: Selection of LigPrep from Application

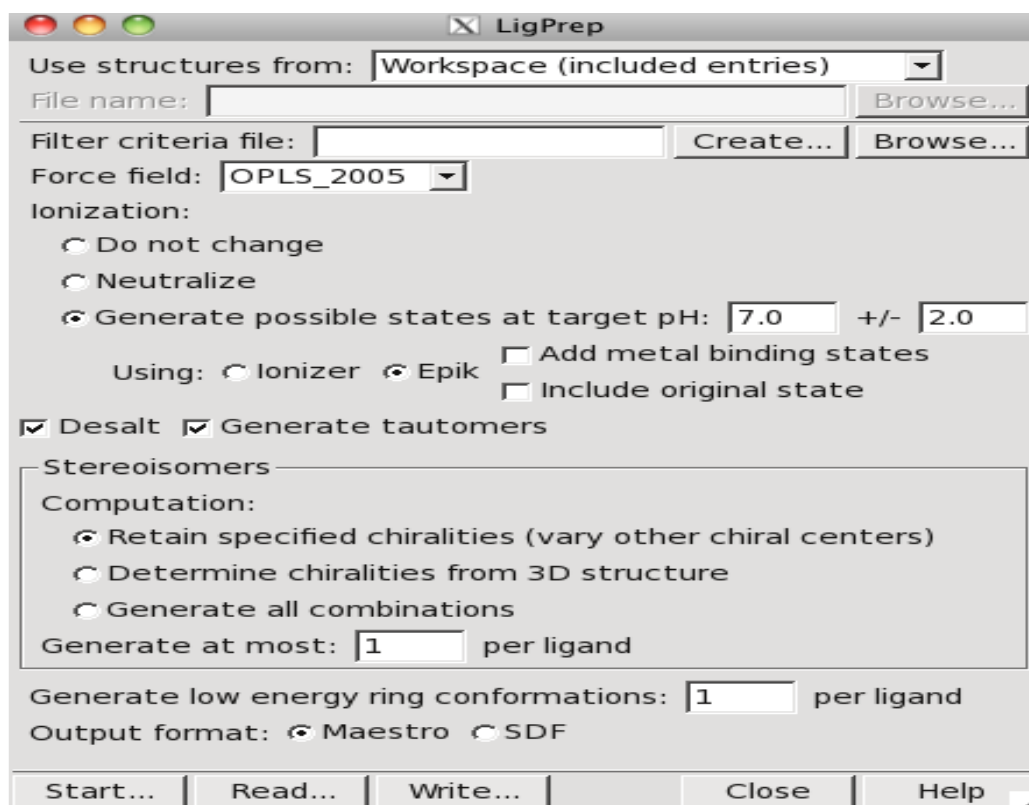


Fig: Ligand preparation window display

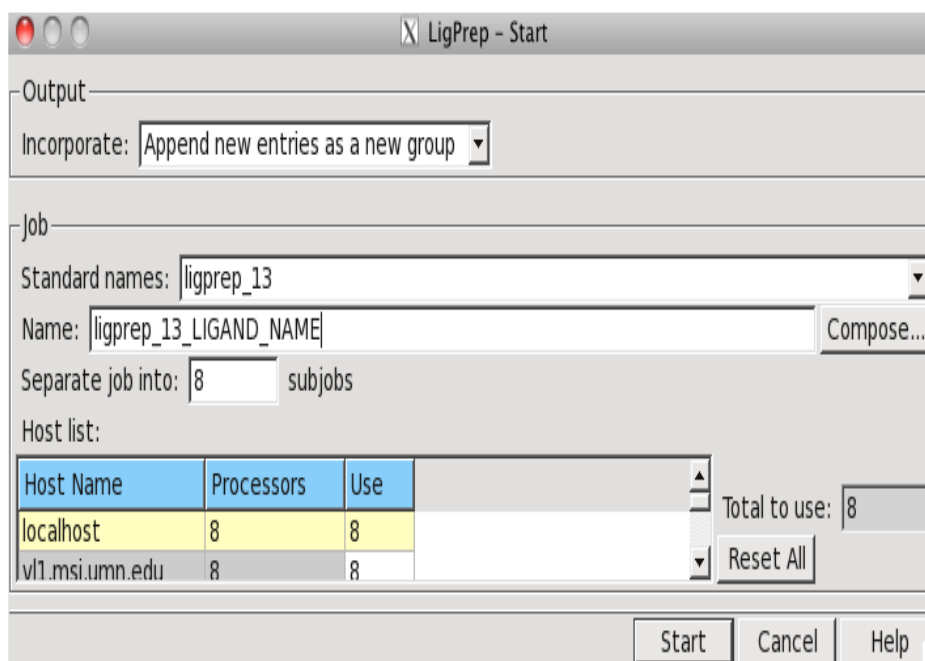


Fig: Ligand preparation-start

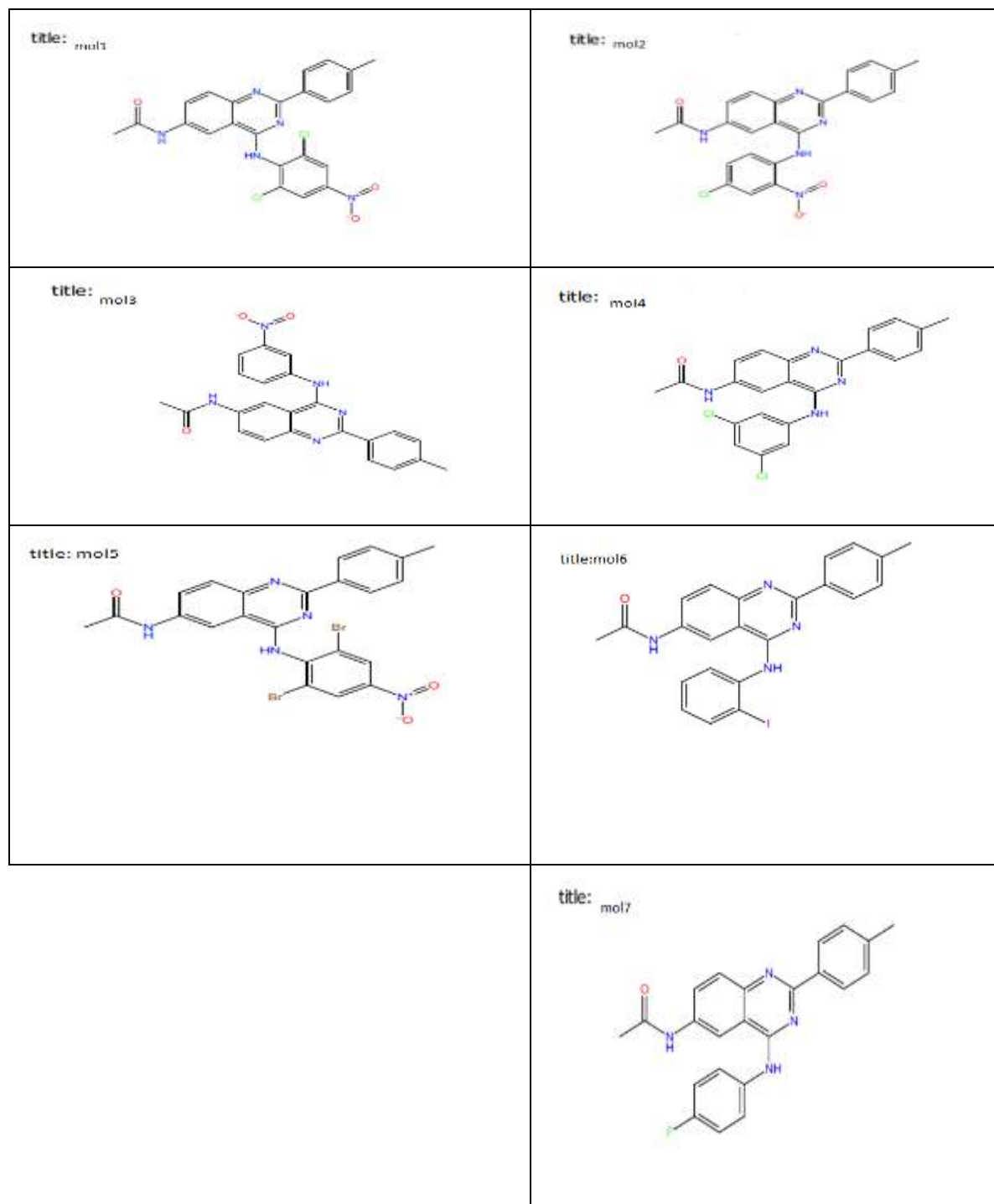


Fig: Chemical structures of different quinazoline derivatives in their minimized positions. Non-carbon hydrogens are colored in blue.

Receptor Grid Generation

These are some steps to be followed for generation of receptor grid.

1. Choose Tasks > Docking > Grid Generation or Applications > Glide > Receptor Grid Generation.
2. Display the prepared receptor in the Workspace.
3. Pick the ligand to define the grid centre.
4. Adjust the size of the active site in the Site tab to accommodate larger ligands, if necessary.
5. Add any hydrogen-bond, metal, positional, or hydrophobic constraints in the Constraints tab.
6. Pick any rotatable hydroxyl groups in the active site if such groups could rotate during docking.
7. Start the grid generation job

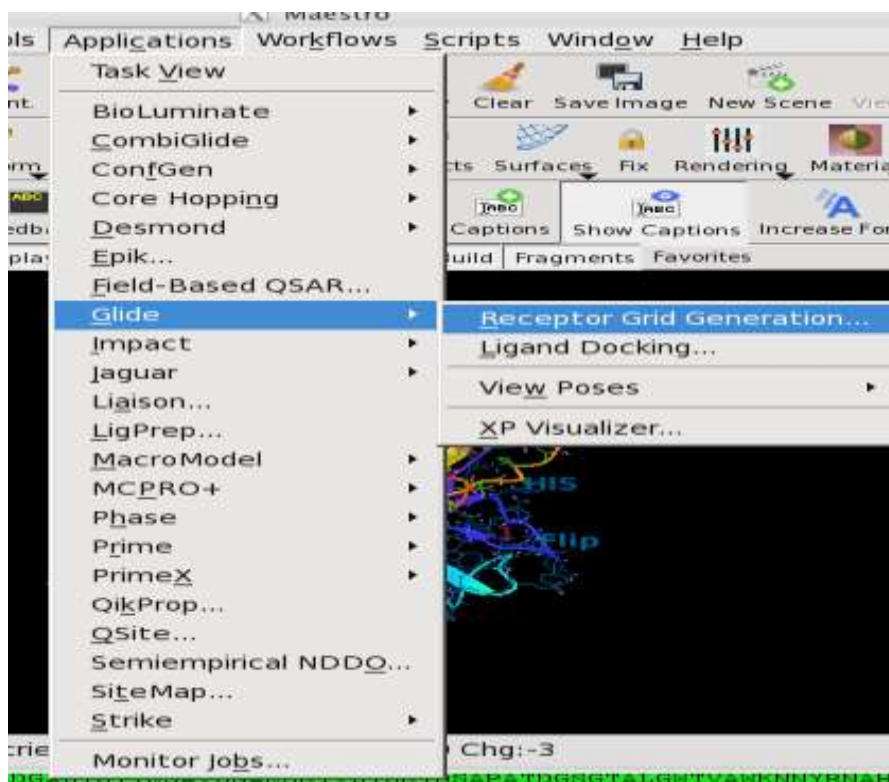


Fig: Selection of Glide -Receptor grid generation from Application panel

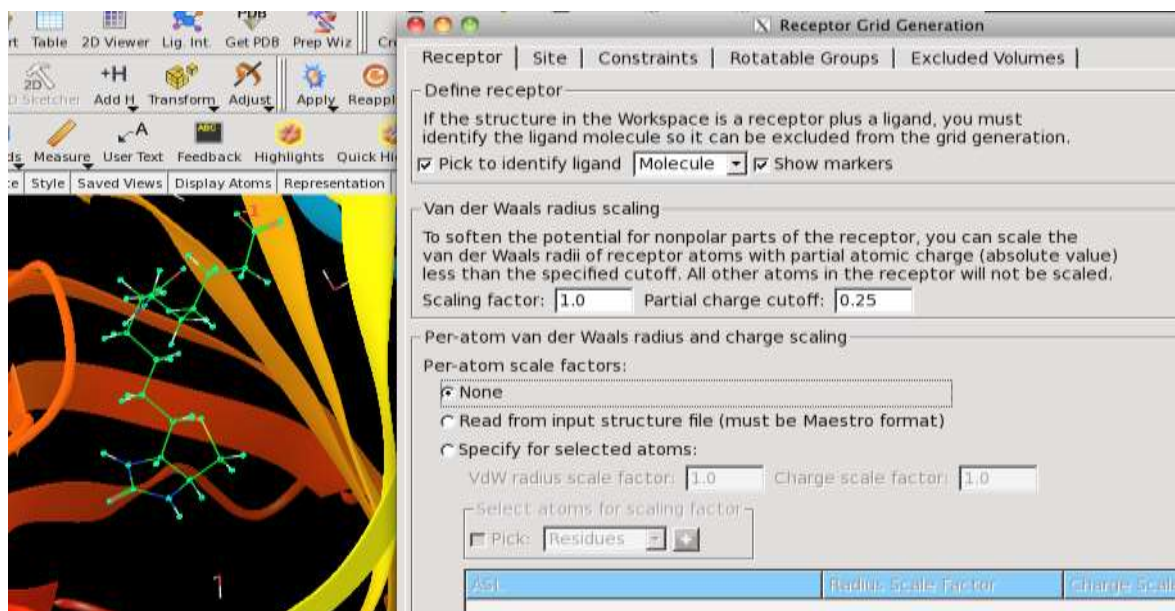


Fig: Receptor grid generation

Ligand Docking

Glide ligand docking job requires a set of previously calculated receptor grids and one or more ligand structures. Open the Ligand Docking panel; choose Ligand Docking from the Glide submenu of the Applications menu.

The Ligand Docking panel has six tabs such as settings, ligands, core, constraints, similarity and output.

Specifying the Receptor Grid

Click Browse in the Receptor grid section of the Settings tab to open a file selector and choose a grid file or a compressed grid archive (zip). The file name, without the extension, is displayed in the Receptor grid base name text box.

Selecting the Docking Precision

There are three choices of docking precision, given under Precision in the Docking section. HTVS (high-throughput virtual screening)-High-throughput virtual screening (HTVS) docking is intended for the rapid screening of very large numbers of ligands. SP (standard precision) docking is appropriate for screening ligands of unknown quality in large numbers. Standard precision is the default.

XP(extraprecision) docking and scoring is a more powerful and discriminating procedure, which takes longer to run than SP. XP is designed to be used on ligand poses that have a high score using SP docking. If want to dock a set of ligands using a progression of precision, then use the Virtual Screening Workflow to set up and run the docking jobs.

Selection of Initial Poses

The selection of initial poses section of the box control the way poses pass through the filters for the initial geometric and complementarity “fit” between the ligand and receptor molecules. The grids for this stage contain values of a scoring functions, it would be to place ligand atoms of given general types in given elementary cubes of the grid. These cubes have a constant spacing of 1 Å.

The “rough score” for a given pose of the ligand relative to the receptor is simply the sum of the appropriate grid scores for each of its atoms. Poses that pass these initial screens enter the final stage of the algorithm, which involves evaluation and minimization of a grid approximation to the OPLS-AA non-bonded ligand-receptor interaction energy. Keep initial poses per ligand for the initial phase of docking. This text box sets the maximum number of poses per ligand to pass to the grid refinement calculation. The value must be a positive integer. The default setting depends on the type of scoring window for keeping initial poses.

Visualizing Docking Results

The View Poses facility in the Project Table panel enables to display the ligand poses with the receptor in the Workspace, along with hydrogen bonds, bad and ugly contacts, and per residue interaction information. For Glide SP and XP docking runs, visualize the contributions to the XP docking score, provided that descriptor information was requested in the docking run. The Project Table panel offers a special facility for viewing poses from a pose viewer file. To use this facility select a single entry group. The group must contain the receptor as the first entry in the group, followed by the ligands. This is the normal situation when import a pose viewer file into the project. To start viewing poses, choose Setup from the View Poses submenu. The receptor is locked in the Workspace, and the first ligand entry is included.

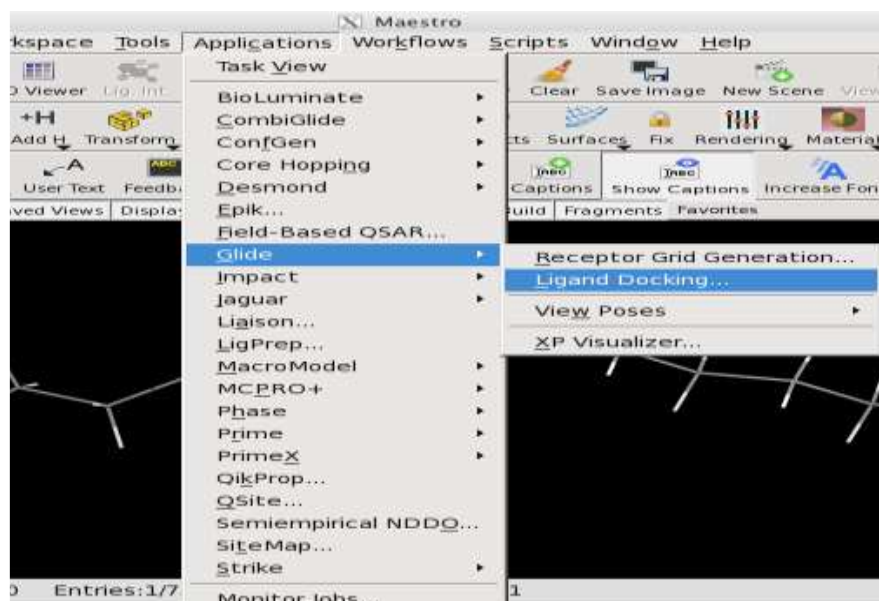


Fig: Selection of ligand docking from Application panel

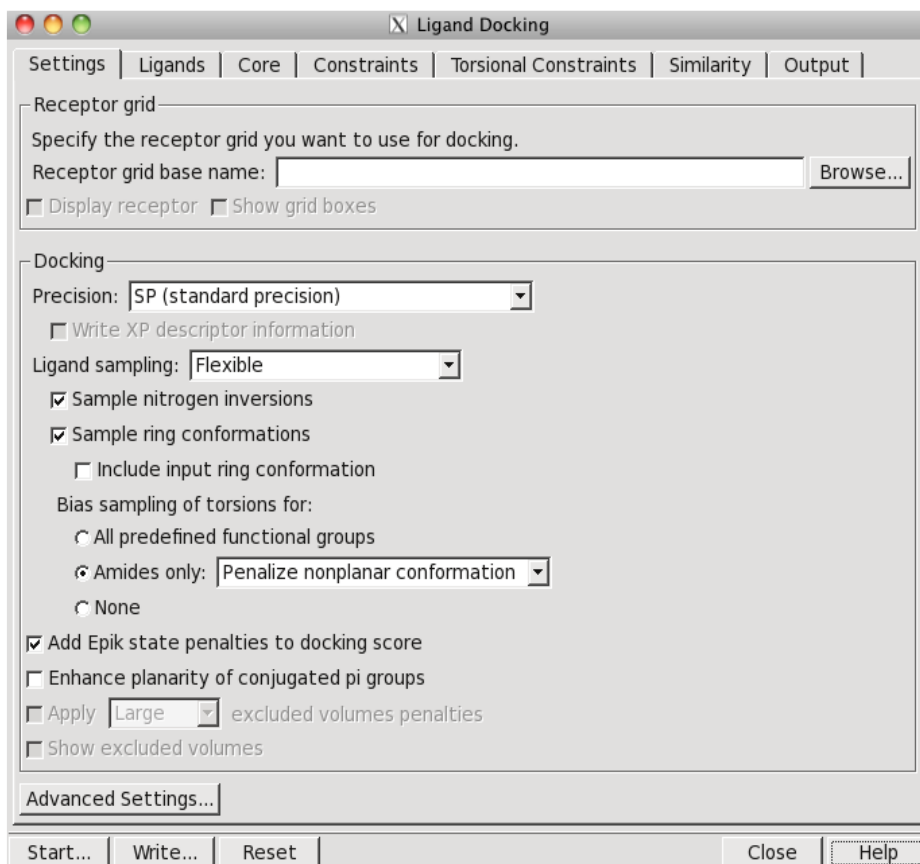


Fig: Ligand docking –settings

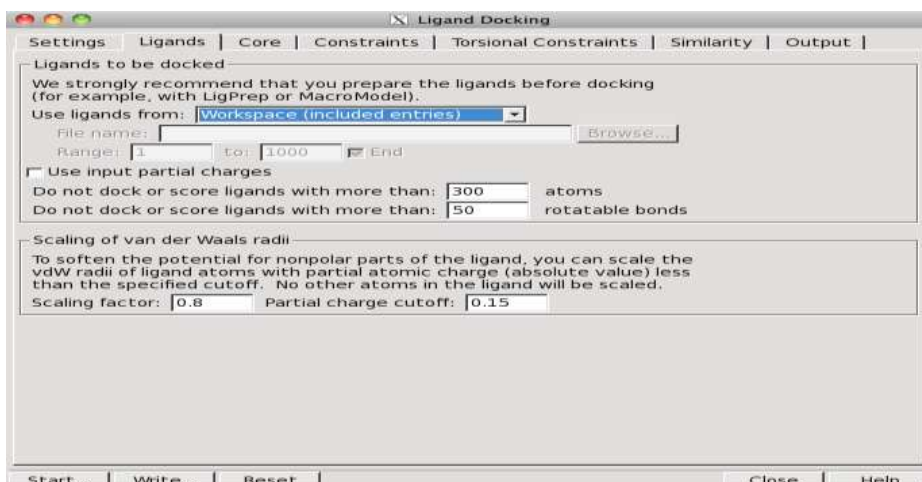


Fig: Ligand docking-Ligand

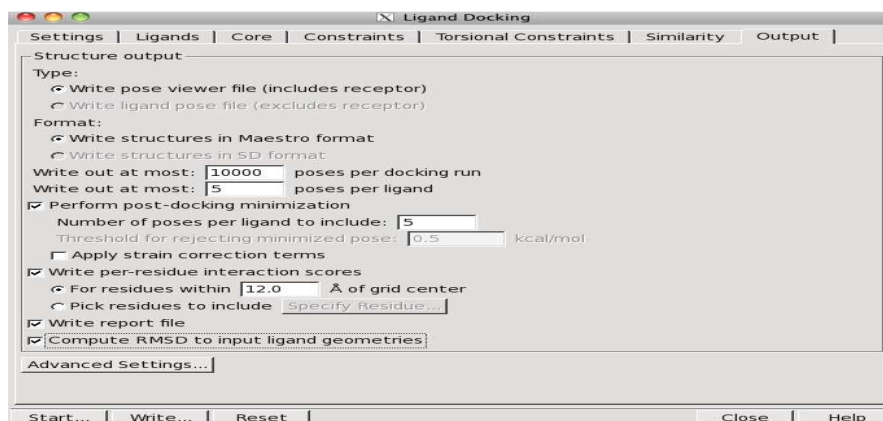


Fig: Ligand docking -output

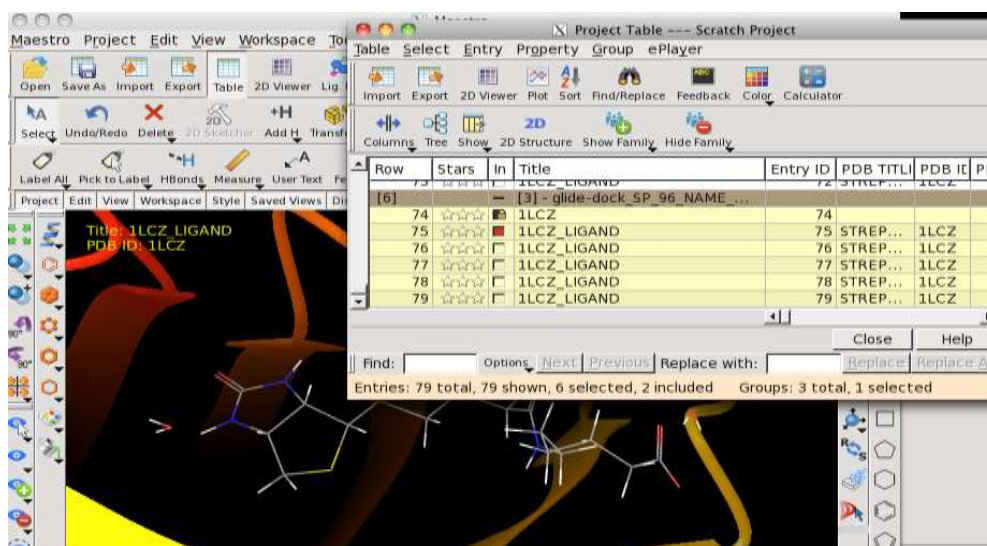


Fig: Project Table

Results and Discussion:

Virtual docking

Glide docking method have applied to inhibitors of tyrosine protein kinases to build a binding affinity model for EGFR that was then used to compute the free energy from binding energy of binding for this kinase.

The ligand preparation procedure generated different training sets of the inhibitors whose scoring function is given in below Table. These different structures were found by using different orientations of the inhibitors and different positions of the hydrogens. The results of docking and scoring are given in below Table. According to the table we see that among all the energy parameters the largest contribution for binding energy comes from Vander Waals interactions.

Table: Energy data of the structures generated by the docking program.

Compounds	E _{vdw}	E _{coul}	E _{site}	Docking score	Energy
Mol 1	-48.282925	-6.286361	-0.19705	-8.36263	-54.569286
Mol 2(comp.1)	-50.720325	-6.945927	-0.31644	-8.217244	-57.666253
Mol 4(comp.3)	-55.158234	-3.377333	-0.03047	-8.190933	-58.535567
Mol 3(comp.2)	-54.134922	-6.023509	-0.17859	-8.031208	-60.158431
Mol 6(comp.5)	-48.148769	-3.985412	-0.1011	-7.02276	-52.134181
Mol7	-52.787178	-5.365469	-0.13503	-6.954658	-58.152647
Mol5(comp.4)	-56.551281	-3.541861	-0.12247	-6.908445	-60.093142

The energy data are written according to the structure generated by the docking program. The best docked poses are written in table. All energies are given in Kcal/mol.

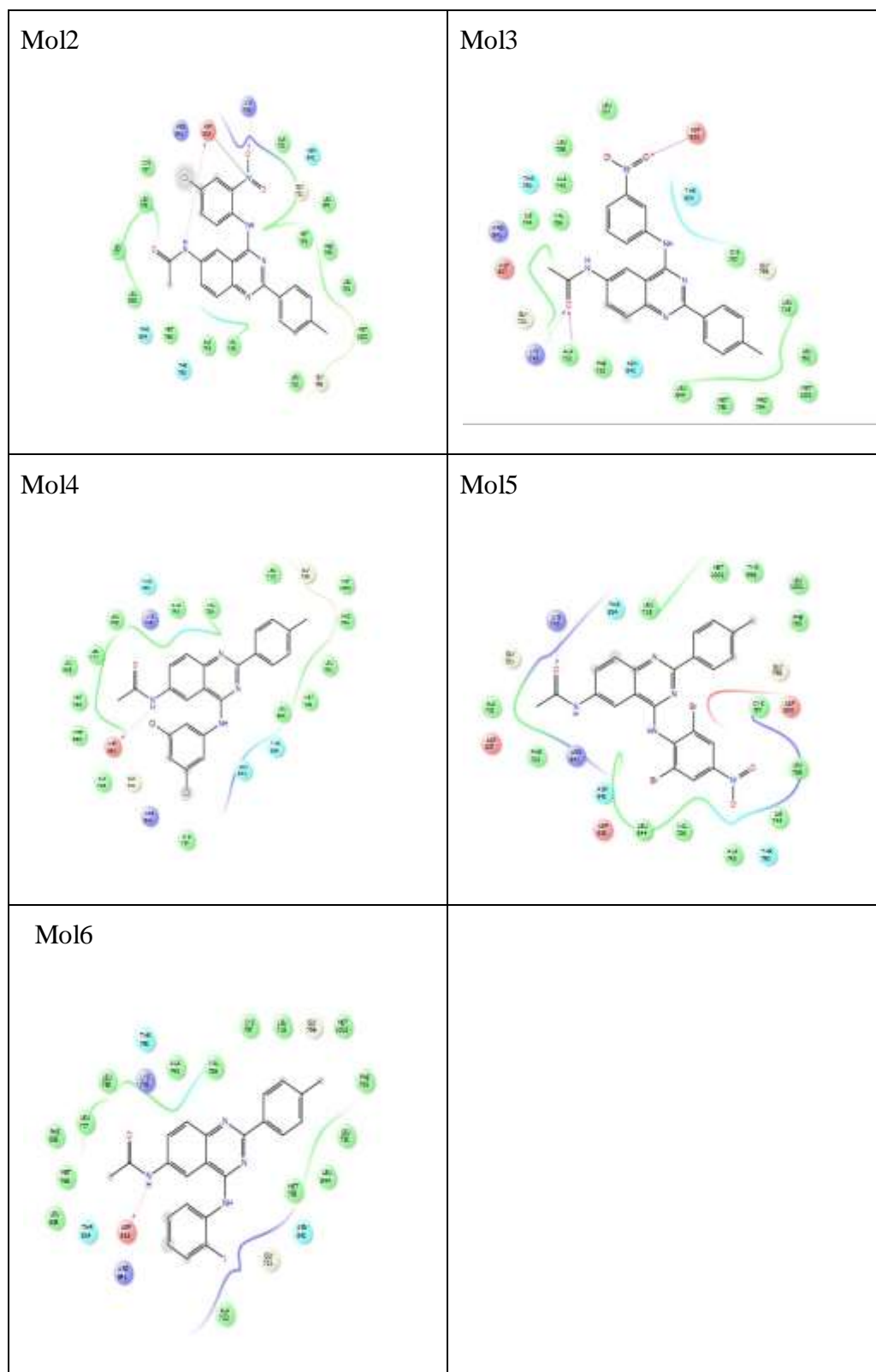


Fig: Ligand interaction diagram with Epidermal Growth Factor receptor.

Induced fit results

In virtual docking the ligands are docked into binding site of the receptor where the receptor is held rigid and the ligand is free to move. We have also taken into account receptor flexibility by induced fit docking. In induced fit docking, we obtained different poses of all the best docked analogues. The results of the induced fit docking are given in below Table, which displays the best docked poses. From the results of the induced fit docking, it is clear that there are some considerable changes in the docking scores and energies of the docked complexes.

Table: Results of the induced fit docking

Compounds	Docking score	Energy
Mol 1	-8.36263	-54.569286
Mol 2 (comp.1)	-8.217244	-57.666253
Mol 4 (comp.3)	-8.190933	-58.535567
Mol 3 (comp.2)	-8.031208	-60.158431
Mol 6 (comp.5)	-7.02276	-52.134181
Mol 7	-6.954658	-58.152647
Mol 5 (comp.4)	-6.908445	-60.093142

Docking energy is written only for the best docked poses. All energy values are given in Kcal/mol.

Conclusion:

The glide score can be used as a semi-quantitative descriptor for the ability of ligands to bind to a specific conformation of the protein receptor. Generally speaking for low glide score good ligand affinity to the receptor may be expected. According to the glide score the results of the inhibition for the EGFR may be arranged in the following manner: Mol1 > Mol2 > Mol4 > Mol3 > Mol6 > Mol7 > Mol5.

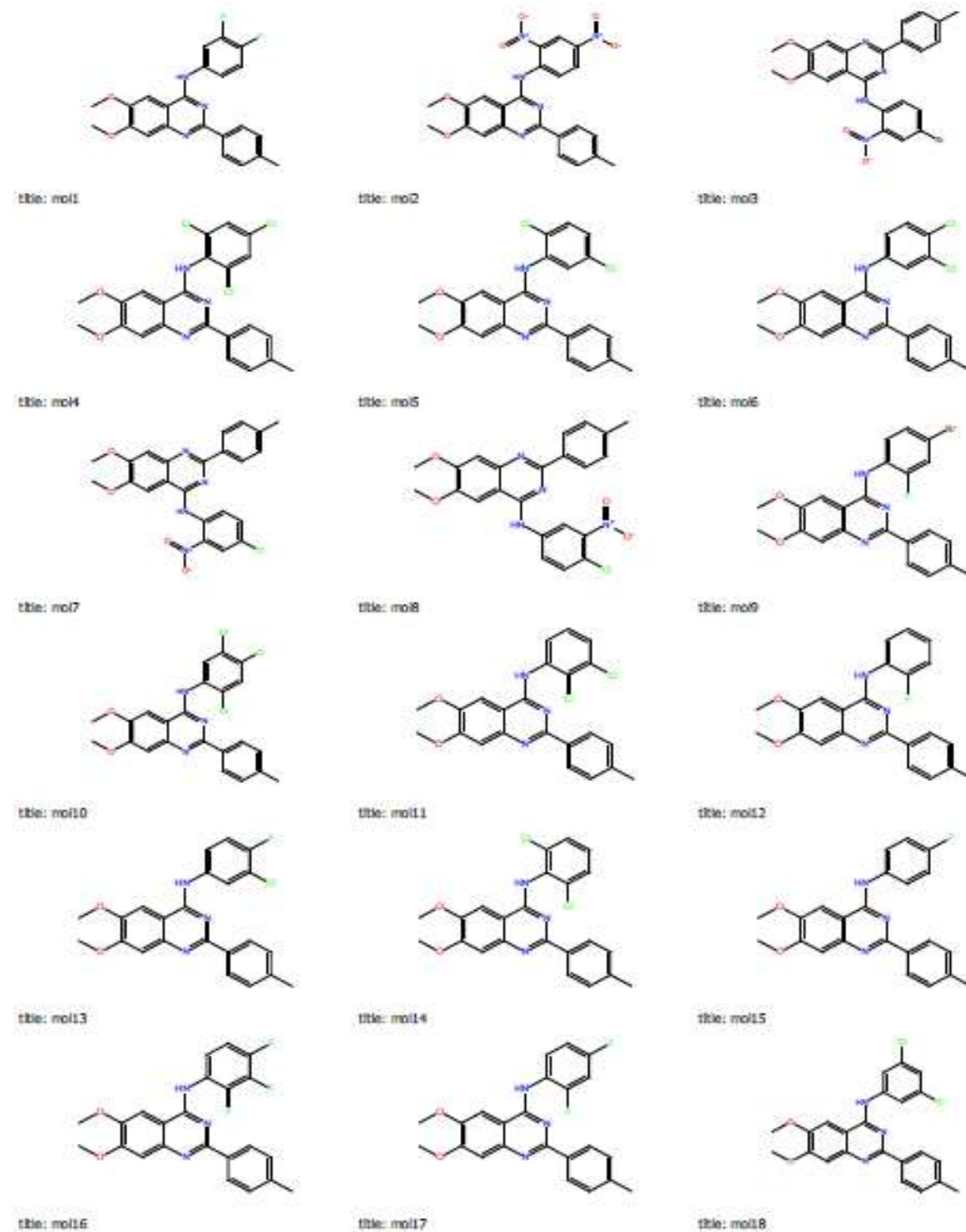
Docking studies performed by GLIDE has confirmed that above inhibitors fit into the binding pocket of the EGF receptor. From the results we may observe that for successful docking, intermolecular hydrogen bonding and lipophilic interactions between the ligand and the receptor are very important.

A comparison of the induced fit and virtual docking gives the role of protein flexibility. It is obvious from the results that a combined method of soft docking and side chain optimization gives better results. It is also clear that an average distribution of docking free energy ranging from 2 kcal/mol or more, is sufficient to mis-rank a potential drug candidate as a weak binder. However, by combining the MM-GB/SA and relaxed complex methods we are able to show the best ranked binding modes.

4.3 DESIGNING OF 4-ANILINOQUINAZOLINE DERIVATIVES

Methodology

Preparing a Library of Compounds.

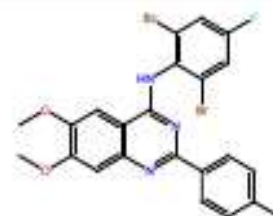




title: mo19



title: mo20



title: mo21



title: mo22



title: mo23



title: mo24



title: mo25



title: mo26



title: mo27



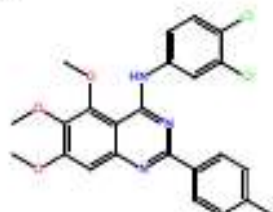
title: mo28



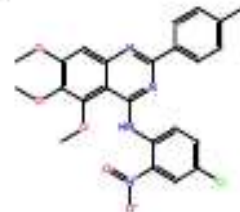
title: mo29



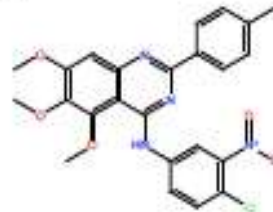
title: mo30



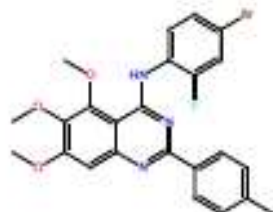
title: mo31



title: mo32



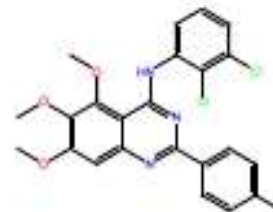
title: mo33



title: mo34



title: mo35



title: mo36

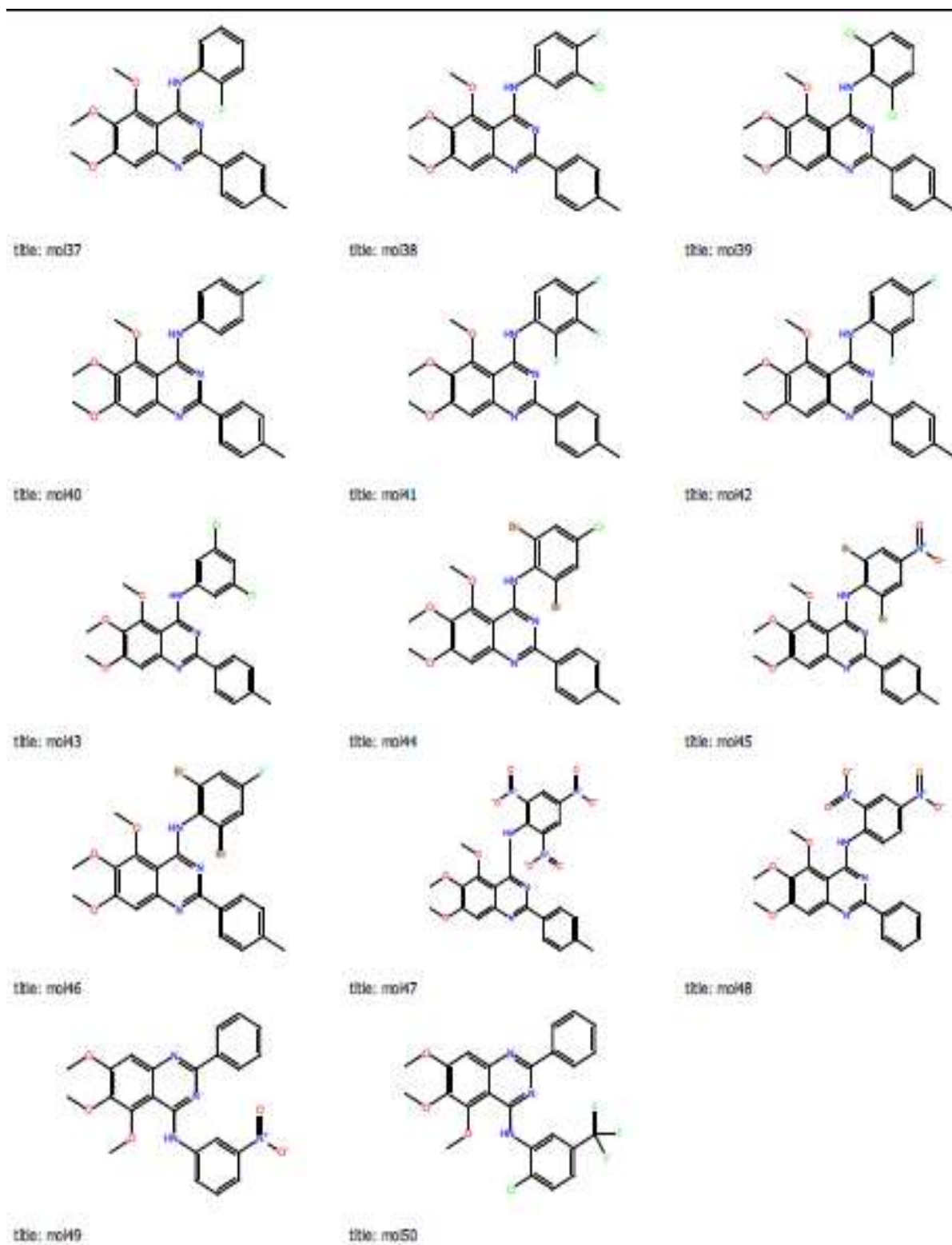


Fig: 2D structures of proposed analogues of 4-anilinoquinazoline.

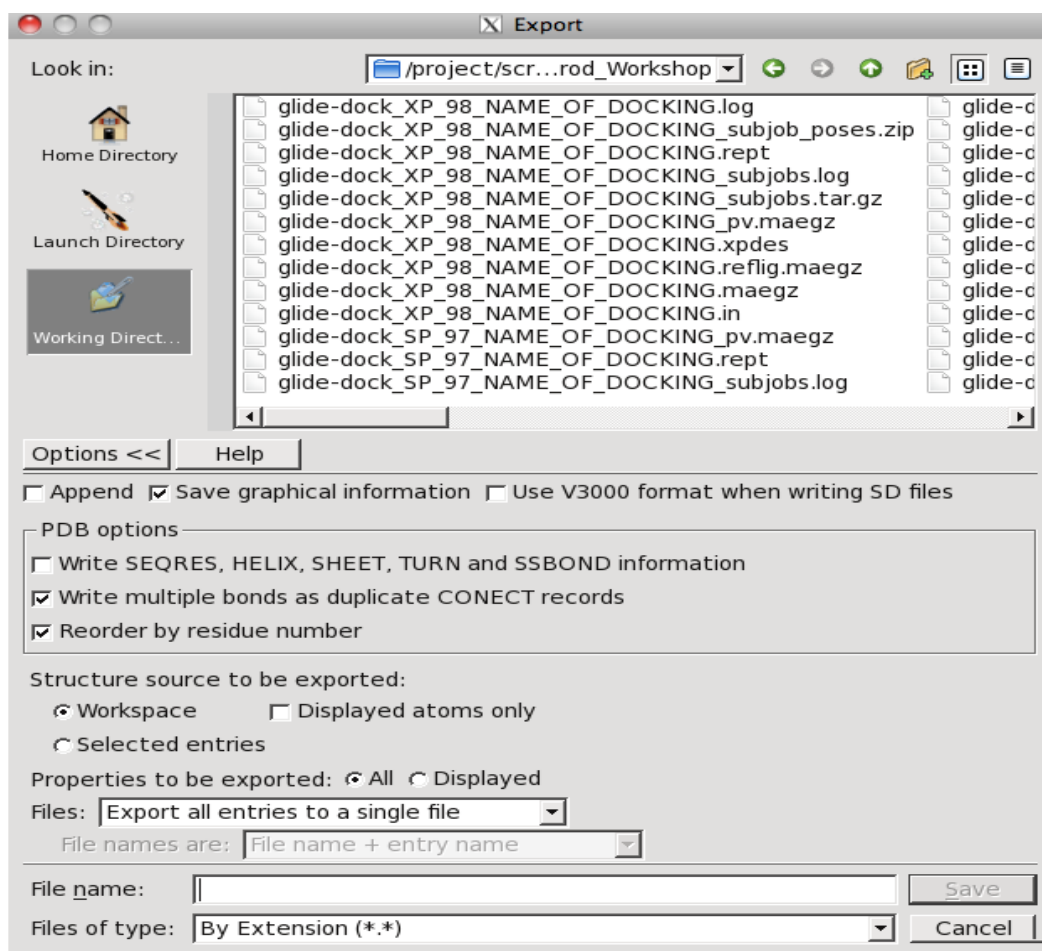


Fig: Saving structures

2. Preparing the Protein

1. Enter the PDB ID of your protein in the PDB text box and click Import.
2. Examine the structure in the Workspace for the following structural issues (colored atoms).
 - Red residues have missing atoms. Select Fill in missing side chains using Prime.
 - Light blue residues have adjacent missing residues (missing loops). Do one of the following:
 - Select Cap termini if the missing residues are not important for the modeling task, especially for long loops.
 - Select Fill in missing loops using Prime. Follow up with a full Prime loop prediction if the loop is important. Good for short loops (up to 5 residues).

- Select neither, but do a full Prime loop prediction (or use Prime X with the diffraction data, if available).
 - Green residues have alternate positions. If you want to use the alternate, select the residues, right-click and choose Switch Alternate Positions. If you want both, duplicate the protein and prepare both alternates.
 - Dark blue residues have mistyped atoms. Fix these in the Atom Properties tab of the Build panel before proceeding.
3. If you want to align the protein to another protein, select Align to, and specify the other protein.
 4. If the structure has hydrogens, select remove original hydrogens to fix problems like bad placement or bad labels.
 5. Select Create disulfide bonds (unless you don't want disulfide bonds).
 6. If you want to keep selenium atoms, deselect Convert selenomethionine to methionine. Conversion is only necessary if you want to use the OPLS_2001 force field for modeling.
 7. Set a range for keeping structural waters, or deselect Delete waters beyond to keep all waters.
 8. Click Preprocess.

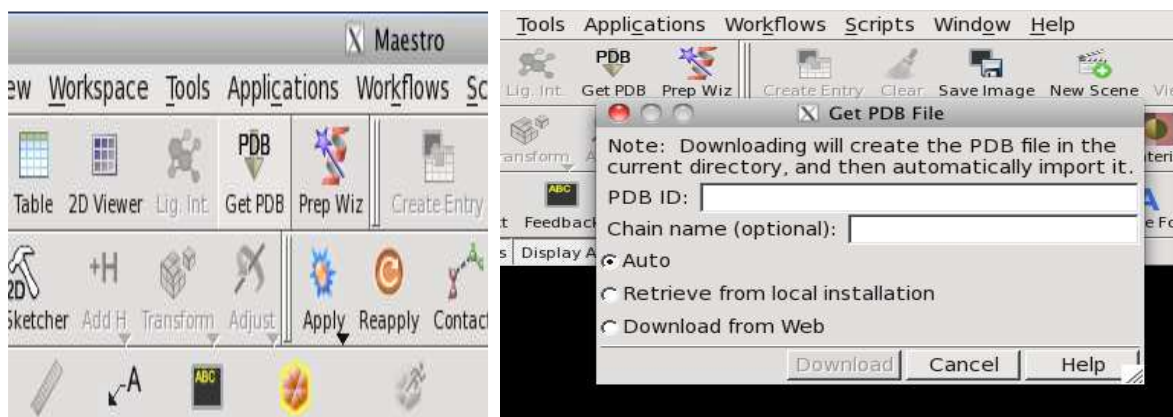


Fig: 5.5.3. Importing a PDB File from the PDB Data bank from maestro.

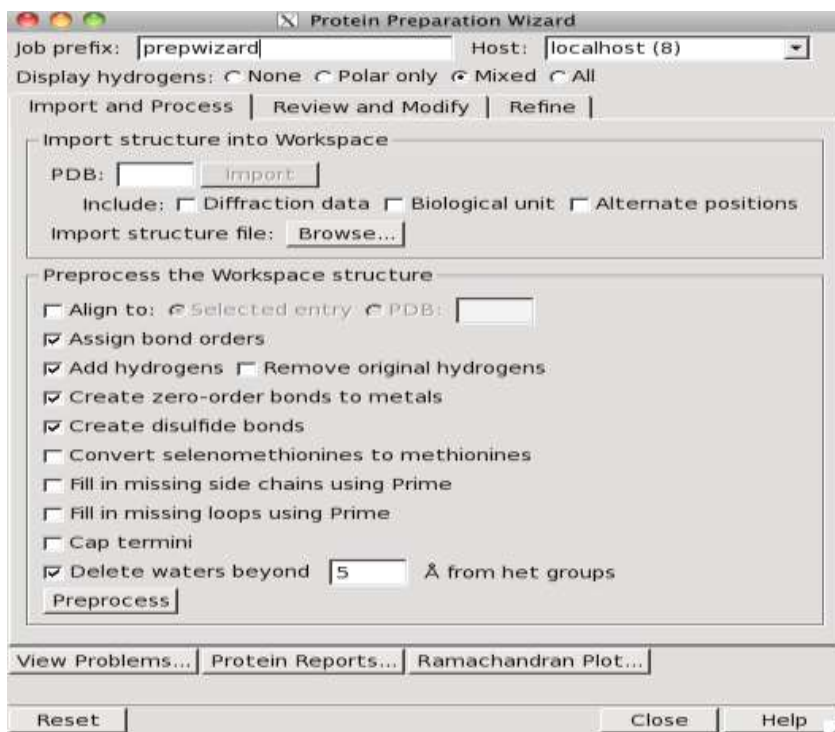


Fig: Protein preparation

i. Fix structural problems:

After preprocessing, the Protein Preparation-Problems dialog box opens if there are unfixed problems.

- If there are mistyped atoms, fix them in the Build panel (Edit > Build > Atom Properties)
- Overlapping hydrogens are mostly fixed by H-bond optimization and terminal flips, or by minimization. Check again at the end of the preparation.
- Fix missing atoms by capping, side-chain prediction or loop prediction, if you didn't do this the first time around. You can do this by running the Preprocess step again with different options selected.

ii. Review and modify:

In the Review and Modify tab, examine the structure and delete parts you don't want to use for modeling.

1. Delete unwanted chains, waters, and het groups, by selecting them in the tables and clicking delete.

2. Click Generate States to run Epik for ionization and tautomeric states of the het groups (ligand). Include metal-binding states if the het group is bonded to a metal.
3. Examine the states and select the state that you think is most reasonable. This step is important for optimizing the H-bond network.

Job prefix: Host:

Display hydrogens: ☐ None ☐ Polar only ☒ Mixed ☐ All

Import and Process | **Review and Modify** | Refine

Analyze Workspace

☒ Fit on select ☐ Display selection only ☐ Pick

Select Hets/Waters within Å of selected chains

Select Lone Waters

Chain Name	Water No.	Chain	esidue No.
A	1	A	513
B	2	A	529
	3	A	575
	4	B	552

Het No.	Het Name
1	A:BH7 (401)
2	B:BH7 (400)

☐ Metal binding states pH: +/-

Selected 1 chain, 3 waters, and 1 het.

Fig: Review and modify tab.

iii. Optimize the H-bond network:

Optimize orientation of polar hydrogens, flip terminal amides and histidines, adjust protein protonation states.

1. Select Exhaustive sampling for a more thorough but longer optimization.
2. Select a pH range option for protonation or deprotonation of residues.
3. Click Optimize.

iv. Run restrained minimization

Minimize the structure with harmonic restraints on the heavy atoms, to remove strain.

1. Select Hydrogens only if you don't want to allow the heavy atoms to move at all.
2. Click Minimize to make settings and start the minimization job.

H-bond assignment

Restrained minimization

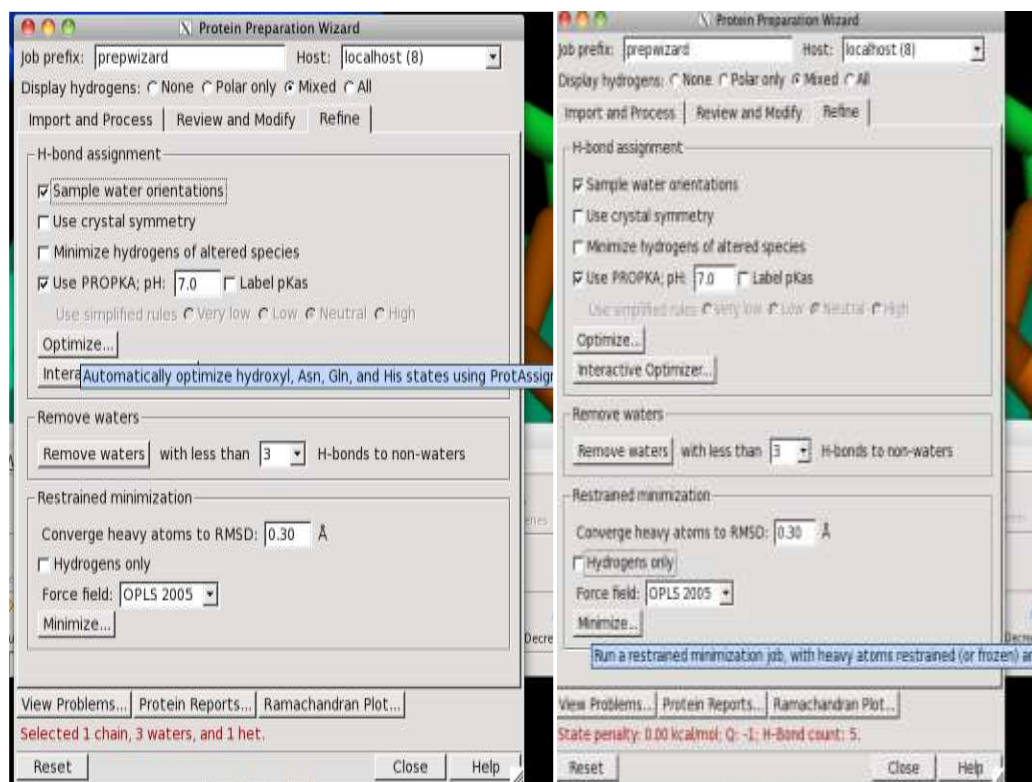


Fig: Refine tab

v. Check the results:

After the entire process is done, you should carefully check your results:

- Open the Problems panel (View Problems) to check for any remaining errors.
- Use the Protein Reports panel to check for other possible problems.
- Use the Ramachandran Plot panel to locate residues with unusual dihedrals.

3. Preparing the Ligands

1. Choose the source of the structures from the Use structures from option menu, and supply the file name if using a file.
2. Filter the structures by property by functional group counts-click Create to set up the filter.

3. Choose the force field. You usually only need to do this if the default doesn't cover some atom types in your ligands.
4. Choose an ionization option. Use of Epik is recommended.
5. Leave Desalt selected, to remove molecules other than the ligand.
6. Deselect Generate tautomers if you don't want to generate tautomers, for example to prepare just the original structures.
7. Choose an option for generating stereoisomers.
8. Increase the number of ring conformations if you have flexible rings that are likely to change conformation.
9. Select an output file format, and start the job.

4. Generating the Receptor Grid

1. Choose the task docking then select grid generation application then glide then receptor grid generation.
2. Display the prepared receptor in the Workspace.
3. Pick the ligand to define the grid center.
4. Adjust the size of the active site in the site tab to accommodate larger ligands, if necessary.
5. Add any hydrogen-bond, metal, positional, or hydrophobic constraints in the Constraints tab.
6. Pick any rotatable hydroxyl groups in the active site if such groups could rotate during docking.
7. Start the grid generation job.

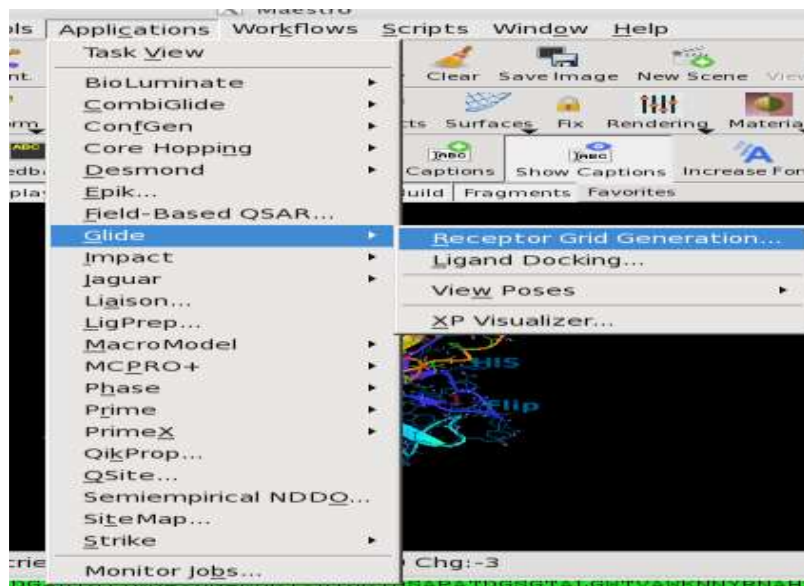
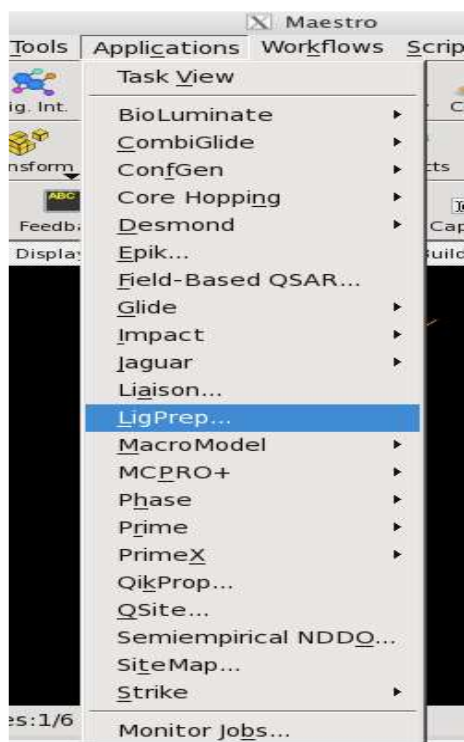


Fig: Receptor Grid generation with Glide.

5. Docking the Ligands

1. Choose tasks docking then glide docking or applications then glide then ligand docking.
2. Specify the receptor grid to use.
3. Select the docking precision:
 - HTVS for initial screen of millions of compounds (limited conformational search but fast)
 - SP for thousands of compounds (better coverage of conformational space)
 - XP for tens or hundreds of compounds (high accuracy on docked poses)
4. If you chose XP, select Write XP descriptor information if you want to visualize interaction terms.
5. Select Add Epik state penalties to docking score, if Epik was used in ligand preparation
6. Specify the ligand file to use, in the Ligands tab.
7. If you want to set up constraints to a reference ligand core or calculate RMSD to this core, you can do this in the Core tab.

8. Select the receptor constraints you want to use in the Constraints tab, and supply any required information.
9. If the ligands are very flexible, you can apply constraints on ligand torsions in the Torsional Constraints tab to reduce the torsional degrees of freedom.
10. Set the number of poses per ligand and total number of poses in the Output tab.
11. Use post-docking minimization if you want to improve pose geometries.
12. Select Write per-residue interaction scores for residues within N Å of grid center if you want to examine interactions of ligand poses with the receptor, and set the cut off distance.
13. Click Start to run the job. If the ligand file is large, distribute the job over multiple processor if possible.



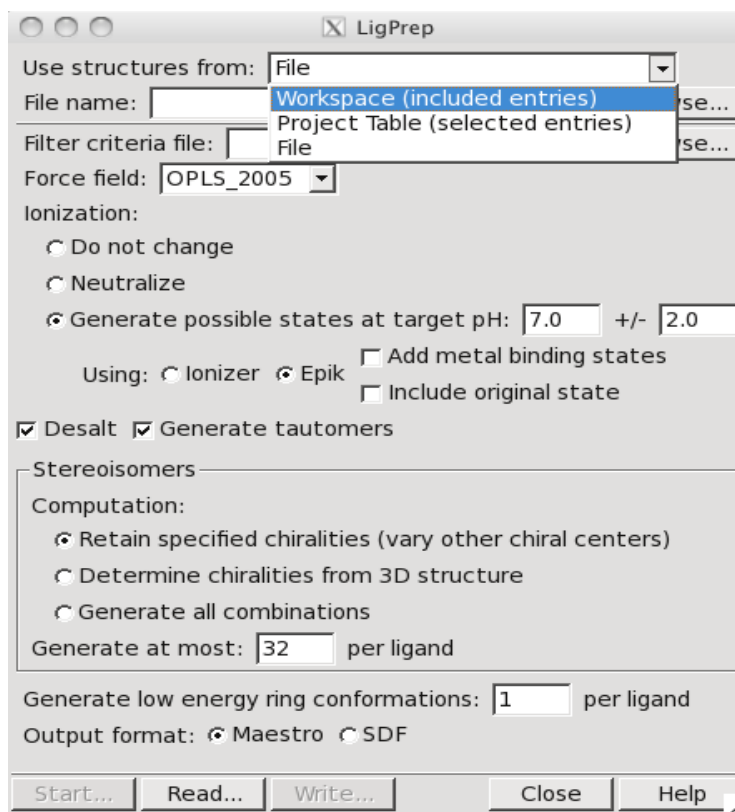


Fig: Ligand Preparation with LigPrep

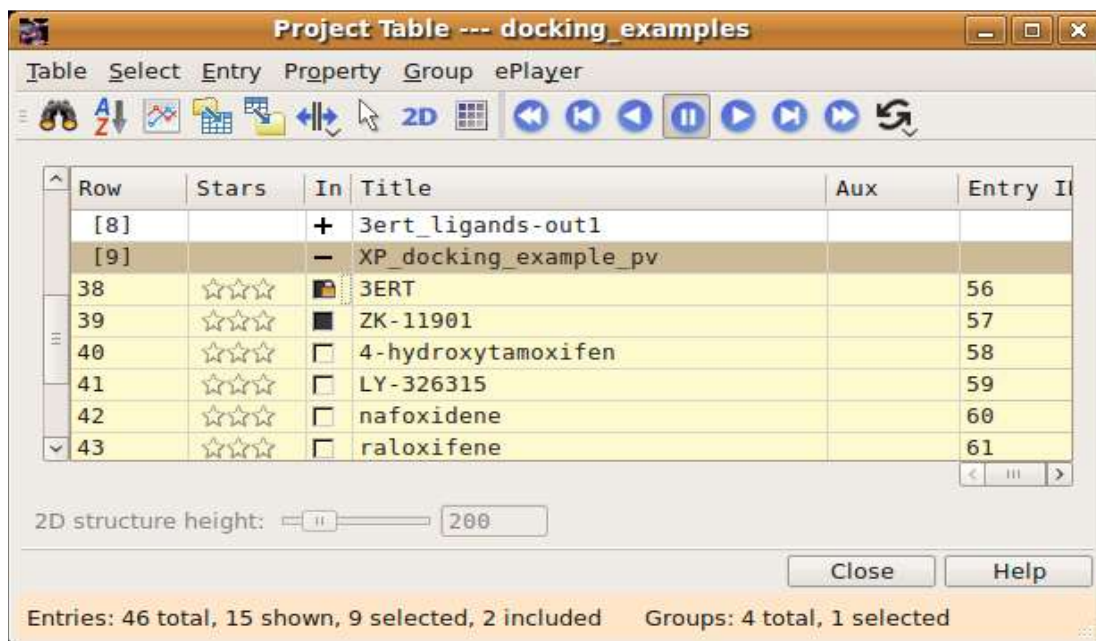


Fig: Ligand docking.

6. Examining Poses

1. Import the pose file *jobname-pv.mae* into Maestro. Ensure that the option for pose viewer files, turn on pose viewing is selected.
2. In the Project Table panel, turn on display of H-bonds and contacts with Entry > View Poses > Display H-bonds and Entry > View Poses > Display Contacts. If you wrote out per-residue interaction scores, turn on Entry > View Poses > Display Per residue interactions.
3. Use the LEFT ARROW and RIGHT ARROW keys to step through the poses, and examine their interactions with the receptor.
4. When you have finished examining poses, right-click on the receptor entry in the Project Table and choose Unfix to exit the pose viewing mode.

7. Visualizing Docking Results

1. The View Poses facility in the Project Table panel enables to display the ligand poses with the receptor in the Workspace, along with hydrogen bonds, bad and ugly contacts, and per-residue interaction information.
2. For Glide SP and XP docking runs, visualize the contributions to the XP docking score, provided that descriptor information was requested in the docking run. The Project Table panel offers a special facility for viewing poses from a pose viewer file.
3. To use this facility you must select a single entry group. The group must contain the receptor as the first entry in the group, followed by the ligands.
4. This is the normal situation when import a pose viewer file into the project. To start viewing poses, choose Setup from the View Poses submenu. The receptor is locked in the Workspace, and the first ligand entry is included.

Results and Discussion

1. Virtual docking

We have applied the GLIDE docking method to 50 analogues of 4-anilinoquinazoline which are inhibitors of tyrosine protein kinases to build a binding affinity model for the

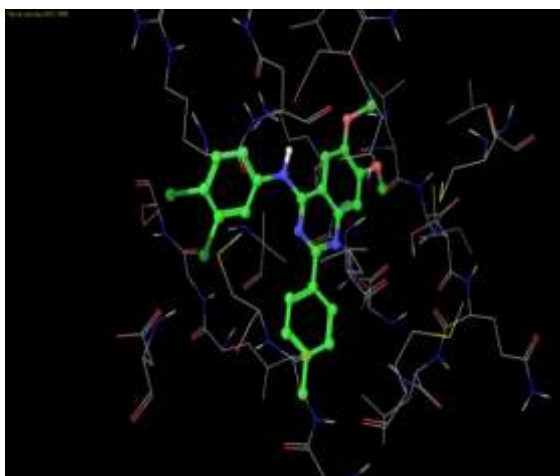
epidermal growth factor receptor that was then used to compute the free energy of binding for this kinase.

The ligand preparation procedure generated different training sets of the inhibitors whose scoring function is given in below Table. These different structures were found by using different orientations of the inhibitors and different positions of the hydrogens. The results of docking and scoring are given in below Table. According to the table we see that among all the energy parameters the largest contribution for binding energy comes from Vander Waals interactions.

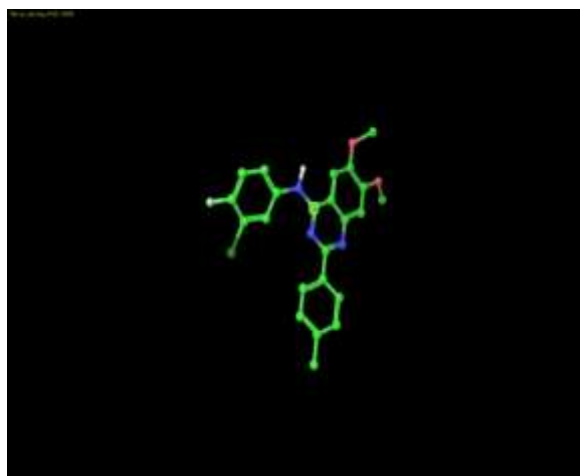
Table: Average Vander Waals (vdw), electrostatic (coul) and Site energy (site) after GLIDE docking.

Analogues	E _{vdw}	E _{coul}	E _{site}	Docking score	Energy
Mol37	-5.4	-0.3	-0.5	-8.6	-5.7
Mol12 (SCI)	-6.5	-0.1	-0.2	-7.1	-6.6
Mol35	-6.0	-0.1	-0.3	-7.0	-6.1
Mol5 (SCII)	-5.5	-0.2	-0.2	-6.9	-5.7
Mol41	-5.8	-0.1	-0.7	-6.9	-5.9
Mol4 (SCIV)	-6.7	-0.0	-0.2	-6.8	-6.7
Mol17	-5.8	-0.2	-0.4	-6.7	-6.0
Mol11 (SCIII)	-5.6	-0.4	-0.3	-6.6	-6.0

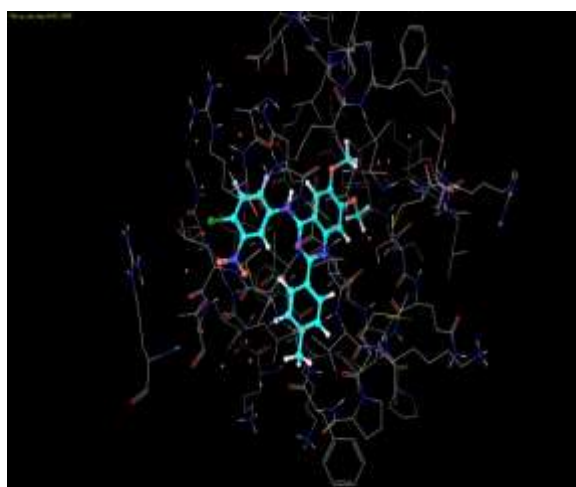
The energy data are written according to the structure generated by the docking program. The best docked poses are written in table. All energies are given in Kcal/mol.



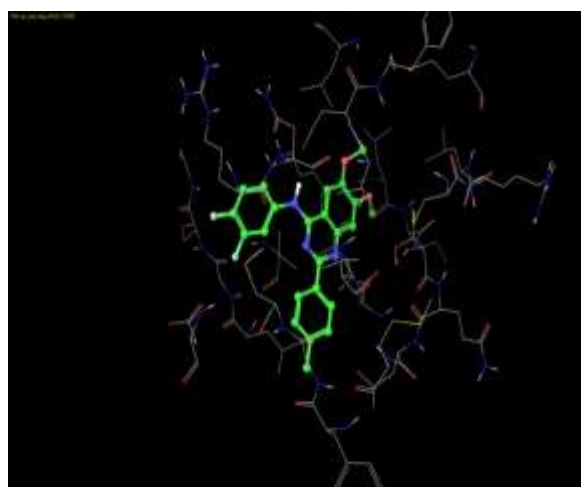
(a)



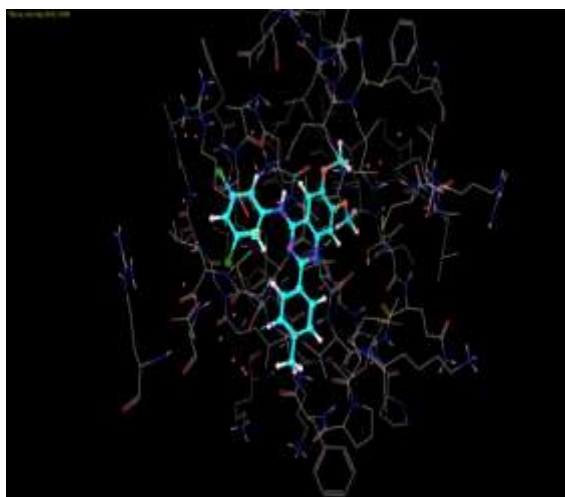
(b)



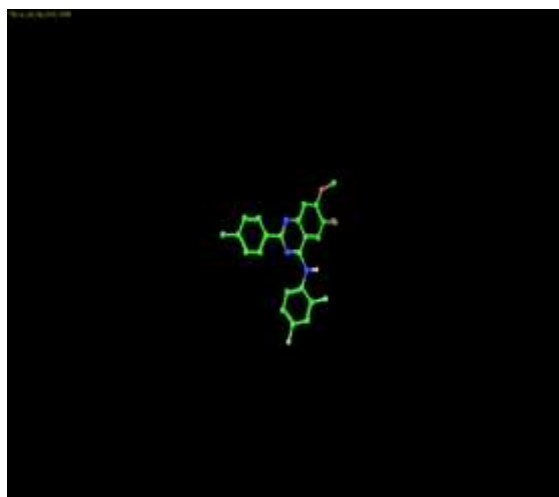
(c)



(d)



(e)



(f)

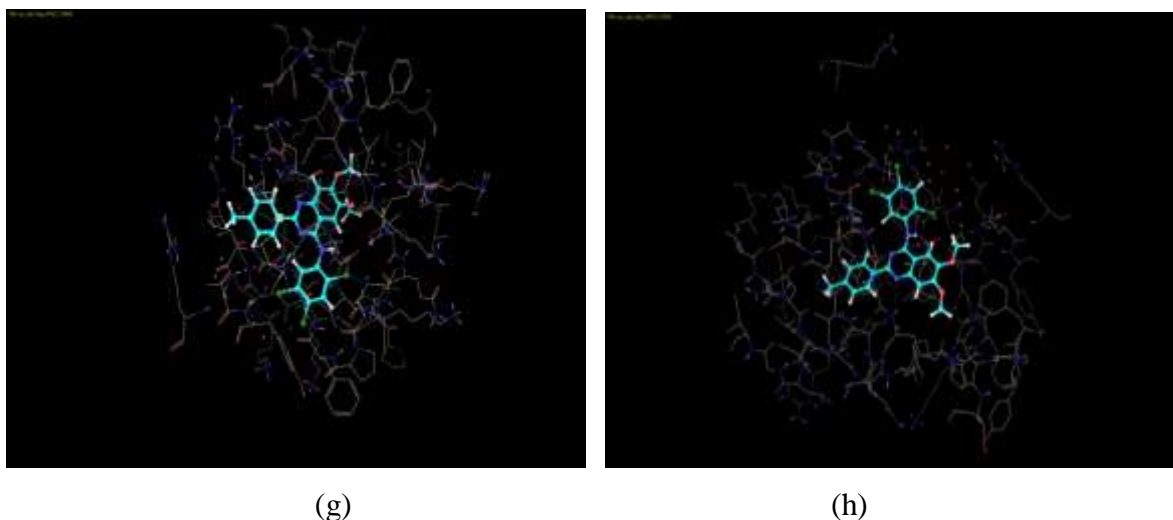


Figure: Structures of the different kinase inhibitors bound to the protein 3w32. Only residues that undergo significant movement or are hydrogen bonded to the ligand are shown.

2. Induced fit results

In virtual docking the ligands are docked into binding site of the receptor where the receptor is held rigid and the ligand is free to move. We have also taken into account receptor flexibility by induced fit docking. In induced fit docking, we obtained different poses of all the best docked analogues. The results of the induced fit docking are given in below Table, which displays the best docked poses. From the results of the induced fit docking, it is clear that there are some considerable changes in the docking scores and energies of the docked complexes.

Table: Results of the induced fit docking

Analogues	Docking Energy	Docking score
Mol37	-5.7	-8.6
Mol12 (SCI)	-6.6	-7.1
Mol35	-6.1	-7.0
Mol5 (SCII)	-5.7	-6.9
Mol41	-5.9	-6.9
Mol4 (SCIV)	-6.7	-6.8
Mol17	-6.0	-6.7
Mol11 (SCIII)	-6.0	-6.6

Docking energy is written only for the best docked poses. All energy values are given in Kcal/mol

CONCLUSION

The glide score can be used as a semi-quantitative descriptor for the ability of ligands to bind to a specific conformation of the protein receptor. Generally speaking for low glide score good ligand affinity to the receptor may be expected. According to the glide score the results of the inhibition for the EGF receptor may be arranged in the following manner: mol37> mol12> mol35>mol15> mol35> mol5>mol41> mol4>mol17>mol11.

Docking studies performed by GLIDE has confirmed that above inhibitors fit into the binding pocket of the EGF receptor. From the results we may observe that for successful docking, intermolecular hydrogen bonding and lipophilic interactions between the ligand and the receptor are very important.

A comparison of the induced fit and virtual docking gives the role of protein flexibility. It is obvious from the results that a combined method of soft docking and side chain optimization gives better results. It is also clear that an average distribution of docking free energy ranging from 2 kcal/mol or more, is sufficient to mis-rank a potential drug candidate as a weak binder. However, by combining the MM-GB/SA and relaxed complex methods we are able to show the best ranked binding modes.

4.4 DESIGNING OF PYRIDO[2,3-D]PYRIMIDINE DERIVATIVES

Protein and ligand preparation

The character of glide results depends on reasonable starting structures of both ligand and protein. Schrödinger offers a comprehensive protein preparation facility in the Protein Preparation Wizard, which is designed to ensure chemical correctness and to optimize protein structures for use with Glide and other products. Schrödinger also offers a comprehensive ligand preparation was subjected to energy minimization by LigPrep module of the software.

Choosing the protein site

Proteins can exhibit induced fit effects on the binding of a ligand, in which the protein conformation changes significantly. This will happen only when more than one co-crystallized complex is available. Glide docking experiments employ only protein geometry in those two approaches is commonly taken. One is to select a single well-suited representative structure of protein to dock into. The other is to use a collection of representative structures, into which each of the candidate ligands is docked. If more than one co-crystallized complex is available, you must decide whether to select a single protein site or to choose two or more sites for use in independent docking experiments.

Cases in which the site changes substantially as different ligands bind may require the use of two or more sites, if finding the maximum number of promising ligands is the main objective.

A procedure for making this determination is as follows-

1. Choose a reference complex and superimpose all other complexes to it.
2. Display the protein for the reference complex and the ligands for each of the other complexes. Examine the active-site region to determine whether the superimposed ligands can fit into the reference site.
3. Display the protein in the reference complex and the protein for each of the other complexes, whether any residues in the superimposed protein differ appreciably in position or conformation from those in the reference site.

4. Judge whether the reference site appears compatible with all the co-crystallized ligands or, if not, whether another site appears more compatible.
5. Choose a more representative site for docking or choose two or more sites if there are large differences between the sites and the objective is to find as many prospective strong binders as possible.
6. Write out a separate file for the protein or proteins that will be prepared and also write out separate files for the superimposed ligands.

Protein preparation

A typical PDB structure file consists only of heavy atoms, can contain water, cofactors, metal ions and can be multimeric. Terminal amide groups can also be misaligned, because the X-ray structure analysis usually cannot be distinguished between -O and -NH₂ groups. Ionization and tautomeric states are also generally unassigned. Glide calculations use an all atom force field for exact energy evaluation. Thus, Glide requires ionization states and bond orders to be properly assigned and performs better when side chains are realigned when necessary and steric clashes are relieved.

The crystal structure of Biotin Carboxylase domain was obtained from the PDB database (Mochalkin I, 2009) with PDB ID 2V58 (Miller J.R, 2009) and PDB ID 4kd1 (Martin M.P. 2013) having a CDK2 in complex with Dinaciclib

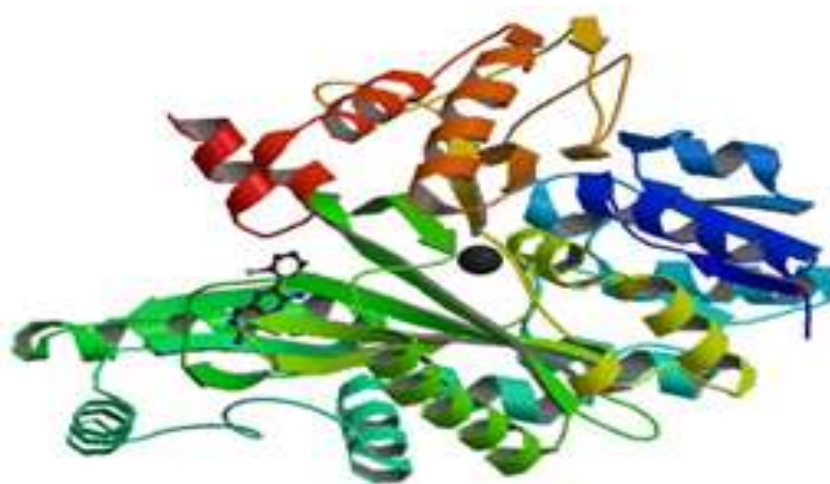


Figure: Crystal structure of biotin carboxylase from *E.coli* in complex with potent inhibitor

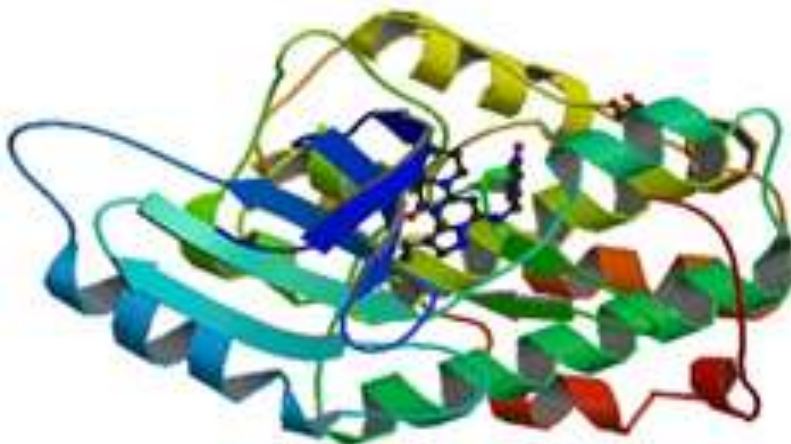


Fig: Crystal structure of CDK2 in complex with Dinaciclib

From Workflows tab, choose protein preparation Wizard.

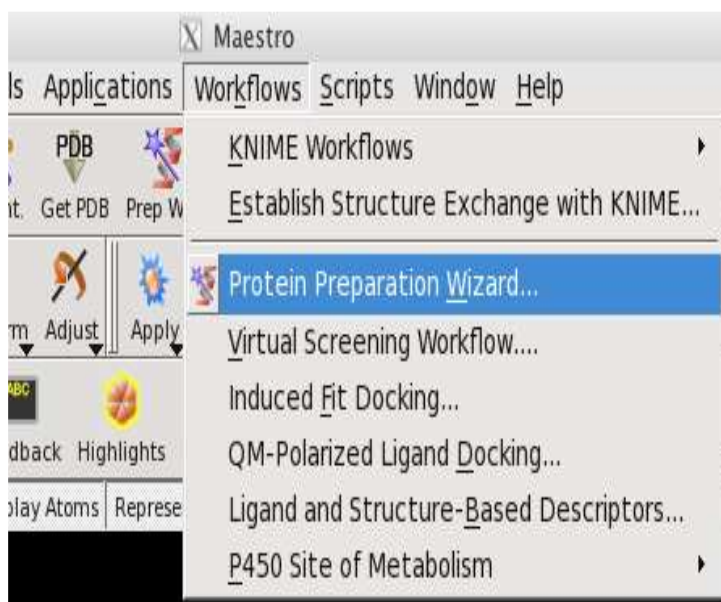


Fig: Protein preparation wizard step

After selecting protein preparation wizard, select import and process tab and import the protein structure from protein data bank and select the options as shown in this window.

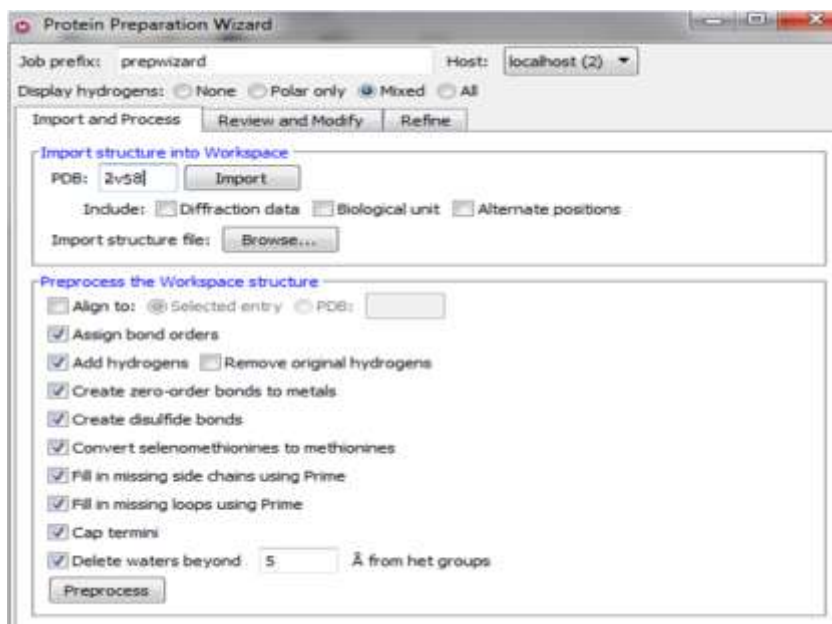


Fig: Protein preparation wizard (import and process step).

The typical structure file from the PDB is not suitable for immediate use in molecular modeling calculations as the PDB structure file consists only of heavy atoms and may include a co-crystallized ligand, water molecules, metal ions, and cofactors. Some structures are multimeric and may need to be reduced to a single unit for that purpose go to next review and modify tab and remove unnecessary water molecule by selecting this chain name i.e. B and delete it.

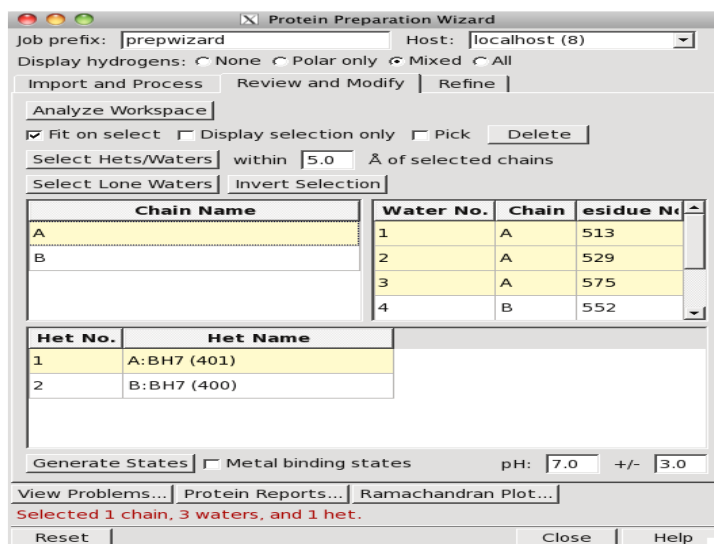


Fig: Protein preparation wizard (review and modify step)

After this process only one chain name is observed in the tab. After that go to the view problem tab if there are any problems then minimize that and move toward refining process. In the refinement process select sample water orientations and set use PROPKA pH 7.0 then optimize it.

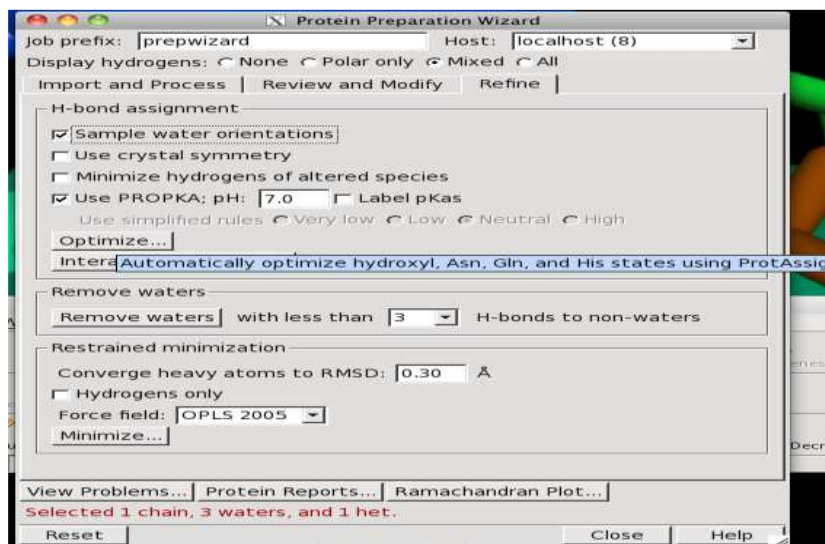


Fig: Protein preparation wizard (Refine step)

After completion of optimization process select 3 H-bond to non-water and in restrained minimization select 0.30 Å converge heavy atoms to RMSD and select force field OPLS 2005 and click on minimize to run this job. After the process is done, a message pops up as shown below. Click Incorporate Now.

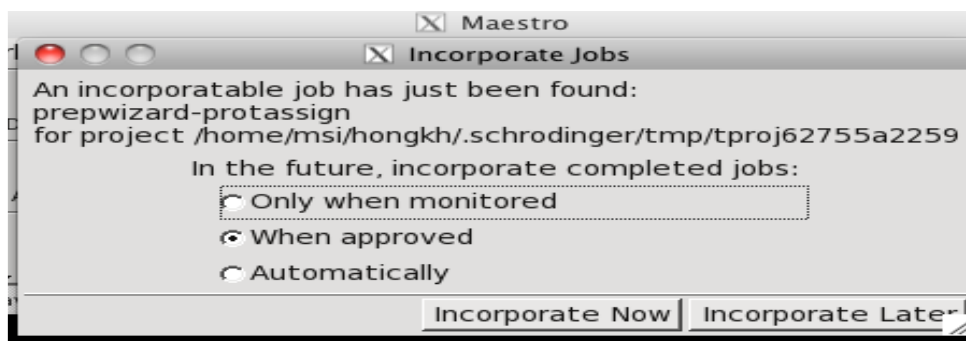


Fig: Incorporation job of prep wizard step

Ligand preparation

Structures supplied to glide must meet the following criteria

1. They must be three-dimensional (3D).
2. They must have ideal bond lengths and bond angles.
3. They must each consist of a single molecule that has no covalent bonds to the receptor, with no accompanying fragments, such as counter ions and solvent molecules.
4. They must have all their hydrogen's
5. They must have a proper protonation state for physiological pH values.

The series of pyridopyrimidine derivatives structures were drawn using the LigPrep module of the Maestro software. Where they were further prepared Choose Tasks from Applications, choose LigPrep. Then, LigPrep window will be displayed. After that browse prepared 2D structure in the format of MDL Molefile [V2000] (*.mol) in LigPrep tab. Set pH 7.0 +/- 2.0, select Desalt, generate tautomers, Retain specified chiralities, select 1 for generating at most per ligand , select 1 for generate low energy ring confirmation and click start to run the job.

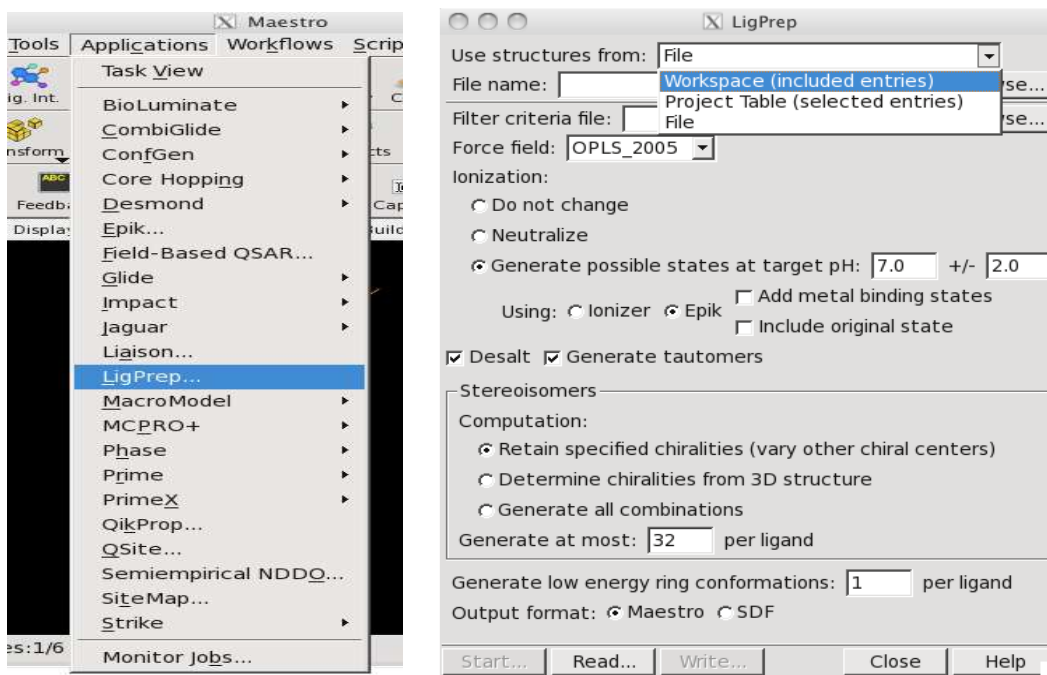
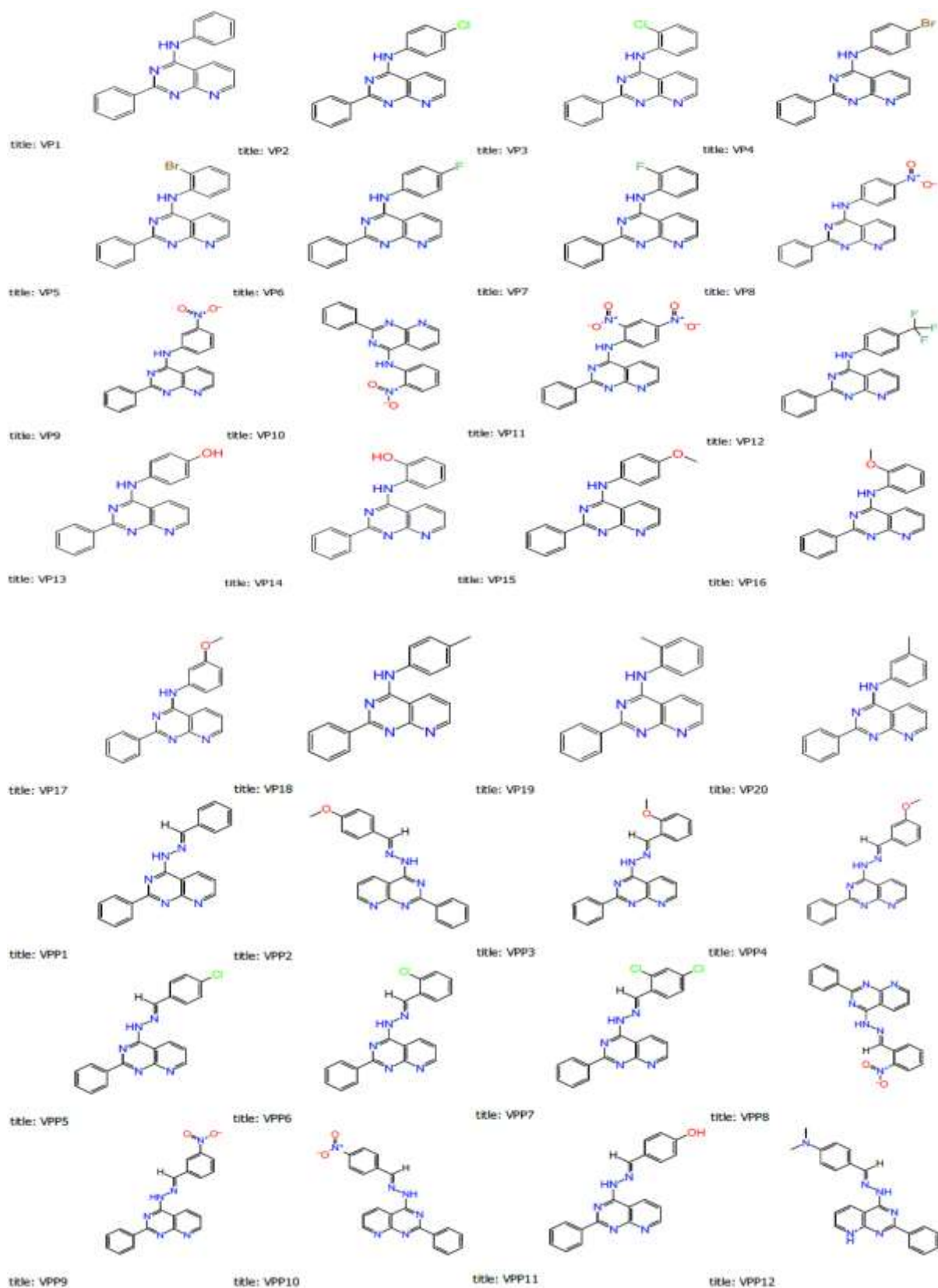
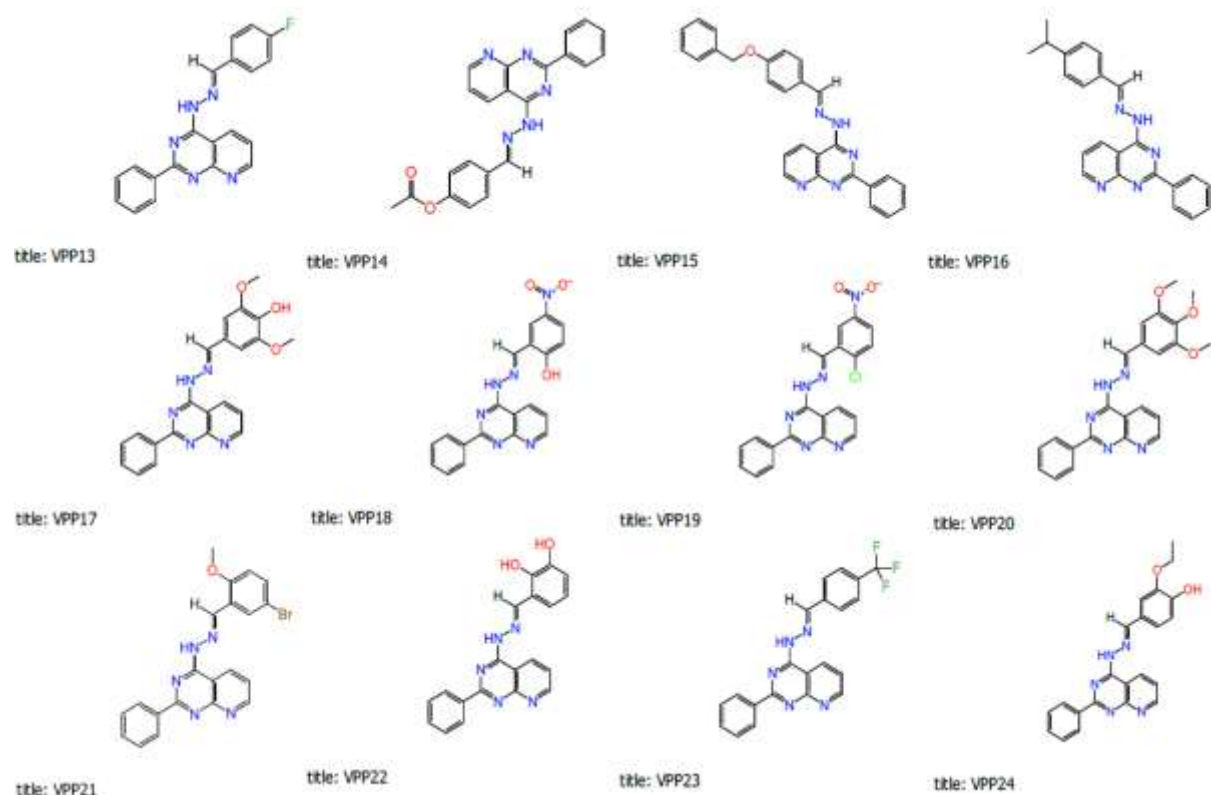


Fig: A) Selection of LigPrep step B) LigPrep step window display.

Table: Prepared ligand for docking





Receptor grid generation

To open the Receptor grid generation panel, choose Receptor Grid Generation from the Applications bar choose the Glide submenu in that receptor grid generation.



Fig: Selection of receptor grid through application.

After selecting receptor grid generation, select receptor tab and pick the ligand to identify i.e. molecule from ligand moiety, the Van der Waals radius scaling factor in the range of 1 and partial charge cut off at 0.25, use the input partial charges as shown in this window.

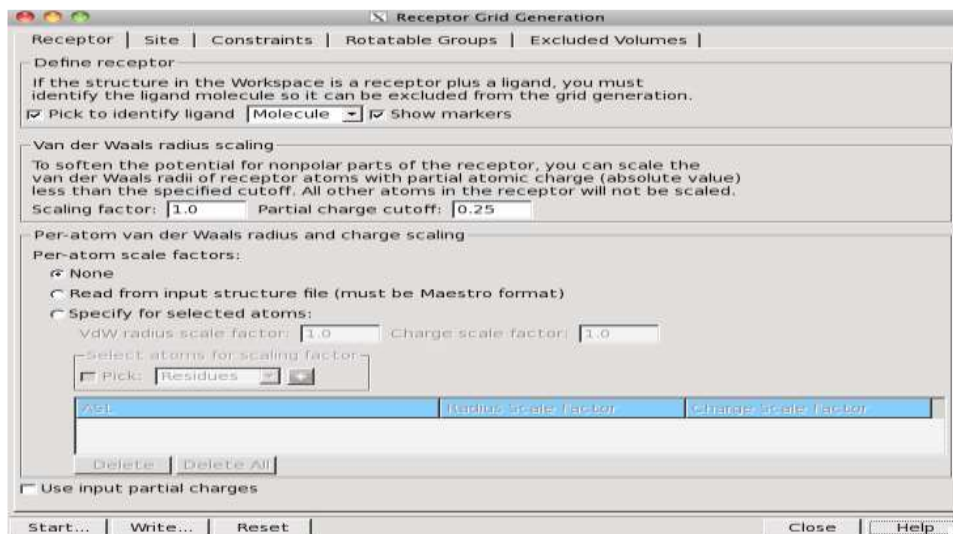


Fig: Receptor grid generation (Receptors ligand selection and other factor)

Then all factors like site, rotatable group, excluded volumes, constraints kept constant. Then run the receptor grid generation following window will come and run it as shown in this window.

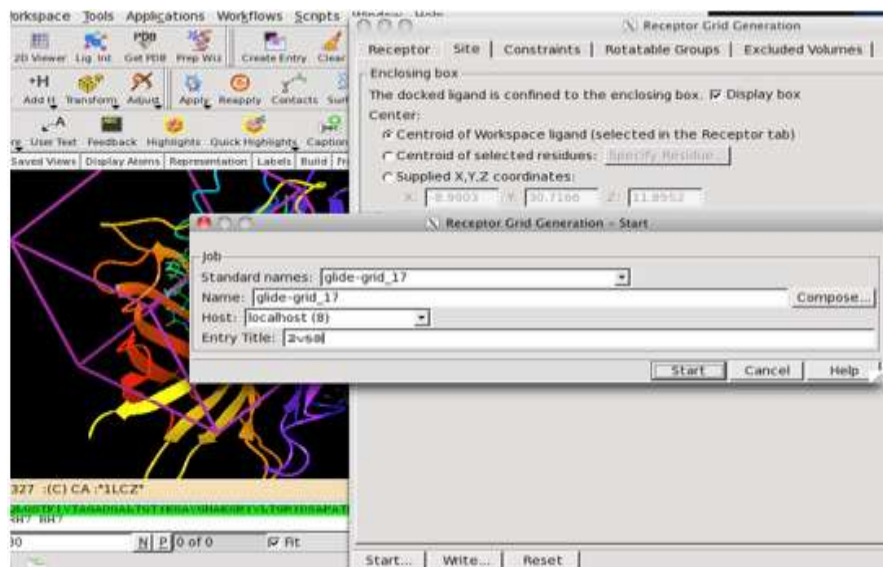


Fig: Receptor grid generation (selection of site and other factor)

Glide docking (ligand docking)

Prepared ligand and receptor were used as the initial coordinates for ligand docking (glide docking) purposes. We have used biotin carboxylase and cyclin dependent kinase 2 as the target receptor. The stage for ligand docking was the receptor grid generation; for that purpose we have used the protein structure. For ligand docking went to Applications>> Glide >> Ligand Docking.

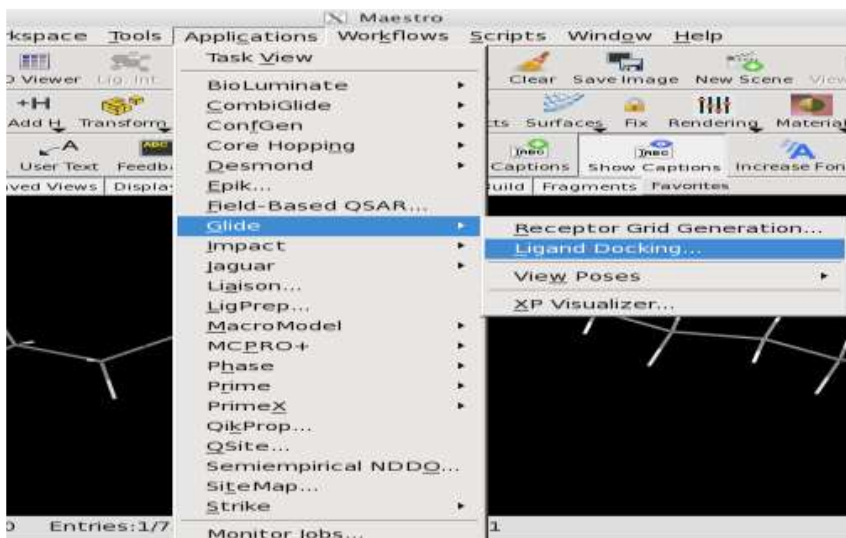


Fig: Selection of Ligand Docking step

The Ligand docking window is shown below. In this tab select settings, select SP (standard precision), select Flexible for ligand sampling, select sample nitrogen inversions, select sample ring confirmation, select penalize non planar conformation for amides only.

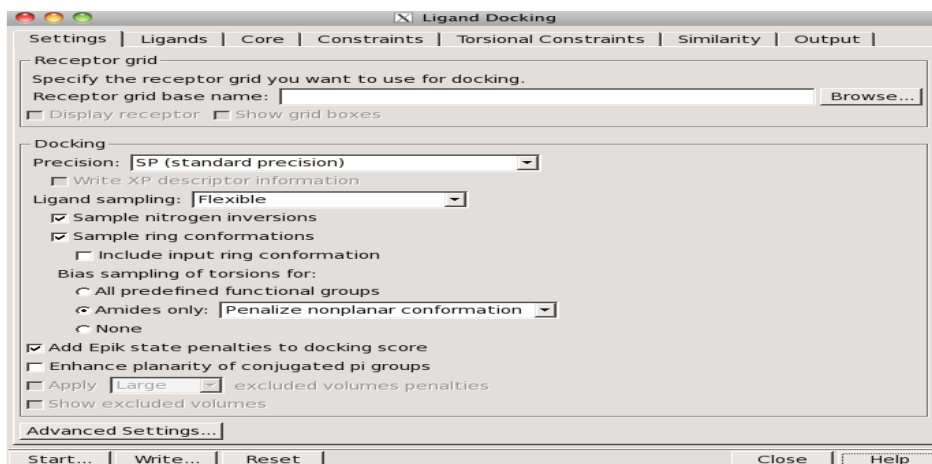


Fig: Ligand docking (selection of settings step)

From Ligands tab, indicate where you will get the ligand from workspace and select value as shown in figure. Click output tab.

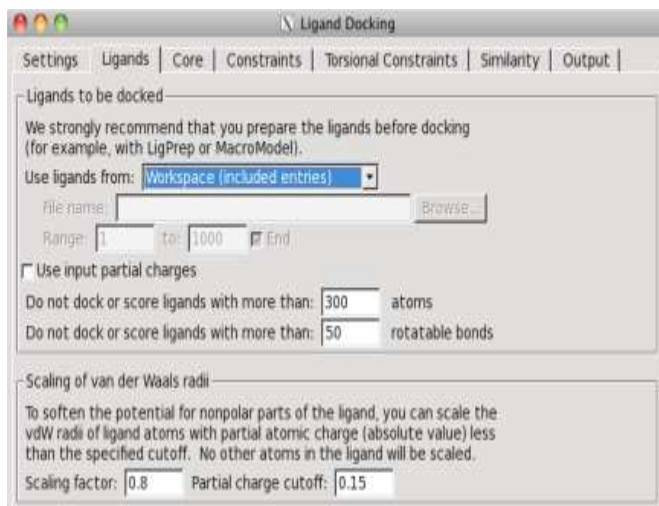


Fig: Ligand docking (Ligand selection step)

From Output tab, choose the options for a docking simulation. Then, click Start.

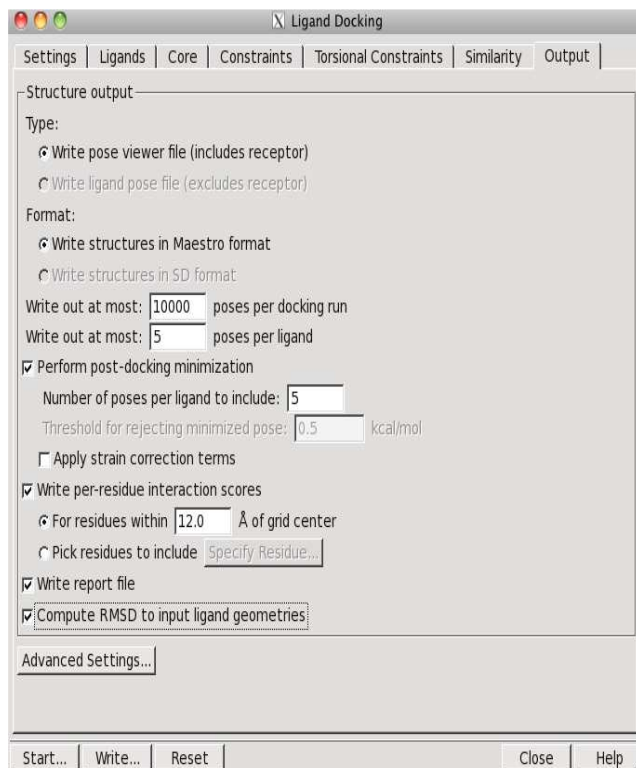


Fig: Ligand docking (output step)

After that, you will see the window below to ask an output file name of the docking simulation. Add the file name and click Start to run the job.

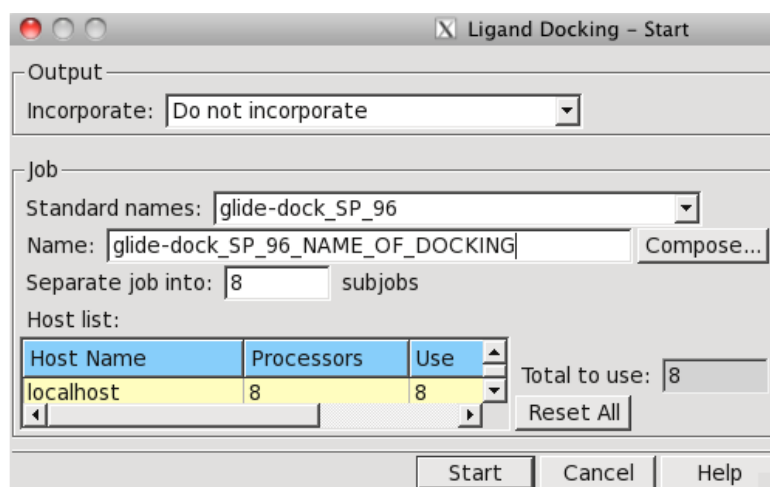


Fig: Ligand docking (final preparation step)

After glide docking, we have performed post-docking minimization to improve the geometry of the docking poses. The post-docking minimization specifies a full force-field minimization of those poses which are considered for the final scoring. After glide docking, the obtained results were used for binding energy calculations and docking scores.

Analysis Docking Poses

The View Poses facility in the Project Table panel enables to display the ligand poses with the receptor in the Workspace, along with hydrogen bonds, bad and ugly contacts, and per-residue interaction information. For Glide SP and XP docking runs, visualize the contributions to the XP docking score, provided that descriptor information was requested in the docking run. The Project Table panel provides a special facility for viewing poses from a pose viewer file. To use this facility you must select a single entry group. The group must contain the receptor as the first entry in the group, followed by the ligands. This is the normal situation when import a pose viewer file into the project. To start viewing poses, choose Setup from the View Poses submenu. The receptor is locked in the Workspace, and the first ligand entry is included.

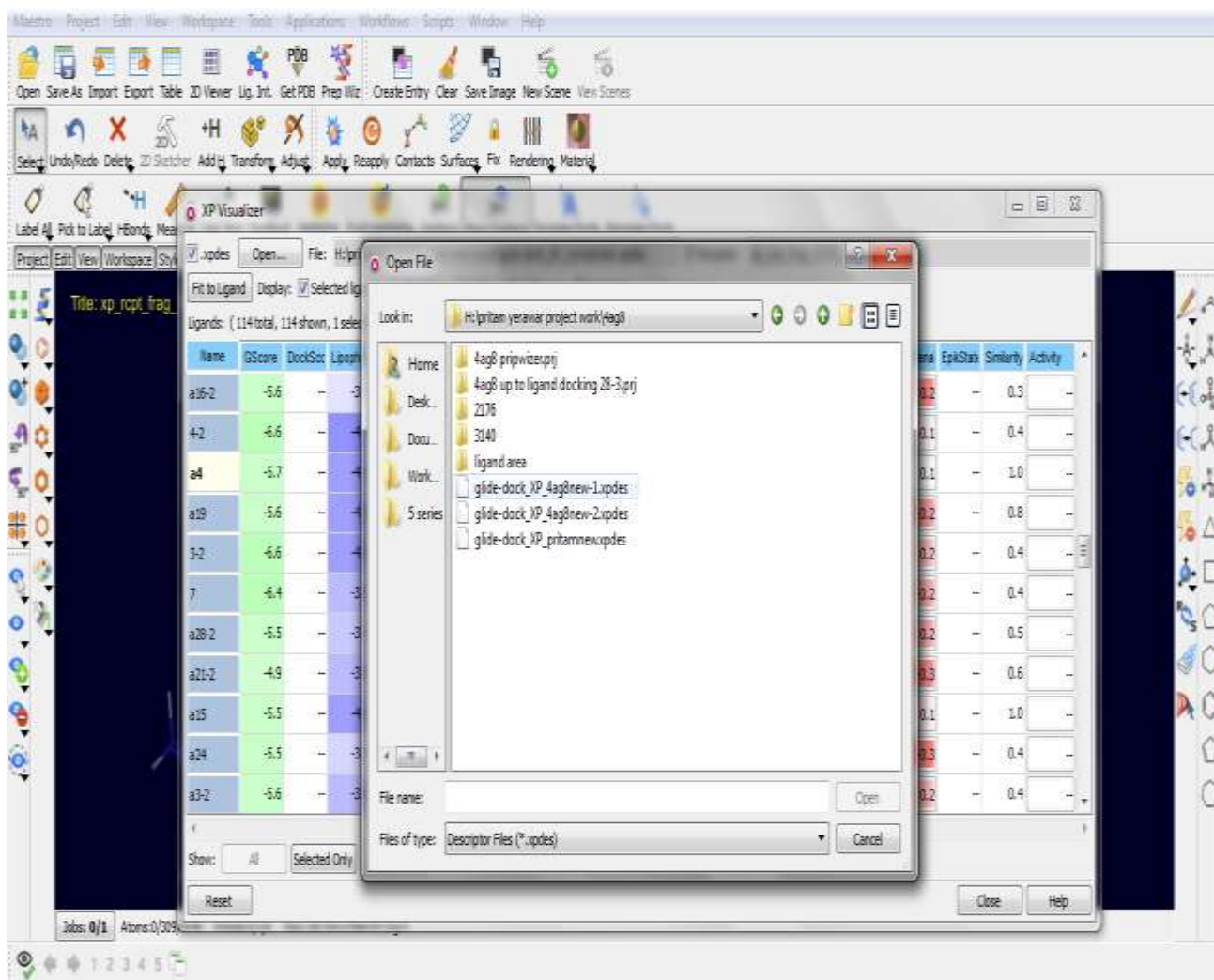


Fig: Analyzing of docking poses through generated (.xpdes) file

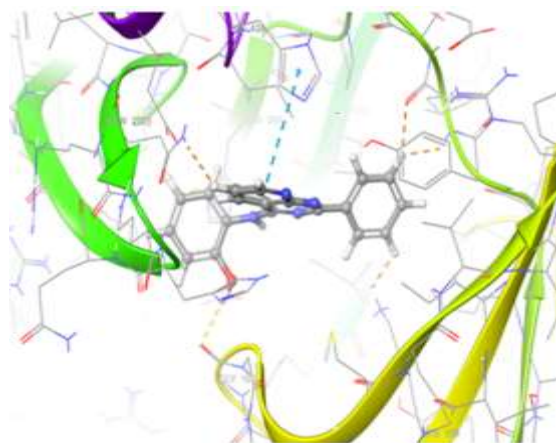
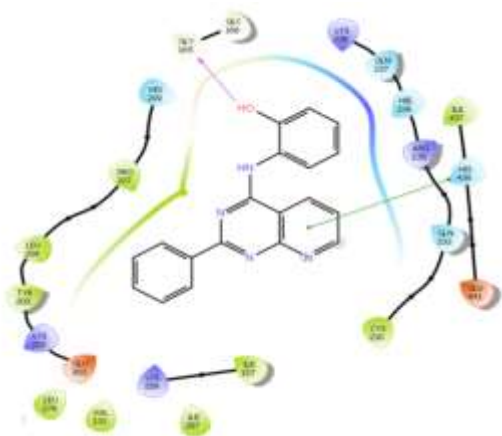
Results and Discussion

Molecular docking studies with PDB 2v58:-

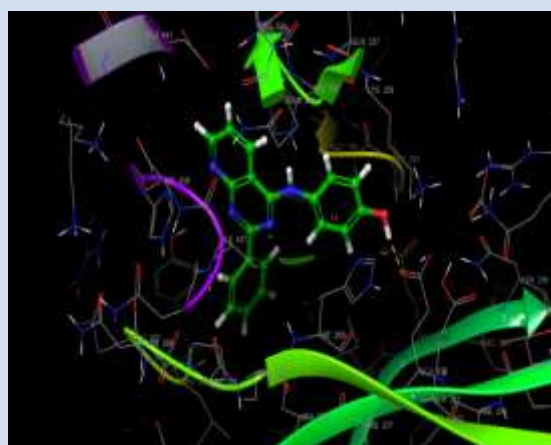
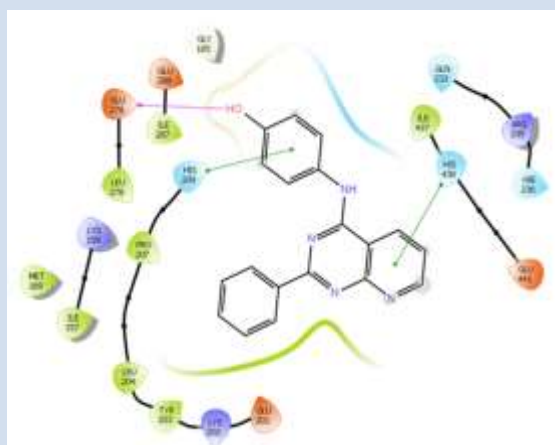
All the compounds were subjected to molecular docking studies to determine the mode of binding and energy changes. The crystal structure of biotin carboxylase (PDB: 2V58) was used for this study and ligands were prepared for docking by method described earlier. The biotin carboxylase is co-crystallized with 6-(2,6-dibromophenyl)pyrido[2,3-d]pyrimidine-2,7-diamine, which we have used as reference ligand for molecular docking studies. It was observed that compound **VP14 (6o)**, **VP13 (6n)**, **VP10 (6r)**, **VP3 (6d)**, **VP20 (6i)** and **VP17 (6l)** showed highest interaction with the enzyme in their molecular docking

studies, the details of docking studies are mentioned in the below table (Supplementary material). The bound ligand in the active site forms covalent nitration with Glu201A, Lys202A, aromatic interactions with Leu204A and Lys159A, it shows weaker interactions with Ile437A and His438. The docked compound **VP3 (6d)**, show a high docking score of -7.58 and Glide energy of -44.50. It forms a salt bridge between pyridopyrimidine nucleus and HIS438. It forms an aromatic interaction with the Lys159, the presence of electronegative substituent like chlorine on the phenylpyridopyrimidine nucleus contributes to its biological activity. Compound **VP17 (6l)**, showed a high docking score of -7.34 and Glide energy of -45.06, the pyridopyrimidine nucleus forms a salt bridge with the residue HIE438 and the phenyl ring formed a salt bridge with HIS226, this may be due to the presence of electron donating group like methoxy on the phenylpyridopyrimidine nucleus. Compound **VP13 (6n)**, show a docking score of -7.76 and Glide energy of -47.34. It forms a salt bridge between pyridopyrimidine nucleus and HIS438, the phenyl ring of substituent forms another salt bridge with HIS209 and a hydrogen bond is formed between hydroxy groups with GLU276. Compound **VP14 (6o)**, showed a high docking score of -7.96 and Glide energy of -46.71, the pyridopyrimidine nucleus forms a salt bridge with the residue HIS438 and the OH group forms a hydrogen bond with GLY165. In case of compounds 6l and 6n there is hydroxyl group (-OH) on the 4th and 2nd positions respectively. Their biological activity, high dock score and hydrogen bond formation with Glu276 and Gly165 suggest importance of strong electron donating character of hydroxyl functional group on the phenylpyridopyrimidine nucleus. Compound **VP10 (6r)**, showed a high docking score of -7.62 and Glide energy of -45.89, the pyridopyrimidine nucleus forms a salt bridge with the residue HIS438 and the phenyl ring formed a salt bridge with HIS209, this may be due to the presence of electron withdrawing group like nitro on the phenylpyridopyrimidine nucleus. Compound **VP20 (6i)**, showed a high docking score of -7.34 and Glide energy of -46.30, the pyridopyrimidine nucleus forms a salt bridge with the residue HIE438 and the phenyl ring formed a salt bridge with HIS236, this may be due to the presence of electron donating group like methyl on the phenylpyridopyrimidine nucleus.

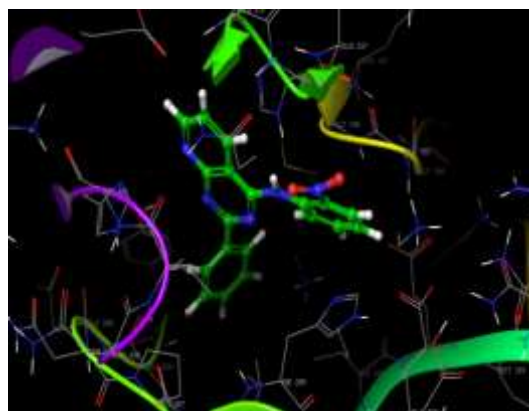
VP14



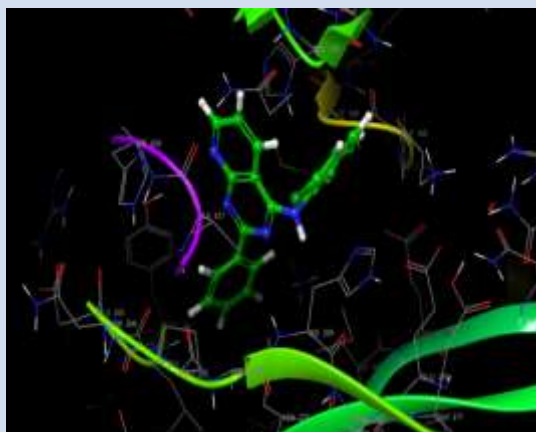
VP13



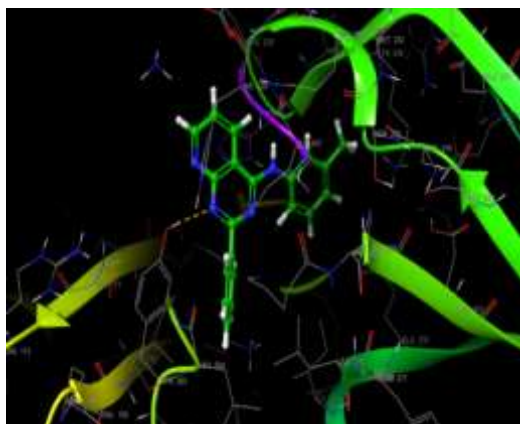
VP10



VP3



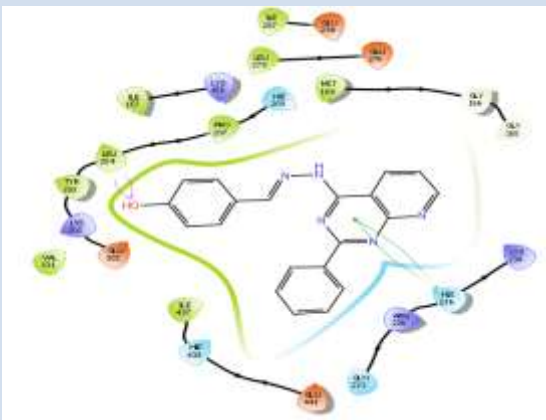
VP20

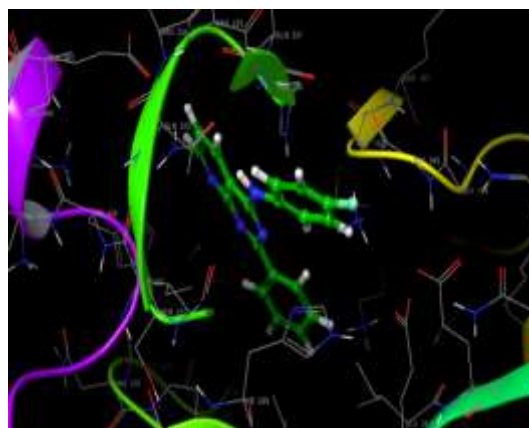
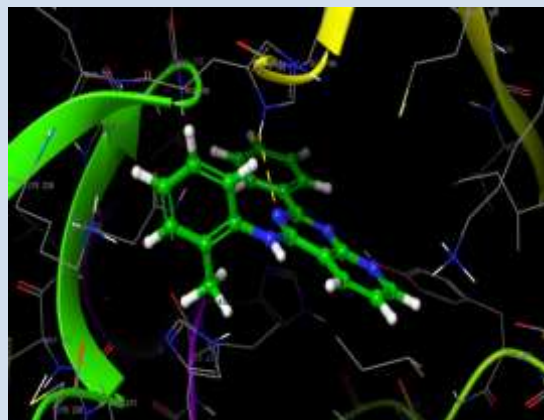
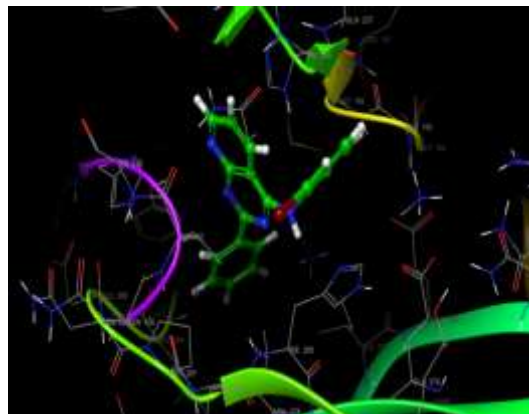


VP17



VPP11





105

Table: Molecular docking study data for docking score, glide score and energy and ecoulomb score for phenylpyridopyrimidine compounds with PDB 2v58:-

Analog ues	Glide Energy	Dockin g score	Glide score	Ecoul score	Analog ues	Glide Energy	Docki ng score	Glide score	Ecoul · Score
VP14	-46.71	-7.96	-7.96	-3.34	VPP1	-36.85	-6.57	-6.57	-5.58
VP13	-47.34	-7.76	-7.76	-7.37	VPP11	-40.79	-6.52	-6.52	-7.29
VP10	-45.89	-7.62	-7.62	-2.54	VP12	-41.09	-6.45	-6.45	-1.89
VP3	-44.50	-7.58	-7.58	-2.07	VP4	-43.03	-6.38	-6.38	-3.61
VP20	-46.30	-7.56	-7.56	-1.19	VP7	-40.56	-6.32	-6.32	-0.84
VP16	-46.30	-7.56	-7.56	-2.83	VPP13	-37.33	-6.31	-6.31	-4.96
VP5	-46.18	-7.48	-7.48	-2.26	VPP14	-42.11	-6.28	-6.28	-5.62
VP19	-45.40	-7.48	-7.48	-1.2	VPP22	-38.72	-6.19	-6.19	-9.14
VP17	-45.06	-7.34	-7.34	-5.78	VPP3	-38.55	-6.07	-6.07	-4.50
VP9	-46.66	-7.11	-7.11	-4.94	VPP24	-37.65	-5.66	-5.66	-5.64
VP8	-45.08	-7.07	-7.07	-4.08	VPP7	-40.56	-5.57	-5.57	-2.09
VP15	-45.39	-6.89	-6.89	-2.24	VPP23	-36.80	-5.57	-5.57	-5.51
VPP12	-39.25	-6.80	-6.80	-6.68	VPP6	-35.44	-5.56	-5.56	-5.17
VP6	-41.07	-6.78	-6.78	-3.53	VPP9	-42.66	-5.26	-5.26	-4.04
VP2	-42.63	-6.65	-6.65	-3.33	VPP20	-39.74	-4.90	-4.90	-6.30
VP18	-41.34	-6.59	-6.59	-3.24	VPP4	-35.99	-4.88	-4.88	-5.39

Molecular docking studies with PDB 4kd1:-

All the compounds were subjected to molecular docking studies to determine the mode of binding and energy changes. The crystal structure (PDB 4KD1) was employed as the receptor with phenylpyridopyrimidine compounds as ligands. The results obtained from the simulation were obtained in the form of dock score; these values represent the minimum energies. Interactions between the ligand and residues were presented in the form of H-bond, van der Waals forces and the pi bonds. The results in the form of 3D and 2D representation were obtained for simplified understanding.

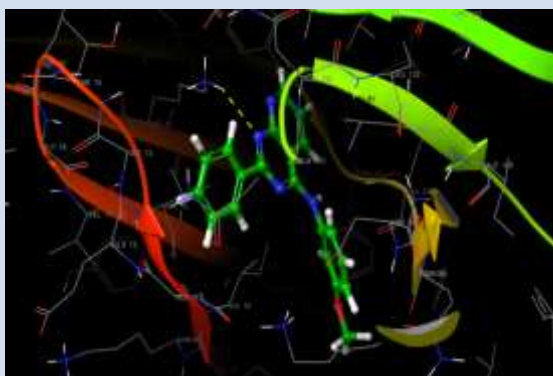
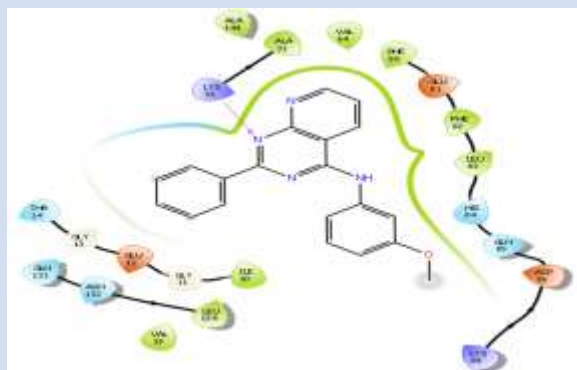
It was observed that compound **VPP20 (7j)**, **VP17 (6l)**, **VPP9 (7n)**, **VP13 (6n)**, **VPP1 (7a)**, **VPP24 (7l)**, **VPP4 (7i)**, **VPP11 (7f)** and **VP10 (6r)** showed highest interaction with the enzyme in their molecular docking studies, the details of docking studies are mentioned in the table 6.1.3 (Supplementary material). The docked compound **VPP20 (7j)**, show a high docking score of -7.53 and Glide energy of -33.02. It forms the hydrazineyl nitrogen forms hydrogen bond with the Leu83. It forms a hydrophobic interaction with phenylpyridopyrimidine, this may be due to the presence of electron donating group like methoxy on the phenylpyridopyrimidine nucleus contributes to its biological activity. Compound **VP17 (6l)**, showed a high docking score of -6.81 and Glide energy of -35.14, the hydrogen bond is formed between nitrogen of at 1st position in pyridopyrimidine nucleus with LYS33. It forms a strong hydrophobic interaction with phenylpyridopyrimidine. Compound **VPP9 (7n)**, showed a high docking score of -6.55 and Glide energy of -29.76, the compound is perfectly fitted in the crystal structure of CDK2 and it forms an strong hydrophobic interaction with phenylpyridopyrimidine this may be due to the presence of electron withdrawing group like nitro on the phenylpyridopyrimidine nucleus. Compound **VP13 (6n)**, showed a high docking score of -6.48 and Glide energy of -30.85, the hydrogen bond is formed between hydroxyl group with GLN85. Compound **VPP4 (7i)**, showed a docking score of -5.94 and Glide energy of -43.39, the hydrogen bond is formed between nitrogen of at 1st position in pyridopyrimidine nucleus with LYS33. It forms a strong hydrophobic interaction with hydrazineyl group and phenylpyridopyrimidine nucleus. Compound **VPP24 (7l)**, showed a docking score of -6.00 and Glide energy of -34.51, the compound is perfectly fitted in the crystal structure of CDK2 and it forms an strong hydrophobic interaction with hydrazineyl group and phenylpyridopyrimidine nucleus.

whereas strong hydrophilic interaction with aromatic region, this may be due to the presence of electron donating group like ethoxy on the aromatic ring contributes to its biological activity.

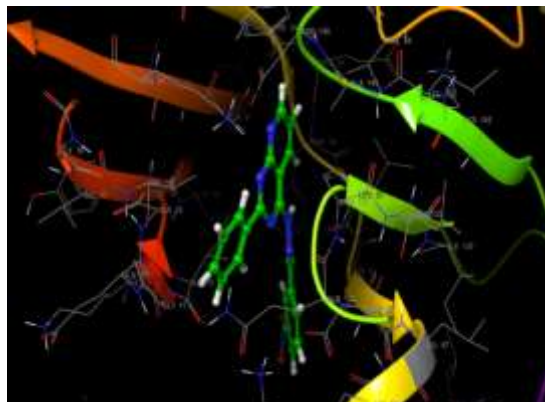
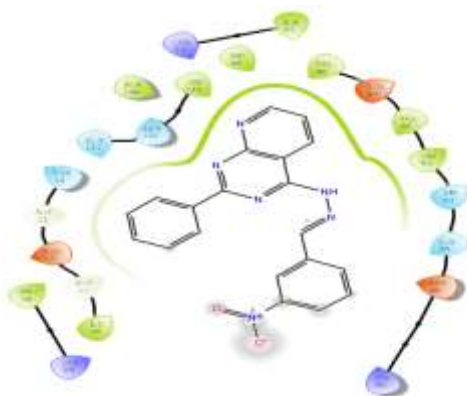
VPP20



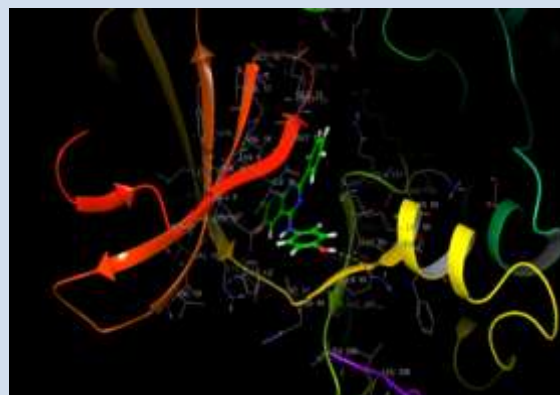
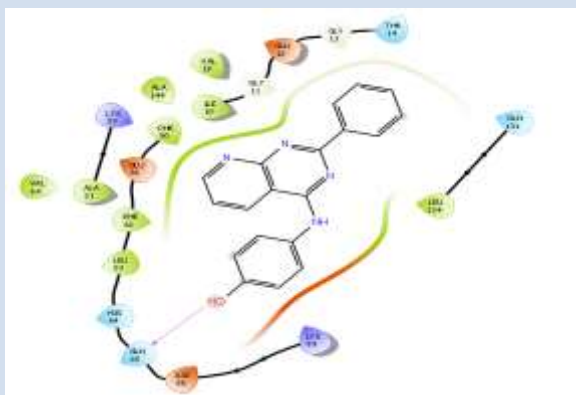
VP17



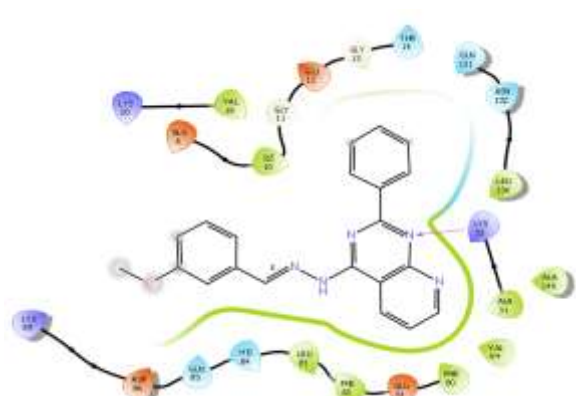
VPP9



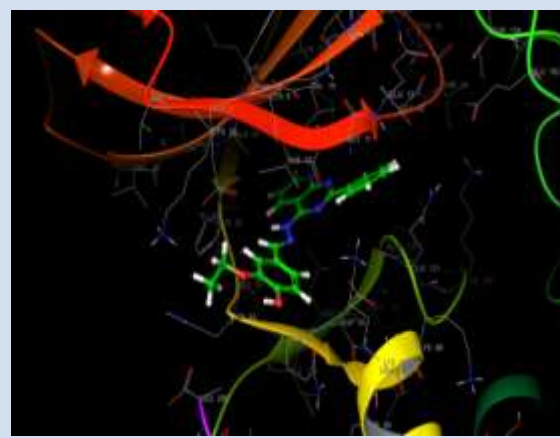
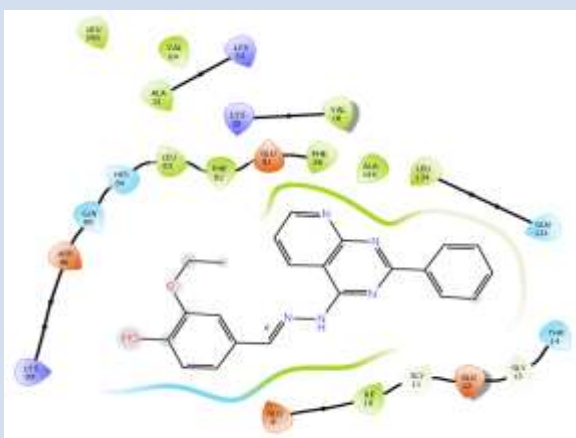
VP13



VPP4

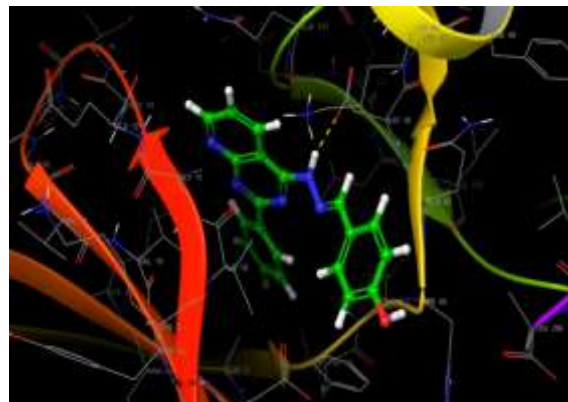


VPP24



VPP11

The diagram illustrates a complex network of nodes and connections, likely representing a biological or chemical pathway. The central structure is a complex organic molecule, possibly a protein or a small molecule, with a benzene ring and a quinoline-like system. The network consists of numerous nodes, each labeled with a number and a name, connected by lines of varying colors and thicknesses. The nodes are color-coded: blue, green, orange, and purple. The connections are represented by lines of different colors (blue, green, orange, purple) and thicknesses, indicating different types of relationships or pathways between the nodes and the central structure.



VP10



Fig: Molecular interaction between CDK and compound

Table:- Molecular docking study data for docking score, glide score and energy for phenylpyridopyrimidine compounds with PDB-4kd1:-

Analogue s	Glide Energy	Docking score	Glide score	Analogues	Glide Energy	Docking score	Glide score
VPP20	-33.02	-7.53	-7.53	VPP23	-36.31	-5.09	-5.09
VP17	-35.14	-6.81	-6.81	VP6	-37.50	-4.96	-4.96
VPP9	-29.76	-6.55	-6.55	VPP6	-34.12	-4.87	-4.87
VP13	-30.85	-6.48	-6.48	VPP13	-35.03	-4.83	-4.83
VPP1	-24.96	-6.37	-6.37	VP5	-38.99	-4.82	-4.82
VPP24	-34.51	-6.00	-6.00	VP2	-34.28	-4.56	-4.56
VPP4	-43.39	-5.94	-5.94	VPP14	-32.29	-4.54	-4.54
VPP11	-28.26	-5.94	-5.94	VP14	-33.66	-4.49	-4.49
VP10	-28.58	-5.91	-5.91	VP8	-38.97	-4.42	-4.42
VP19	-30.26	-5.65	-5.65	VP15	-36.15	-4.21	-4.21
VP18	-33.42	-5.62	-5.62	VP16	-35.31	-4.16	-4.16
VPP22	-37.21	-5.60	-5.60	VP12	-36.00	-3.89	-3.89
VP7	-35.92	-5.38	-5.38	VP20	-32.96	-3.84	-3.84
VPP3	-37.43	-5.36	-5.36	VP9	-36.48	-3.60	-3.60
VPP7	-42.04	-5.33	-5.33	VP3	-37.24	-3.57	-3.57
VPP12	-34.87	-5.20	-5.20	VP4	-37.99	-3.42	-3.42

Conclusion of Molecular Docking Study:-

The glide score (docking score) can be used as a semi-quantitative descriptor for the ability of ligands to bind to a specific conformation of the protein receptor. Generally speaking for low glide score having good ligand affinity to the receptor may be expected.

According to the glide score the results:-

For biotin carboxylase inhibitor may be arranged in the following manner: **VP14> VP13> VP10> VP3> VP20> VP16> VP5> VP19> VP17> VP9 > VP8> VP15> VPP12> VP6** i.e. compound 6o, 6n, 6r, 6d, 6i, 6m, 6f, 6j, 6l, 6q, 6p, 6k, 7p, 6a, 6c, 6h respectively, showed high docking score on BC.

For CDK inhibitor may be arranged in the following manner: **VPP20> VP17> VPP9> VP13> VPP1> VPP24> VPP4> VPP11> VP10** i.e. compound 7j, 6l, 7n, 6n, 7a, 7l, 7i, 7f, 6r respectively, showed high docking score on CDK.

Docking studies performed by GLIDE has confirmed that above inhibitors fit into the binding pocket of the biotin carboxylase and CDK. From the results we may observe that for successful docking, intermolecular hydrogen bonding and lipophilic interactions between the ligand and the receptor are very important.

A comparison of the induced fit and virtual docking gives flexibility role of protein. It is obvious from the results that a combined method of soft glides docking and side chain optimization gives desirable results. It is also clear that an average distribution of docking free energy ranging from 2 kcal/mol or more, is sufficient to mis-rank a potential drug candidate as a weak binder. However, by combining the MM-GB/SA and relaxed complex methods we are able to show the best ranked binding modes.

5. SYNTHESIS OF ANTICANCER DRUG MOLECULES

Materials and Methods

1. All the chemicals used were purchased from commercial sources such as Alfa Aesar, SD fine Chemicals, spectrochem and purified using standard procedure if required.
2. Melting points were recorded on open capillary tube on super fit melting point apparatus and are uncorrected.
3. The purity of all the final compounds was assessed by TLC.
4. Readymade TLC plates were procured from Merck (TLC Silica gel 60 on Aluminum sheets (20 x 20 cm) and cut to suitable sizes as required)
5. Completion of the reaction was monitored by TLC with n-Hexane Ethyl Acetate Methanol (in varying proportion) system.
6. TLC plates were visualized using UV lamp.
7. IR spectra were recorded in KBr disk on “Schimadzu FTIR Model I.R. Affinity” and are reported in centimeters (cm^{-1}).
8. ^1H NMR spectra were recorded using AVANCE II 400 NMR Spectrometer with tetramethylsilane (TMS) as the internal standard in DMSO.
9. Mass spectra were recorded using Mass Spectrometer; the spectra are recorded on WATERS, Q-TOF MS ES^+ and MICROMASS (LC-MS) instrument.

Characterization Studies

After synthesis of a new compounds it is identified by means of physical and chemical parameters like melting point, boiling point, solubility, chemical tests, elemental analysis etc. other analytical methods like TLC, UV, IR, NMR and Mass spectroscopy, were also applied in characterization of newly synthesized compounds, a brief outline of which is given below.

Thin layer chromatography

Thin layer chromatography is a method of analysis in which the stationary phase is a finely subdivided solid which is spread over as a thin layer on a rigid plate and mobile phase, a liquid, allowed to migrate across the surface of the plate.

The technique is widely used for the identification of the organic compounds with characteristic R_F values. This method is also applied to determine the progress of reaction

and to examine the purity of end product. Prepared silica gel plates were used Ethyl acetate: N-hexane in various proportions as (4:6, 5:5, 6:4) and Ethyl Acetate: Petroleum ether: Methanol (4:6:2 drops, 3:7:3 drops) was used as a mobile phase. After the development of the chromatogram the spots were detected by placing the plate in iodine chamber R_f value was calculated for each compound by using formula,

$$R_f \text{ value} = \frac{\text{Distance travelled by solute}}{\text{Distance travelled by solvent}}$$

Infrared spectral studies

The important advantage of IR over the other technique is that it gives fingerprints ($1300 - 650 \text{ cm}^{-1}$) information about the structure (functional group, bonding with each other) of molecules easily.

IR spectra were recorded in KBr on “Schimadzu FTIR model no. I.R.Affinity1” and are reported in cm^{-1} .

Nuclear magnetic resonance spectra

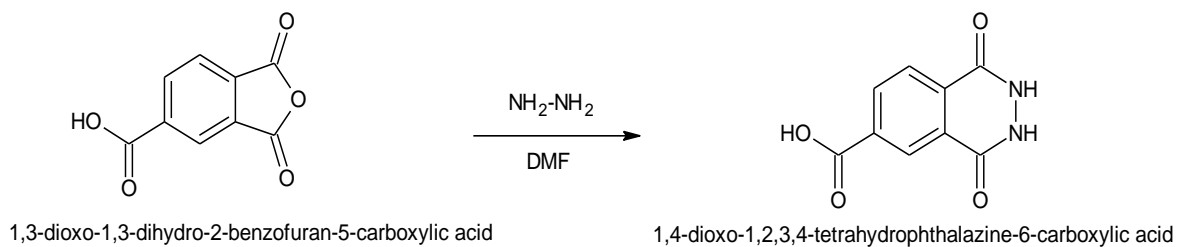
This technique is useful in assuming the structure of molecule. Synthesized compounds were subjected to ^1H NMR spectral studies on the “BRUKER AVANCE II 400 NMR spectrometer”.

Mass Spectral Studies

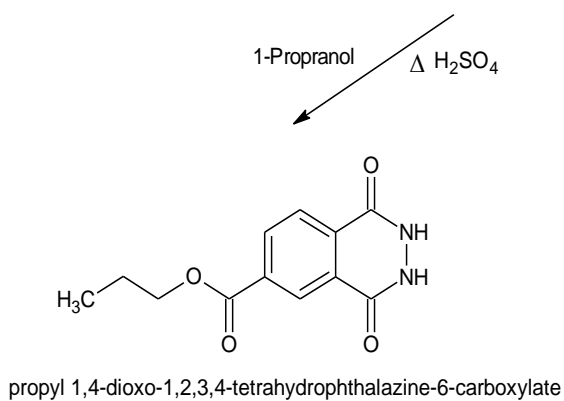
Mass spectra were reported at “Sophisticated Analytical Instrumentation Faculty, Punjab University, Chandigarh” with Mass spectrometer, Make: Varian Inc. USA; Model: 410 prostar Binary LC with 500 MS IT PDA Detectors.

5.1 SYNTHESIS OF PHTHALAZINE DERIVATIVES

5.1.1 Synthesis of 1,6-Disubstituted Phthalazine Derivatives

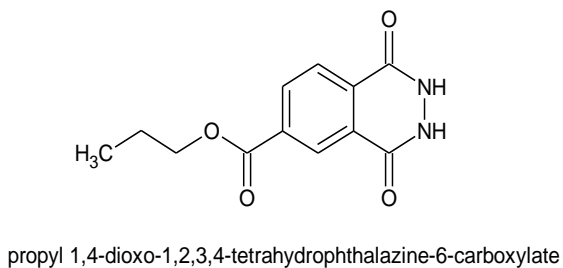


Step-I

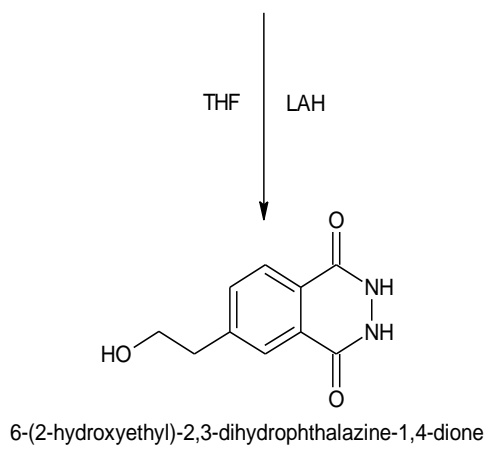


Step- II

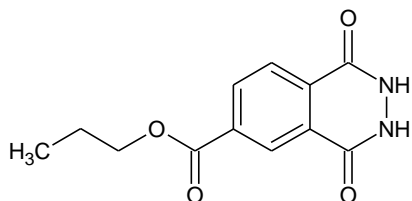
Ester Derivative



Alcohol Derivative



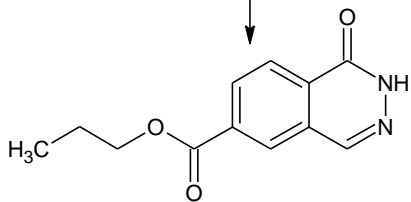
Step-III



propyl 1,4-dioxo-1,2,3,4-tetrahydrophthalazine-6-carboxylate

Step II-IV

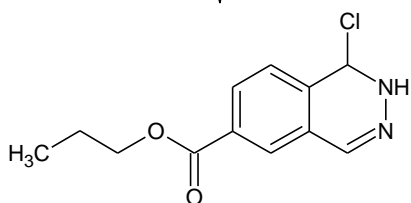
THF NaBH_4



propyl 1-oxo-1,2-dihydrophthalazine-6-carboxylate

Step-V

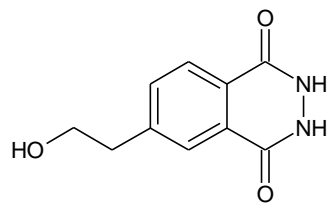
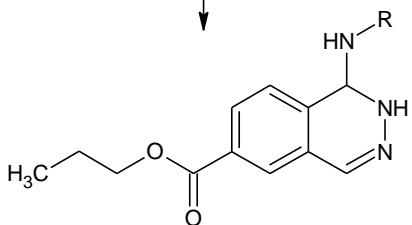
Chlorination POCl_3



propyl 1-chloro-1,2-dihydrophthalazine-6-carboxylate

Step-VI

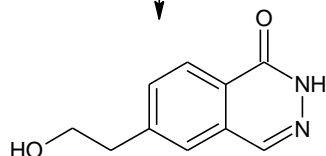
Substituted Aniline Isopropanol



6-(2-hydroxyethyl)-2,3-dihydrophthalazine-1,4-dione

Step III-IV

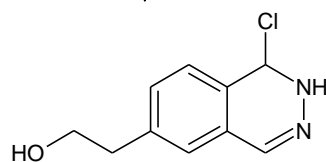
THF NaBH_4



6-(2-hydroxyethyl)phthalazin-1(2H)-one

Step-V

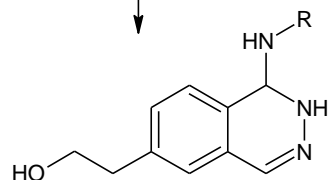
Chlorination POCl_3



2-(1-chloro-1,2-dihydrophthalazin-6-yl)ethanol

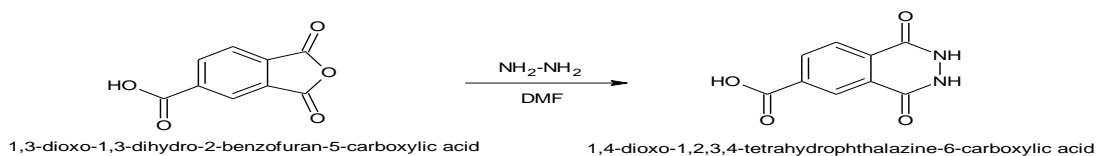
Step-VI

Substituted Aniline Isopropanol



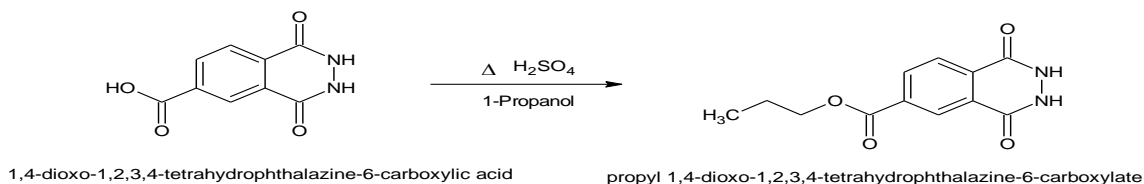
General Steps of Synthesis

Step-I Preparation of 1, 4-dioxo-1, 2, 3, 4-tetrahydrophthalazine-6-carboxylic acid⁵¹



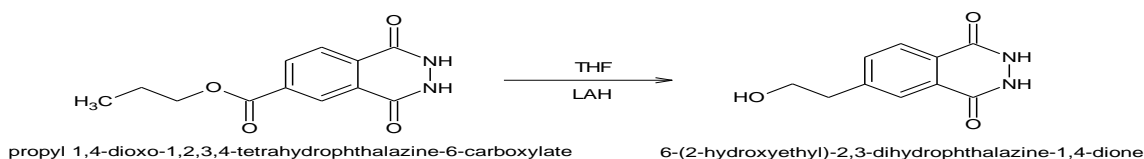
A Solution of 19.2 g of trimetallic anhydride in 200ml of dimethyl formamide was heated at 100^{0c} and solution of 9.6g hydrazine in 100ml of dimethyl formamide was added over about 1 minute. A tar ball formed which eventually broken up on continued heating and stirring for an hour, cooled, filtered and washed with dimethyl formamide and ether.

Step-II: Preparation of Propyl 1,4- dioxo-1,2,3,4-tetrahydrophthalazine-6-carboxylate



The crude acid from step-1 was refluxed with stirring in 1600ml ethanol containing 50ml conc. sulphuric acid for 20 hr. The reaction mixture was cooled, filtered and washed with ethanol and dried.

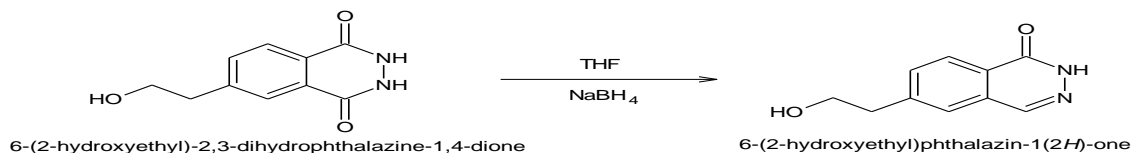
Step-III Preparation of 6-(2-hydroxyethyl)-2, 3-dihydrophthalazine-1,4-dione



The solid ester from step-II (28.8g) was added to the solution of 8g lithium aluminium hydride (LH) in 500ml tetrahydrofuran (THF) at 5^{0c}(ice bath cooling with little heat of evolution), then the temperature of reaction mixture was allowed to rise at room temperature. The mixture was stirred for 4 hr. Then excess of lithium aluminium hydride was destroyed by 60ml ethyl acetate, follow by 40ml water, then 180 ml 6N hydrochloric acid. The mixture was diluted with another 500ml of water and tetrahydrofuran was removed under vacuum. Then product was filtered off, washed with dilute hydrochloric acid and finally washed with neutral water before drying.

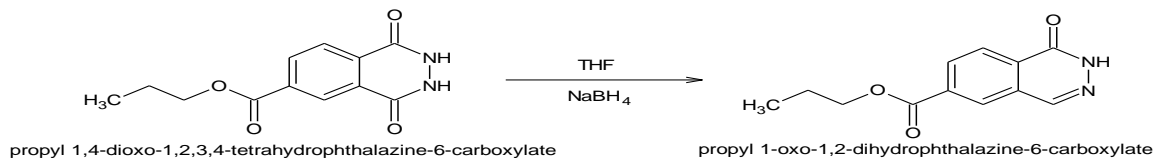
Step IV

1. Preparation of 6-(2-hydroxyethyl)phthalazin-1(2H)-one



NaBH₄ (126.2g, 3.32mol) was added to slowly to stirred solution of step-iii in dry THF (750ml) at 0-10^{0c} Anhydrous methanol was added to reaction mixture drop wise at 0-10^{0c} o-10^{0c} and reaction mixture was stirred at room temperature for 3hr . The mixture was concentrated under reduced pressure. The residue was poured in 10% hydrochloric acid aqueous solution (1000ml), stirred intensively for 3 hr. and separated by filtration. The solid was alkalinized with 10% Na₂CO₃ aqueous solution (1000 mL), stirred for 1 hr and separated by filtration to give compound as a white crystal.

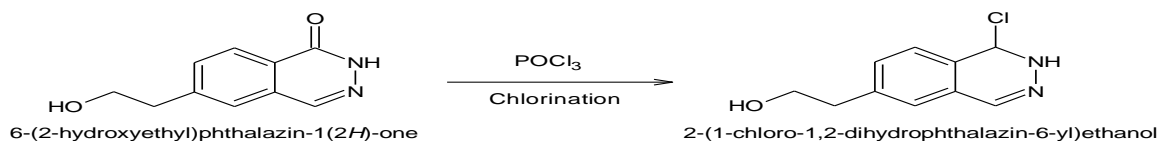
2. Preparation of propyl 1-oxo-1,2-dihydrophthalazine-6-carboxylate



NaBH₄ (126.2g, 3.32mol) was added to slowly to stirred solution of step-ii in dry THF (750ml) at 0-10^{0c} Anhydrous methanol was added to reaction mixture drop wise at 0-10^{0c} o-10^{0c} and reaction mixture was stirred at room temperature for 3hr . The mixture was concentrated under reduced pressure. The residue was poured in 10% hydrochloric acid aqueous solution (1000ml), stirred intensively for 3 hr. and separated by filtration. The solid was alkalinized with 10% Na₂CO₃ aqueous solution (1000 mL), stirred for 1 hr and separated by filtration to give compound as a white crystal.

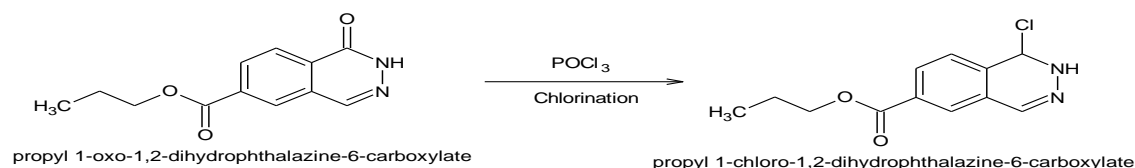
Step-V

1. Preparation of 2-(1-chloro-1,2-dihydrophthalazine-6-yl)ethanol



Step IV (1) Compound (17.5 g, 0.07 mol) was added to a stirred solution of POCl₃ (170mL) and CH₃CN (80mL) at room temperature, and then 3 drops of DMF were added to the mixture. The reaction mixture was heated to 90 °C for 3hr. The mixture was concentrated under reduced pressure. The residue was poured into ice water (500 mL), alkalized with a 10%Na₂CO₃ aqueous solution to pH7-8 and separated by filtration to give compound as a red solid.

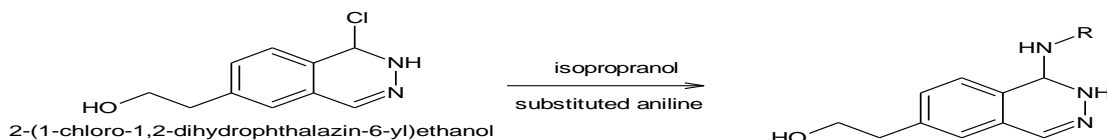
2. Preparation of propyl 1-chloro-1,2-dihydrophthalazine-6-carboxylate



Step IV (2) Compound (17.5 g, 0.07 mol) was added to a stirred solution of POCl₃ (170mL) and CH₃CN (80mL) at room temperature, and then 3 drops of DMF were added to the mixture. The reaction mixture was heated to 90 °C for 3hr. The mixture was concentrated under reduced pressure. The residue was poured into ice water (500 mL), alkalized with a 10%Na₂CO₃ aqueous solution to pH7-8 and separated by filtration to give compound as a red solid.

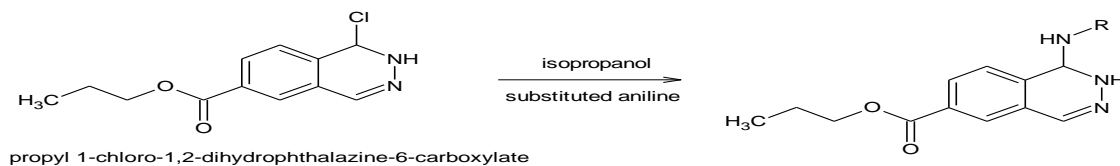
Step-VI

1. Preparation of 1-(substituted phthalazine) 6-yl ethanol



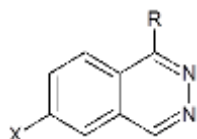
Product from step V (1) (0.181 g, 0.7mmol) & substituted aniline (0.177 g, 0.7mmol.) in isopropanol (20ml) was heated at reflux and stirred for 4hr. The white solid was filtered while hot, recrystallized from methanol or DMF to give product.

2. Preparation of 1-(substituted phthalazine) 6-carboxylate

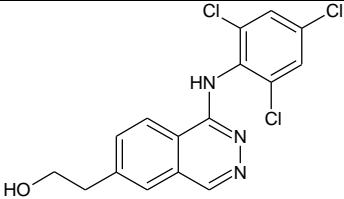
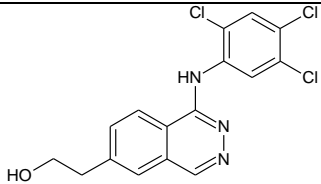
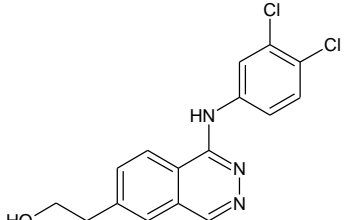
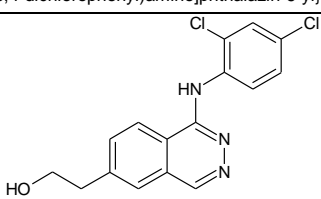
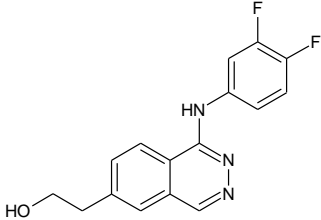
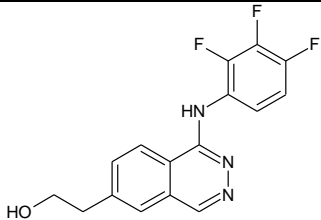
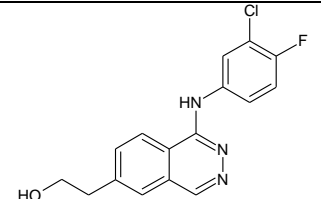


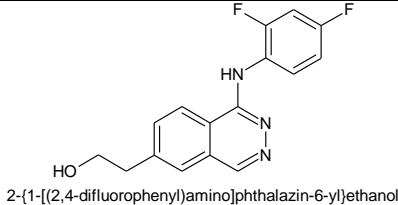
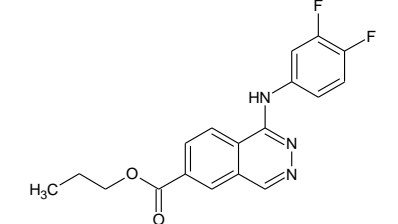
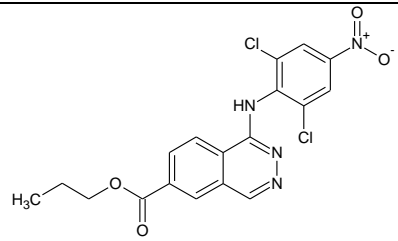
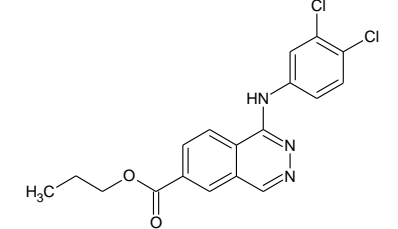
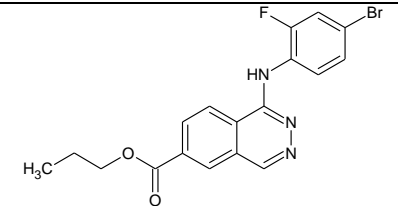
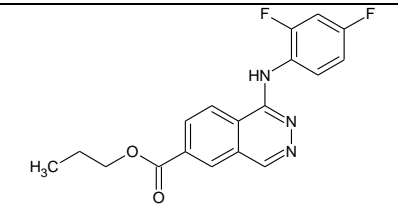
Product from step V (2) (0.181 g, 0.7mmol) & substituted aniline (0.177 g, 0.7mmol.) in isopropanol (20ml) was heated at reflux and stirred for 4hr. The white solid was filtered while hot, recrystallized from methanol or DMF to give product.

Table. Structure of Synthesized Aminophthalazine Derivative



Compound code	Structure	R	X
1.	<p>2-[(3,5-difluorophenyl)amino]phthalazin-6-yl)ethanol</p>	3,4-Di Fluoro Aniline	HOC ₂ H ₅
2.	<p>2-[(2,5-dichlorophenyl)amino]phthalazin-6-yl)ethanol</p>	2,5 Dichloro aniline	HOC ₂ H ₅
3.	<p>propyl 1-[(3,5-difluorophenyl)amino]phthalazine-6-carboxylate</p>	3,5 Difluoro aniline	COOC ₃ H ₇
4.	<p>propyl 1-[(3-chloro-4-fluorophenyl)amino]phthalazine-6-carboxylate</p>	3- Chloro, 4 -Fluoro aniline	COOC ₃ H ₇
5.	<p>2-[(4-bromo-2-fluorophenyl)amino]phthalazin-6-yl)ethanol</p>	4 -Bromo, 2- Fluro aniline	HOC ₂ H ₅

6.	 <p>2-{1-[(2,4,6-trichlorophenyl)amino]phthalazin-6-yl}ethanol</p>	2,4,6 Trichloro aniline	HOC ₂ H ₅
7.	 <p>2-{1-[(2,4,5-trichlorophenyl)amino]phthalazin-6-yl}ethanol</p>	2,4,5 Trichloro aniline	HOC ₂ H ₅
8.	 <p>2-{1-[(3,4-dichlorophenyl)amino]phthalazin-6-yl}ethanol</p>	3,4 dichloro aniline	HOC ₂ H ₅
9.	 <p>2-{1-[(2,4-dichlorophenyl)amino]phthalazin-6-yl}ethanol</p>	2,4 Dichloro aniline	HOC ₂ H ₅
10.	 <p>2-{1-[(3,4-difluorophenyl)amino]phthalazin-6-yl}ethanol</p>	3,4 Difluoro aniline	HOC ₂ H ₅
11.	 <p>2-{1-[(2,3,4-trifluorophenyl)amino]phthalazin-6-yl}ethanol</p>	2,3,4 Trifluoro aniline	HOC ₂ H ₅
12.	 <p>2-{1-[(3-chloro-4-fluorophenyl)amino]phthalazin-6-yl}ethanol</p>	3 chloro 4 fluoro aniline	HOC ₂ H ₅

13.	 <p>2-[(1-[(2,4-difluorophenyl)amino]phthalazin-6-yl)ethanol</p>	2,4 Difluoro	HOC ₂ H ₅
14.	 <p>propyl 1-[(3,4-difluorophenyl)amino]phthalazine-6-carboxylate</p>	3,4 Difluoro	COOC ₃ H ₇
15.	 <p>propyl 1-[(2,6-dichloro-4-nitrophenyl)amino]phthalazine-6-carboxylate</p>	2,6 Dichloro 4 nitro aniline	COOC ₃ H ₇
16.	 <p>propyl 1-[(3,4-dichlorophenyl)amino]phthalazine-6-carboxylate</p>	3,4 Dichloro aniline	COOC ₃ H ₇
17.	 <p>propyl 1-[(4-bromo-2-fluorophenyl)amino]phthalazine-6-carboxylate</p>	4 -Bromo, 2 -fluoro aniline	COOC ₃ H ₇
18.	 <p>propyl 1-[(2,4-difluorophenyl)amino]phthalazine-6-carboxylate</p>	2,4 Difluoro aniline	COOC ₃ H ₇

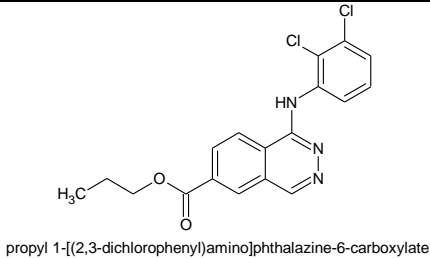
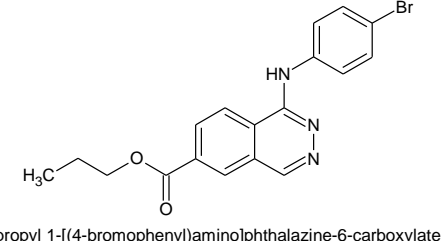
19.	 <p>propyl 1-[(2,3-dichlorophenyl)amino]phthalazine-6-carboxylate</p>	2,3 Dichloro aniline	COOC ₃ H ₇
20.	 <p>propyl 1-[(4-bromophenyl)amino]phthalazine-6-carboxylate</p>	4- Bromo aniline	COOC ₃ H ₇

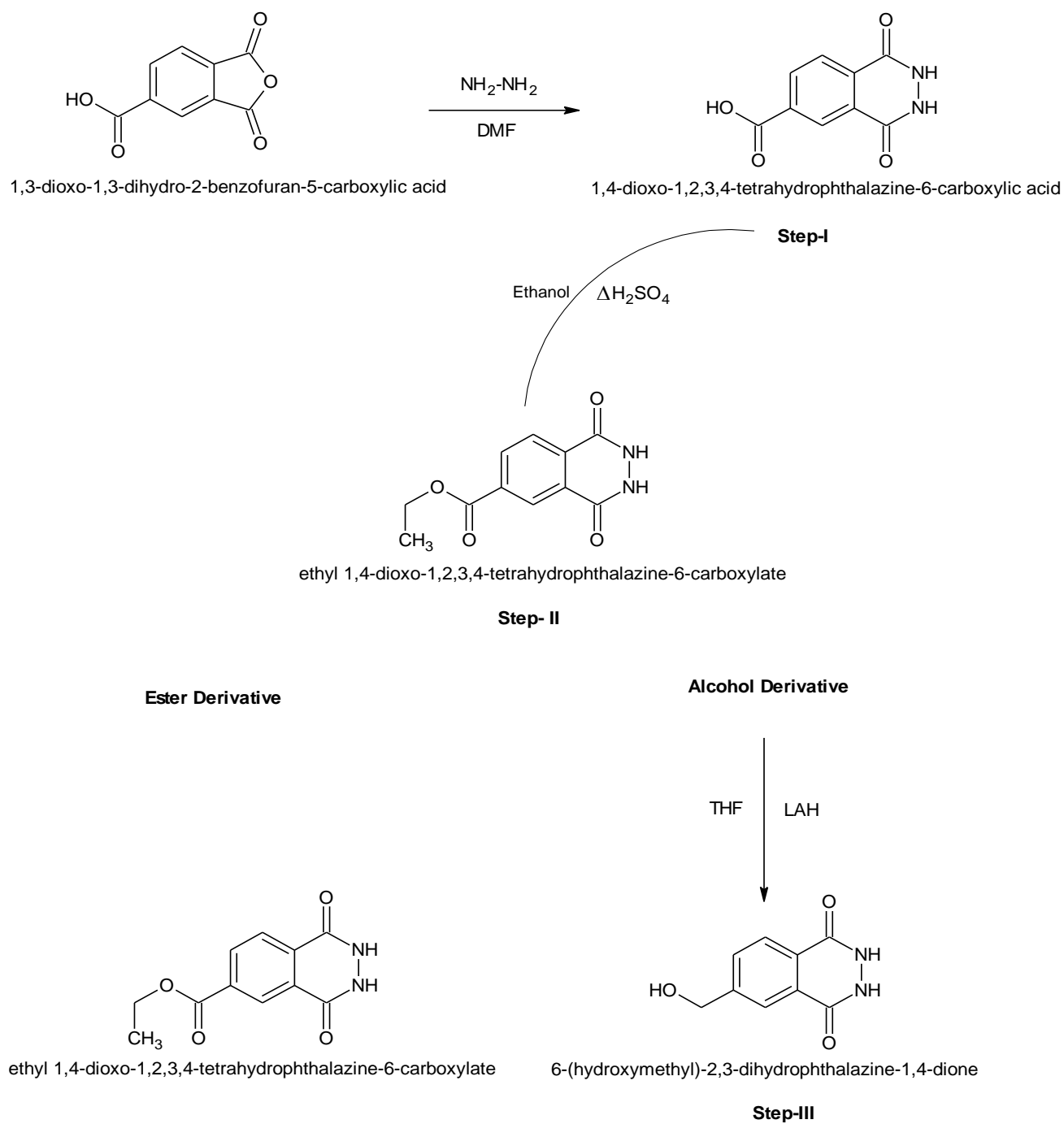
Table: Physiochemical data of synthesized compound

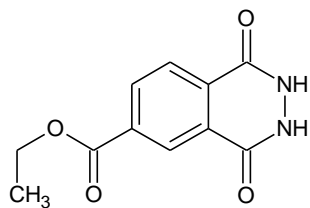
Comp. Code	Color	MP °C	Rf value	Comp. Code	% Yield	Color	MP °C	Rf value	% Yield
1	Shiny cream	189	.28	11	54.25%	Yellowish Green	193	.28	64.34%
2	Dull brown	187	.24	12	62.25%	Green	192	.26	59.23%
3	Green	188	.26	13	58.54%	Dark Brown	186	.34	58.55%
4	Green	192	.36	14	54.52%	Greenish Brown	185	.25	63.56%
5	Greenish brown	205	.34	15	62.13%	Yellow	207	.32	60.20%
6	Dark cream	202	.26	16	51.43%	Dull Brown	169	.24	57.78%
7	Dark green	168	.28	17	56.43%	Dark green	205	.32	56.56%
8	Cream	186	.32	18	58.82%	Brown	186	.26	57.77%
9	Dark Brown	158	.24	19	57.765	Greenish Black	169	.24	59.66%
10	Light Brown	187	.32	20	53.34%	Cream	206	.24	58.23%

All compounds are soluble in DMSO and 2-Propanol.

5.1.2. Synthesis for Aminophthalazine Derivatives

Scheme for Synthesis of Aminophthalazine Derivatives:

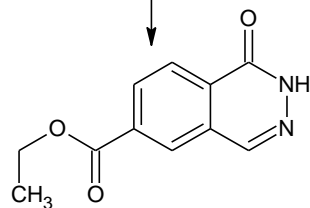




ethyl 1,4-dioxo-1,2,3,4-tetrahydrophthalazine-6-carboxylate

Step II-IV

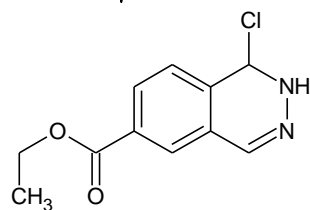
THF NaBH_4



ethyl 1-oxo-1,2-dihydrophthalazine-6-carboxylate

Step-V

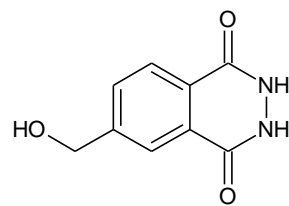
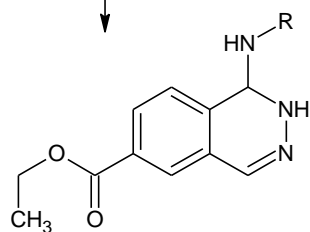
Chlorination POCl_3



ethyl 1-chloro-1,2-dihydrophthalazine-6-carboxylate

Step-VI

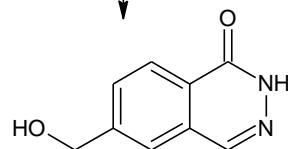
Substituted Aniline Isopropanol



6-(hydroxymethyl)-2,3-dihydrophthalazine-1,4-dione

Step III-IV

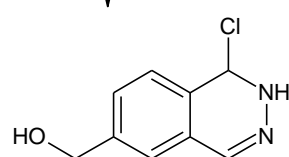
THF NaBH_4



6-(hydroxymethyl)phthalazin-1(2H)-one

Step-V

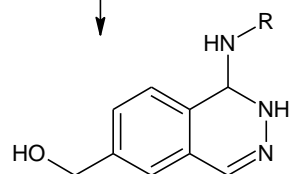
Chlorination POCl_3



(1-chloro-1,2-dihydrophthalazin-6-yl)methanol

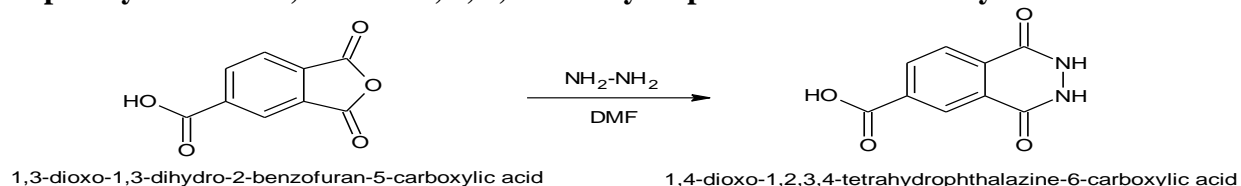
Step-VI

Substituted Aniline Isopropanol



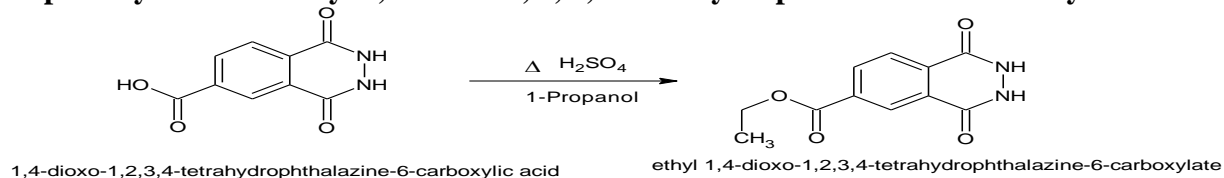
General Procedure for the Synthesis Aminophthalazine Derivatives

Step-I: Synthesis of 1, 4-dioxo-1, 2, 3, 4-tetrahydrophthalazine-6-carboxylic acid



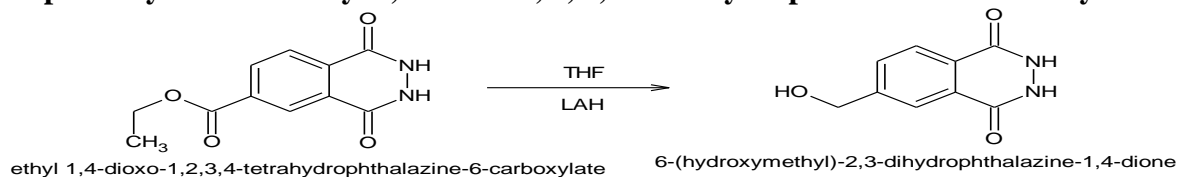
A solution of 19.2 g of trimetallic anhydride in 200 ml of dimethyl formamide was heated at 100°C and solution of 9.6 g hydrazine in 100 ml of dimethyl formamide was added over about 1 minute. A tar ball formed which eventually broken up on continued heating and stirring for an hour, cooled, filtered and washed with dimethyl formamide and ether, affording 95% yield as a yellow solid.

Step-II: Synthesis of ethyl 1, 4-dioxo-1, 2, 3, 4-tetrahydrophthalazine-6-carboxylate



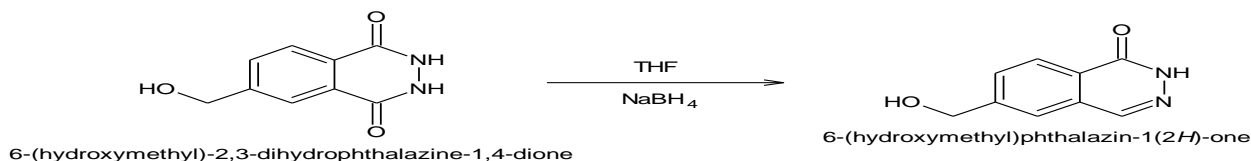
The crude acid from step-1 was refluxed with stirring in 1600 ml ethanol containing 50 ml conc. sulphuric acid for 20 h. The reaction mixture was cooled, filtered and washed with ethanol and dried, affording 90% yield as a white amorphous solid.

Step-III: Synthesis of ethyl 1, 4-dioxo-1, 2, 3, 4-tetrahydrophthalazine-6-carboxylate ⁽⁶⁶⁾



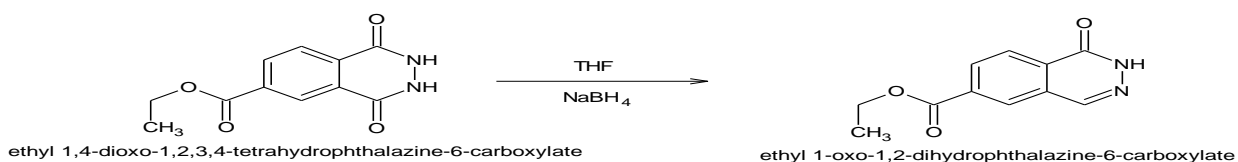
The solid ester from step-II (28.8 g) was added to the solution of 8 g lithium aluminium hydride (LAH) in 500 ml tetrahydrofuran (THF) at 5°C (ice bath cooling with little heat of evolution), then the temperature of reaction mixture was allowed to rise at room temperature. The mixture was stirred for 4 h Then excess of lithium aluminium hydride was destroyed by 60 ml ethyl acetate, follow by 40 ml water, then 180 ml 6 N hydrochloric acid. The mixture was diluted with another 500 ml of water and tetrahydrofuran was removed under vacuum. Then product was filtered off, washed with dilute hydrochloric acid and finally washed with neutral water before drying, affording 75% yield as a cream white amorphous solid

Step IV: 1. Synthesis of 6-(hydroxymethyl) phthalazin-1(2H)-one



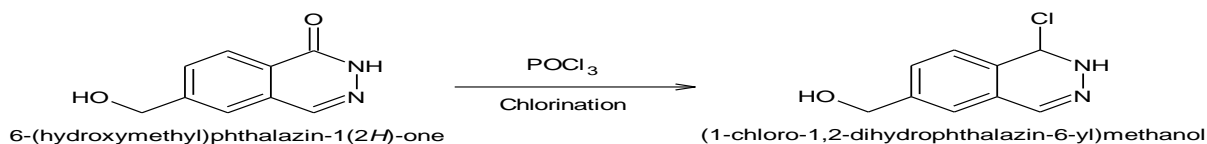
NaBH₄ (126.2 g, 3.32 mol) was added to slowly. Stirred solution of step-iii in dry THF (750 ml) at 0-10⁰C anhydrous methanol was added to reaction mixture drop wise at 0-10⁰C and reaction mixture was stirred at room temperature for 3 h. The mixture was concentrated under reduced pressure. The residue was poured in 10% HCl aqueous solution (1000 ml), stirred intensively for 3 h and separated by filtration. The solid was alkalized with 10% Na₂CO₃ aqueous solution (1000 ml), stirred for 1 h and separated by filtration to give compound as a white crystal, affording 60% yield as a cream white amorphous solid.

Step II-IV: 2. Synthesis of ethyl 1-oxo-1, 2-dihydrophthalazine-6-carboxylate ⁽⁷³⁾



NaBH₄ (126.2g, 3.32mol) was added to slowly. Stirred solution of step-ii in dry THF (750 ml) at 0-10⁰C anhydrous methanol was added to reaction mixture drop wise at 0-10⁰C and reaction mixture was stirred at room temperature for 3 h. The mixture was concentrated under reduced pressure. The residue was poured in 10% hydrochloric acid aqueous solution (1000 ml), stirred intensively for 3 h and separated by filtration. The solid was alkalized with 10% Na₂CO₃ aqueous solution (1000 ml), stirred for 1 h and separated by filtration to give compound as a white crystal, affording 55% yield as a white amorphous solid.

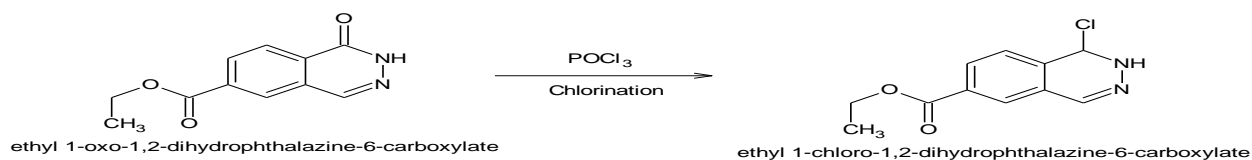
Step-V: 1. (1-chloro-1, 2-dihydrophthalazin-6-yl) methanol



Step IV (a) compound (17.5 g, 0.07 mol) was added to a stirred solution of POCl₃ (170 ml) and CH₃CN (80 ml) at room temperature, and then 3 drops of DMF were added to the mixture. The reaction mixture was heated to 90 ⁰C for 3 h. The mixture was concentrated

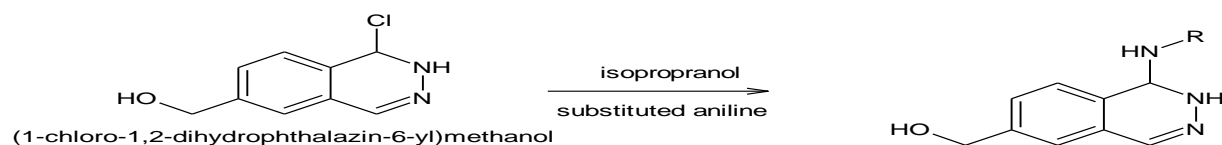
under reduced pressure. The residue was poured into ice water (500 ml), alkalized with a 10% Na_2CO_3 aqueous solution to pH 7-8 and separated by filtration to give compound as a red solid, affording 85% yield.

Step-V: 2. Ethyl 1-chloro-1, 2-dihydrophthalazine-6-carboxylate



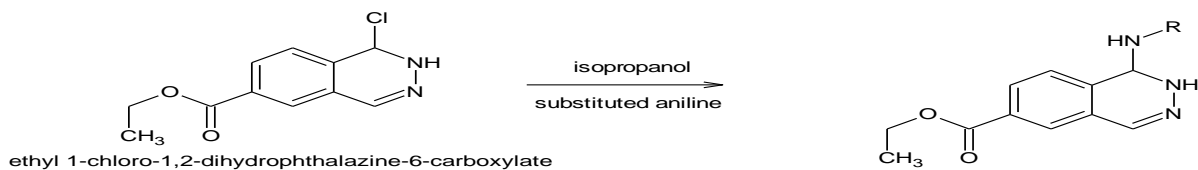
Step IV compound (17.5 g, 0.07 mol) was added to a stirred solution of POCl_3 (170 ml) and CH_3CN (80 ml) at room temperature, and then 3 drops of DMF were added to the mixture. The reaction mixture was heated to 90°C for 3 h. The mixture was concentrated under reduced pressure. The residue was poured into ice water (500 ml), alkalized with a 10% Na_2CO_3 aqueous solution to pH 7-8 and separated by filtration to give compound as a red solid, affording 85% yield.

Step-VI: 1. Synthesis of final compound



Product from step V 1 (0.181 g, 0.7mmol) & substituted aniline (0.177 g, 0.7 mmol) in isopropanol (20 ml) was heated at reflux and stirred for 4 h. The white solid was filtered while hot, recrystallized from methanol or DMF to give product, affording 80% yield.

Step-VI: 2. Synthesis of final compound



Product from step V 2 (0.181 g, 0.7 mmol) & substituted aniline (0.177 g, 0.7 mmol.) in isopropanol (20ml) was heated at reflux and stirred for 4 h. The white solid was filtered while hot, recrystallized from methanol or DMF to give product, affording 85% yield.

Physicochemical Data of Synthesized Aminophthalazine Derivatives

Table: Physicochemical Data of Synthesized Aminophthalazine Derivatives

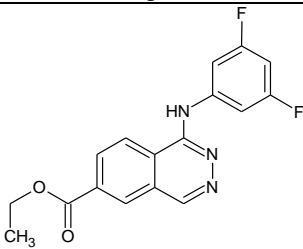
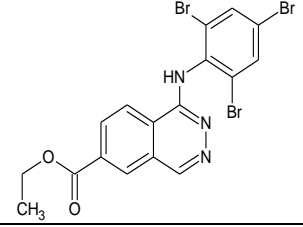
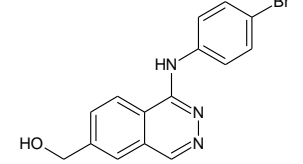
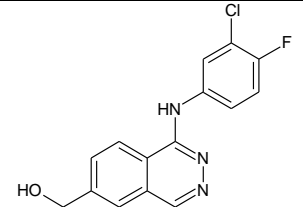
Comp. No.	Structure of Synthesized Compound	Chemical Name of Compound	Molecular formula	Molecular weight
1		ethyl 1-[(3,5-difluorophenyl) amino] phthalazine-6-carboxylate	C ₁₇ H ₁₃ F ₂ N ₃ O ₂	329.30
2		ethyl 1-[(2,4,6-tribromophenyl) amino] phthalazine-6-carboxylate	C ₁₇ H ₁₂ Br ₃ N ₃ O ₂	530.00
3		{1-[(4-bromophenyl)amino]phthalazin-6-yl}methanol	C ₁₅ H ₁₁ BrN ₃ O	303.72
4		{1-[(3-chloro-4-fluorophenyl)amino]phthalazin-6-yl}methanol	C ₁₅ H ₁₂ BrN ₃ O	330.19

Table: Physicochemical Data of Synthesized Aminophthalazine Derivatives

Comp. No.	Nature	Colour	Solubility	Melting point (°C)	Yield (%)	Rf. Values
1	Solid	Light brown	DMSO	208-210 ⁰ C	90%	0.40
2	Solid	Light brown	DMSO	180-182 ⁰ C	85%	0.48
3	Solid	Dark brown	DMSO	186-188 ⁰ C	82.2%	0.58
4	Solid	Dark brown	DMSO	188-190 ⁰ C	80%	0.50

5.2. SYNTHESIS OF QUINAZOLINE DERIVATIVES

5.2.1. Synthesis of *N*-[2-(4-methylphenyl)-4-(substituted aniline)-3, 4-dihydroquinazolin-6-yl] acetamide

Scheme for Synthesis of Proposed Compounds

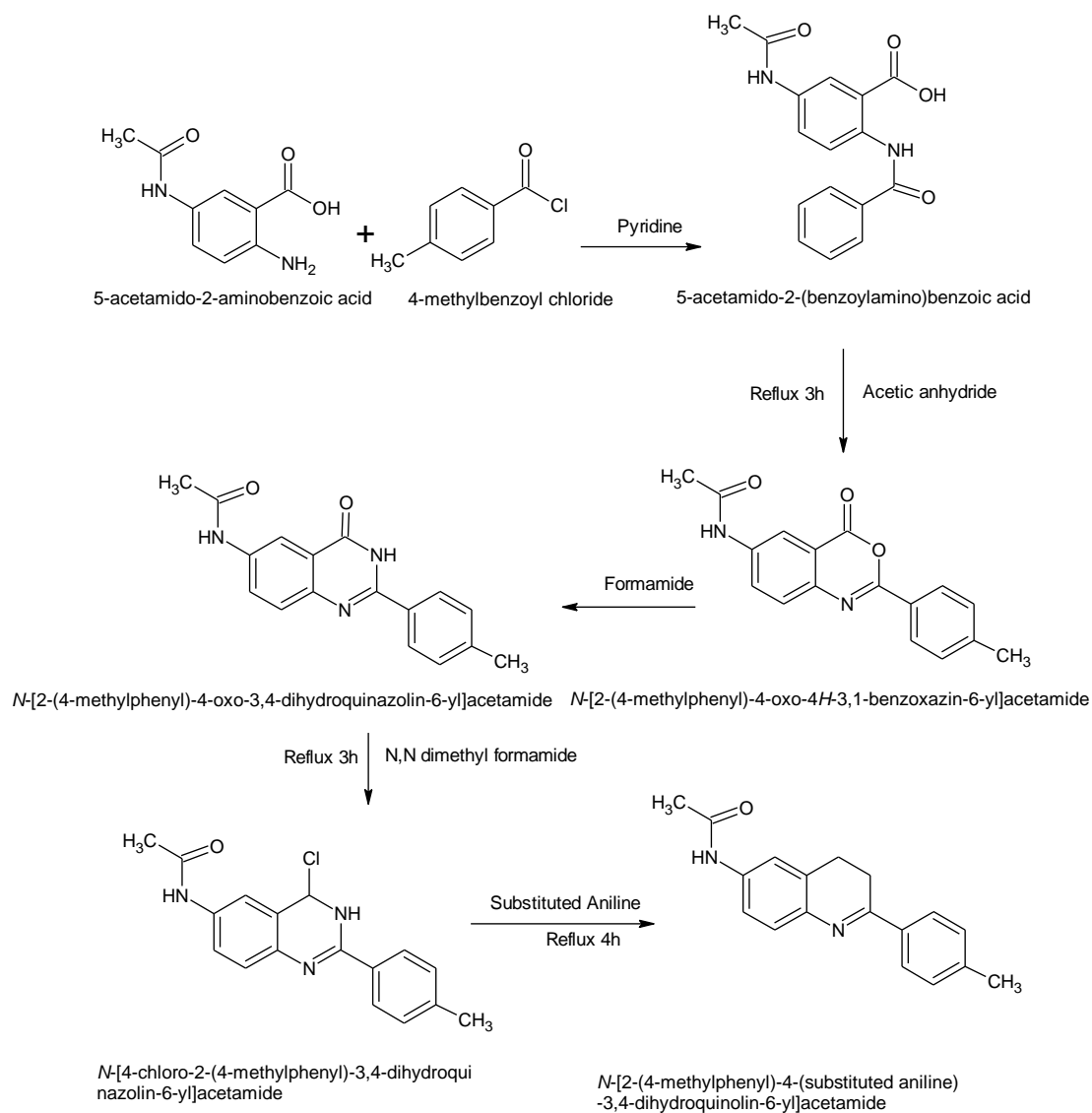
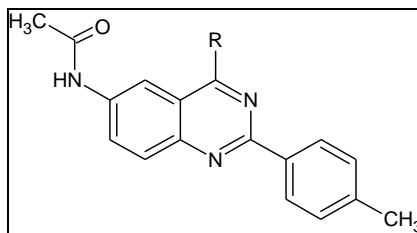


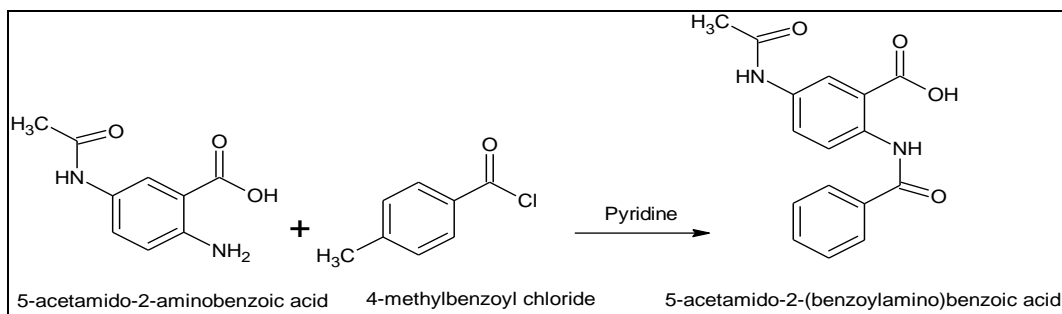
Table: Synthesized Compounds



Compound Code	R	Resulting Structure
1		<p><i>N</i>-4-[(2,5-dichlorophenyl)amino]-2-(4-methylphenyl)quinazolin-6-ylacetamide</p>
2		<p><i>N</i>-2-(4-methylphenyl)-4-[(2,4,6-trichlorophenyl)amino]quinazolin-6-ylacetamide</p>
3		<p><i>N</i>-2-(4-methylphenyl)-4-[(2,4,5-trichlorophenyl)amino]quinazolin-6-ylacetamide</p>
4		<p><i>N</i>-4-[(2,6-dichloro-4-nitrophenyl)amino]-2-(4-methylphenyl)quinazolin-6-ylacetamide</p>

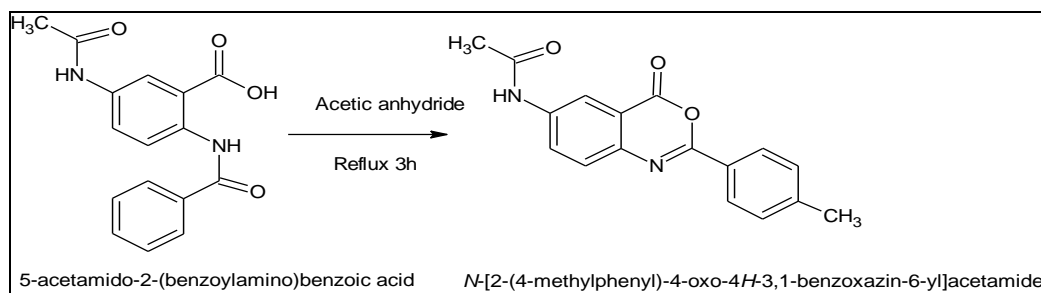
Procedure for the synthesis of quinazoline derivatives:

Step I: Synthesis of 5-acetamido -2 (benzoylamino) benzoic acid:



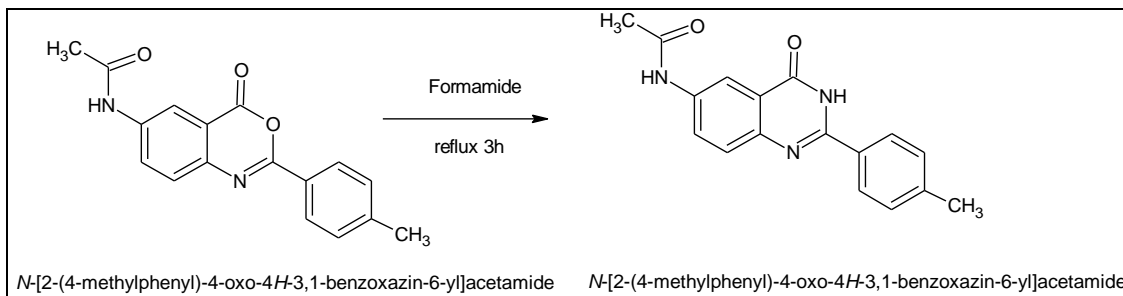
5-acetamido-2-aminobenzoic acid (22mmol, 3.43g) and 4-methyl benzoyl chloride (22mmol, 3.40g) were stirred with pyridine (80ml) at room temperature for 6h. The solvent removed under reduced pressure, the obtained solid was washed with acid water. Filter the crystalline residue, washed with water, dried and then recrystallized from ethanol, affording 80% yield as a white solid.

Step II: Synthesis of N-[2-(4-methylphenyl)-4-oxo-4H-3, 1-benzoxazin-6-yl] acetamide:



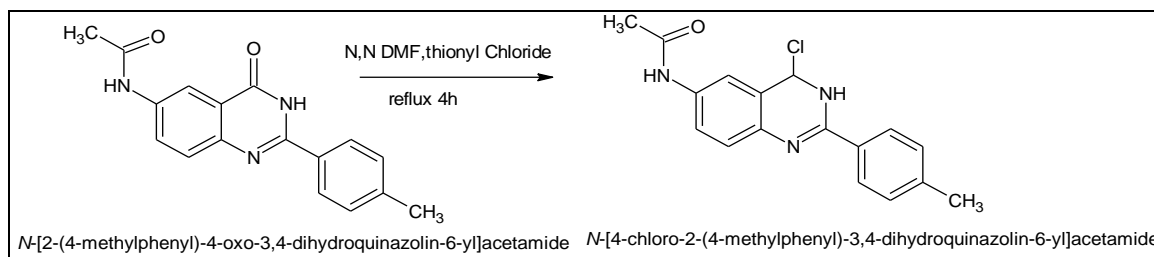
Product obtained from previous step (20mmol, 5.79g) was heated under reflux in acetic anhydride (100ml) for 3h. The obtained solid was then filtered while hot and dried. 65% yield was obtained with grey color solid.

Step III: Synthesis of N [2-(4methylphnyl)-4-oxo-4H-3, 1-benzoxazin-6yl] acetamide:



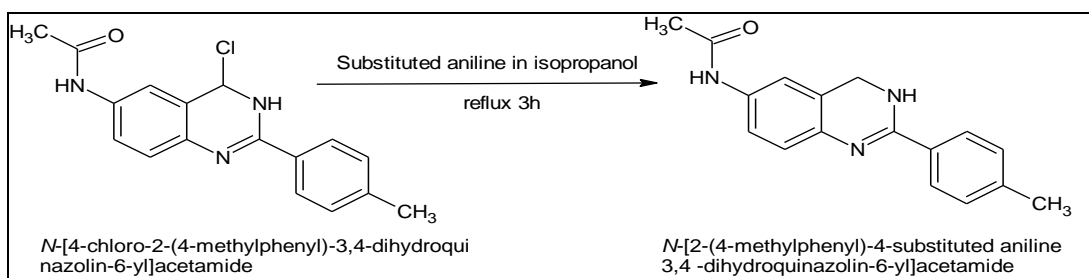
N-[2-(4-methylphenyl)-4-oxo-4H-3, 1-benzoxazin-6-yl] acetamide (10mmol, 2.71g) was heated with formamide (50ml) under reflux for 3h. Then, cooled, filtered the solid while hot and dried. The yield of 59% was obtained with a white color solid.

Step IV: Synthesis N-[4-chloro-2-(4-methylphenyl) 3, 4-dihydroquinazolin-6yl]acetamide



N [2-(4methylphnyl)-4-oxo-4H-3, 1-benzoxazin-6yl]acetamide (0.38mol, 102g) was stirred with thionyl chloride (500ml). Then, added 20ml DMF slowly and heated to reflux for 4h. Excess of thionyl chloride was removed under pressure and chloroform (500ml) added in it. Washed twice with sodium carbonate (100ml) and water (100ml), filtered and dried over Na₂SO₄, affording the 61% yield as a reddish yellow solid.

Step V: Synthesis of N-[2-(4-methylphenyl)-4-(substituted aniline)-3, 4-dihydro quinazolin-6-yl] acetamide:



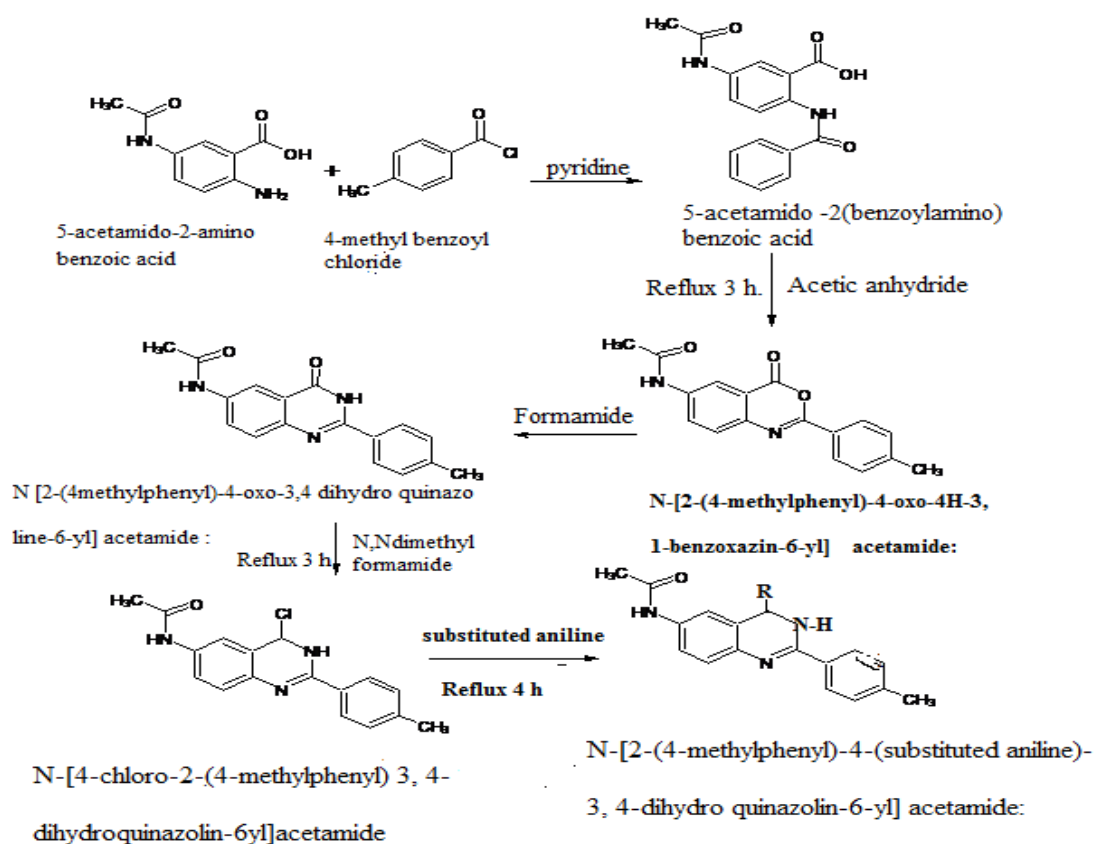
N-[4-chloro-2-(4-methylphenyl)-3, 4-dihydroquinazolin-6yl] acetamide (0.7mmol, 0.181g) and substituted aniline (0.7mmol, 0.177g) in an isopropanol (20ml) was then heated to reflux and stirred for 3h. The yellow solid was filtered while hot and recrystallized from methanol or DMF. 78% yield was obtained with reddish yellow color solid.

All the compounds were found to be soluble in DMSO. The mobile phase for thin layer chromatography was with n-Hexane: Ethyl Acetate: Methanol in varying proportions.

Table: Physicochemical properties of synthesized Quinazoline derivatives

C. code	Molecular formula	Color	Nature	M. wt.	Melting Point	Yield (%)	Rf. Values
1	C ₂₃ H ₁₈ Cl ₂ N ₄ O	Reddish yellow	Solid	437.32	234-238°C	79%	0.34
2	C ₂₃ H ₁₇ Cl ₃ N ₄ O	Reddish yellow	Solid	471.76	234-238°C	70%	0.32
3	C ₂₃ H ₁₇ Cl ₃ N ₄ O	Reddish yellow	Solid	471.76	276-282°C	82%	0.24
4	C ₂₃ H ₁₇ Cl ₂ N ₅ O ₃	Reddish yellow	Solid	482.31	304-310°C	74%	0.43

5.2.2. Synthesis of N-[2-(4-methylphenyl)-4-(substituted aniline)-3, 4-dihydro quinazolin-6-yl] acetamide



R=1] 4-chloro,2-nitro aniline

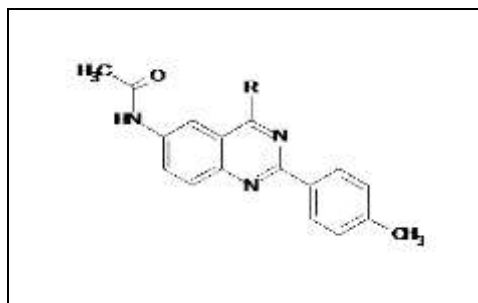
R=3] 3,5 dichloro aniline

R=5] 2-iodo aniline

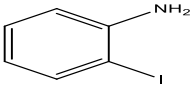
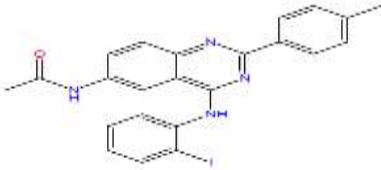
R=2] 3-nitro aniline

R=4] 2,6 dibromo,4-nitro aniline

Table: Synthesized Compounds



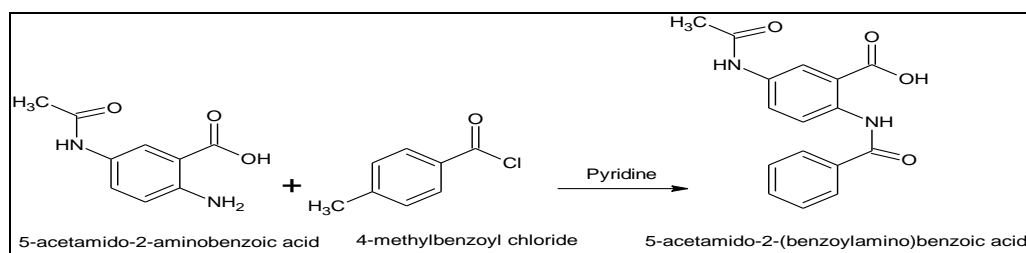
C. Code	R	Resulting Structure
1	<p>4-chloro 2-nitroaniline</p>	<p>N-{2 (4-methylphenyl)-4-[(4-chloro,2-nitro phenyl)amino]quinazoline-6-yl}acetamide</p>
2	<p>3-nitro aniline</p>	<p>N-{2 (4-methylphenyl)-4-[(3-nitro phenyl) amino] quinazoline-6-yl}acetamide</p>
3	<p>3,5 dichloro aniline</p>	<p>N-{2 (4-methylphenyl)-4-[(3,5dichloro phenyl) amino]quinazoline-6-yl}acetamide</p>
4	<p>2,6 dibromo 4-nitro aniline</p>	<p>N-{2 (4-methylphenyl)-4-[(2,6 dibromo ,4 nitro phenyl) amino]quinazoline-6-yl}acetamide</p>

5	 <p>2-iodo aniline</p>	 <p>N-{2 (4-methylphenyl)-4-[(2-iodo phenyl) amino] quinazoline-6-yl} acetamide</p>
---	---	---

Procedure for the synthesis of quinazoline derivatives

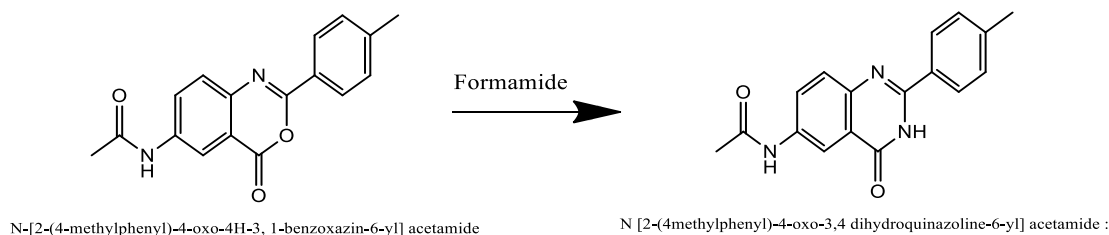
Step I: Synthesis of 5-acetamido -2-(benzoylamino)benzoic acid:

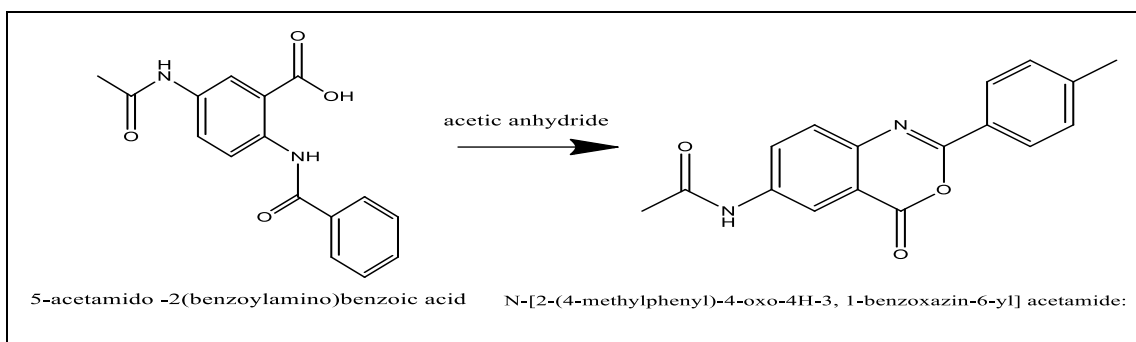
5-acetamido-2-aminobenzoic acid (22mmol, 3.43g) and 4-methyl benzoyl chloride (22mmol, 3.40g) were stirred with pyridine (80ml) at room temperature for 6h. The solvent removed under reduced pressure, the obtained solid was washed with acid water. Filter the crystalline residue, washed with water, dried and then recrystallized from ethanol, affording 80% yield as a white solid.



Step II: Synthesis of N-[2-(4-methylphenyl)-4-oxo-4H-3, 1-benzoxazin-6-yl] acetamide:

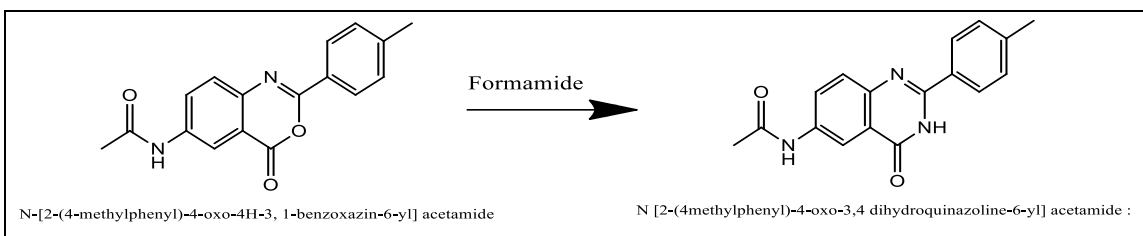
Product obtained from previous step (20mmol, 5.79g) was heated under reflux in acetic anhydride (100ml) for 3h. The obtained solid was then filtered while hot and dried. 72% yield was obtained with grey color solid.





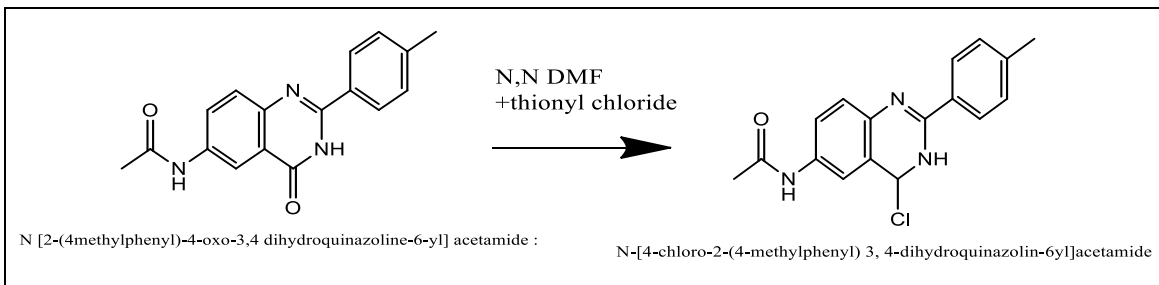
Step III: Synthesis of N [2-(4methylphenyl)-4-oxo-3,4 dihydroquinazoline-6-yl] acetamide:

N-[2-(4-methylphenyl)-4-oxo-4H-3,1-benzoxazin-6-yl]acetamide (10mmol, 2.71g) was heated with formamide (50ml) under reflux for 3h. Then, cooled, filtered the solid while hot and dried. The yield of 65% was obtained with a white color solid.



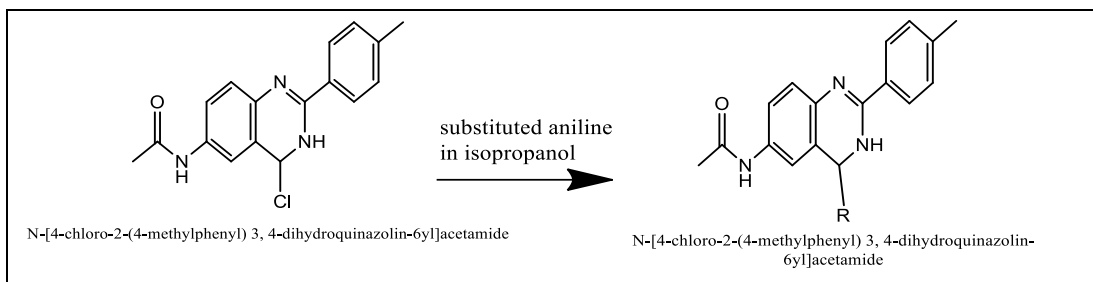
Step IV: Synthesis N-[4-chloro-2-(4-methylphenyl)3,4-dihydroquinazolin-6-yl]acetamide

N [2-(4methylphenyl)-4-oxo-3,4 dihydroquinazoline-6-yl]acetamide (0.38mol, 102g) was stirred with thionyl chloride (500ml). Then, added 20ml DMF slowly and heated to reflux for 4h. Excess of thionyl chloride was removed under pressure and chloroform (500ml) added in it. Washed twice with sodium carbonate (100ml) and water (100ml), filtered and dried over Na_2SO_4 , affording the 60% yield as a reddish yellow solid.



Step V: Synthesis of N-[2-(4-methylphenyl)-4-(substituted aniline)-3, 4-dihydroquinazolin-6-yl] acetamide:

N-[4-chloro-2-(4-methylphenyl)-3, 4-dihydroquinazolin-6yl] acetamide (0.7mmol, 0.181g) and substituted aniline (0.7mmol, 0.177g) in an isopropanol (20ml) was then heated to reflux and stirred for 3h. The reddish yellow solid was filtered while hot and recrystallized from methanol or DMF. 55 % yield was obtained with reddish brown color solid.



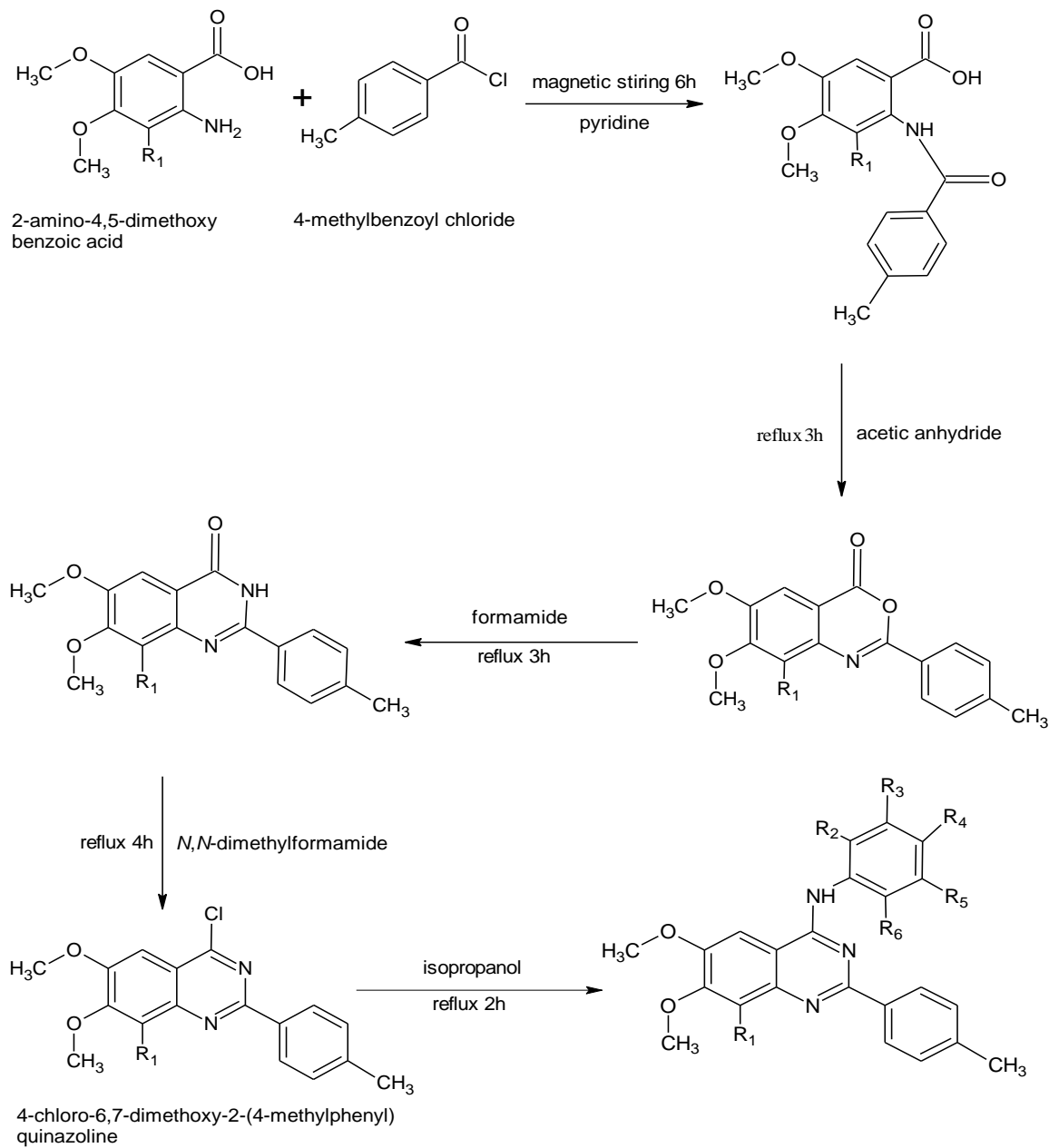
All the compounds were found to be soluble in DMSO. The mobile phase for thin layer chromatography was n-hexane: ethyl acetate: methanol in varying proportion.

Table: Physicochemical properties of synthesized Quinazoline derivatives

C. code	Molecular formula	Color	Nature	Mol.wt.	Melting Point	Yield (%)	Rf. Value
1	C ₂₃ H ₁₈ ClN ₅ O ₃	Reddish brown	Solid	447.87	235-237 ^o C	53%	0.35
2	C ₂₃ H ₁₉ N ₅ O ₃	Reddish brown	Solid	413.43	234-238 ^o C	55%	0.32
3	C ₂₃ H ₁₈ Cl ₂ N ₄ O	Reddish brown	Solid	437.32	272 - 281 ^o C	52%	0.27
4	C ₂₃ H ₁₇ Br ₂ N ₅ O ₃	Reddish brown	Solid	571.22	302-308 ^o C	54%	0.39
5	C ₂₃ H ₁₉ IN ₄ O	Reddish brown	Solid	494.33	310-318 ^o C	53 %	0.42

5.3. SYNTHESIS OF 4-ANILINOQUINAZOLINE DERIVATIVES

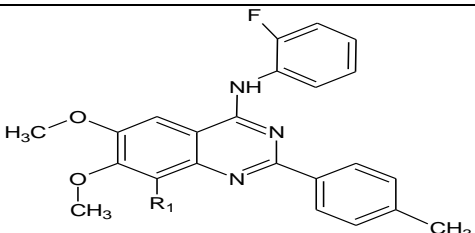
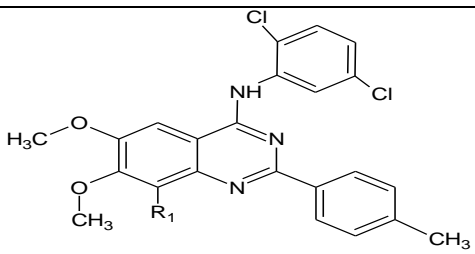
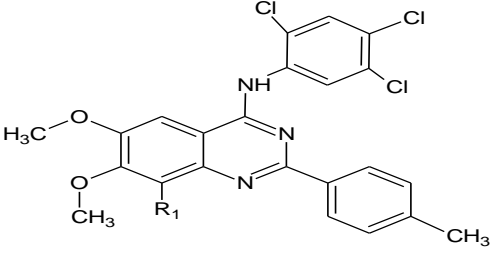
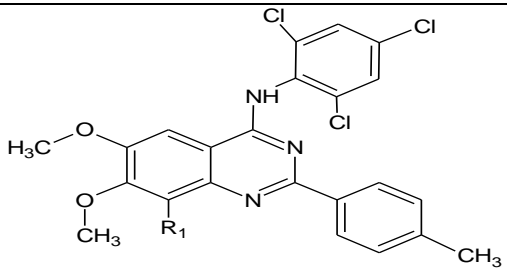
Scheme for Synthesis of 4-Anilinoquinazoline



Where,

$R_1 = \text{H or OCH}_3$.

Table: 6.1.1 Structures of synthesized compounds.

Comp. No	R ₁	R ₂	R ₃	R ₄	R ₅	R ₆	Structure
1	H	F	H	H	H	H	 <p>6,7-dimethoxy-2-(methylphenyl)-N-(2-fluorophenyl) quinazoline-amine</p>
2	H	Cl	H	H	Cl	H	 <p>6,7-dimethoxy-2-(methylphenyl)-N-(2,5-dichlorophenyl) quinazoline-amine</p>
3	H	Cl	H	Cl	Cl	H	 <p>6,7-dimethoxy-2-(methylphenyl)-N-(2,4,5-trichlorophenyl) quinazoline-amine</p>
4	H	Cl	H	Cl	H	Cl	 <p>6,7-dimethoxy-2-(methylphenyl)-N-(2,4,6-trichlorophenyl) quinazoline-amine</p>

General procedure for Preparation of derivatives

STEP I: 4, 5-dimethoxy-2[(4-methylbenzoyl) amino] benzoic acid. (1)

2-amino 4, 5-dimethoxy benzoic acid (20 mmol, 3.43g) and 4-methylbenzoyl chloride (22 mmol, 3.40 g) were stirred at room temperature in pyridine (8ml) for 6 h. The solvent was removed under reduced pressure; the obtained residue was washed with acidulated water, filtered, washed with water, dried, and recrystallized from ethanol, affording 60% yield as white solid.

STEP II: 6, 7-dimethoxy-2(4-methylphenyl) quinoline-4(3H)-one. (2)

A benzoic acid derivative (1) (20 mmol, 5.79g) was heated under reflux in acetic anhydride (100 ml) for 3 h. The solid obtained was filtered while hot and dried, obtained in 55% yield.

STEP III: 6, 7-dimethoxy-2(4-methylphenyl) quinazoline-4(3H)-one. (3)

Benzoxazine (2) (10 mmol, 2.71g) was heated under reflux in formamide (50 ml) for 3 h. The solid obtained was filtered while hot and dried, obtained in 55% yield.

STEP IV: 6, 7-dimethoxy-2(4-methylphenyl) quinazoline. (4)

6, 7-dimethoxy 2-(4-methylphenyl) quinazoline-4(3H) one (3) (24, 102g, 0.38 mol) was added to thionyl chloride (500 ml) with magnetic stirring. DMF (20 ml) was then slowly added drop wise and the mixture was heated to reflux for 4 h. Most of the excess of thionyl chloride was then removed under reduced pressure and the yellow residue was dissolved in chloroform (500 ml), washed with a saturated solution of sodium carbonate (2×100 ml) and water (2×100 ml), and dried (Na₂SO₄). The chloroform was then removed under reduced pressure to give an off-white powder, which was recrystallized from ethyl acetate to give the product, affording 60% yield.

STEP V: 6, 7-dimethoxy-2(4-methylphenyl) 4-anilinoquinazoline. (5)

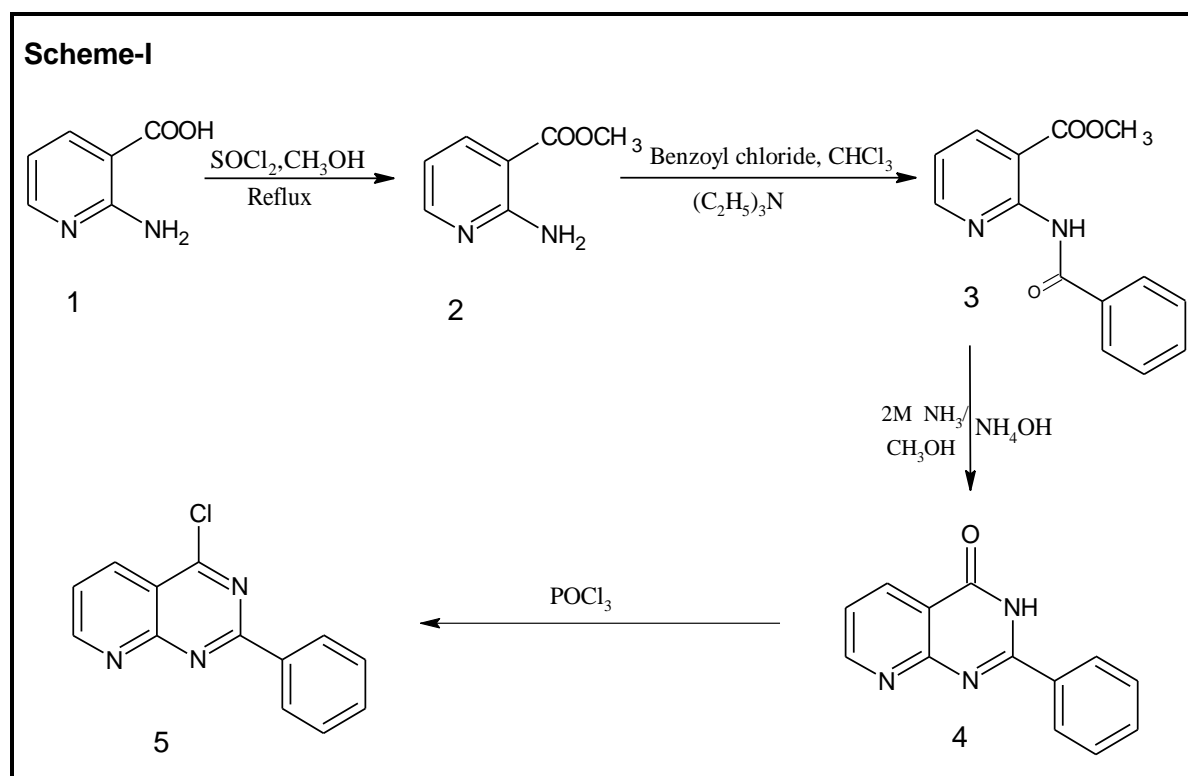
Product from step IV (0.181g, 0.7mmol) and substituted aniline (0.177g, 0.7mmol) in isopropanol (20ml) was heated at reflux and stirred for 4 h. The white solid was filtered while hot, recrystallized from methanol or DMF to give product, with 50% yield.

Table: Physicochemical data of synthesized 4-anilinoquinazoline derivatives

Comp. Code	Nature	Color	Mol. Formula	Mol. Weight	Rf value	M.P. (°C)	Yield (%)
1	Solid	Light yellow	C ₂₃ H ₂₀ FN ₃ O ₂	389.42	0.72	280°C	70.56%
2	Solid	Light yellow	C ₂₃ H ₁₉ Cl ₂ N ₃ O ₂	440.32	0.69	292 °C	60.34%
3	Solid	Light yellow	C ₂₃ H ₁₈ Cl ₃ N ₃ O ₂	474.76	0.62	297 °C	55.78%
4	Solid	Light yellow	C ₂₃ H ₁₈ Cl ₃ N ₃ O ₂	474.76	0.68	299 °C	55.89%

5.4. SYNTHESIS OF PYRIDOPYRIMIDINE DERIVATIVES

Scheme for Synthesis of pyrido[2,3-d]pyrimidine derivatives:



Scheme for Synthesis of 2-phenyl-N-(substituted phenyl) pyrido[2,3-d]pyrimidin-4-amine derivatives (6a-r):-

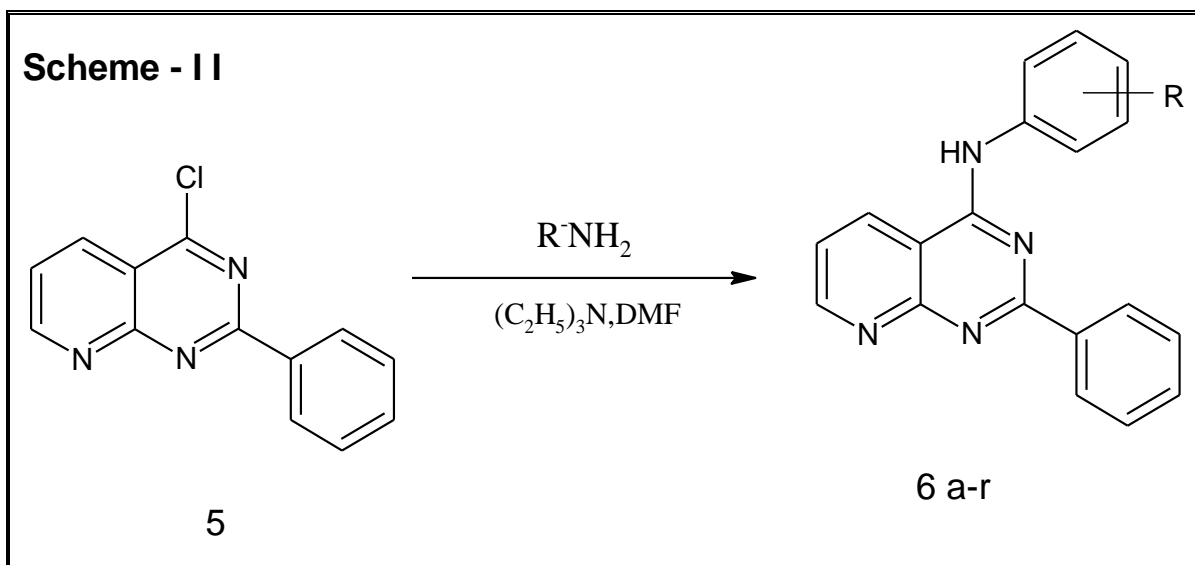
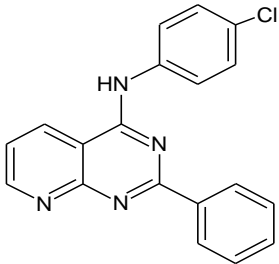
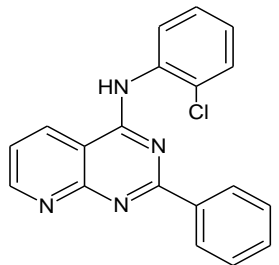
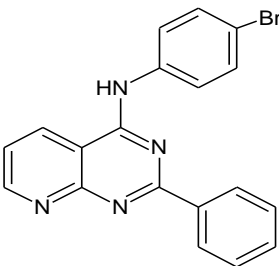
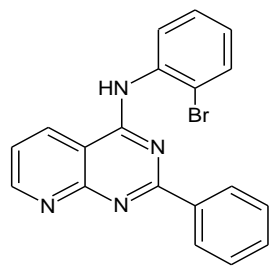
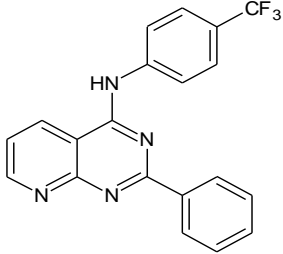
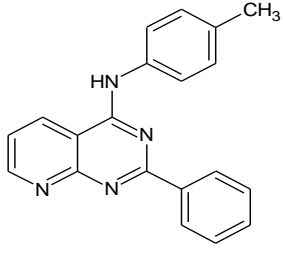
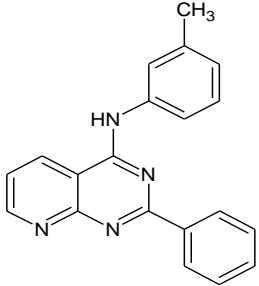
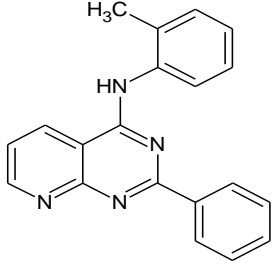
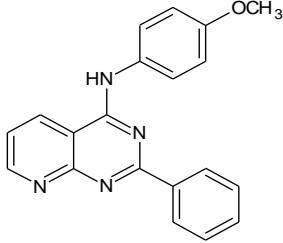
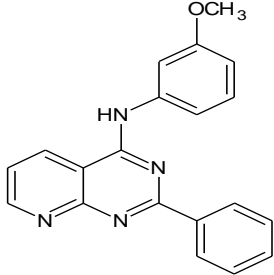
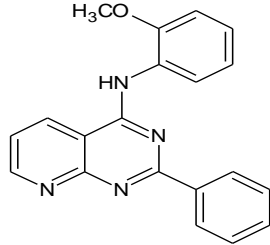
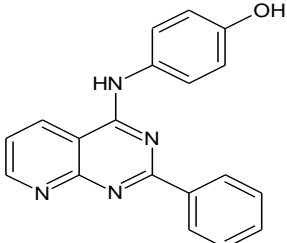


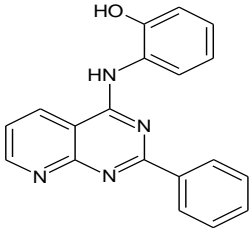
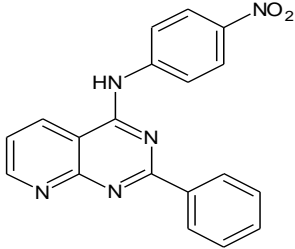
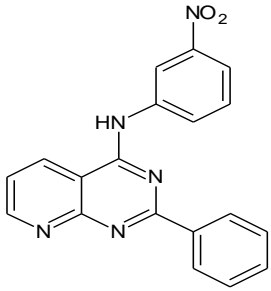
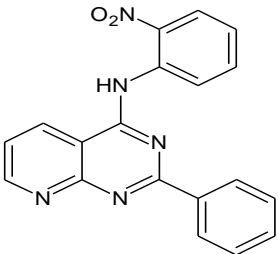
Table: - Structure of 2-phenyl-N-(substituted phenyl) pyrido[2,3-d] pyrimidin-4-amine (6a-r):-

Compound No.	R	Structure and IUPAC Name
6a	4-F	<p><i>N</i>-(4-Fluorophenyl)-2-phenylpyrido[2,3-d]pyrimidin-4-amine</p>
6b	2-F	<p><i>N</i>-(2-Fluorophenyl)-2-phenylpyrido[2,3-d]pyrimidin-4-amine</p>

6c	4-Cl	 <p><i>N</i>-(4-Chlorophenyl)-2-phenylpyrido[2,3-d]pyrimidin-4-amine</p>
6d	2-Cl	 <p><i>N</i>-(2-Chlorophenyl)-2-phenylpyrido[2,3-d]pyrimidin-4-amine</p>
6e	4-Br	 <p><i>N</i>-(4-Bromophenyl)-2-phenylpyrido[2,3-d]pyrimidin-4-amine</p>
6f	2-Br	 <p><i>N</i>-(2-Bromophenyl)-2-phenylpyrido[2,3-d]pyrimidin-4-amine</p>

6g	4-CF ₃	 <p>2-Phenyl-N-(4-(trifluoromethyl)phenyl)pyrido[2,3-d]pyrimidin-4-amine</p>
6h	4-CH ₃	 <p>2-Phenyl-N-(p-tolyl)pyrido[2,3-d]pyrimidin-4-amine</p>
6i	3-CH ₃	 <p>2-Phenyl-N-(m-tolyl)pyrido[2,3-d]pyrimidin-4-amine</p>
6j	2-CH ₃	 <p>2-Phenyl-N-(o-tolyl)pyrido[2,3-d]pyrimidin-4-amine</p>

6k	4-OCH ₃	 <p><i>N</i>-(4-Methoxyphenyl)-2-phenylpyrido[2,3-d]pyrimidin-4-amine</p>
6l	3-OCH ₃	 <p><i>N</i>-(3-Methoxyphenyl)-2-phenylpyrido[2,3-d]pyrimidin-4-amine</p>
6m	2-OCH ₃	 <p><i>N</i>-(2-Methoxyphenyl)-2-phenylpyrido[2,3-d]pyrimidin-4-amine</p>
6n	4-OH	 <p>4-((2-Phenylpyrido[2,3-d]pyrimidin-4-yl)amino)phenol</p>

6o	2-OH	 <p>2-((2-Phenylpyrido[2,3-d]pyrimidin-4-yl)amino)phenol</p>
6p	4-NO ₂	 <p><i>N</i>-(4-Nitrophenyl)-2-phenylpyrido[2,3-d]pyrimidin-4-amine</p>
6q	3-NO ₂	 <p><i>N</i>-(3-Nitrophenyl)-2-phenylpyrido[2,3-d]pyrimidin-4-amine</p>
6r	2-NO ₂	 <p><i>N</i>-(2-Nitrophenyl)-2-phenylpyrido[2,3-d]pyrimidin-4-amine</p>

Scheme for Synthesis of 4-(2-(substituted benzylidene)hydrazineyl)-2-phenylpyrido[2,3-d]pyrimidine derivatives (7a-p):-

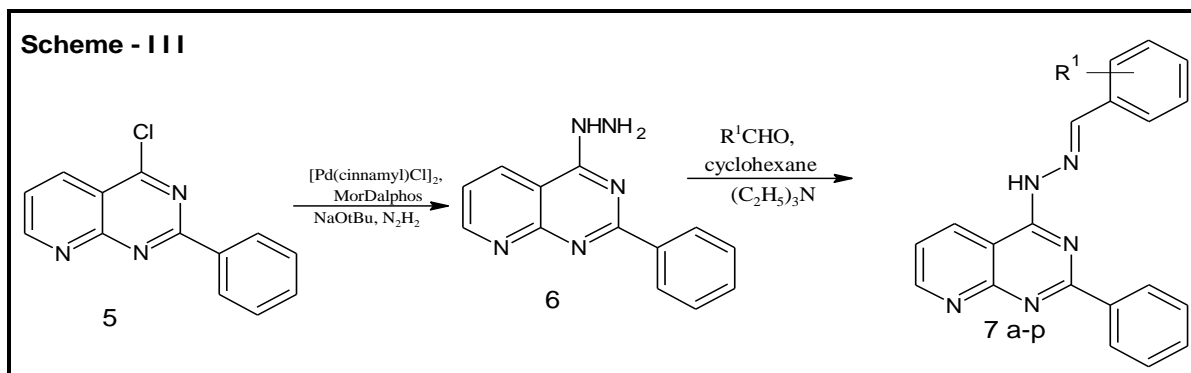
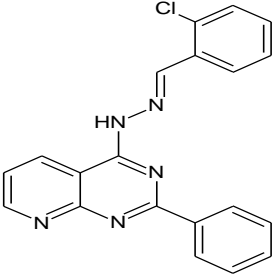
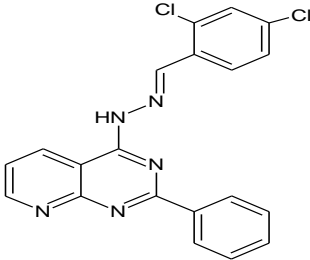
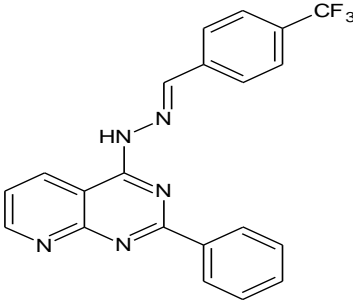
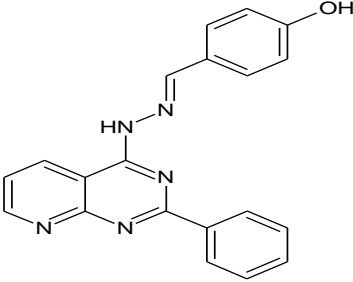
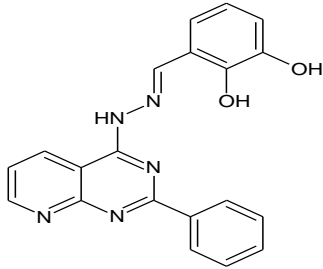
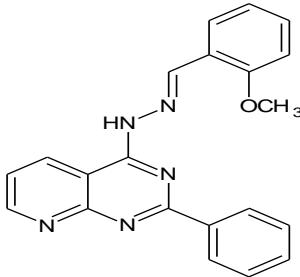
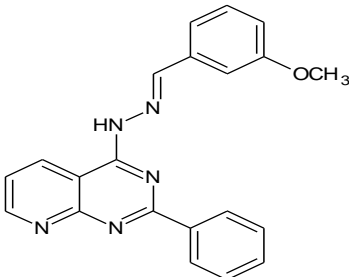
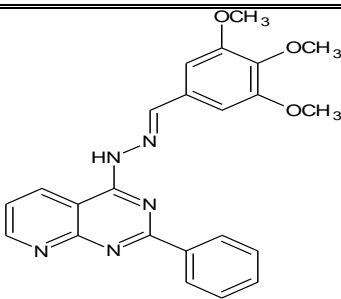
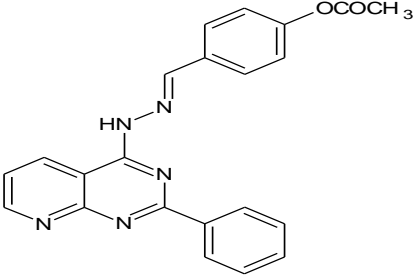
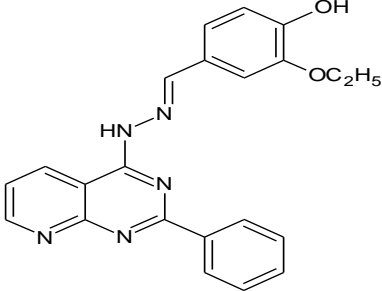
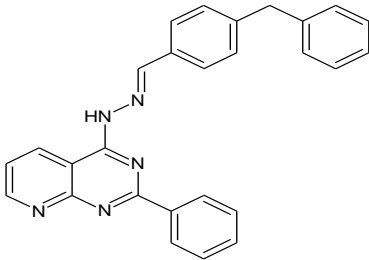
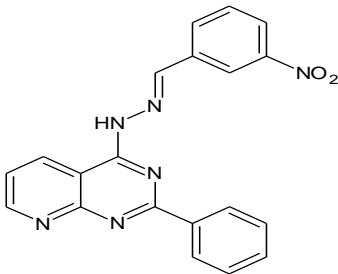


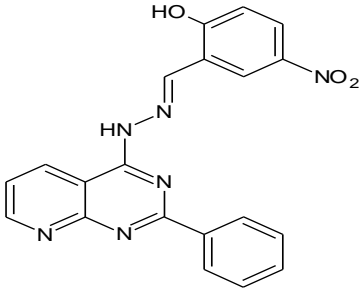
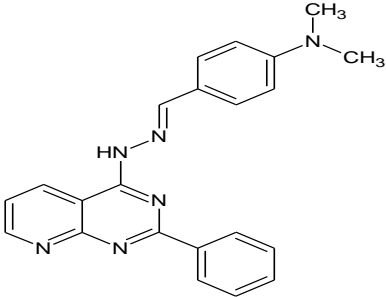
Table: - Structure of 4-(2-(substituted benzylidene)hydrazineyl)-2-phenylpyrido [2,3-d]pyrimidine (7a-p):-

Compound No.	R1	Structure and IUPAC Name
7a	-H	<p>4-(2-Benzylidenehydrazineyl)-2-phenylpyrido[2,3-d]pyrimidine</p>
7b	4-F	<p>4-(2-(4-Fluorobenzylidene)hydrazineyl)-2-phenylpyrido[2,3-d]pyrimidine</p>

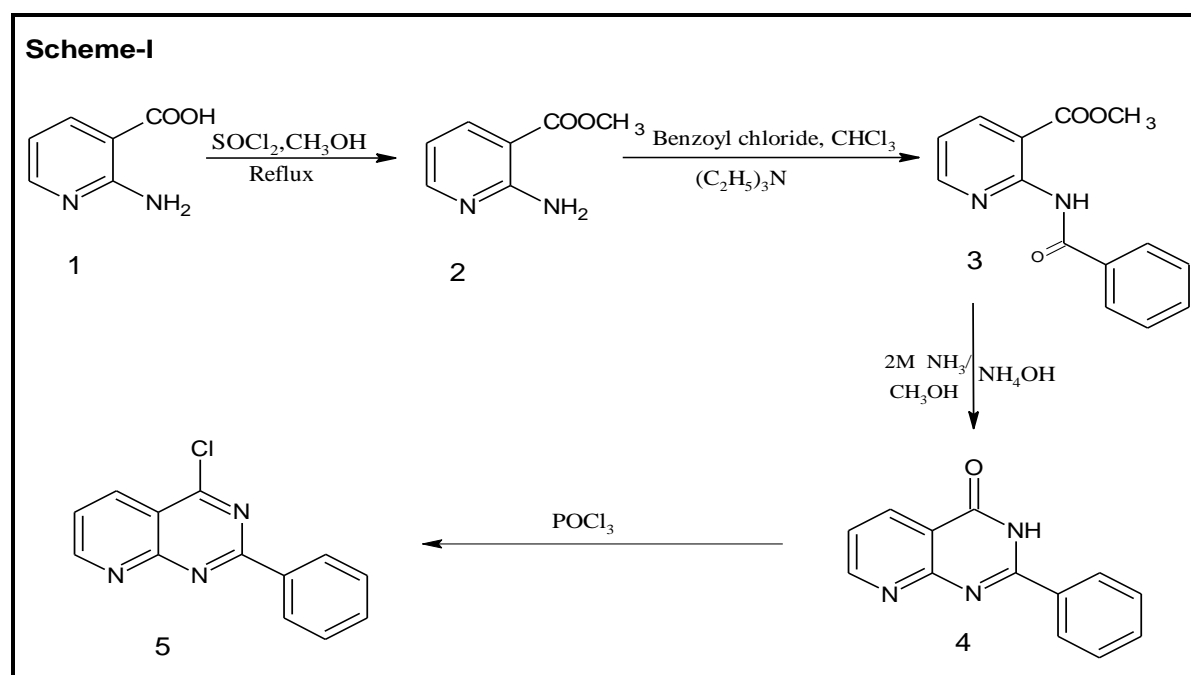
7c	2-Cl	 <p>4-(2-(2-Chlorobenzylidene)hydrazineyl)-2-phenylpyrido[2,3-d]pyrimidine</p>
7d	2,4-Cl	 <p>4-(2-(2,4-Dichlorobenzylidene)hydrazineyl)-2-phenylpyrido[2,3-d]pyrimidine</p>
7e	4-CF ₃	 <p>4-(2-(4-(Trifluoromethyl)benzylidene)hydrazineyl)-2-phenylpyrido[2,3-d]pyrimidine</p>
7f	4-OH	 <p>4-((2-(2-Phenylpyrido[2,3-d]pyrimidin-4-yl)hydrazineylidene)methyl)phenol</p>

7g	2,3-OH	 <p>3-((2-(2-Phenylpyrido[2,3-d]pyrimidin-4-yl)hydrazineylidene)methyl)benzene-1,2-diol</p>
7h	2-OCH ₃	 <p>4-(2-(2-Methoxybenzylidene)hydrazineyl)-2-phenylpyrido[2,3-d]pyrimidine</p>
7i	3-OCH ₃	 <p>4-(2-(3-Methoxybenzylidene)hydrazineyl)-2-phenylpyrido[2,3-d]pyrimidine</p>
7j	3,4,5-OCH ₃	 <p>2-Phenyl-4-(2-(3,4,5-trimethoxybenzylidene) hydrazineyl)-pyrido[2,3-d]pyrimidine</p>

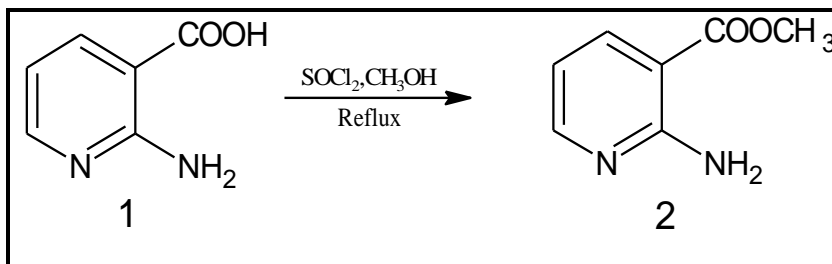
7k	4- OCOCH ₃	 <p>4-((2-(2-Phenylpyrido[2,3-d]pyrimidin-4-yl)hydrazineylidene)-methyl)phenyl acetate</p>
7l	3-OC ₂ H ₅ , 4-OH	 <p>2-Ethoxy-4-((2-(2-phenylpyrido[2,3-d]pyrimidin-4-yl)-hydrazineylidene)methyl)phenol</p>
7m	4- CH ₂ C ₆ H ₅	 <p>4-(2-(4-Benzylbenzylidene)hydrazineyl)-2-phenylpyrido[2,3-d]pyrimidine</p>
7n	3-NO ₂	 <p>4-(2-(3-Nitrobenzylidene)hydrazineyl)-2-phenylpyrido[2,3-d]pyrimidine</p>

7o	2-OH, 5-NO ₂	 <p>4-Nitro-2-((2-(2-phenylpyrido[2,3-d]pyrimidin-4-yl)hydrazineylidene)methyl)phenol</p>
7p	4- N(CH ₃) ₂	 <p><i>N,N</i>-dimethyl-4-((2-(2-phenylpyrido[2,3-d]pyrimidin-4-yl)hydrazineylidene)methyl)-aniline</p>

Scheme for Synthesis-

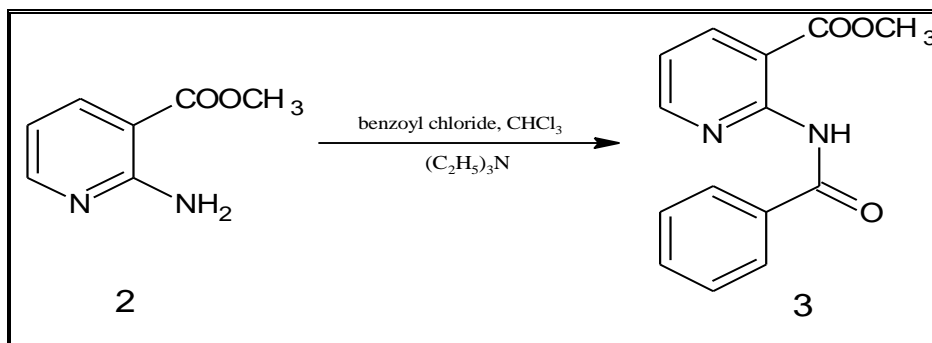


Synthesis of methyl 2-aminonicotinate (2)-



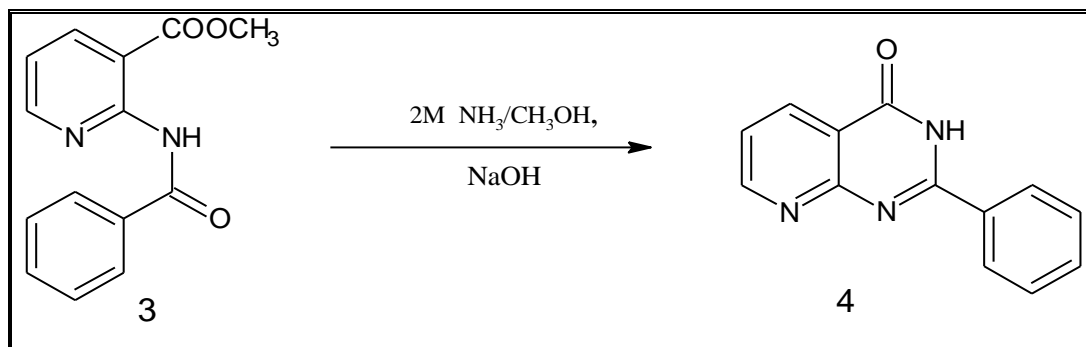
2-Aminopyridine 3-carboxylic acid (13.8g, 0.1 mole) was dissolved in 400 mL of anhydrous methanol, to this solution thionyl chloride (11.8mL, 14.03g, 0.1 mole) was added drop wise for half hour with constant stirring. On complete addition, it was refluxed for twelve hours after which the reaction mixture was cooled to room temperature. The solvent from the mixture was evaporated under vacuum and remaining residue was dissolved in chloroform. The chloroform layer was collected and washed with 5% hydrochloric acid and 10% sodium bicarbonate followed by water. This layer was further dried over sodium sulphate and concentrated to give methyl 2-aminonicotinate.

Synthesis of methyl 2-benzamidonicotinate (3)-



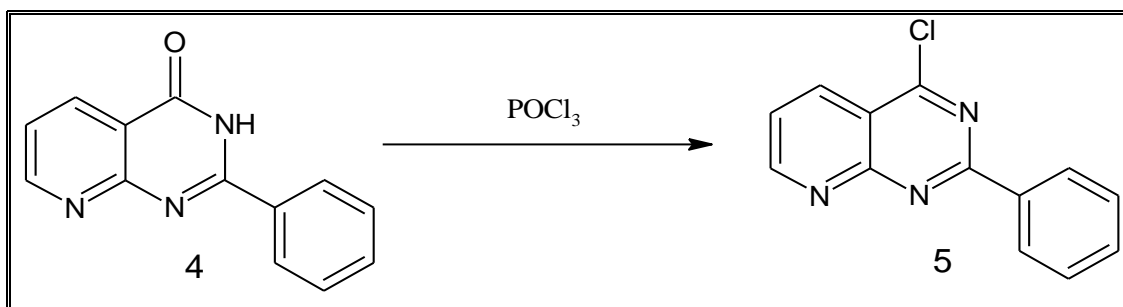
To a solution of methyl 2-aminonicotinate (7.60g, 0.5 mole) in 50 mL chloroform was added triethylamine (2.5 mL, 0.2 mole). To this solution benzoyl chloride (3.04 mL, 2.22g, 0.02 mole) in chloroform was added drop wise over a period of one hour with continues stirring. It was further stirred on room temperature for next twenty hours. After that the mixture was filtered to remove any residue formed, the solution was washed with 10% sodium bicarbonate and 5% hydrochloric acid. It was further treated with ethyl acetate in presence of hexane to give methyl-2-benzamidonicotinate as solid product.

Synthesis of 2-phenylpyrido[2,3-d]pyrimidin-4(3H)-one (4)-



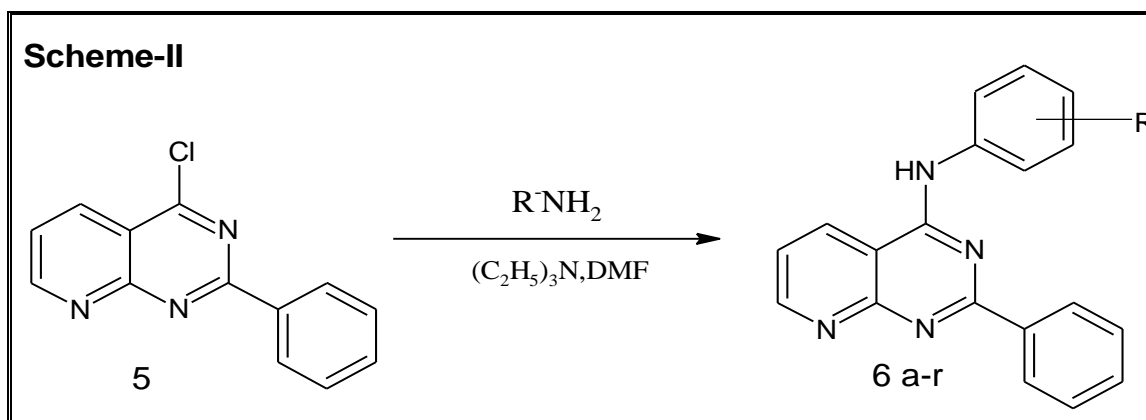
Compound **3** (5.12g, 0.02 mole) was dissolved in 10 mL of methanol and to this a 28% solution of ammonium hydroxide was added. This mixture was then heated for five hours and then 40 mL of sodium hydroxide was added with vigorous stirring followed by refluxing for twelve hours. It was allowed to cool down to room temperature leading to formation of a precipitate which was further filtered and dried to obtain white solid as 2-phenylpyrido[2,3-d]pyrimidin-4(3H)-one.

Synthesis of 4-chloro-2-phenylpyrido[2,3-d]pyrimidine (5)-



Compound **4** (2.23 g, 0.01 mole) was refluxed with phosphorus oxychloride for five hour during which all the starting material was dissolved and utilized. Excess of phosphorus oxychloride was removed under vacuum and the remaining residue was poured in ice-cold water and chloroform. The chloroform layer was separated and treated with sodium bicarbonate. The chloroform layer was further washed with brine and then purified using silica gel column with chloroform as an eluent to provide 4-chloro-2-phenylpyrido[2,3-d]pyrimidine.

General Synthesis of 2-phenyl-*N*-(substituted phenyl) pyrido[2,3-*d*] pyrimidin-4-amine derivatives (6a-r)-



Compound **5** was reacted with various anilines in 4 mL of dry DMF, to this solution 86 microliters of diisopropylamine (DIPA) was added and heated over a period of three to six hours. This reaction mixture was cooled to room temperature and residue was filtered out and purified using column chromatography to yield respective derivatives. Total eighteen derivatives were synthesized, these compounds are enlisted as follows;

1. *N*-(4-Fluorophenyl)-2-phenylpyrido[2,3-*d*]pyrimidin-4-amine (**6a**)-
2. *N*-(2-Fluorophenyl)-2-phenylpyrido[2,3-*d*]pyrimidin-4-amine (**6b**)-
3. *N*-(4-Chlorophenyl)-2-phenylpyrido[2,3-*d*]pyrimidin-4-amine (**6c**)-
4. *N*-(2-Chlorophenyl)-2-phenylpyrido[2,3-*d*]pyrimidin-4-amine (**6d**)-
5. *N*-(4-Bromophenyl)-2-phenylpyrido[2,3-*d*]pyrimidin-4-amine (**6e**)-
6. *N*-(2-Bromophenyl)-2-phenylpyrido[2,3-*d*]pyrimidin-4-amine (**6f**)-
7. 2-Phenyl-*N*-(4-(trifluoromethyl)phenyl)pyrido[2,3-*d*]pyrimidin-4-amine (**6g**)-
8. 2-Phenyl-*N*-(*p*-tolyl)pyrido[2,3-*d*]pyrimidin-4-amine (**6h**)-
9. 2-Phenyl-*N*-(*m*-tolyl)pyrido[2,3-*d*]pyrimidin-4-amine (**6i**)-
10. 2-Phenyl-*N*-(*o*-tolyl)pyrido[2,3-*d*]pyrimidin-4-amine (**6j**)-
11. *N*-(4-Methoxyphenyl)-2-phenylpyrido[2,3-*d*]pyrimidin-4-amine (**6k**)-
12. *N*-(3-Methoxyphenyl)-2-phenylpyrido[2,3-*d*]pyrimidin-4-amine (**6l**)-

13. *N*-(2-Methoxyphenyl)-2-phenylpyrido[2,3-*d*]pyrimidin-4-amine (6m)-

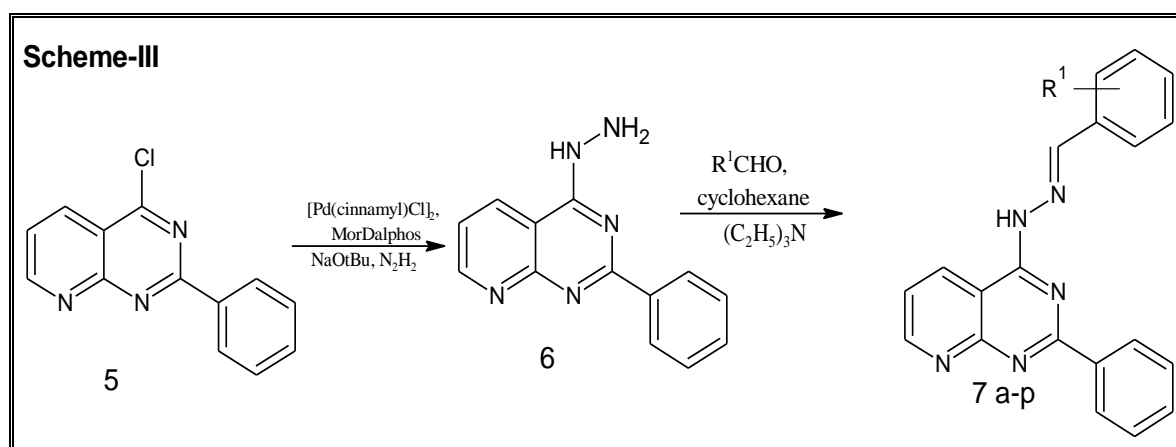
14. 4-((2-Phenylpyrido[2,3-*d*]pyrimidin-4-yl)amino)phenol (6n)-

15. 2-((2-Phenylpyrido[2,3-*d*]pyrimidin-4-yl)amino)phenol (6o)-

16. *N*-(4-Nitrophenyl)-2-phenylpyrido[2,3-*d*]pyrimidin-4-amine (6p)-

17. *N*-(3-Nitrophenyl)-2-phenylpyrido[2,3-*d*]pyrimidin-4-amine (6q)-

18. *N*-(2-Nitrophenyl)-2-phenylpyrido[2,3-*d*]pyrimidin-4-amine (6r)-



Synthesis of 4-hydrazineyl-2-phenylpyrido[2,3-*d*] pyrimidine (6)-

This reaction was carried out in an inert atmosphere glove box, a PTFE septum capped vial was injected with analytical grade toluene, to this was added a mixture of palladium(π -cinnamyl)chloride ($[\text{Pd}(\text{cinnamyl})\text{Cl}]_2$) (2.5 mol%) and Di(1-adamantyl)-2-morpholinophenylphosphine (MorDalphos) (5.5 mol%), this mixture was stirred for ten min. subsequently sodium tert-butoxide (1.5 mol%) was added and care was taken that the solids should not form. After removal from the glove box, 4-chloro-2-phenylpyrido[2,3-*d*]pyrimidine (2.5 mol) and hydrazine hydrate (2.5 mol) was added via syringe and stirred for another five hour. The completion was observed over a TLC with reaction solution withdrawal at every twenty min interval. On completion of reaction the solution from tube was filtered and washed with dichloromethane: methanol system for three times and then with brine and dried over sodium sulphate. The product (4-hydrazineyl-2-phenylpyrido[2,3-

d] pyrimidine) obtained was stored in amber colored vacuum sealed bottles and used within twelve hours of synthesis.

General Synthesis of 4-(2-(substituted benzylidene)hydrazineyl)-2-phenylpyrido[2,3-d]pyrimidine (7a-p)

Compounds **7a-p** was obtained from the reaction of compound **6** with various aldehydes to obtain various derivatives. In 4 mL of cyclohexane 4-hydrazineyl-2-phenylpyrido[2,3-d] pyrimidine (1 mmol. eq.) was mixed and stirred continuously. To this solution aldehyde (1 mmol. eq.) was added followed by catalytic amount of triethylamine. The mixture was stirred at 35-40 °C for four to seven hour depending on the completion of reaction as determined by TLC. This reaction mixture was cooled to room temperature and residue was filtered out and purified using column chromatography to yield respective derivatives. Total sixteen derivatives were synthesized; these compounds are enlisted as follows;

1. **4-(2-Benzylidenehydrazineyl)-2-phenylpyrido[2,3-d]pyrimidine(7a)-**
2. **4-(2-(4-Fluorobenzylidene)hydrazineyl)-2-phenylpyrido[2,3-d]pyrimidine (7b)-**
3. **4-(2-(2-Chlorobenzylidene)hydrazineyl)-2-phenylpyrido[2,3-d]pyrimidine (7c)-**
4. **4-(2-(2,4-Dichlorobenzylidene)hydrazineyl)-2-phenylpyrido[2,3-d]pyrimidine (7d)-**
5. **4-(2-(4-(Trifluoromethyl)benzylidene)hydrazineyl)-2-phenylpyrido[2,3-d] pyrimidine (7e)-**
6. **4-((2-(2-Phenylpyrido[2,3-d]pyrimidin-4-yl)hydrazineylidene)methyl) phenol (7f)-**
7. **3-((2-(2-Phenylpyrido[2,3-d]pyrimidin-4-yl)-hydrazineylidene)-methyl)- benzene -1,2-diol (7g)-**
8. **4-(2-(2-Methoxybenzylidene)hydrazineyl)-2-phenylpyrido[2,3-d]pyrimidine (7h)-**
9. **4-(2-(3-Methoxybenzylidene)hydrazineyl)-2-phenylpyrido[2,3-d]pyrimidine (7i)-**
10. **2-Phenyl-4-(2-(3,4,5-trimethoxybenzylidene)hydrazineyl)pyrido[2,3-d] pyrimidine (7j)-**

11. 4-((2-(2-Phenylpyrido[2,3-d]pyrimidin-4-yl)hydrazineylidene)methyl) phenyl acetate (7k)-

12. 2-Ethoxy-4-((2-(2-phenylpyrido[2,3-d]pyrimidin-4-yl)hydrazineylidene) methyl) phenol (7l)-

13. 4-(2-(4-Benzylbenzylidene)hydrazineyl)-2-phenylpyrido[2,3-d]pyrimidine (7m)-

14. 4-(2-(3-Nitrobenzylidene)hydrazineyl)-2-phenylpyrido[2,3-d]pyrimidine (7n)-

15. 4-Nitro-2-((2-(2-phenylpyrido[2,3-d]pyrimidin-4-yl)hydrazineylidene) methyl)-phenol (7o)-

16. *N,N*-dimethyl-4-((2-(2-phenylpyrido[2,3-d]pyrimidin-4-yl)hydrazineylidene) methyl)-aniline (7p)-

Total eighteen derivatives of 2-phenyl-*N*-(substituted phenyl) pyrido[2,3-d] pyrimidin-4-amine (6a-r) were synthesized, these compounds are enlisted as follows:-

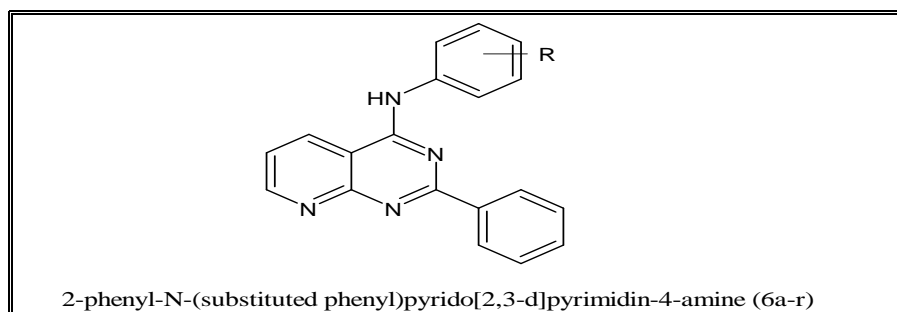
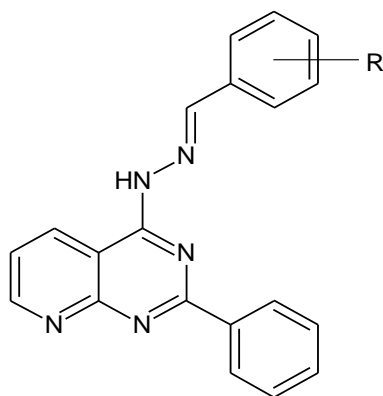


Table: Substituent of 2-phenyl-*N*-(substituted phenyl)pyrido[2,3-d] pyrimidin-4-amine derivatives (6a-r)-

Compound No.	Functional group	Compound No.	Functional group	Compound No.	Functional group
6a	4-F	6g	4-CF ₃	6m	2-OCH ₃
6b	2-F	6h	4-CH ₃	6n	4-OH
6c	4-Cl	6i	3-CH ₃	6o	2-OH
6d	2-Cl	6j	2-CH ₃	6p	4-NO ₂
6e	4-Br	6k	4-OCH ₃	6q	3-NO ₂
6f	2-Br	6l	3-OCH ₃	6r	2-NO ₂

Compound **5** was further treated with hydrazine hydrate in presence of a mixture of palladium(π -cinnamyl)chloride ([Pd(cinnamyl)Cl]₂) (2.5 mol%) and Di(1-adamantyl)-2-morpholinophenylphosphine (MorDalphos) to provide with 4-hydrazineyl-2-phenylpyrido[2,3-d] pyrimidine **6**. Treatment with different substituted aldehydes gave sixteen derivatives of 4-(2-(substituted benzylidene)hydrazineyl)-2-phenylpyrido[2,3-d]pyrimidines **7a-p**. In the series of compounds (**7a-p**), the characteristic properties of derivatives involved singlets at 1.98 ppm corresponding to the methyl group of the acetyl derivative (**7k**), singlet at 2.82 ppm of methyl group of the phenyl derivative (**7m**) and singlet at 1.8 ppm of methyl group of the dimethyl amine derivative (**7p**). The methoxy derivatives (**7h**), (**7i**) and (**7j**) showed a methyl proton at 2.55, 2.53 and 2.51 ppm respectively. In case of compounds (**7f**), (**7g**), (**7l**) and (**7o**) showed characteristic -OH singlets at 10.59, 10.59, 10.19 and 10.11 ppm respectively. All compounds were subjected to determination of molecular weight following a mass spectral analysis; all compounds were found to be in agreement with the theoretical values. Total sixteen derivatives of 4-(2-(substituted benzylidene)hydrazineyl)-2-phenylpyrido[2,3-d]pyrimidines (**7a-p**) were synthesized, these compounds are enlisted as follows:-



4-(2-(substituted benzylidene)hydrazineyl)-2-phenylpyrido[2,3-d]pyrimidines (**7a-p**)

Table: Substituent of 4-(2-(substituted benzylidene)hydrazineyl)-2-phenylpyrido[2,3-d]pyrimidines (7a-p)-

Compound No.	Functional group	Compound No.	Functional group	Compound No.	Functional group
7a	-H	7g	2,3-OH	7m	4-CH ₂ C ₆ H ₅
7b	4-F	7h	2-OCH ₃	7n	3-NO ₂
7c	2-Cl	7i	3-OCH ₃	7o	2-OH, 5-NO ₂
7d	2,4-Cl	7j	3,4,5-OCH ₃	7p	4-N(CH ₃) ₂
7e	4-CF ₃	7k	4-OCOCH ₃		
7f	4-OH	7l	3-OC ₂ H ₅ ,4-OH		

6. ANTICANCER ACTIVITY

***In-vitro* Cytotoxicity assay:-**

All the compounds (**7a-p**) were screened in vitro for their *In vitro* CDK enzyme assay anti-proliferative activity against two cell lines.

Cytotoxicity Assay:-

In-vitro growth inhibition effect of test compounds (**7a-p**) was assessed by colorimetric or spectrophotometric determination by using Sulforhodamine B (SRB) solution at 0.05% (w/v).

SRB Solution preparation:-

Experimental Drugs (**7a-p**) were solubilized in dimethylsulfoxide at 100mg/ml and diluted to 1mg/ml using water and stored frozen prior to use.

Procedure

***In vitro* enzyme assay**

IC₅₀ was calculated using GraphPad Prism version 5 for Windows. The curves were fit using a nonlinear regression model with a log (inhibitor) versus response formula. The experiment was performed in duplicates.

Experimental procedure was followed by the manufactured instruction (LANCE, Perkin Elmer, MA, USA). The reaction was initiated by ATP addition to a mixture containing the kinase (CDK 2/5), peptide substrates (ULingt-4E-BP), and inhibitors (**7a-p**). After 1 hour, EDTA containing solution was added to stop the reaction and phosphorylated peptides were captured by Eu-labeled anti-phosphopeptide antibodies. After 1-hour incubation, fluorescence was measured with 320 nm or 340 nm excitation and 665 nm emission of the Envision reader.

Cell cytotoxicity assay-

IC₅₀ was calculated using GraphPad Prism version 5 for Windows. The curves were fit using a nonlinear regression model with a log (inhibitor) versus response formula. The experiment was performed in triplicates.

For viability experiments, cells were seeded in 96-well plates at 30% confluency and exposed to chemicals the next day. After 72 hours, cells were fixed with 10% TCA (TriChloroAcetic acid). Then, cells were stained with 0.05% SRB solutions, and 10mM Tris base is added to solubilize the protein-bound SRB dye. Absorbance at 564nm is measured on each well and cytotoxicity was calculated as % cell growth inhibition.

$$\% \text{ cell survival} = \{(\text{At}-\text{Ab})/(\text{Ac}-\text{Ab})\} \times 100$$

Where At, Ab and Ac are absorbance of test, blank and control, respectively.

Result and discussion:-

All the final compounds (7a-p) were tested for their inhibitory activity at 25 nM against CDK2 and CDK5; the results of IC₅₀ are mentioned in below Table. Among the final compounds, compounds with halogens substituted on the R₁ position (7b-e) showed higher inhibition at 25 nM, compounds with acetyl group (7k) showed poor activity in both CDK2 and CDK5. Disubstituted compounds also showed low inhibition (7g, 7j, 7l and 7o), whereas the phenyl substituent on the R₁ position (7m) exhibited poor inhibition of CDK2 and good inhibition of CDK5 activity. Compounds 7i and 7n showed promising inhibitory activity and the IC₅₀ in CDK2 (7i: 7.1 ± 2.1; 7n: 2.6 ± 0.1) and CDK5 (7i: 2.3 ± 0.5; 7n: 4.7 ± 1.4).

Table: IC₅₀ evaluation of 4-(2-(substituted benzylidene)hydrazineyl)-2-phenylpyrido[2,3-d]pyrimidine (7a-p) compounds:-

Comp No.	R ₁	IC ₅₀ (nM)		Comp No.	R ₁	IC ₅₀ (nM)	
		CDK2/ cyclinA	CDK5/ p35			CDK2/ cyclinA	CDK5/ p35
7a	-H	17 ± 7	11 ± 7	7i	3-OCH ₃	7.1 ± 2.1	2.3 ± 0.5
7b	4-F	15 ± 7	22 ± 5	7j	3,4,5-OCH ₃	50 ± 14	26 ± 14
7c	2-Cl	39 ± 7	32 ± 4	7k	4-OCOCH ₃	47 ± 6	78 ± 16
7d	2,4-Cl	16 ± 8	10 ± 4	7l	3-OC ₂ H ₅ , 4-OH	96 ± 15	65 ± 22
7e	4-CF ₃	16 ± 4	7 ± 8	7m	4-CH ₂ C ₆ H ₅	111 ± 14	28 ± 8
7f	4-OH	5.5 ± 1.7	31 ± 7	7n	3-NO ₂	2.6 ± 0.1	4.7 ± 1.4
7g	2,3-OH	28 ± 5	17 ± 7	7o	2-OH, 5-NO ₂	163 ± 24	29 ± 11
7h	2-OCH ₃	53 ± 16	93 ± 17	7p	4-N(CH ₃) ₂	49 ± 8	72 ± 14

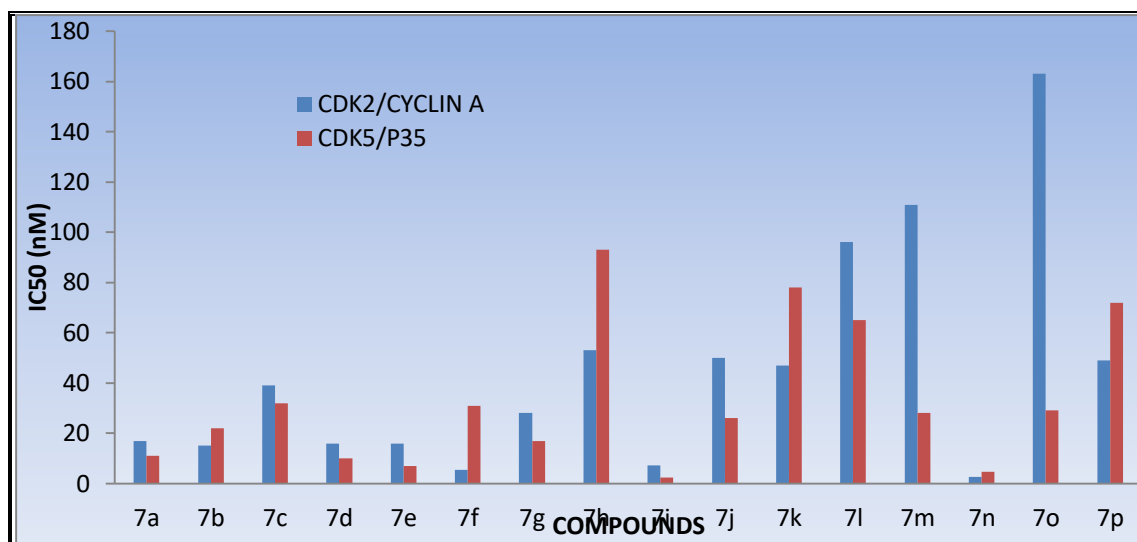


Fig: Graph of IC₅₀ evaluation of synthesized compounds 7a-p

Further to evaluate the kinase selectivity of these two compounds 7i and 7n, Kinase selectivity assay was performed (Table-8.2.3.2). Compounds 7i and 7n showed single digit nanomolar inhibition concentration (IC₅₀) towards CDK2 and CDK5 (7i: CDK2= 8.2 nM, CDK5= 3.6 nM), and double digit values of nM concentration for remaining kinase in the study. To study the growth inhibitory action of these compounds anti-proliferative activity was carried out on two cell lines, viz., colon cancer cell lines HCT116 and breast cancer cell lines MCF7. Both the compounds showed the anti-proliferative activity (Table-8.23.3) in the micromolar concentration range (7i: HCT116= 3.10 μ M, MCF7= 3.04 μ M and 7n: HCT116= 2.19 μ M, MCF7= 2.43 μ M). These concentration are quit high for being a good anticancer drug, possible reasons for this moderate performance may be physicochemical variations or various other mechanistic reasons which would need to be further studied.

Table: CDK selectivity assay of Compound 7i and 7n

Sr. No.	Protein kinase	7i	7n
1.	CDK1/cyclinB(h)	22 nM	25 nM
2.	CDK2/cyclinA	8.2 nM	3.6 nM
3.	CDK4/cyclinD3(h)	>1000 nM	500 nM
4.	CDK5/p35	9.1 nM	8.2 nM
5.	CDK6/cyclinD3(h)	>1000 nM	>1000 nM
6.	CDK7/cyclinH/MAT1(h)	333 nM	371 nM
7.	CDK9/cyclin T1(h)	32 nM	24 nM

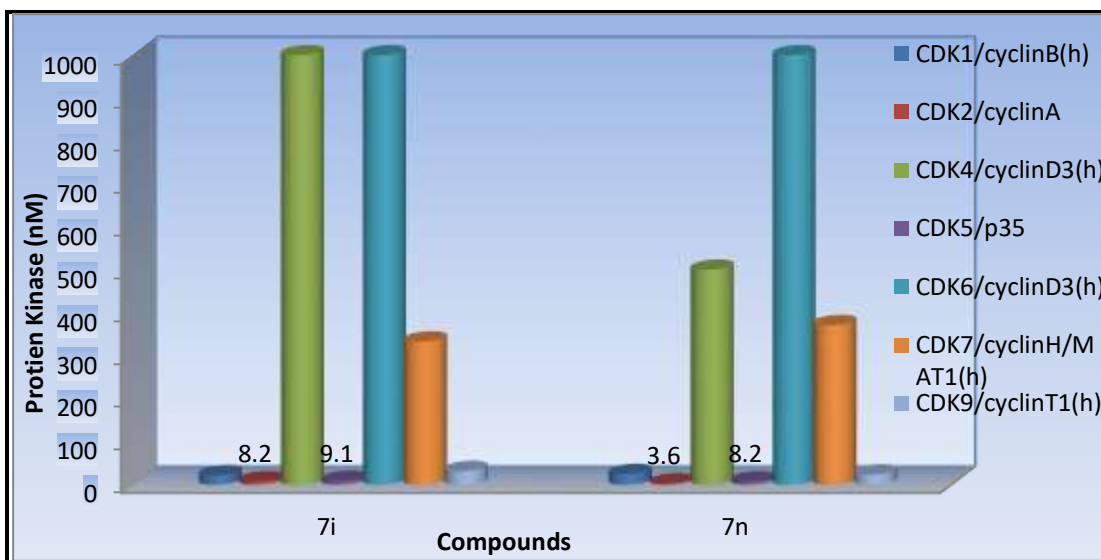


Fig: Graph of CDK selectivity assay for the compound 7i and 7n.

Table: Anti-proliferative activity of Compound 7i and 7n:-

Compound	Cell line	
	HCT116	MCF7
7i	3.10 μ M	3.04 μ M
7n	2.19 μ M	2.43 μ M

Conclusion:-

New compounds had been synthesized with an attempt to potentate them by fulfilling the structural requirement for special biological activity.

The anticancer activity is evaluated by using the software package Schrödinger. The approach was based on structure based screening of several commercial databases. Glide is validated software designing for calculating the accurate binding interaction energies of the 3-D structures of a known protein receptor with ligand or another protein molecule.

The series of 2-phenyl-*N*-(substituted phenyl) pyrido[2,3-*d*] pyrimidin-4-amine, 4-(2-(substituted benzyldene)hydrazineyl)-2-phenylpyrido[2,3-*d*]pyrimidine and its derivatives structures were used in order to prepare ligand for glide docking. The co-crystal structure of compounds was obtained from Protein Data Bank (PDB-ID: 2v58 and 4kd1) in order to prepare protein for docking studies (using the 'protein preparation tools' in glide dock). The results of the docking studies are presented in the form of glide Score are shown in above table. From results of glide dock, above ligands fit into the binding pocket of the biotin carboxylase and it has to be potent antibacterial activity. The ligand structure VP14, VP13, VP10, VP3, VP20, VP16, VP5, VP19, VP17, VP9, VP8, VP15, VPP12, VP6, VP2, VP18 i.e. compound 6o, 6n, 6r, 6d, 6i, 6m, 6f, 6j, 6l, 6q, 6p, 6k, 7p, 6a, 6c, 6h respectively, showed high docking score on BC. For Kinase inhibitor may be arranged in the following manner: VPP20> VP17> VPP9> VP13> VPP1> VPP24> VPP4> VPP11> VP10 i.e. compound 7j, 6l, 7n, 6n, 7a, 7l, 7i, 7f, 6r respectively, showed high docking score on CDK.

Total thirty four analogs have been synthesized by using various aldehyde and various substituted anilines substituents. The synthesized pyridopyrimidine derivatives had been purified by recrystallization and all the reactions involved in synthesis were monitored using TLC with Ethyl Acetate: n-Hexane and Ethyl Acetate: Petroleum ether: Methanol (in varying proportion) as solvent systems. Spectral data of all synthesized compounds were confirmed by IR Spectra, ¹HNMR and Mass Spectra. The synthesized pyridopyrimidine analogues were evaluated for their *in vitro* antibacterial and anticancer activity.

The series of pyridopyrimidines yielded eighteen compounds (6a-r) that were characterized on the basis of spectral data. We have synthesized series of pyridopyrimidines that yielded sixteen compounds (**7a-p**) which were evaluated for anticancer activity on the basis of structure based designing with Dinaciclib. Compounds **7i** and **7n** were found to show promising activity, IC₅₀ and kinase selectivity. These compounds also showed moderate anti-proliferative activity. Kinase selectivity assay shows selective nature of these two compounds toward CDK2 and CDK5 compared to other kinases under investigation.

7. CONCLUSION:-

The present work entitled “Design, Synthesis and Screening of Some Novel Tyrosine Kinase Inhibitors as Anticancer Agents”, aims to design and synthesize tyrosine kinase inhibitor analogs in hope that tyrosine kinase inhibitor kills cancer cells without harming normal cells much. The new chemical entities were designed by using the pharmacophore structure of known tyrosine kinase inhibitor molecules that acts as anticancer agent.

The designing and virtual screening of total 232 novel anticancer agents from seven different series viz. 1,6-Diphthalazine analogues, Aminophthalazine analogues, N-[4-Amino-2-(4-Methylphenyl)quinazoline-6-yl]acetamide analogues, N-[2-(4-methylphenyl)-4-(substituted aniline)-3, 4-dihydro quinazolin-6-yl] acetamide analogues, 4-anilinoquinazoline analogues, 2-phenyl-*N*-(substituted phenyl) pyrido[2,3-*d*] pyrimidin-4-amine analogues and 4-(2-(substituted benzylidene)hydrazineyl)-2-phenylpyrido[2,3-*d*]pyrimidine analogues had been carried out using molecular modeling and docking studies by Schrodinger’s Maestro Glide Docking version 2012 software. Total 71 compounds had been synthesized from seven different schemes outlined viz. 1,6-Diphthalazine derivatives, Aminophthalazine derivatives, N-[4-Amino-2-(4-Methylphenyl)quinazoline-6-yl]acetamide derivatives, N-[2-(4-methylphenyl)-4-(substituted aniline)-3, 4-dihydro quinazolin-6-yl] acetamide derivatives, 4-anilinoquinazoline derivatives, 2-phenyl-*N*-(substituted phenyl) pyrido[2,3-*d*] pyrimidin-4-amine derivatives and 4-(2-(substituted benzylidene)hydrazineyl)-2-phenylpyrido[2,3-*d*]pyrimidine derivatives. Amongst designed and synthesized novel compounds total 16 were screened for In-vitro Protein Kinase Inhibition Assay as Anticancer Agents.

Total 48 Novel analogs from 1,6-Diphthalazine derivatives series were designed and docked into the active sites of EGFR receptor PDB ID (1YWN, 2P2H, 3XIR, 3EWH, 3VHE, 3VNT, 4AG8, 4ASE) for studying the binding mode of designed compounds and further screening to sort out the best compound having good binding affinity which was compared with binding mode of EGFR receptor Inhibitors like Vatalanib results. The results of the docking studies are presented in the form of Glide Dock Score. The 1YWN, 2P2H, 3XIR, 3EWH, 3VHE, 3VNT, 4AG8, 4ASE glide dock score are presented as negative values, indicating that more the negative values more are the binding interactions. According to the results we see that among all the energy parameters the largest contribution for binding

energy comes from Vander Waals interactions. The results of the inhibition for the VEGF receptor may be arranged in the following manner: Vmol 21> Vmol 17>mol 16> mol 15> mo21> mol 23>mol 6> mol 9>mol17. Docking studies performed by GLIDE has confirmed that above inhibitors fit into the binding pocket of the VEGF receptor.

The GLIDE docking was applied for proposed 56 ligands from Aminophthalazine derivatives series to build a binding affinity model for the vascular epidermal growth factor receptor that was then used to compute the free energy of binding for this kinase. According to the glide score, the results of the inhibition for the VEGFR human tyrosine kinase receptor may be arranged in the following manner: 22>a22>a11> 1. Docking studies performed by GLIDE has confirmed that above inhibitors fit into the binding pocket of the VEGFR kinase receptor.

Glide docking method have been applied to total 27 inhibitors of tyrosine protein kinases from N-[4-Amino-2-(4-Methylphenyl)quinazoline-6-yl]acetamide series to build a binding affinity model for EGFR that was then used to compute the free energy of binding energy of binding for this kinase. According to the glide score the results of the inhibition for the EGFR may be arranged in the following manner: mol21> mol50> mol24>mol30> mol1> mol2>mol39> mol5. Docking studies performed by GLIDE has confirmed that above inhibitors fit into the binding pocket of the EGF receptor.

Glide docking method have been applied to 7 tyrosine protein kinase inhibitor from N-[2-(4-methylphenyl)-4-(substituted aniline)-3, 4-dihydro quinazolin-6-yl] acetamide series to build a binding affinity model for EGFR that was then used to compute the free energy of binding energy of binding for this kinase. According to the glide score the results of the inhibition for the EGFR may be arranged in the following manner: Mol1> Mol2 > Mol4 >Mol3 > Mol6 > Mol7 > Mol5. Docking studies performed by GLIDE has confirmed that above inhibitors fit into the binding pocket of the EGF receptor.

We have applied the GLIDE docking method to 50 analogues of 4-anilinoquinazoline which are inhibitors of tyrosine protein kinases to build a binding affinity model for the epidermal growth factor receptor that was then used to compute the free energy of binding for this kinase. According to the results we see that among all the energy parameters the largest contribution for binding energy comes from Vander Waals interactions. According to

the glide score the results of the inhibition for the EGF receptor may be arranged in the following manner: mol37> mol12> mol35>mol15> mol35> mol5>mol41> mol4>mol17>mol11. Docking studies performed by GLIDE has confirmed that above inhibitors fit into the binding pocket of the EGF receptor.

The molecular docking studies of total 18 analogs of 2-phenyl-*N*-(substituted phenyl)pyrido[2,3-*d*] pyrimidin-4-amine series on PDB 2v58 showed that compound VP14 (6o), VP13 (6n), VP10 (6r), VP3 (6d), VP20 (6i) and VP17 (6l) exhibited highest interaction with the enzyme in their molecular docking studies. For biotin carboxylase inhibitor may be arranged in the following manner: VP14> VP13> VP10> VP3> VP20> VP16> VP5> VP19> VP17> VP9 > VP8> VP15> VPP12> VP6 i.e. compound 6o, 6n, 6r, 6d, 6i, 6m, 6f, 6j, 6l, 6q, 6p, 6k, 7p, 6a, 6c, 6h respectively, showed high docking score on BC. The molecular docking studies of total 16 analogs of 4-(2-(substituted benzylidene)hydrazineyl)-2-phenylpyrido[2,3-*d*]pyrimidine series on PDB 4kd1 showed that compound VPP20 (7j), VP17 (6l), VPP9 (7n), VP13 (6n), VPP1 (7a), VPP24 (7l), VPP4 (7i), VPP11 (7f) and VP10 (6r) exhibited highest interaction with the enzyme in their molecular docking studies. For CDK inhibitor may be arranged in the following manner: VPP20> VP17> VPP9> VP13> VPP1> VPP24> VPP4> VPP11> VP10 i.e. compound 7j, 6l, 7n, 6n, 7a, 7l, 7i, 7f, 6r respectively, showed high docking score on CDK. Docking studies performed by GLIDE has confirmed that above inhibitors fit into the binding pocket of the biotin carboxylase and CDK.

From the results we may observe that for successful docking, intermolecular hydrogen bonding and lipophilic interactions between the ligand and the receptor are very important. A comparison of the induced fit and virtual docking gives the role of protein flexibility. It is obvious from the results that a combined method of soft docking and side chain optimization gives better results. It is also clear that an average distribution of docking free energy ranging from 2 kcal/mol or more, is sufficient to mis-rank a potential drug candidate as a weak binder. However, by combining the MM-GB/SA and relaxed complex methods we are able to show the best ranked binding modes.

All new chemical entities synthesized had been purified by recrystallization and all the reactions involved in synthesis were monitored using TLC. All synthesized compounds were

characterized by spectral data and were confirmed on basis of IR Spectra, ¹HNMR and Mass Spectra.

Amongst designed and synthesized compounds series of pyridopyrimidines (7a-p) were evaluated for anticancer activity on the basis of structure based designing with Dinaciclib. Compounds 7i and 7n exhibited promising activity, IC₅₀ and kinase selectivity. These compounds also showed moderate anti-proliferative activity. Kinase selectivity assay showed selective nature of these two compounds toward CDK2 and CDK5 compared to other kinases under investigation.

FUTURE SCOPE:

As the tyrosine kinase enzyme is the promising target for the designing and development of more selective, potent and safer anticancer agents, the novel molecules designed and screened in present study needs to be explored further in order to get promising FDA approved drugs in our hand. For this, extensive In-silico screening and In-vitro screening of more number of analogues of the scaffold studied needs to be carried out on more number of tyrosine kinase proteins along with In-vivo screening there In vivo studies. The toxicity studies of the more potent analogues need be explore further. Also, there is scope for further optimization of the scaffold structure to get more potent and safe compounds.

ACKNOWLEDGMENT:

The Principle Investigator and Co-Investigator are thankful to University Grants Commission (UGC), New Delhi for providing the financial support to present study on “Designing, Synthesis and Screening of Some Novel Tyrosine Kinase Inhibitors as Anticancer Agents. We are also thankful to the Honorable Vice Chancellor Sir of the Swami Ramanand Teerth Marathwada University Nanded and Director, School of Pharmacy, Swami Ramanand Teerth Marathwada University Nanded for providing all necessary facilities required for the completion of this project.

REFERENCES:

1. D.J.Brown, Wiley online library, Chemistry of Heterocyclic Compounds: Fused Pyrimidines, Quinazolines, JAN 2008.,Part I, Volume 24;
2. J. A. Lowe III, R. L. Archer, D. S. Chapin, J. B. Cheng, D. Helweg, J. L Johnson, Kenneth, L. A. Lebel, P. F. Moore, J. A. Nielson, L. L. Russo and J. T. Shirley, J. Med. Chem., 1991.,34 ; 624-628 .
3. H. B. Cottam, H. Shih, L. R. Tehrani, B. Wasson and D. A. Carson, J. Med. Chem., 1996.,39; 2-9.
4. A. Schlapbach, R. Heng and F. D. Padov, Bioorg. Med. Chem. Lett., 2004 ., 14; 357- 360.
5. A. Raghu Ram Rao and V. Malla Reddy, Pharmazie, 1992.,47; 793-795.
6. A. Raghu Ram Rao and V. Malla Reddy, Arzneim. Forsch. /Drug Res, 1993.,43;663-667.
7. 14. G. Daidone, B. Maggio, D. Raffa, S. Plescia, M. L. Bajardi, A. Caruso, V. M. C. Cutuli and M. Amico-Roxas, Eur. J. Med. Chem., 1994., 29; 707-711 .
8. P. Rani, Archana, V. K. Srivastava and A. Kumar. Ind. J. Chem., 41B, 2642-2646
10. K. Karnakar, J. Shangkar, S. N. Murthy, K. Ramesch, Y. V. D. Nageshwar, Synlett, 2011, 1089-1096.
11. J. Zhang, D. Zhu, C. Yu, C. Wan, Z. Wang, Org. Lett., 2010, 12, 2841-2843.
12. C. Wang, S. Li, H. Liu, Y. Jiang, H. Fu, J. Org. Chem., 2010, 75, 7936-7938.
13. B. Han, X.-L. Yang, C. Wang, Y.-W. Bai, T.-C. Pan, X. Chen, W. Yu, J. Org. Chem., 2012, 77, 1136-1142.
14. X. Yang, H. Liu, R. Qiao, Y. Jiang, Y. Zhao, Synlett, 2010, 101-106.
15. Y. Wang, H. Wang, J. Peng, Q. Zhu, Org. Lett., 2011, 13, 4596-4599.
16. F. Portela-Cubillo, J. S. Scott, J. C. Walton, J. Org. Chem., 2009, 74, 4934-4942.
17. Sorbera L.A., Bartoli J, Castaner J. Albaconazole. Drugs Fut, 2003.,28(6); 529.
18. Dictionary of organic compounds. London:Chapman & Hall,1996.ISBN 0412-54090-8.
19. Dell A.; Williams D. H; Morris H. R; Smith G.A.; Feeney J; RobertsG, J. Am. Chem. Soc., 1975.,97:2497.
- 20.

21. 34. Wang.Y, Serradell. N, Rosa.E, Castaner.R,"BI-1356". *Drugs of the Future* , 2008.,33 (6):473–477.
22. 35. Tiwari.A. Linagliptin, a dipeptidyl peptidase-4 inhibitor for treatment of type-II diabetes. *Curr Opin Investig Drugs*, 2009.,10(10);1091-104.
23. 40. Kim.Y. H, Choi.H, Lee.J, Hwang.I.C, Moon.S.K, Kim.S.J et al.,Quinazolines as potent and highly selective PDE5 inhibitors as potential therapeutics for male erectile dysfunction. *Bioorganic & Medicinal Chemistry Letters* 2008.,18;6279–6282.
24. 41. Raymond E, Faivre S, Armand J,"Epidermal growth factor receptor tyrosine kinase as a target for anticancer therapy",2000 ., 1: 15–23; 41– 2.
25. 42. Pao W, Miller V, Zakowski M, et al. "EGF receptor gene mutations are common in lung cancers from "never smokers" and are associated with sensitivity of tumors to gefitinib and erlotinib". *Proceedings of the National Academy of Sciences of theUnited States of America*, 2004.,101(36);13306–11.
26. 43. Higa GM & Abraham J , "Lapatinib in the treatment of breast cancer" *Expert Review of Anticancer Therapy*, 2007., (Future Drugs)7(9);1183–92.
27. 47. Khaled Abouzid and Samia Shouman, Design, synthesis and in vitro antitumor activity of 4-aminoquinoline and 4-aminoquinazoline derivatives targeting EGFR tyrosine kinase, *Bioorganic & Medicinal Chemistry* ,2008., 16 ; 7543–7551.
28. 49. Adel S. El-Azab , Mohamed A. Al-Omar, Design, synthesis and biological evaluation of novel quinazoline derivatives as potential antitumor agents: Molecular docking study, *European Journal of Medicinal Chemistry* 2010.,45 ; 4188-4198.
29. 53. Wang Yong-kang, JIN Jing et al., Synthesis and antitumor activity of novel 2-(1-substitutedpiperidin-4-ylamino)quinazolines as antitumor agents, *Acta Pharmaceutica Sinica* 2012., 47 (9); 1164–1178.
30. 54. Maneesh Kumar Srivastav and S. M. Shantakumar, Design and Synthesis of Novel 2-Trichloromethyl-4- Substituted Quinazoline Derivatives as Anti-tubercular Agents, *Chem Sci Trans.*, 2013., 2(3) ;1056-1062 .DOI:10.7598/cst2013.490.
31. 55. Xiaoqing Wu, Mingdong Li, Design and synthesis of novel Gefitinib analogues with improved anti-tumor activity, *Bioorganic & Medicinal Chemistry* 2010., 18 ;3812–3822.

32. Peter, B., Robert, H.B., Craig, S.H., Laurent, F.A.H., Mark, H., Jason, G.K., Jane, K., Teresa, K., Donald, J.O., Stuart, E.P., Emma, J.W., Ingrid, . Design, synthesis and in vitro antitumor activity of 4-amino quinoline and 4-amino quinazoline derivatives targeting EGFR tyrosine kinase. *Bioorg. Med. Chem. Lett.* 16, 4908.
33. Ranson, M., 2004. Epidermal growth receptor tyrosine kinase inhibitors. *Br. J. Cancer* 90, 2250.
34. Fabbro, D., Ruetz, S., Buchdunger, E., Cowan-Jacob, S.W., Fendrich, G., Liebetanz, J., O'Reilley, T., Traxler, P., Chaudhari, B., Fretz, H., Zimmermann, J., Meyer, T., Carvatti, G., Furet, P., Manley, P.W., 2002. Protein kinases as targets for anti-cancer agents: from inhibitors to useful drugs. *Pharmacol. Ther.* 93, 79–98.
35. Jeff B. Smaill, Brian D. Palmer, Gordon W. Rewcastle, William A. Denny,, Dennis J. McNamara, Ellen M. Dobrusin, Alexander J. Bridges,‡ Hairong Zhou, H. D. Hollis Showalter, R. Thomas Winters, Wilbur R. Leopold, David W. Fry, Tyrosine Kinase Inhibitors. 15. 4-(Phenylamino)quinazoline and 4-(Phenylamino)pyrido[d]pyrimidine Acrylamides as Irreversible Inhibitors of the ATP Binding Site of the Epidermal Growth Factor Receptor; 1999, 42, 1803-1815 (1998).
36. William A. Denny; The 4-anilinoquinazoline class of inhibitors of the *erbB* family of receptor tyrosine kinases; 56 (2001) 51–56; (2000).
37. Malleshappa N. Noolvi, Harun M. Patel; A comparative QSAR analysis and molecular docking studies of quinazoline derivatives as tyrosine kinase (EGFR) inhibitors: A rational approach to anticancer drug design; 2011.
38. Anja Lu`th, Werner Lowe; Syntheses of 4-(indole-3 yl) quinazolines e A new class of epidermal growth factor receptor tyrosine kinase inhibitors; 2007: *European Journal of Medicinal Chemistry* 43 (2008) 1478e1488.
39. Khaled Abouzid a, Samia Shouman; Design, synthesis and in vitro antitumor activity of 4-aminoquinoline and 4-aminoquinazoline derivatives targeting EGFR tyrosine kinase; 16 (2008) 7543–7551.
40. Clauuen, Holger; Buning, Christian; Rarey, Matthias and Lengauer, Thomas (2001), “FLEXE: Efficient Molecular Docking Considering Protein Structure variations”, *J. Mol. Biol.*, 308, 377-395.

41. Wei, BQ; Weaver, LH; Ferrari, AM; Matthews, BW and Shoichet, BK (2004), "Testing a flexible-receptor docking algorithm in a model binding site", *J. Mol. Biol.*, 337 (5), 1161-82.
42. Taylor, RD; PJ, Jewsbury and JW, Essex1 (2002), "A review of protein-small molecule docking methods", *Journal of Computer-Aided Molecular Design*, 16, 151-166.
43. Bruyère C and Meijer L. Targeting cyclin-dependent kinases in anti-neoplastic therapy. *Curr. Opin. Cell Bio.* **2013**, 25 (6), 772-779. DOI: [10.1016/j.ceb.2013.08.004](https://doi.org/10.1016/j.ceb.2013.08.004)
44. Parry D.; Guzi T.; Shanahan F.; Davis N.; Prabhavalkar D.; Wiswell D.; Seghezzi W.; Paruch K.; Dwyer M. P. and Doll R. Dinaciclib (SCH 727965), a novel and potent cyclin-dependent kinase inhibitor. *Mol. Cancer Ther.* **2010**, 1535-7163. MCT-10-0324. DOI: [10.1021/ml100051d](https://doi.org/10.1021/ml100051d)
45. Crawford T. D.; Ndubaku C. O.; Chen H.; Boggs J. W.; Bravo B. J.; DeLaTorre K.; Giannetti A. M.; Gould S. E.; Harris S. F.; Magnuson S. R.; McNamara E.; Murray L. J.; Nonomiya J.; Sambrone A.; Schmidt S.; Smyczek T.; Stanley M.; Vitorino P.; Wang L.; West K.; Wu P. and Weilan Ye. Discovery of Selective 4-Aminopyridopyrimidine Inhibitors of MAP4K4 Using Fragment-Based Lead Identification and Optimization. *J. Med. Chem.* **2014**, 57, 3484-3493. DOI: [10.1021/jm500155b](https://doi.org/10.1021/jm500155b).
46. Saurat T.; Buron F.; Rodrigues N.; Tauzia M de.; Colliandre L.; Bourg S.; Bonnet P.; Guillaumet G.; Akssira M.; Corlu A.; Guillouzo C.; Berthier P.; Rio P.; Jourdan M.; Bénédicti H and S. Routier. [Design, synthesis and biological activity of pyridopyrimidine scaffolds as novel PI3K/mTOR dual inhibitors](#). *J. Med. Chem.* **2014**, 57, 613-631.
47. Smaill J. B.; Rewcastle G. W.; Loo J. A.; Greis K. D.; Chan O. H.; Reyner E. L.; Lipka E.; Showalter H. DH.; Vincent P. W.; Elliott W. L. and Denny W. A. Tyrosine kinase inhibitors. 17. Irreversible inhibitors of the epidermal growth factor receptor: 4-(phenylamino)quinazoline- and 4-(phenylamino)pyrido[3,2-d]pyrimidine-6-acrylamides bearing additional solubilizing functions. *J. Med. Chem.* **2000**, 43, 1380-1397. <https://doi.org/10.1021/jm990482t>

48. Gong H.; Qi H.; Sun W.; Zhang Y.; Jiang D.; Xiao J.; Yang X.; Wang Y and Li S., Design and Synthesis of a Series of Pyrido[2,3-d]pyrimidine Derivatives as CCR4 Antagonists. *Molecules*, **2012**, 17, 9961-9970. [DOI:10.3390/molecules17089961](https://doi.org/10.3390/molecules17089961)

RESEARCH OUTCOMES: PG STUDENTS AWARDED

The following is the list of Post Graduate Students who have been benefited out of the present sanctioned Major Research Project entitled “Design, Synthesis and Screening of Some Novel Tyrosine Kinase Inhibitors as Anticancer Agents” sanctioned by University Grants Commission (UGC), New Delhi.

Sr. No.	Name of Student	Title of Dissertation Topic	Year of Degree Award
01	Miss. Waghmare Chetana	Design, Synthesis & Pharmacological Activities Of Some Novel N-[4-Amino-2-(4-Methyl Phenyl Quinazoline-6-YL] Acetamide Derivative	2012-2013
02	Miss. Chevale Shital	Design, Synthesis & Biological Evaluation of some Novel 4- Anilino Quinazoline Derivative	2012-2013
03	Miss Anita Yadav	Design, Synthesis And Biological Activity Of Some Novel 1,6-disubstituted phthalazine Derivatives	2012-2013
04	Mr. Venkatesh Patawar	Design, Synthesis & Biological Evaluation Of Some Novel Quinazoline Derivatives	2012-2013
05	Mr. Pritam Yerawar	Design, Synthesis & Biological Activity of Some Novel Aminophthalazine Derivative	2012-2013
06	Mr. Gacche Rohit	Design, Synthesis & Anticancer Activity of Some Novel 4-AnilinoQuinazoline Derivatives.	2012-2013
07	Miss. Rangari Manjusha	Design, Synthesis & Biological Evaluation of some Novel 4- Anilino Quinazoline Derivatives	2013-2014

08	Miss. Mayadevi Ghuge	Design, Synthesis & Biological Evaluation of some Novel 2,3-Disubstituted Quinazolinone Derivatives	2013-2014
09	Miss. Trupti Mamde	Design, Synthesis, Characterization & Biological Evaluation Of Some Novel 4-Anilinoquinazline Derivatives	2013-2014
10	Mr. Lahane Shivahar	Synthesis, Characterization& Biological Activity Of Some Novel 3-Hydrazinyl Quinazolin 2 (1H) ONE Derivatives	2013-2014

RESEARCH OUTCOMES: PhD STUDENTS REGISTERED/AWARDED

The following PhD students have been benefited out of the present sanctioned Major Research Project entitled “Design, Synthesis and Screening of Some Novel Tyrosine Kinase Inhibitors as Anticancer Agents” sanctioned by University Grants Commission (UGC), New Delhi.

Sr. No.	Name of Student	Title of Dissertation Topic	Year of Registration
01	Vivek B. Panchabhai	“Design, Synthesis and Evaluation of some Novel Heterocyclic Compounds”	2012 - 2013
02	Parag G. Ingole	“Design, Synthesis and Screening of some Novel Heterocyclic Compounds As Anticancer Agents”	2012 - 2013

RESEARCH OUTCOMES:

RESEARCH PAPERS PUBLISHED:

1. Recent Advances in Drug Development of Anticancer Drug Through CADD, Mehtre S M, Kalyankar T M, Butle S R, Inventi Impact: Molecular Modeling, Vol. 2012m 2249-359X
2. Synthetic And Biological Profile of 4H-3, 1-Benzoxazin-4-one: A Review, Akash A. Pawar, S. R. Butle, Pawar P. U., Phulwale V. P., Patawar K. V., Upadhye S. P., Chilwant K. M., Sarate S. M. World Journal Of Pharmaceutical Research, Vol 5, Issue 6, 2016, pp-556-570, ISSN - 2277-7105.
3. Synthesis And Biological Evaluation Of 2-Pheylpyrido[2,3-D]Pyrimidine Derivatives As Cyclin-Dependent Kinase (CDK) Inhibitors, Bhagwanrao P. V., Ingole P. G., Butle S. R., Indian Drugs, ISSN: 0019-462X, 2019: 56 (05) 50-58
4. Synthesis, Evaluation and Pharmacological Screening of 2,3-Benzoquinoline Derivatives For Their Possible Anti-inflammatory And Anticancer Activity, Santosh Rathod, Ajay Kshirsagar, Santosh Butle, Nitin Ipper, International Research Journal of Pharmacy, 2019, 10(7), pp – 114, ISSN - 2230-8407

RESEARCH PAPERS ACCEPTED

1. Design, Synthesis and Antibacterial Studies of Some New Pyridopyrimidine Derivatives as Biotin Carboxylase Inhibitors, Vivek B. Panchabhai, Parag G. Ingole, S. R. Butle, Bulletin of Faculty of Pharmacy, Cairo University , ISSN:- 1110-0931. DOI:- 10.21608/bfpc.2019.10149.1017
2. “Synthesis, characterization and molecular Docking Studies on Some New N-substituted 2-phenylpyrido[2,3-d]pyrimidine derivatives.” Research Journal of Pharmacy and Technology (RJPT), ISSN:- 0974-3618

RESEARCH PAPERS COMMUNICATED

1. Epidermal Growth Factor Receptor Inhibitor A New Target for Anticancer Therapy: A Review, S. R. Butle, Shital Chewale, Communicated to Eurasian Journal of Pharmacy.

RESEARCH OUTCOMES: POSTER PRESENTED

1. Poster Presented in 69th Indian Pharmaceutical Congress 2017 on Synthesis, Characterization and Antimicrobial Screening of Some Novel 1, 2, 4, 5-tetrasubstituted imidazole derivatives, S. B. Choudhary, A. Pawar, S. R. Butle, Department of Pharmaceutical Chemistry, School of Pharmacy, Swami Ramanand Teerth Marathwada University, Nanded (MS), India.
2. Poster Presented in 69th Indian Pharmaceutical Congress 2017 on Synthesis, characterization and biological evaluation of some novel pyrimido [4, 5-b] quinoline derivatives, Kiran Kadam, Naveed Shaikh, Santosh R. Butle, Department of Pharmaceutical Chemistry, School of Pharmacy, Swami Ramanand Teerth Marathwada University, Vishnupuri, Nanded.
3. Poster Presented in National Seminar on Green Chemistry-Role in Environmental Protection 2018 organized by Pravara Rural College of Pharmacy Pravaranagar on “Synthesis, Characterization and Biological Evaluation of Some Novel Substituted 2,3-Benzoquinoline Derivatives”, S. R. Butle, S. D. Pusadkar, Department of Pharmaceutical Chemistry, School of Pharmacy, Swami Ramanand Teerth Marathwada University, Nanded (MS), India.
4. Poster Presented in National Seminar on Green Chemistry-Role in Environmental Protection 2018 organized by Pravara Rural College of Pharmacy Pravaranagar on “Synthesis, Characterization & Antimicrobial Screening of 3-(substituted phenyl)-2-phenylquinazolin-4(3*H*)-one derivatives”, S. R. Butle, Kavita A. Gaikwad, Sumeet Ukalkar, Pooja Pawar, Department of Pharmaceutical Chemistry, School of Pharmacy, Swami Ramanand Teerth Marathwada University, Nanded (MS), India.
5. Poster Presented in National Seminar on Green Chemistry-Role in Environmental Protection 2018 organized by Pravara Rural College of Pharmacy Pravaranagar on “Synthesis, Characterization and Biological Evaluation Some Novel substituted Primidi [4,5 D] Pyrimidine Derivatives”, S. R. Butle, Swati Sonkamble, Komal B Bhoge, Pooja Kachawe, Shyam Shelke, Ajay D. Kshirsagar, Department of Pharmaceutical Chemistry, School of Pharmacy, Swami Ramanand Teerth Marathwada University, Nanded (MS), India.

6. Poster Presented in National Conference on Applications of Computational Chemistry in Pharmaceutical Research 2019 organized by Channabasweshwar Pharmacy College Latur on “Designing of Novel 4-Anilinoquinazoline Derivatives by Using Computational approach: Molecular Docking”, Butle S. R., Pekamwar S. S., Chewale S. L., Yambal V. V., Khedkar V. C., Bajare N. D., Department of Pharmaceutical Chemistry, School of Pharmacy, Swami Ramanand Teerth Marathwada University, Nanded (MS), India.
7. Poster Presented in National Conference on Applications of Computational Chemistry in Pharmaceutical Research 2019 organized by Channabasweshwar Pharmacy College Latur on “Designing of Some Novel 2,3-Disubstitutedquinazolinone Derivatives by Using Docking Studies”, S. S. Pekamwar, Butle S. R., M. H. Ghuge, Y. G. Parakh, S. A. Yadav, Department of Pharmaceutical Chemistry, School of Pharmacy, Swami Ramanand Teerth Marathwada University, Nanded (MS), India.
8. Poster Presented in National Conference on Applications of Computational Chemistry in Pharmaceutical Research 2019 organized by Channabasweshwar Pharmacy College Latur on “Docking Studies of Some Novel N-[4-Amino-2-(4-Methylenyl) Quinazolin-6-yl] Acetamide Derivatives”, S. R. Butle, S. S. Pekamwar, C. M. Waghmare, R. T. Bhagat, P. S. Ladda, Department of Pharmaceutical Chemistry, School of Pharmacy, Swami Ramanand Teerth Marathwada University, Nanded (MS), India.
9. Poster Presented in National Conference on Applications of Computational Chemistry in Pharmaceutical Research 2019 organized by Channabasweshwar Pharmacy College Latur on “Design of Some Novel 6,7,8-trimethoxy-4-anilinoquinazoline Derivatives By Using Docking Studies”, S. S. Pekamwar, S. R. Butle, P.J. Totala. A. A. Kank, A. S. Patil, Department of Pharmaceutical Chemistry, School of Pharmacy, Swami Ramanand Teerth Marathwada University, Nanded (MS), India.
10. Poster Presented in National Conference on Novel Approaches in Drug Regulatory Affairs (DRA-2019) organized by SSS's College of Pharmacy Nanded on “Desig, Synthesis, Characterization and Biological evaluation of Some Novel 4-

Anilinoquinazoline Derivatives”, S. R. Butle, T. P. Mamde, R. T. Bhagat, M. M. Butle, Department of Pharmaceutical Chemistry, School of Pharmacy, Swami Ramanand Teerth Marathwada University, Nanded (MS), India.